Institute for Molecular Science

annual review

2012

Published by

Institute for Molecular Science
National Institutes of Natural Sciences
Myodaiji, Okazaki 444-8585, Japan
Phone: +81-564-55-7418 (Secretary Room)
Fax: +81-564-54-2254 (Secretary Room)
URL: http://www.ims.ac.jp/

Editorial Committee 2012

Chairperson	JIANG, Donglin	
Vice-Chairperson	NISHIMURA, Katsuyuki	
	YASUIKE, Tomokazu	FUKUDA, Ryoichi
	TAKEI, Nobuyuki	MIZUSE, Kenta
	KONOMI, Taro	NOMURA, Yutaka
	FURUKAWA, Ko	IIJIMA, Takahiro
	HIGASHIBAYASHI, Shuhei	KIMURA, Tetsunari
	YAMAGUCHI, Takumi	KAMO, Kyoko
	NAKAMURA, Rie	

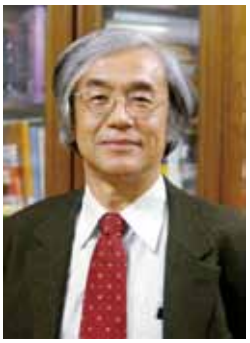

This Annual Review 2012 is a summary of research activities performed in the Institute for Molecular Science (IMS) during September 2011–August 2012. IMS is one of the world's core research facilities for molecular science and is a center for inter-university joint research in Japan, as well. It sets an extremely wide range of research goals, from understanding the behavior of individual molecules to that of collective molecular processes on the scale of life forms and in space. Currently, the IMS is engaged in four areas of research: Theoretical and computational molecular science, photo-molecular science, materials molecular science and life and coordination-complex molecular science. It operates seven research facilities, including the UVSOR Facility.

The staff at IMS are making steady progress in basic research on molecular structures, reactions and functions demonstrating "novel molecular capabilities," as reported in this Review. In addition to these individual research activities, IMS conducts the six special programs in the institute basis; (i) Two computational chemistry programs: TCCI (Theoretical and Computational Chemistry Initiative) as a part of CMSI (Computational Materials Science Initiative) in HPCI (High Performance Computational Infra), and Nano-science simulation for the "Grand Challenge Applications" of the next generation supercomputer projects (the latter was till March 2012), (ii) Nano-network project, including the joint research initiative using 920MHz NMR, (iii) Extreme photonics in collaboration with RIKEN, (iv) COE of molecular and materials simulations as a joint program of NINS, (v) Quantum Beam Development Program in collaboration with Kyoto University and Nagoya University, and (vi) Networked Laboratories for the Frontiers of Photon Science and Technology in collaboration with Japan Atomic Energy Research Institute, Osaka University and Kyoto University. With two IMS own international programs for Asia, namely, EXODASS (EXchange prOgram for the Development of Asian Scientific Society) and Asian Core, IMS has invited active young scientists from various East Asian countries to carry out collaborative researches. EXODASS Program is the post-JENESYS starting from 2011, aims to provide the opportunity for young researchers (*e.g.*, master's and doctoral students and postdoctoral researchers) from Asian countries to stay in IMS laboratories related to the basic research for environmental and energy problems. Asian Core programs now also becomes IMS own project and continue to strengthen the tie among the four key institutes of Chemical Physics in Asia, namely, KAIST in Korea, IASM in Taiwan, ICCAS in China and IMS in Japan.

Three professors, Professor Tanaka, Professor Nagase, and Professor Hirata, are retired at the end of March 2012 and now become our emeritus professors. Two associate professors, Professor Yonemitsu and Professor Mitsuke, were promoted to full professsors of Chuo and Josai Universities, respectively. We are grateful to all five professors for their great contribution to IMS. As for our new faculty, five new members have joined to the our faculty. Dr. Akiyama, an expert of biomolecular systems, and Dr. Murahashi, an organometallic chemist, and Dr. Yamamoto, a solid-state chemist, becomes our full professors. Two young theoretical chemical physicists, Dr. Ishizaki and Dr. Shikano have joined us as the independent young researchers (of new associate professor positions).

IMS is continuing to employ a new scientific perspective to examine the boundary between "micro" and "macro" phenomena, which is "an intrinsic arena for the generation of life" and "for the evolution of functioning molecular materials." We do expect your advice and support for creating this new era of molecular science.

September, 2012

OHMINE, Iwao
Director-General, Institute for Molecular Science

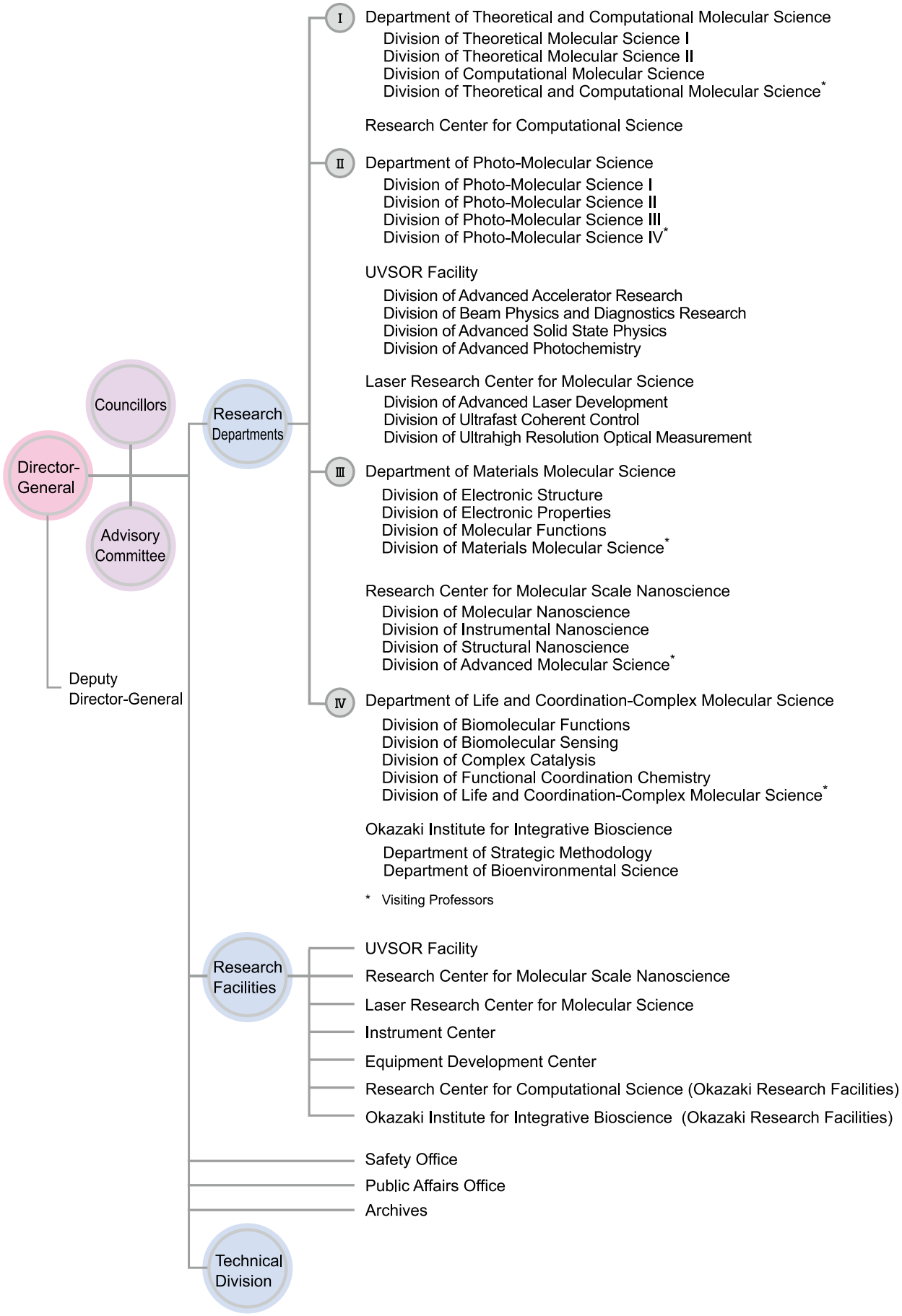
Councillors
Director-General
Advisory Committee
Deputy Director-General
Research Departments
Research Facilities
Technical Division
I
Department of Theoretical and Computational Molecular Science
Division of Theoretical Molecular Science I
Division of Theoretical Molecular Science II
Division of Computational Molecular Science
Division of Theoretical and Computational Molecular Science*
Research Center for Computational Science
II
Department of Photo-Molecular Science
Division of Photo-Molecular Science I
Division of Photo-Molecular Science II
Division of Photo-Molecular Science III
Division of Photo-Molecular Science IV*
UVSOR Facility
Division of Advanced Accelerator Research
Division of Beam Physics and Diagnostics Research
Division of Advanced Solid State Physics
Division of Advanced Photochemistry
Laser Research Center for Molecular Science
Division of Advanced Laser Development
Division of Ultrafast Coherent Control
Division of Ultrahigh Resolution Optical Measurement
III
Department of Materials Molecular Science
Division of Electronic Structure
Division of Electronic Properties
Division of Molecular Functions
Division of Materials Molecular Science*
Research Center for Molecular Scale Nanoscience
Division of Molecular Nanoscience
Division of Instrumental Nanoscience
Division of Structural Nanoscience
Division of Advanced Molecular Science*
IV
Department of Life and Coordination-Complex Molecular Science
Division of Biomolecular Functions
Division of Biomolecular Sensing
Division of Complex Catalysis
Division of Functional Coordination Chemistry
Division of Life and Coordination-Complex Molecular Science*
Okazaki Institute for Integrative Bioscience
Department of Strategic Methodology
Department of Bioenvironmental Science
* Visiting Professors
UVSOR Facility
Research Center for Molecular Scale Nanoscience
Laser Research Center for Molecular Science
Instrument Center
Equipment Development Center
Research Center for Computational Science (Okazaki Research Facilities)
Okazaki Institute for Integrative Bioscience (Okazaki Research Facilities)
Safety Office
Public Affairs Office
Archives

COUNCIL

OHMINE, Iwao	**Director-General**

Senior Scientific Advisors

YANAGIDA, Toshio	Specially Appointed Professor, Osaka University
FLEMING, Graham R.	Professor, University of California, Berkeley

Foreign Councillors

WOLYNES, Peter	Professor, Rice University
WALMSLEY, Ian A.	Professor, University of Oxford

The Council is the advisory board for the Director-General.

Distinguished Consultants

NAGAKURA, Saburo	Professor Emeritus, Institute for Molecular Science, The Graduate University for Advanced Studies, and The University of Tokyo
INOKUCHI, Hiroo	Research Director, Toyota Physical and Chemical Research Institute
ITO, Mitsuo	Professor Emeritus, Institute for Molecular Science, The Graduate University for Advanced Studies, and Tohoku University
KAYA, Koji	Deputy Director General, Next-Generation Supercomputer R&D Center, RIKEN
NAKAMURA, Hiroki	Visiting Professor, National Chiao Tung University

Advisory Committee

ASAKURA, Kiyotaka	Professor, Hokkaido University
KANDORI, Hideki	Professor, Nagoya Institute of Technology (Vice chair)
KOHNO, Hirohiko	Professor, Tohoku University
MIZUTANI, Yasuhisa	Professor, Osaka University
MORI, Takehiko	Professor, Tokyo Institute of Technology
TERASAKI, Akira	Professor, Kyushu University
TSUKUDA, Tatsuya	Professor, The University of Tokyo
UMEMURA, Daisuke	Professor, Kanagawa University
YAMAGATA, Yuriko	Professor, Kumamoto University
YAMANOUCHI, Kaoru	Professor, The University of Tokyo
AONO, Shigetoshi	Professor, Institute for Molecular Science
KATO, Koichi	Professor, Institute for Molecular Science
KATOH, Masahiro	Professor, Institute for Molecular Science
KOSUGI, Nobuhiro	Professor, Institute for Molecular Science (Chair)
OHMORI, Kenji	Professor, Institute for Molecular Science
OHSHIMA, Yasuhiro	Professor, Institute for Molecular Science
OKAMOTO, Hiromi	Professor, Institute for Molecular Science
SAITO, Shinji	Professor, Institute for Molecular Science
UOZUMI, Yasuhiro	Professor, Institute for Molecular Science
YAMAMOTO, Hiroshi	Professor, Institute for Molecular Science
YOKOYAMA, Toshihiko	Professor, Institute for Molecular Science

Administration Bureau

ANAZAWA, Kazuo	Director, Okazaki Administration Office Director, General Affairs Department
HIGUCHI, Hironori	Director, Financial Affairs Department
HIRANO, Shigeichi	Head, General Affairs Division
NODA, Yoshito	Head, International Relations and Research Cooperation Division
SATO, Toshiaki	Head, Financial Affairs Division
TANIGUCHI, Jun	Head, Procurement Division
TORAZAWA, Takahiko	Head, Facilities Division

Emeritus Professors

NAGAKURA, Saburo	Professor Emeritus, The Graduate University for Advanced Studies and The University of Tokyo
HIROTA, Eizi	Professor Emeritus, The Graduate University for Advanced Studies
KIMURA, Katsumi	Archives, IMS and Professor Emeritus, Japan Advanced Institute of Science and Technology
MOROKUMA, Keiji	Senior Research Fellow, Fukui Institute for Fundamental Chemistry, Kyoto University
INOKUCHI, Hiroo	Research Director, Toyota Physical and Chemical Research Institute
MARUYAMA, Yusei	Professor, Hosei University
YOSHIHARA, Keitaro	Fellow, Toyota Physical and Chemical Research Institute
HANAZAKI, Ichiro	Professor Emeritus, The Graduate University for Advanced Studies
IWAMURA, Hiizu	Professor, Nihon University
SAITO, Shuji	Professor Emeritus, The Graduate University for Advanced Studies
IWATA, Suehiro	Fellow, Toyota Physical and Chemical Research Institute
ITO, Mitsuo	Professor Emeritus, The Graduate University for Advanced Studies and Tohoku University
KAYA, Koji	Deputy Director General, Next-Generation Supercomputer R&D Center, RIKEN
KITAGAWA, Teizo	Professor, The University of Hyogo
KOABAYASHI, Hayao	Visiting Professor, Nihon University
NAKAMURA, Hiroki	Visiting Professor, National Chiao Tung University
NISHI, Nobuyuki	Professor, Tokyo Institute of Technology and Nagoya Institute of Technology
YAKUSHI, Kyuya	Fellow, Toyota Physical and Chemical Research Institute
URISU, Tsuneo	Specially Appointed Professor, Nagoya University
NAGASE, Shigeru	Senior Research Fellow, Fukui Institute for Fundamental Chemistry, Kyoto University
HIRATA, Fumio	Visiting Professor, College of Life Sciences, Ritsumeikan University
TANAKA, Koji	Professor, Institute for Integrated Cell-Material Sciences, Kyoto University

ACTIVITIES IN EDUCATION AND COLLABORATION

Graduate Programs

IMS promotes pioneering and outstanding researches by young scientists as a core academic organization in Japan. IMS trains graduate students in Departments of Structural Molecular Science and Functional Molecular Science, Graduate School of Physical Sciences, the Graduate University for Advanced Studies (SOKENDAI). By virtue of open seminars in each research division, Colloquiums and Molecular Science Forum to which speakers are invited from Japan and all over the world, as well as other conferences held in IMS, graduate students have regular opportunities to be exposed to valuable information related to their own as well as other scientific fields. Graduate students can benefit from these liberal and academic circumstances, all of which are aimed at extending the frontiers of fundamental molecular science and to facilitate their potential to deliver outstanding scientific contributions. Recently, we started Course-by-Course Education Program in Graduate School of Physical Sciences. Students choose one of the courses of Basic, Advanced research skills, Project research, and Development research, and can stay abroad, join some big projects, or stay in private companies to improve their research achievements. For more details on Departments of Structural Molecular Science and Functional Molecular Science, young scientists are encouraged to visit IMS through many opportunities such as the IMS Open Campus in May, Graduate-School Experience Program (Taiken Nyugaku) in August, Open Lectures in summer and winter, *etc*.

International Collaboration and Exchange Programs

IMS has accepted many foreign scientists and hosted numerous international workshops and conferences (*e.g.* Okazaki Conference) since its establishment in 1975 and is now universally recognized as an international research institute that is open to foreign countries. In 2004, IMS initiated a program to further promote international collaborations. As a part of this program, IMS faculty members can (1) nominate senior foreign scientists for short-term visits, (2) invite young scientists for long-term stays, and (3) undertake visits overseas to conduct international collaborations. In 2006, IMS started JSPS Asian CORE Program on “Frontiers of material, photo- and theoretical molecular sciences” (2006–2011). This program aims to develop a new frontier in the molecular sciences and to foster the next generation of leading researchers through the collaboration and exchange among IMS and core Asian institutions: ICCAS (China), KAIST (Korea), and IAMS (Taiwan). After this JSPS Asian CORE Program was successfully completed in March 2011, we have launched IMS Asian CORE Program to further promote collaborations with those four key institutes. From 2008, IMS also started JSPS JENESYS and our own EXODASS Programs on “Improvement of Fundamental Research Base for Environmental and Energy Problems.” IMS provides the opportunity for young researchers from ASEAN countries to stay in the laboratories related to the basic research for environmental and energy problem for 14–90 days. Through the experience, we encourage them to continue the basic research in their own countries as well as to build up the future collaboration.

Joint Studies Programs

As one of the important functions of an inter-university research institute, IMS facilitates joint studies programs for which funds are available to cover the costs of research expenses as well as the travel and accommodation expenses of individuals. Proposals from domestic scientists are reviewed and selected by an interuniversity committee. See the details on pages 115–116. The programs are conducted under one of the following categories. In addition to the normal programs, IMS provides “Urgent Joint Studies Programs” for the researchers suffering from the earthquake on March 11, 2011 to recover and rebuild their research activities at March, 2011. We continue to provide this supporting programs in 2012. In this programs, the proposals in the category 5, 6, 7, and 8 are accepted.

(1) Joint Studies on Special Projects (a special project of significant relevance to the advancement of molecular science can be carried out by a team of several groups of scientists).
(2) Research Symposia (a symposium on timely topics organized as a collaborative effort between outside and IMS scientists). Since October, 2010, three sub-categories are set up in Research Symposia: (i) general type as in the past, (ii) Research Symposia in cooperation with foreign scientists in Asian countries, (iii) Research Symposia in cooperation with scientific societies.
(3) Research Symposia graduate students plan.
(4) International Research Conference (Okazaki Conference).
(5) Cooperative Research (a research program conducted by outside scientists with collaboration from an IMS scientist).
(6) Use of Facilities (a research program conducted by outside scientists using the research facilities of IMS, except the UVSOR facility).
(7) Joint Studies Programs using beam lines of UVSOR Facility.
(8) Use of Facility Program of the Computer Center (research programs conducted by outside scientists at research facilities in the Research Center for Computational Science).

RESEARCH ACTIVITIES

Theoretical and Computational Molecular Science

It is our goal to develop new theoretical and computational methods based on quantum mechanics, statistical mechanics, and molecular simulation in order to predict and understand the structures, reactions, and functions of molecules in gas, solution, and condensed phases as well as in nano- and bio-systems prior to or in cooperation with experiments.

Theoretical Study and Design of Functional Molecules: New Bonding, Structures, and Reactions

Department of Theoretical and Computational Molecular Science
Division of Theoretical Molecular Science I

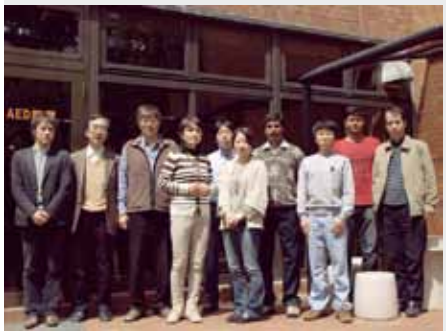

NAGASE, Shigeru	Professor (–March, 2012)*
LUO, Gangfu	IMS Fellow†
KATOUDA, Michio	Post-Doctoral Fellow‡
GUO, Jing-Doing	Post-Doctoral Fellow*
KARTHIKEYAN, Subramanlan	Post-Doctoral Fellow§
ZHOU, Xin	Post-Doctoral Fellow‖
SAKAKI, Shigeyoshi	Visiting Scientist*
YAMADA, Mariko	Secretary
KONDO, Naoko	Secretary

In theoretical and computational chemistry, it is an important goal to develop functional molecules prior to or in cooperation with experiment. Thus, new bonds and structures provided by heavier atoms are investigated together with the reactivities. In addition, chemical modification and properties of nanocarbons are investigated to develop functional nanomolecular systems. Efficient computational methods are also developed to perform reliable quantum chemistry calculations for small and large molecular systems.

1. Quest for Stable Multiple Bonds between Lead Atoms

The heavier analogues of alkynes, REER (E = Si, Ge, Sn, Pb), have attracted special interest in main-group element chemistry. Accordingly, all the heavier analogues have been synthesized and isolated uo to now. The X-ray crystal structure of the heaviest analogue, Ar*PbPbAr* (Ar* = C_6H_3-2,6-(C_6H_2-2,4,6-^{i}Pr$_3$)$_2$), has shown that the Pb–Pb bond distance is much longer than Pb–Pb single bond distances. Theoretical calculations have revealed that Ar*PbPbAr* has no π bond between Pb atoms. Therefore, it has been widely accepted that the heaviest Pb analogues of alkynes take a singly bonded structure, unlike the Si, Ge, and Sn cases. However, we have pointed out that Ar*PbPbAr* has a triply bonded structure in solution and crystal structures are not very helpful for compounds with bulky groups.[1)]

The Pb–Pb bond distance of 3.071 Å calculated for the triply bonded structure of Ar*Pb–PbAr* is considerably longer than the Pb–Pb single bond distance of 2.844 Å in $Ph_3PbPbPh_3$. Since we have found that electropositive silyl groups decreases the Pb–Pb bond distance, several bulky silyl groups were tested using density functional calculations.[2)] The optimized structure of $R^{Si}PbPbR^{Si}$ (R^{Si} = Si^{i}Pr{CH(SiMe$_3$)$_2$}$_2$) is depiched in Figure 1, the two Pb atoms being triply bonded. The Pb–Pb bond distance of 2.696 Å is remarkably shorter than the Pb–Pb single bond distance of 2.844 Å in Ph_3Pb-$PbPh_3$, and it is considerably shorter than the shortest Pb–Pb double bond distance of 2.903 Å known to date. However, the triply bonded structure is 4.3 kcal/mol less stable than the singly bonded structure. We are still searching for good substituent groups that stabilize a triply bonded structure with a sufficiently short Pb–Pb bond.

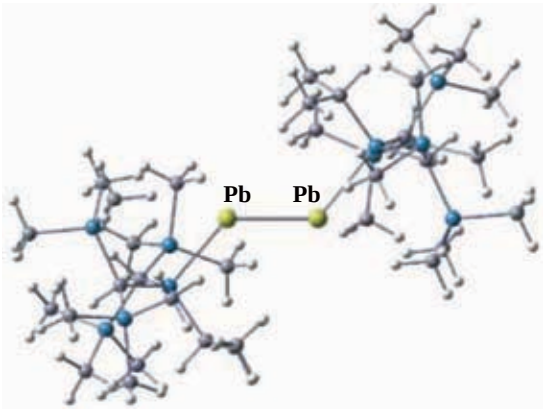

Figure 1. Triply bonded structure of $R^{Si}PbPbR^{Si}$.

As a new type of double bonds, diatomic molecules stabilized by the coordination of dative N-heterocyclic carbenes are of considerable interest currently. This stabilization has been performed for the synthesis and isolation of L:→Si=Si←:L and L:→Ge=Ge←:L (L = :C[N(2,6-^{i}Pr$_2$-C_6H_3)CH]$_2$). The Si–Si and Ge–Ge bond distances compare well with typical double bond distances of R_2Si=SiR_2 and R_2Ge=GeR_2. Because the heaviest Pb case remains unknown, we have investigated L:→Pb=Pb←:L.[2)] The optimized structure is shown in Figure 2. Molecular orbital analysis confirms that the two Pb atoms are doubly bonded. It is notable that the Pb–Pb double bond distance of 2.833 Å is considerably shorter than the shortest Pb–Pb double bond distance of 2.903 Å known to date and

differs little from the Pb–Pb bond distance of Pb_2. It is expected that L:→Pb=Pb←:L is an interesting synthetic target.

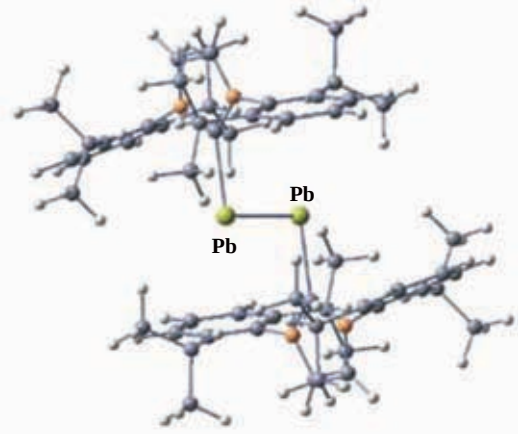

Figure 2. Optimized structure of L:→Pb=Pb←:L.

2. Short Bonds between Transition Metals

As a novel transition metal complex with an unsupported two-coordinate Fe atom, R*FeFe(η^5-C_5H_5)$(CO)_2$ (R* = C_6H-2,6-Ar_2-3,5-$^i Pr_2$ where Ar = C_6H_2-2,5,6-$^i Pr_3$) has recently been synthesized and investigated.[3] X-ray crystal analysis shows that the Fe–Fe bond distances of 2.393 Å is much shorter than the known unsupported Fe–Fe bond distances (2.687–3.138 Å), suggesting that R*FeFe(η^5-C_5H_5)$(CO)_2$ has the shortest unsupported Fe–Fe bond. Interestingly, calculations show that the Fe–Fe bond is greatly shortened in the bicyclic four-membered ring presented in Figure 3a.[2]

Figure 3. Bicyclic four-membered ring complexes.

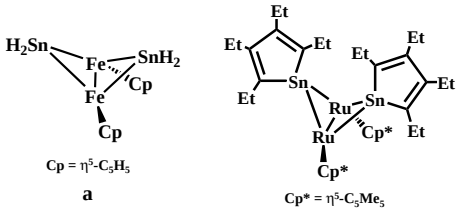

It is remarkable that the Fe–Fe bond distance of 2.045 Å is much shorter than the shortest Fe–Fe bond distance of 2.127 Å reported to date. This bond shortening assisted by two Sn atoms is very recently realized for the bicyclic four-membered Ru_2Sn_2 ring complex presented in Figure 3b.[4] The Ru–Ru bond distance of 2.343 Å determined through X-ray crustal analysis agrees well with the calculated value of 2.363 Å. It is shorter than the Ru–Ru distance of 2.449–2.469 Å in the related bridge complexes, for which it is assumed that the two Ru atoms are triply bonded. Localized molecular orbital analysis reveals that one clear σ bond exists between the Ru atoms, while two three-centered σ orbitals are delocalized over each of the three-membered Ru_2Sn rings, which make an important contribution to Ru–Ru bonding. As a result, the Ru–Ru bond has a somewhat multiple-bond character.

It is also predicted theoretically that the Ru–Ru bond distance in the bicyclic four-membered Ru_2Sn_2 ring is shortened further in the bicyclic six-membered Ru_2Sn_4 ring. Experimental confirmation is in progress.

3. Nano-Carbon Systems

We have performed theoretical calculations for (a) polarized nonresonant Raman spectra of graphene nanoriboins[5] and (b) transport properties of transition metal intercalated graphene.[6] In collaboration with experiment, we have also performed calculations for (c) stable radical anions inside fullerene cages,[7] (d) the core-shell interplay in carbide cluster metallofullerenes,[8] (e) the cocrystal of La@C_{82} and nickel porphyrin with high electron mobility,[9] and (f) chemical understanding of carbide cluster metallofullerenes.[10]

References

1) N. Takagi and S. Nagase, *Organometallics* **26**, 3627–3629 (2007).
2) S. Nagase, *Pure Appl. Chem.*, in press.
3) H. Lei, J. -D. Guo, J. C. Fettinger, S. Nagase and P. P. Power, *J. Am. Chem. Soc.* **132**, 17399–17401 (2010).
4) T. Kuwabara, M. Saito, J. -D. Guo and S. Nagase, to be submitted for publication.
5) G. Luo, L. Wang, H. Li, R. Qui, J. Zhou, L. Li, Z. Gao, W. -N. Mei, J. Lu and S. Nagase, *J. Phys. Chem. C* **115**, 24463–24468 (2011).
6) J. Zhou, L. Wang, R. Qin, J. Zheng, W. N. Mei, P. A. Dowben, S. Nagase, Z. Gao and J. Lu, *J. Phys. Chem. C* **115**, 25273–25280 (2011).
7) T. Tsuchiya, M. Wielopolski, N. Sakuma, N. Mizorogi, T. Akasaka, T. Kato, D. M. Guldi and S. Nagase, *J. Am. Chem. Soc.* **133**, 13280–13283 (2011).
8) H. Kurihara, X. Lu, Y. Iiduka, H. Nikawa, M. Hachiya, N. Mizorogi, Z. Slanina, T. Tsuchiya, S. Nagase and T. Akasaka, *Inorg. Chem.* **51**, 746–750 (2012).
9) S. Sato, H. Nikawa, S. Seki, L. Wang, G. Luo, J. Lu, M. Haranaka, T. Tsuchiya, S. Nagase and T. Akasaka, *Angew. Chem., Int. Ed.* **51**, 1589–1591 (2012).
10) H. Kurihara, X. Lu, Y. Iiduka, H. Nikawa, N. Mizorogi, Z. Slanina, T. Tsuchiya, S. Nagase and T. Akasaka, *J. Am. Chem. Soc.* **134**, 3139–3144 (2012).

* Present Address; Fukui Institute for Fundamental Chemistry, Kyoto University, Kyoto 606-8103
† Present Address; Department of Physics, Peking University, Beijing 100871, P. R. China
‡ Present Address; Riken Advanced Institute for Computational Science, Kobe 650-0047
§ Present Address; Department of Chemistry, Sungkyunkwan University, Suwon 440-746, Korea
|| Present Address; Harbin Institute of Technology, Harbin 150080, P. R. China

Electron and Electromagnetic Field Dynamics in Nanostructures

Department of Theoretical and Computational Molecular Science
Division of Theoretical Molecular Science I

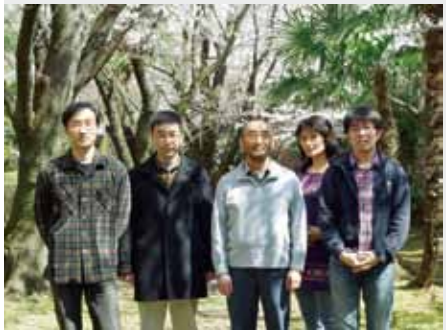

NOBUSADA, Katsuyuki	Associate Professor
YASUIKE, Tomokazu	Assistant Professor
IIDA, Kenji	IMS Fellow
NODA, Masashi	Post-Doctoral Fellow
YAMADA, Mariko	Secretary

We have developed theoretical methods to calculate photo-induced electron dynamics in nanostructured materials such as nanoparticles, quantum-dot arrays, and adsorbate-surface systems. Specifically, we have formulated generalized theory of a light-matter interaction beyond a dipole approximation with the aim of understanding the near-field excitation of nanostructures. Furthermore, a highly efficient computational program of massively parallel calculations for electron dynamics has been developed to investigate optical response of nanostructures more than ten-nanometers. Structural and electronic properties of gold-thiolate clusters have also been elucidated in collaboration with an experimental group.

1. Massively-Parallel TDDFT Calculations Based on Finite Difference Method in Real-Time and Real-Space

A highly efficient computational program of massively parallel calculations for electron dynamics has been developed in an effort to apply the method to optical response of nanostructures more than ten-nanometers. The approach is based on time-dependent density functional theory calculations in real-time and real-space. The computational code is implemented by using very simple algorithms with a finite difference method in space derivative and Taylor expansion in time-propagation. Since the computational program is free from the algorithms of eigenvalue problems and fast-fourier-transformation, which are usually implemented in conventional quantum chemistry or band structure calculations, the program is highly suitable for massively parallel calculations. The method is applied to optical response of nanostructures constructed from C_{60} as benchmark systems. We achieved 8.15% peak performance on the K computer with 1920 nodes (15360 cores) and 3.25% peak performance with 12288 nodes (98304 cores). The peak performance decreases with increasing the nodes because of the network communications due to summing up electron density. The computed absorption spectrum of a face-centered cubic unit of solid C_{60} well reproduces the experimental result.

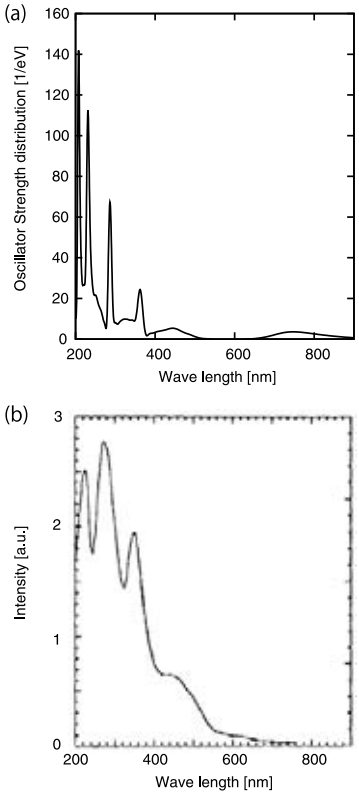

Figure 1. (a) Absorption spectrum of a face-centered cubic unit associated with a solid thin film of C_{60} in comparison with (b) the experimental observation.

2. Enhanced Raman Spectrum of Pyrazine with the Aid of Resonant Electron Dynamics in a Nearby Cluster[1)]

We have investigated the electron dynamics relevant to the

Raman enhancement of pyrazine by a nearby Na_4 cluster. The present time-dependent analysis allows us to illustrate that the electronic excitation in Na_4 is closely associated with surface-enhanced Raman scattering in pyrazine. More specifically, it was clearly demonstrated that some specific enhanced vibrational modes strongly couple with the plasmonic electron motion of Na_4. The displacement along the enhanced mode leads to a change of the electron dynamics in the entire region of the system, whereas the non-enhanced mode causes only a localized change in the junction area between pyrazine and Na_4. The strong obstructive mode to the plasmonic electron motion is strongly enhanced. In the present system, all the obstructive modes are readily understood by the characteristics of the atoms in-phase oscillating in the *x*-direction at the side of Na_4. This picture gives a clear explanation for the enhancement. The present results show the potential ability of cluster-enhanced Raman scattering. A microcluster selectively adsorbed by a specific molecule can be designed using recently developed techniques for the chemical synthesis of clusters. Such artificially designed clusters significantly enhance the Raman scattering of analyte molecules and therefore provide a new way of utilizing enhanced Raman scattering in various research fields.

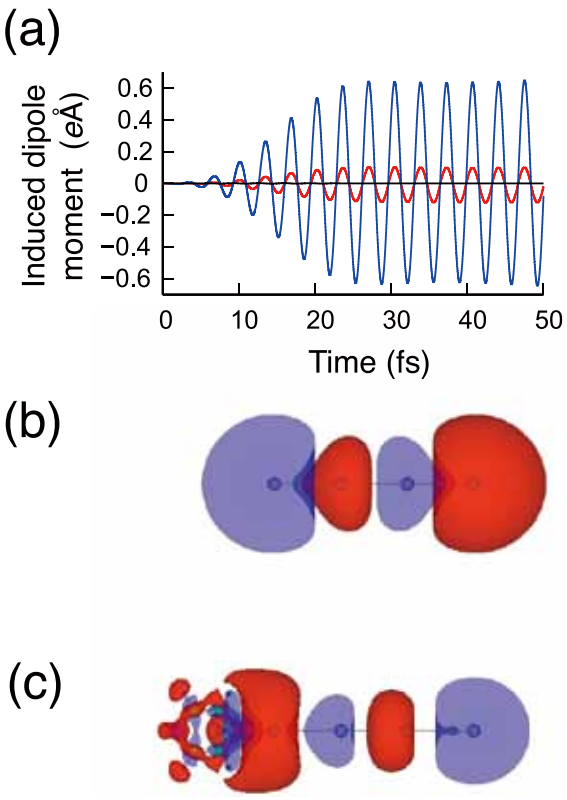

Figure 2. (a) Time-dependent induced dipole moments (*x*-component) in the $C_4H_4N_2$ (red) and Na_4 (blue) sides of $C_4H_4N_2$–Na_4 under *x*-polarized laser excitation at $\omega = 1.23$ eV. The dipole moment of isolated $C_4H_4N_2$ under the same excitation condition is also shown (black). Fourier component (1.23 eV) of the time-dependent induced density of (b) Na_4 and (c) $C_4N_2H_4$–Na_4.

3. Palladium Doping of Magic Gold Cluster $Au_{38}(SC_2H_4Ph)_{24}$: Formation of $Pd_2Au_{36}(SC_2H_4Ph)_{24}$ with Higher Stability than $Au_{38}(SC_2H_4Ph)_{24}$[2)]

Gold clusters protected by thiolates have attracted considerable attention as building blocks for new functional materials because they exhibit size-specific physical and chemical properties. Among these, $Au_{25}(SR)_{18}$, $Au_{38}(SR)_{24}$, $Au_{68}(SR)_{34}$, $Au_{102}(SR)_{44}$, and $Au_{144}(SR)_{60}$ are promising, because they exhibit higher thermodynamic and chemical stabilities than clusters of other sizes. Many studies have been conducted on the isolation, size-selective synthesis, stabilities, structures, chemical and physical properties, and applications of these stable clusters. In this study, a phenylethanethiolate-protected $Pd_2Au_{36}(SC_2H_4Ph)_{24}$ cluster, which is a two-Pd atom-doped cluster of the well studied magic gold cluster $Au_{38}(SC_2H_4Ph)_{24}$, was synthesized in high purity and its stability was investigated. The experimental and theoretical results demonstrate that $Pd_2Au_{36}(SC_2H_4Ph)_{24}$ is more stable than $Au_{38}(SC_2H_4Ph)_{24}$ against degradation in solution and core etching by thiols.

4. Effect of Copper Doping on Electronic Structure, Geometric Structure, and Stability of Thiolate-Protected Au_{25} Nanoclusters[3)]

Several recent studies have attempted to impart $[Au_{25}(SR)_{18}]^-$ with new properties by doping with foreign atoms. In this study, we investigated the effect of copper doping on the electronic structure, geometric structure, and stability of $[Au_{25}(SR)_{18}]^-$ with the aim of investigating the effect of foreign atom doping of $[Au_{25}(SR)_{18}]^-$. $Cu_nAu_{25-n}(SC_2H_4Ph)_{18}$ was synthesized by reducing complexes formed by the reaction between metal salts (copper and gold salts) and PhC_2H_4SH with $NaBH_4$. Mass analysis revealed that the products contained $Cu_nAu_{25-n}(SC_2H_4Ph)_{18}$ (n = 1–5) in high purity. Experimental and theoretical analysis of the synthesized clusters revealed that copper doping alters the optical properties and redox potentials of the cluster, greatly distorts its geometric structure, and reduces the cluster stability in solution. These findings are expected to be useful for developing design guidelines for functionalizing $[Au_{25}(SR)_{18}]^-$ through doping with foreign atoms.

References

1) M. Noda, T. Yasuike, K. Nobusada and M. Hayashi, *Chem. Phys. Lett.* **550**, 52–57 (2012).
2) Y. Negishi, K. Igarashi, K. Munakata, W. Ohgake and K. Nobusada, *Chem. Commun.* **48**, 660–662 (2012).
3) Y. Negishi, K. Munakata, W. Ohgake and K. Nobusada, *J. Phys. Chem. Lett.* **3**, 2209–2214 (2012).

Advanced Electronic Structure Theory in Quantum Chemistry

Department of Theoretical and Computational Molecular Science
Division of Theoretical Molecular Science I

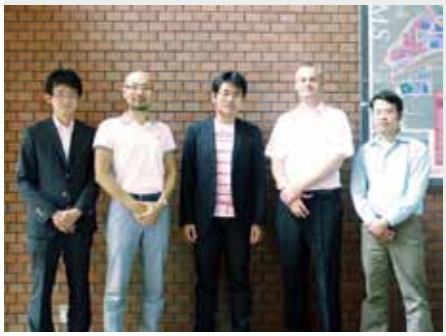

YANAI, Takeshi	Associate Professor
KURASHIGE, Yuki	Assistant Professor
CHALUPSKY, Jakub	IMS Fellow
TRAN, Lan	Graduate Student
SAITOW, Masaaki	Graduate Student*
YAMADA, Mariko	Secretary

Aiming at predictive computational modelings of molecular electronic structures with *ab initio* quantum chemistry calculations, our scientific exploration is to establish a cutting-edge theoretical methodology that allows one to compute accurately and efficiently the complex electronic structures, in which strongly-interacting electrons play a crucial role to characterize the nature of molecules. The complicated electronic structures can be handled accurately with the multi-reference theory, which deals with multiple important electronic configurations on equal footing. However, with the standard multireference methods such as the complete active space self-consistent field (CASSCF), the tractable size of the reference space is limited to small active space because the complexity of the calculations grows exponentially with the reference size. The existing multireference methods are nevertheless usefully applied to chemical theory problems such as exploring chemical reactions of bonding, dissociation and isomerization along the reaction coordinates, electronically excited states, unstable electronic structures of radical systems, and multiple covalent bindings in molecular metal complexes, *etc*. Our resultant works to be reported here are (1) to develop a type of the multireference correlation model named Canonical Transformation (CT) theory, which can efficiently describe short-range dynamic correlation on top of the multi-configurational staring wave function, (2) to construct the extensive complete active space self-consistent field (CASSCF) method combined with *ab initio* density matrix renormalization group (DMRG) method for making unprecedentedly larger active spaces available for the CASSCF calculations, and (3) to develop an efficient second-order perturbation theory that can use large active space with the DMRG-SCF reference wavefunction.

1. Canonical Transcorrelated Theory with Projected Slater-Type Geminals[1)]

An effective Hamiltonian perturbed with explicit inter-

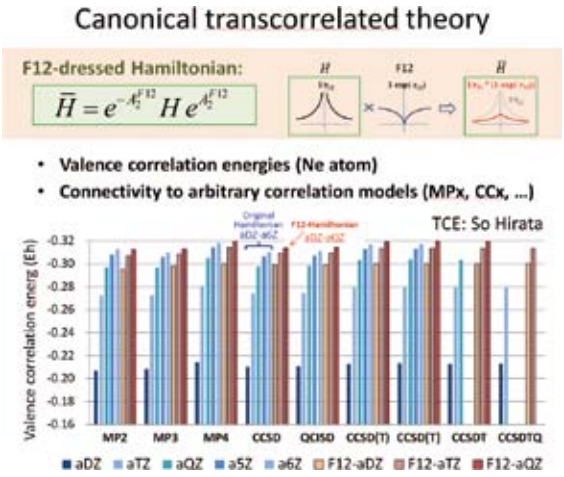

Figure 1. Canonical Transcorrelation method with F12 correlation factor.

electronic correlation is derived from similarity transformation of Hamiltonian using a unitary operator with Slater-type geminals. The Slater-type geminal is projected onto the excitation (and de-excitation) component as in the F12 theory. Simplification is made by truncating higher-body operators, resulting in a correlated Hamiltonian which is Hermitian and has exactly the same complexity as the original Hamiltonian in the second quantized form. It can thus be easily combined with arbitrary correlation models proposed to date. The present approach constructs a singularity-free Hamiltonian *a priori*, similarly to the so-called transcorrelated theory, while the use of the canonical transformation[2)] assures that the effective Hamiltonian is two-body and Hermite. Our theory is naturally extensible to multireference calculations on the basis of the generalized normal ordering. The construction of the effective Hamiltonian is non-iterative. The numerical assessments demonstrate that the present scheme improves the basis set convergence of the post-mean-field calculations at a similar rate to the explicitly correlated methods proposed by others

that couple geminals and conventional excitations.

In this study, we propose a canonical transcorrelated Hamiltonian with the F12 operator:

$$\hat{\bar{H}}^{\mathrm{F12}} \equiv \hat{H} + [\hat{H}, \hat{A}^{\mathrm{F12}}]_{1,2} + \tfrac{1}{2}[[\hat{F}, \hat{A}^{\mathrm{F12}}]_{1,2}, \hat{A}^{\mathrm{F12}}]_{1,2}$$

which is derived in two ways of formal approximations: (i) terminating the expansion at the second order and (ii) replacing the uncorrelated Hamiltonian $\underline{H}$ at the second order term (*i.e.*, the double commutator) by the Fock operator F. Note that F is the effective one-particle approximation to $\underline{H}$. This truncation of the infinite expansion is correct through the second order in perturbation.

We use an anti-Hermitian generator with projected geminal functions to make the transcorrelated H Hermite:

$$\hat{A}^{\mathrm{F12}} = \tfrac{1}{2} G_{ij}^{\alpha\beta} (\hat{E}_{ij}^{\alpha\beta} - \hat{E}_{\alpha\beta}^{ij}),$$
$$G_{ij}^{\alpha\beta} = \frac{3}{8}\langle \alpha\beta | \hat{Q}_{12} F_{12} | ij \rangle + \frac{1}{8}\langle \alpha\beta | \hat{Q}_{12} F_{12} | ji \rangle,$$
$$F_{12} = -\gamma^{-1} \exp(-\gamma r_{12}),$$

in which we have fixed the amplitudes by those determined by the first-order cusp condition. The explicit electron correlation with the *projected* Slater-type geminals is built into a Hamiltonian through the canonical transformation. The present approach provides a formulation to effectively remove high-energy orbital components by using the F12 factor as a regulator for renormalizing them into the smaller-size orbital space. The features of the canonical transcorrelated theory are:

(1) The resulting effective Hamiltonian is already perturbed with a considerable amount of the dynamic correlation associated with the interelectronic Coulomb singularity;
(2) It remains Hermitian and has exactly the same size, dimension, and quartic complexity as the bare Hamiltonian;
(3) There is no adjustable parameter in the geminal excitations with Ten-no's fixed amplitude ansatz, since the F12 amplitudes for the present transformation are predetermined and calculated in a non-iterative manner;
(4) The theory is extensible to multireference models on the basis of the generalized normal ordering of Mukherjee and Kutzelnigg;
(5) In contrast to the standard F12 theories which couple the F12 and conventional excitations in the amplitude equations or Valeev's *a posteori* F12 corrections, we have introduced an *a priori* F12 transformed Hamiltonian that can be readily used in conjunction with arbitrary correlation models to describe the remaining orbital correlation.

We have demonstrated its applications to various solvers in quantum chemical methods, such as CCSD(T), QCISD, MP4, CCSDT, CCSDTQ, and so forth. The benchmarks on small molecules have revealed that the numerical performance of our explicit correlation scheme is comparable to that of other F12 theories. In our method, the F12 correction and the orbital correlation are treated separately at different steps, and thus it is indicated that they are more or less additively separable. (**Figure 1**)

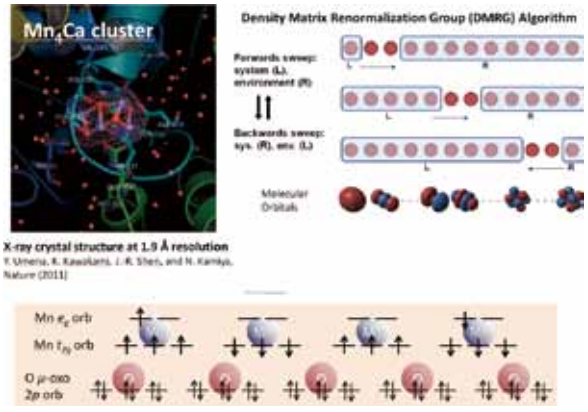

Figure 2. Determination of oxidation state of Mn_4CaO_5 cluster in photosystem II from a multireference wavefunction theory based on Denisty Matrix Renormalization Group method.

2. Oxidation State of Mn_4Ca Cluster in Photosystem II: A Quantum-Chemical Density-Matrix Renormalization Group Study[3)]

The X-ray diffraction (XRD) structure of photosystem II at a resolution of 1.9 Å was recently reported, entailing atomic-details of the Mn_4Ca cluster. Meanwhile, there is an earlier study suggesting that the high-valent $Mn^{III–IV}$ ions of the cluster are potentially damaged by X-rays and reduced towards the lower-valent Mn^{II}, involving structural deformation. Thus, the record-resolution XRD measurement used a low-level X-ray dose to avoid such damage. We report a theoretical analysis identifying the oxidation states of the Mn ions as fingerprints to be compared with the widely-accepted oxidation state. Super high-dimensional multireference wavefunctions were calculated to account for nonperturbative interactions arising from four Mn 3d and five μ-oxo 2p shells. (**Figure 2**)

References

1) T. Yanai and T. Shiozaki, *J. Chem. Phys.* **136**, 084107 (9 pages) (2012).
2) T. Yanai, Y. Kurashige, E. Neuscamman and G. K.-L. Chan, *Phys. Chem. Chem. Phys.* **14**, 7809–7820 (2012).
3) Y. Kurashige, G. K.-L. Chan and T. Yanai, submitted.

* carrying out graduate research on Cooperative Education Program of IMS with Rikkyo University

Developing the Statistical Mechanics Theory of Liquids in Chemistry and Biophysics

Department of Theoretical and Computational Molecular Science
Division of Theoretical Molecular Science II

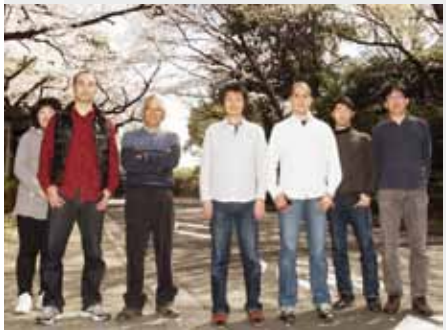

HIRATA, Fumio	Professor (–March, 2012)*
YOSHIDA, Norio	Assistant Professor†
MARUYAMA, Yutaka	Post-Doctoral Fellow
PHONGPHANPHANEE, Saree	Post-Doctoral Fellow
SINDHIKARA, Daniel J.	Post-Doctoral Fellow
KIYOTA, Yasuomi	Post-Doctoral Fellow
SUETAKE, Yasumi	Secretary
KONDO, Naoko	Secretary
YAMADA, Mariko	Secretary

"Molecular recognition" is an essential elementary process for protein to function. The process is a thermodynamic process which is characterized with the free energy difference between two states of a host-guest system, namely, associated and dissociated states. It is readily understood that the structural fluctuation of protein gives a big effect on the free energy barrier. In that respect, the "molecular recognition" is a thermodynamic process which is conjugated with the structural fluctuation of protein.

We have been developing a new theory concerning the molecular recognition, based on the 3D-RISM/RISM theory which is a statistical mechanics of liquids. The theory has successfully "probed" small ligands such as water molecules and ions bound in a small cavity of protein.[1–3)]

1. Elucidating the Molecular Origin of Hydrolysis Energy of Pyrophosphate in Water[4)]

The molecular origin of the energy produced by the ATP hydrolysis has been one of the long-standing fundamental issues. A classical view is that the negative hydrolysis free energy of ATP originates from intra-molecular effects connected with the backbone P–O bond, so called "high-energy bond." On the other hand, it has also been recognized that solvation effects are essential in determining the hydrolysis free energy. Here, using the 3D-RISM-SCF (three-dimensional reference interaction site model self-consistent field) theory that integrates the ab initio quantum chemistry method and the statistical mechanical theory of liquids, we investigate the molecular origin of hydrolysis free energy of pyrophosphate, an ATP analog, in water. We demonstrate that our theory quantitatively reproduces the experimental results without the use of empirical parameters. We clarify the crucial role of water in converting the hydrolysis free energy in the gas phase determined solely by intra-molecular effects, which ranges from endothermic, thermoneutral to highly exothermic depending on the charged state of pyrophosphate, into moderately exothermic in the aqueous phase irrespective of the charged state as observed in experimental data. We elucidate that this is brought about by different natures of solute–water interactions depending on the charged state of solute species: the hydration free energy of low-charged state is mainly subjected to short-range hydrogen-bonds, while that of high-charged state is dominated by long-range electrostatic interactions. We thus provide unambiguous evidence on the critical role of water in determining the ATP hydrolysis free energy.

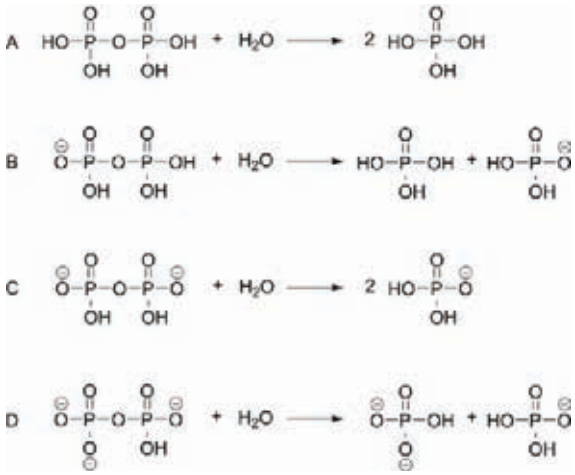

Scheme 1. Schematic description of the hydrolysis reaction of pyrophosphate for the four possible charged states.

Table 1. The reaction free energies in the gas phase and in the aqueous phase at 298.15 K and 1.0 atm computed by DFT at the B3LYP/6-31+(d) level and the 3D-RISM-SCF theory. Units are in kcal/mol.

Reaction	gas phase (DFT)	aqueous phase (3D-RISM/RISM)	Exp.
A	–1.7	–8.9	–9.5
B	21.3	–6.2	–7.5
C	–56.6	–8.1	–7.7
D	–119.0	–7.7	–7.1

2. Placevent: An Algorithm for Predicting of Explicit Solvent Atom Distribution—Application to HIV-1 Protease and F-ATP Synthase[5)]

Location of water and ions in native structure of protein is of essential importance for its stability and for its functions. However, determination of the position of those species in protein is not an easy task for any experimetal methods currently available, X-ray, NMR, neutron diffraction, and the molecular simulation.

We have created a simple algorithm for automatically predicting the explicit solvent atom distribution of biomolecules. The explicit distribution is coerced from the 3D continuous distribution resulting from a 3D-RISM calculation. This procedure predicts optimal location of solvent molecules and ions given a rigid biomolecular structure and the solvent composition. We show examples of predicting water molecules near the KNI-272 bound form of HIV-1 protease and predicting both sodium ions and water molecules near the rotor ring of F-ATP synthase. Our results give excellent agreement with experimental structure with an average prediction error of 0.45–0.65 Å. Further, unlike experimental methods, this method does not suffer from the partial occupancy limit. Our method can be performed directly on 3D-RISM output within minutes. It is extremely useful for examining multiple specific solvent–solute interactions, as a convenient method for generating initial solvent structures for MD calculations, and may assist in refinement of experimental structures.

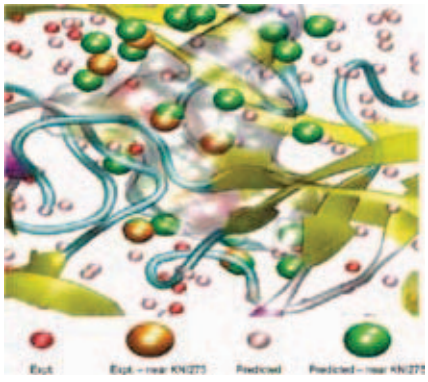

Figure 1. Water molecules near KNI-275. KNI-275 is shown as a translucent surface, HIV-1 protease as a cartoon. Crystal water molecules near KNI-275 are shown in orange, elsewhere in red. Water molecules placed by this method near KNI-275 are shown in green, elsewhere in pink.

3. Modified Andersen Method for Accelerating 3D-RISM Calculations Using Graphics Processing Unit[6)]

Increasing attention has been paid to the 3D-RISM theory due mainly to its capability of treating "solvation" of biomolecules such as protein and DNA without using any adjustable parameters, which is the case in the continuum model. The method was highlighed in several symposiums in the latest ACS meeting held in Philadelphia. Superiority of 3D-RISM to the continuum models, the Poisson-Boltzmann and generalized Born equations, was addressed unambiguously by several talks in the symposiums as far as physical soundness, amount of information produced, applicability to drug design, and so on, are concerned. However, there still remains one point which makes people stick to the continuum models. That is the computation cost. The cost to perform the 3D-RISM calculation is far higher than that of the continuum models. We have proposed a fast algorithm to solve the 3D-RISM equation on a graphics processing unit (GPU). It was the large memory space required for convergence of iteration that banned 3D-RISM from GPU. In order to overcome the difficulty, we replaced the conventional MDIIS algorithm by Anderson's method with some modification. Using this method on a Tesla C2070 GPU, we reduced the total computational time by a factor of eight, 1.4 times by the modified Andersen method and 5.7 times by GPU, compared to calculations on an Intel Xeon machine (8 cores, 3.33 GHz) with the conventional method.

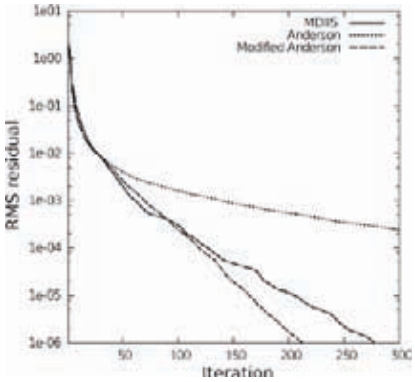

Figure 2. Root mean square residual against the number of iteration steps for the calculation of 3D site distribution profiles of water around a DNA molecule by 3D-RISM. Solid, dotted, and dashed lines are for MDIIS, Anderson, and Modified Anderson algorithms, respectively.

References

1) F. Hirata, *Molecular Theory of Solvation*, Kluwer; Dordrecht, Netherlands (2003).
2) A. Kovalenko and F. Hirata, *J. Chem. Phys.* **110**, 10095–10112 (1999).
3) T. Imai, R. Hiraoka, A. Kovalenko and F. Hirata, *J. Am. Chem. Soc. (Communication)* **127**, 15334–15335 (2005).
4) J. Hong, N. Yoshida, S.-H. Chong, C. Lee, S. Ham and F. Hirata, *J. Chem. Theory Comput.* **8**, 2239 (2012).
5) D. Sindhiara, N.Yoshida and F. Hirata, *J. Comput. Chem.* **33**, 1536 (2012).
6) Y. Maruyama and F. Hirata, *J. Chem. Theory Comput.* **8**, 2239–2246 (2012).

* Present Address; College of Life Sciences, Ritsumeikan University
† Present Address; Graduate School of Sciences, Kyushu University

Theory of Photoinduced Phase Transitions

Department of Theoretical and Computational Molecular Science
Division of Theoretical Molecular Science II

YONEMITSU, Kenji	Associate Professor (–March, 2012)*
TANAKA, Yasuhiro	Assistant Professor
NISHIOKA, Keita	IMS Fellow†
MIYAZAKI, Mitake	Visiting Scientist‡
KONDO, Naoko	Secretary

Photoirradiation of materials usually creates electrons and holes, which are often accompanied by local structural deformation. With the help of cooperativity, the electronic and/or structural deformation can proliferate to change the physical property such as conductivity, permittivity, and magnetic susceptibility. The resultant nonequilibrium phase may not be reached by changing temperature or pressure because the energy of a photon is much higher than thermal energies. Our theoretical researches are focused on the mechanisms and dynamics of photoinduced phase transitions, how they are controlled, and how the photoinduced electron–lattice states are different from those which are realized in thermal equilibrium.[1)]

1. Normal Mode Analysis for Intra- and Inter-Molecular Electron–Phonon Coupled Systems

The ground-state properties of a molecular compound $Et_2Me_2Sb[Pd(dmit)_2]_2$ are theoretically studied, which shows a dimer-Mott character in $Pd(dmit)_2$ layers at high temperature and charge order mainly stabilized by electron–phonon interactions at low temperature. An effective extended Peierls-Hubbard model is constructed with intra- and inter-molecular electronic and phonon degrees of freedom. Using a mean-field approximation, the energies and optimized structures are calculated for isolated neutral, monovalent, divalent $Pd(dmit)_2$ dimers and their two-dimensional crystallized states. The optical conductivities of the latter are calculated by a single configuration interaction method. Through these numerical calculations, model parameters have been evaluated by comparing the theoretical and experimental ground-state properties.

Then, the normal mode analysis is performed for the intradimer C=C stretching vibrations and intradimer intermonomer stretching vibrations. Molecular vibrations with different symmetries are coupled to different combinations of electrons and holes within a molecule, so that their frequencies depend on the molecular charge in different manners. This information is useful to analyze photoinduced transient states, where the relation between their frequencies and the molecular charge is modified from the equilibrium counterpart.

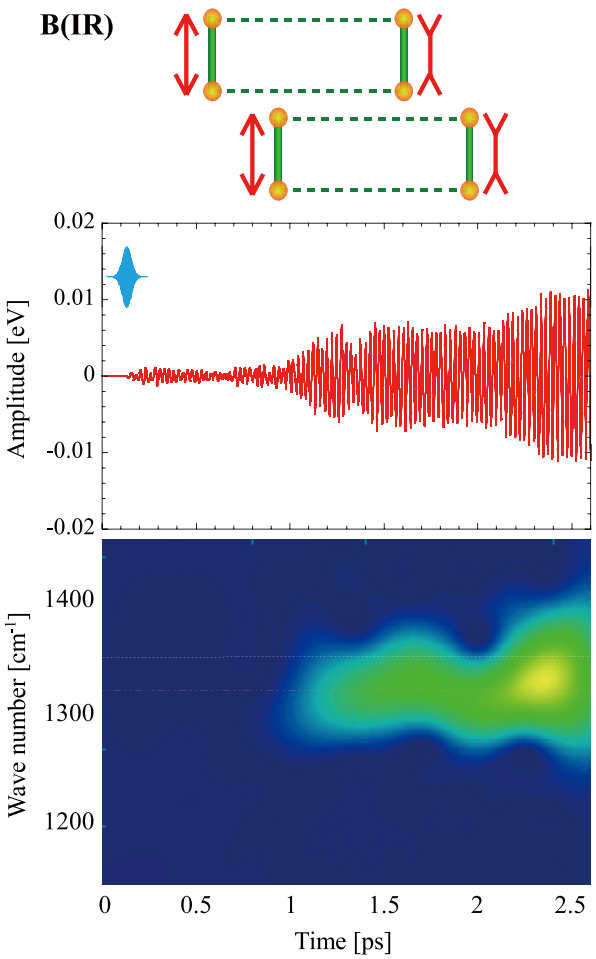

Figure 1. C=C stretching phonon mode B (infrared active) schematically represented in the upper panel. Its time evolution (middle panel) and time-frequency spectrogram (lower panel) on the initially neutral dimer are shown when the charge-separated state is photoexcited.

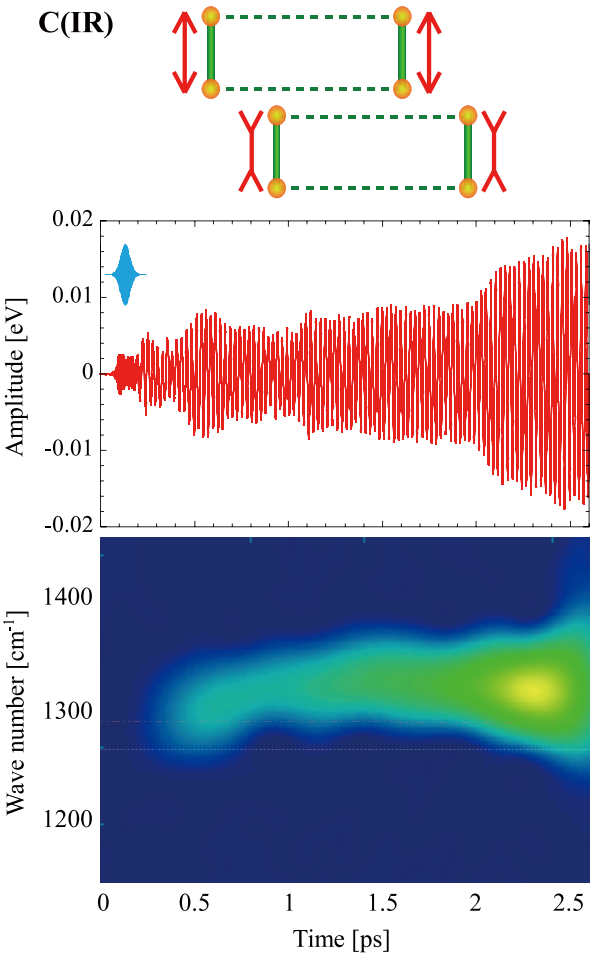

Figure 2. C=C stretching phonon mode C (infrared active) schematically represented in the upper panel. Its time evolution (middle panel) and time-frequency spectrogram (lower panel) on the initially neutral dimer are shown when the charge-separated state is photoexcited.

2. Photoinduced Dynamics in Intra- and Inter-Molecular Electron-Phonon Coupled Systems[2)]

For the photoinduced dynamics in $Et_2Me_2Sb[Pd(dmit)_2]_2$, the time-dependent Schrödinger equation is numerically solved for the Hartree-Fock wave function on the cluster of sixteen dimers (eight sites in each dimer, 128 sites in total). The classical equation of motion is solved for phonons. Photoexcitation is introduced through the Peierls phase in the transfer integrals.

We focus on intradimer C=C stretching vibrations that are infrared active and experimentally observed so far, which are schematically shown in the upper panels of Figures 1 and 2. The middle panels show the time evolution of their amplitudes on the initially neutral dimer when the charge-separated state is photoexcited. The lower panels show their time-frequency spectrograms.

The initially neutral and divalent dimers become monovalent at about 0.5 ps after photoexcitation. After 0.5 or 1 ps, their oscillations are noticeable and sinusoidal. The frequency of the B mode is actually close to that in a monovalent dimer in the equilibrium state. The B mode is coupled with the antibonding-LUMO (electron)–antibonding-HOMO (hole) excitation within the dimer. Their correlation is recovered and becomes close to that in equilibrium after 1 ps.

However, the frequency of the C mode after 1 ps is not close to that in a neutral dimer or that in a monovalent dimer, but it is rather close to the bare frequency (*i.e.*, the frequency if the couplings with electron–hole excitations are turned off) of 1331 cm^{-1}. The C mode is coupled with the antibonding-HOMO (electron)–bonding-HOMO (hole) excitation and the antibonding-LUMO (electron)–bonding-LUMO (hole) excitation within the dimer, so that it is largely softened in equilibrium. Their correlations are largely modified and far from that in equilibrium after 1 ps. This phonon mode appears to oscillate almost independently of electron–hole excitations.

Thus, a usual picture based on the adiabatic potential fails even if phonons are treated classically. The correlation between a phonon and its relevant electron–hole excitation(s) depends on the mode or on the symmetries of the vibrational pattern and the wave functions of electron(s) and hole(s). The analysis of these correlations at an early stage of photoinduced charge-order melting is essential for future manipulation of non-equilibrium phases.

References

1) K. Yonemitsu, *Crystals* **2**, 56–77 (2012).
2) K. Nishioka and K. Yonemitsu, *Phys. Status Solidi C* **9**, 1213–1215 (2012).

* Present Position; Professor, Department of Physics, Faculty of Science and Engineering, Chuo University, 1-13-27 Kasuga, Bunkyo-ku, Tokyo 112-8551
† Present Address; Department of Physics, Faculty of Science and Engineering, Chuo University, 1-13-27 Kasuga, Bunkyo-ku, Tokyo 112-8551
‡ from Hakodate National College of Technology

Theoretical Studies on Condensed Phase Dynamics

Department of Theoretical and Computational Molecular Science
Division of Computational Molecular Science

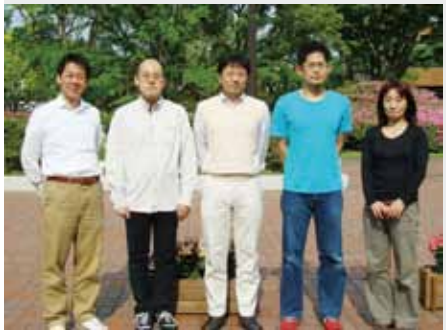

SAITO, Shinji	Professor
KIM, Kang	Assistant Professor
HIGASHI, Masahiro	JSPS Post-Doctoral Fellow
YAGASAKI, Takuma	Post-Doctoral Fellow
IMOTO, Sho	Graduate Student
KAWAGUCHI, Ritsuko	Secretary

Liquids and biological systems show complicated dynamics because of their structural flexibility and dynamical hierarchy. Understanding these complicated dynamics is indispensable to elucidate chemical reactions and relaxation in solutions and functions of proteins. In this year, we investigated ultrafast proton transfer in solution[1)] and dynamics of liquid and supercooled states.[2–5)] In particular, we examined complicated dynamics in terms of nonlinear response functions and multi-time correlation functions.

1. Direct Simulation of Excited-State Intramolecular Proton Transfer and Vibrational Coherence of 10-Hydroxybenzo[*h*]quinoline in Solution[1)]

We investigate an ultrafast excited-state intramolecular proton transfer (ESIPT) reaction and the subsequent coherent vibrational motion of 10-hydroxybenzo-[*h*]quinoline in cyclohexane by the electronically embedded multiconfiguration Shepard interpolation method, which enables us to generate the potential energy surface of the reaction effectively and thus carry out a direct excited-state dynamics simulation with low computational costs. The calculated time scale of the ESIPT and the frequencies and lifetimes of coherent motions are in good agreement with the experimental results. The present study reveals that the coherent motions are caused by not only the proton transfer itself but also the backbone displacement induced by the ESIPT. We also discuss the effects of the solvent on the dynamics of the coherent vibrational modes.

2. Insights in Quantum Dynamical Effects in the Infrared Spectroscopy of Liquid Water from a Semiclassical Study with an *Ab Initio*-Based Flexible and Polarizable Force Field[2)]

The dynamical properties of liquid water play an important role in many processes in Nature. In this paper we focus on the infrared (IR) absorption spectrum of liquid water based on the linearized semiclassical initial value representation (LSC-IVR) with the local Gaussian approximation (LGA) [Liu and Miller, *J. Chem. Phys.* **131**, 074113 (2009)] and an *ab initio* based, flexible, polarizable Thole-type model (TTM3-F) [Fanourgakis and Xantheas, *J. Chem. Phys.* **128**, 074506 (2008)]. Although the LSC-IVR (LGA) gives the exact result for the isolated 3-dimensional shifted harmonic stretching model, it yields a blue-shifted peak position for the more realistic anharmonic stretching potential. By using the short time information of the LSCIVR correlation function, however, it is shown how one can obtain more accurate results for the position of the stretching peak. Due to the physical decay in the condensed phase system, the LSC-IVR (LGA) is a good and practical approximate quantum approach for the IR spectrum of liquid water. The present results offer valuable insight into future attempts to improve the accuracy of the TTM3-F potential or other *ab intio*-based models in reproducing the IR spectrum of liquid water.

3. Energy Relaxation of Intermolecular Motions in Supercooled Water and Ice: A Molecular Dynamics Study[3)]

We investigate the energy relaxation of intermolecular motions in liquid water at temperatures ranging from 220 K to 300 K and in ice at 220 K using molecular dynamics simulations. We employ the recently developed frequency resolved transient kinetic energy analysis, which provides detailed information on energy relaxation in condensed phases like two-color pump-probe spectroscopy. It is shown that the energy cascading in liquid water is characterized by four processes. The temperature dependences of the earlier three processes, the rotational–rotational, rotational–translational, and translational–translational energy transfers, are explained in terms of the density of states of the intermolecular motions. The last process is the slow energy transfer arising from the transitions between potential energy basins caused by the excitation of the low frequency translational motion. This process is absent in ice because the hydrogen bond network rearrangement, which accompanies the interbasin transitions in liquid water, cannot take place in the solid phase. We find that the last process in supercooled water is well approximated by a stretched exponential function. The stretching parameter, β, decreases from 1 to 0.72 with decreasing temperature. This result indicates that the dynamics of liquid water becomes heterogeneous at lower temperatures.

4. Fluctuations and Dynamics of Liquid Water Revealed by Nonlinear Spectroscopy[4)]

Many efforts have been devoted to elucidate the intra- and intermolecular dynamics in liquid water because of its important roles in many fields of science and engineering. Multidimensional nonlinear spectroscopy is a powerful tool to investigate the dynamics. Since nonlinear response functions are described by more than one time variable, it is possible to analyze static and dynamic mode couplings. Here, we review the intra- and intermolecular dynamics of liquid water revealed by recent nonlinear spectroscopic experiments and computer simulations. In particular, we discuss the anharmonic coupling, population relaxation, anisotropy decay, and spectral diffusion of intra- and intermolecular motions of water and their temperature dependence, which play important role in ultrafast dynamics and relaxations in water.

5. Anomalous Temperature Dependence of Isobaric Heat Capacity of Water below 0 °C[5)]

When pure liquid water is cooled below its freezing/melting temperature, it exhibits a number of striking anomalies. Most remarkable among these anomalies is the temperature dependence of the isobaric heat capacity, C_P, that exhibits first a rise, and then a fall, on lowering temperature substantially below 0 °C.[1–4)] In contrast, the isochoric heat capacity, C_V, remains weakly temperature dependent and displays no such anomaly. The reason for this surprisingly large difference is not well understood. To understand this and other anomalies of low temperature water, we examine both *wave number and frequency dependent temperature fluctuation* by long molecular dynamics simulations. Significant differences between constant pressure and constant volume conditions appear below 240 K in the spatio-temporal correlation of temperature fluctuation. Shell-wise decomposition of relative contribution to the temperature fluctuation reveals an increase in contribution from the distant regions, extending even up to the *fifth hydration shell, at low temperatures*, more significant under isobaric than under isochoric conditions. While the temperature fluctuation time correlation function (TFCF) exhibits the expected slow-down with lowering temperature, it shows a rather surprisingly sharp crossover from a markedly fragile to a weakly fragile liquid around 220 K. We establish that this crossover of TFCF (and the related anomalies) arises from a percolation transition in the population of clusters made of liquid-like molecules, defined by coordination number (and consistent with local volumes obtained from Voronoi polyhedra). The disappearance of large liquid-like clusters below 220 K display characteristic features consistent with theory[5)] of percolation. As temperature is further lowered, TFCF exhibits a power law decay and the relaxation time, when fitted to Vogel-Fulcher-Tammann law, reveal a dynamic transition around 160–170 K. Our computed two-dimensional IR and Raman spectra both also signal a dynamical transition around 170 K and additionally carry signatures of the percolation transition at 220 K that could be measured experimentally.

References

1) M. Higashi and S. Saito, *J. Phys. Chem. Lett.* **2**, 2366–2371 (2011).
2) J. Liu, W. H. Miller, G. S. Fanourgakis, S. S. Xantheas, S. Imoto and S. Saito, *J. Chem. Phys.* **135**, 244503 (14 pages) (2011).
3) T. Yagasaki and S. Saito, *J. Chem. Phys.* **135**, 244511 (2011).
4) T. Yagasaki and S. Saito, *Annu. Rev. Phys. Chem.*, submitted.
5) S. Saito, I. Ohmine, and B. Bagchi, submitted.

Theoretical Study on Molecular Excited States and Chemical Reactions

Department of Theoretical and Computational Molecular Science
Division of Computational Molecular Science

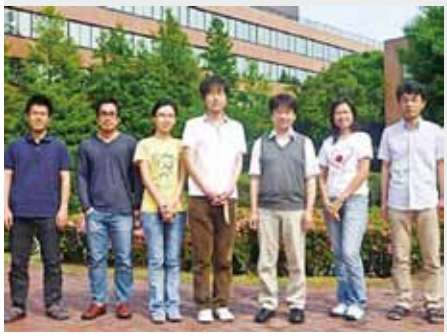

EHARA, Masahiro	Professor
FUKUDA, Ryoichi	Assistant Professor
TASHIRO, Motomichi	IMS Research Assistant Professor
BOBUATONG, Karan	Post-Doctral Fellow*
CHITHONG, Rungtiwa	Visiting Scientist
MAITARAD, Phornphimon	Visiting Scientist
MEEPRASERT, Jittima	Visiting Scientist
HORIKAWA, Takenori	Graduate Student
PROMKATKAEW, Malinee	Graduate Student†
KAWAGUCHI, Ritsuko	Secretary

Molecules in the excited states show characteristic photophysical properties and reactivity. We investigate the molecular excited states and chemical reactions which are relevant in chemistry, physics, and chemical biology with developing the highly accurate electronic structure theory. We are also interested in the excited-state dynamics and energy relaxation so that we also develop the methodology of large-scale quantum dynamics. In this report, we present our recent studies on the development of the CAP/SAC-CI method,[1)] electronic spectra of annulated dinuclear free-base phthalocyanine,[2)] and aerobic oxidation of methanol to formic acid on Au_{20}^- cluster.[3)]

1. Development of CAP/SAC-CI Method for Calculating Resonance States of Metastable Anions[1)]

A "resonance" is an electronically metastable state, that is, a state of an (N+1)-electron system that lies energetically above the ground state of the associated N-electron system and can consequently decay by electron autodetachment. Resonances are intermediates in electron-induced processes and electron-catalyzed reactions. Resonances are part of the continuum and are represented by non-square-integrable (non-L^2) wavefunctions. Computational methods for resonances are thus necessarily combinations of a method to address the continuum nature of the state and a method to address its many-body nature. It is this combination that renders computing the resonance parameters, E_r and τ, of a many-electron system a challenging task.

In this work, we have developed the complex absorbing potential (CAP)/SAC-CI method to investigate resonance states of metastable anions. The method has been implemented in the projected scheme and applied to the π^* resonance state of formaldehyde. The dependence on both valence and diffuse basis sets up to g-function, the number of SAC-CI states in the projection, and the effect of perturbation selection are examined. The potential energy curve and decay width are calculated in the C–O stretching coordinate (Figure 1), and the Franck-Condon factors for transitions from neutral to resonance state are evaluated to interpret the electron transmission (ET) spectrum. (Figure 2)

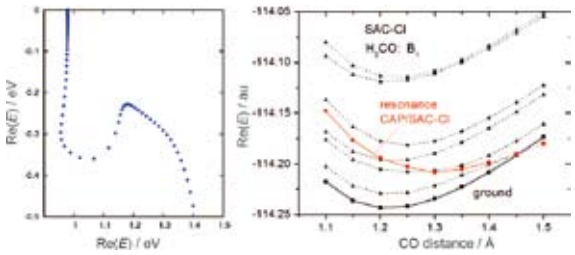

Figure 1. η-trajectory of the $^2B_1$ resonance state of H_2CO (left) and potential energy curves of the ground, electron-attached $^2B_1$ states, and the π^* resonance state by the projected CAP/SAC-CI (right).

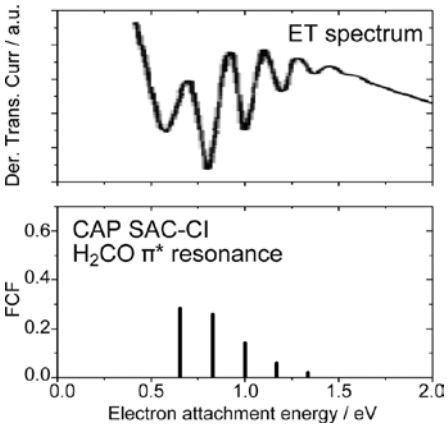

Figure 2. Vibrational structure in π^* resonance of H_2CO by the projected CAP/SAC-CI method compared with the electron transmission spectrum.

2. Electronic Spectra of Annulated Dinuclear Free-Base Phthalocyanines[2)]

There are many applications for organic dyes with strong photoabsorption in the near-IR region, including photo-energy conversion, molecular sensors and devices, and biological

applications. A reliable theory that can treat large conjugated system is urgently required for molecular designs and analysis of the electronic structure of near-IR absorbing materials. The direct SAC-CI method is accurate and efficient for studying large conjugated molecules.

The electronic excited states and electronic absorption spectra of annulated dinuclear free-base phthalocyanine ($C_{58}H_{30}N_{16}$) are studied through quantum chemical calculations using the SAC-CI method. Three tautomers are possible with respect to the position of the pyrrole protons; therefore, the SAC-CI calculations for these tautomers were performed. The lower energy shift of the Q-bands because of dimerization is explained by the decrease in the HOMO–LUMO gaps resulting from the bonding and antibonding interactions between the monomer units. The relative energies of these tautomers are examined using DFT calculations for several peripheral substituents. The relative energies of these tautomers significantly depend on the substituents, and therefore, the abundance ratios of the three tautomers were affected by the substituents. The absorption spectra were simulated from the SAC-CI results weighted by the Boltzmann factors obtained from the DFT calculations. The SAC-CI spectra reproduce the experimental findings well. The thermal-averaged SAC-CI spectra could explain the observed substituent effect on the structure of the Q-bands in terms of the relative stabilities and the abundance ratios of the tautomers.

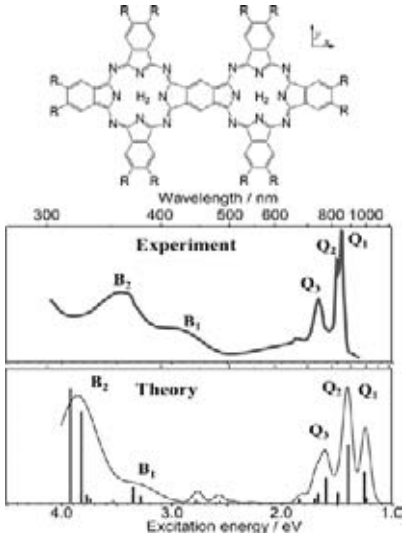

Figure 3. Molecular structure of annulated dinuclear free-base phthalocyanine and its electronic absorption spectra.

3. Aerobic Oxidation of Methanol to Formic Acid on Au_{20}^- Cluster[3)]

During the past two decades, the chemical transformation of hydrocarbons catalyzed by nanometer-sized gold clusters has been of significant interest in industrial and academic research because of its remarkable potential for green chemistry and economic significance Useful and practical reactions with gold catalysts have been extensively developed since the pioneering work of Haruta and co-workers. Among these reactions, aerobic oxidation (oxidation with molecular oxygen) on gold clusters has received special attention because it enables us to perform such reactions at ambient conditions and low temperatures, providing high selectivity to the desired products.

In this work, we investigated the aerobic oxidation of methanol to formic acid catalyzed by Au_{20}^- using density functional theory with the M06 functional. Possible reaction pathways are examined taking account of full structure relaxation of the Au_{20}^- cluster. The proposed reaction mechanism consists of three elementary steps (Figure 4): (1) formation of formaldehyde from methoxy species activated by a superoxo-like anion on the gold cluster; (2) nucleophilic addition by the hydroxyl group of a hydroperoxyl-like complex to formaldehyde resulting in a hemiacetal intermediate; and (3) formation of formic acid by hydrogen transfer from the hemiacetal intermediate to atomic oxygen attached to the gold cluster. A comparison of the computed energetics of various elementary steps indicates that C–H bond dissociation of the methoxy species leading to formation of formaldehyde is the rate-determining step. A possible reaction pathway involving single-step hydrogen abstraction, a concerted mechanism, is also discussed. The stabilities of reactants, intermediates and transition state structures are governed by the coordination number of the gold atoms, charge distribution, cooperative effect and structural distortion, which are the key parameters for understanding the relationship between the structure of the gold cluster and catalytic activity in the aerobic oxidation of alcohol.

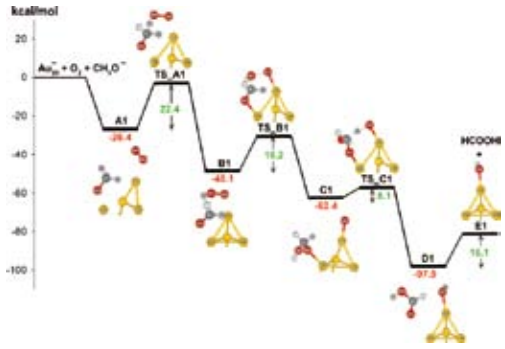

Figure 4. Energy diagram of reaction pathway I in the aerobic oxidation of methanol to formic acid on Au_{20}^- (kcal/mol).

References

1) M. Ehara and T. Sommerfeld, *Chem. Phys. Lett.* **537**, 107–112 (2012).
2) R. Fukuda and M. Ehara, *J. Chem. Phys.* **136**, 114304 (15 pages) (2012).
3) K. Bobuatong, S. Karanjit, R. Fukuda, M. Ehara and H. Sakurai, *Phys. Chem. Chem. Phys.* **14**, 3103–3111 (2012).

* Present Address; Kasetsart University, Bangkok, 10330, Thailand

† carrying out graduate research on Cooperative Education Program of IMS with Kasetsart University

Development of New Algorithms for Molecular Dynamics Simulation and Its Application to Biomolecular Systems

Department of Theoretical and Computational Molecular Science
Division of Computational Molecular Science

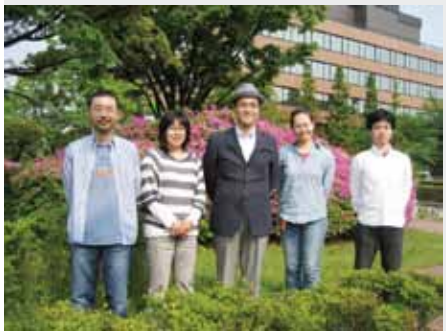

OKUMURA, Hisashi	Associate Professor
ITOH, G. Satoru	Assistant Professor
MORI, Yoshiharu	IMS Research Assistant Professor
NOMURA, Hitomi	Graduate Student*
KAWAGUCHI, Ritsuko	Secretary

In the conventional canonical-ensemble simulations, it is difficult to realize efficient samplings in proteins because the simulations tend to get trapped in a few of many local-minimum states. To overcome these difficulties, we have proposed new generalized-ensemble algorithms, such as multibaric-multithermal algorithm, partial multicanonical algorithm, van der Waals replica exchange method, and Coulomb replica exchange method. It is important to realize efficient samplings in the conformational space and to predict the native structures of proteins. We apply these methods to proteins and peptides.

1. Temperature and Pressure Denaturation of Chignolin: Folding and Unfolding Simulation by Multibaric-Multithermal Molecular Dynamics Method

We performed a multibaric-multithermal molecular dynamics (MD) simulation of a 10-residue protein, chignolin and discussed its folding thermodynamics last year. We further investigated the denaturation mechanisms this year.[1)]

All-atom model for the protein with Amber parm99SB force field were employed in explicit TIP3P water. This MD simulation covered wide ranges of temperature between T = 260~560 K and pressure between P = 0.1~600 MPa and sampled many conformations without getting trapped in local-minimum free-energy states.

Radial distribution function $g(r)$ between the chignolin heavy atoms and the water oxygen atoms, the first peak position of $g(r)$, r_1, the number of hydration water molecules, and the number of hydrophobic contacts were calculated. As the temperature increases, r_1 increases and the number of water molecules around chignolin decreases. It represents that chignolin gains more space to move around and is transferred to a high entropy state, even if it losses potential energy by breaking hydrogen bonds between the protein atoms or between the protein and water. Entropy of the transition state and the unfolded state is higher than the native state. This is the reason why the probabilities of not only the unfolded state such as the extended structure but also the transition state increase as the temperature increases.

On the other hand, the number of hydration water molecules increases with the increasing pressure. There are fewer water molecules near the hydrophobic residues when the protein is folded at the room pressure. As the pressure increases, more water molecules come closer to the hydrophobic residues and the number of hydrophobic contacts decreases. The hydrophobic residues then get separated from one another and the protein is unfolded.

2. Coulomb Replica-Exchange Method: Handling Electrostatic Attractive and Repulsive Forces for Biomolecules

We propose a new type of the Hamiltonian replica-exchange method for molecular dynamics (MD) and Monte Carlo simulations, which we refer to as the Coulomb replica-exchange method. In this method, electrostatic charge parameters in the Coulomb interactions are exchanged among replicas while temperatures are exchanged in the usual replica-exchange method. By varying the atom charges, the Coulomb replica-exchange method overcomes free-energy barriers and realizes more efficient sampling in the conformational space than the

replica-exchange method. Furthermore, this method requires only a smaller number of replicas because only the atom charges of solute molecules are employed as exchanged parameters.

We performed Coulomb replica-exchange MD simulations of an alanine dipeptide in explicit water solvent and compared the results with those of the conventional canonical, replica-exchange, and van der Waals replica-exchange methods. Two force fields of AMBER parm99 and AMBER parm99SB were employed. As a result, the Coulomb replica-exchange method sampled all local-minimum free-energy states more frequently than the other methods for both force fields. Moreover, the Coulomb, van der Waals, and usual replica-exchange methods were applied to a fragment of an amyloid-β peptide (Aβ) in explicit water solvent to compare the sampling efficiency of these methods for a larger system. The Coulomb replica-exchange method sampled structures of the Aβ fragment more efficiently than the other methods. We obtained β-helix, α-helix, 3_{10}-helix, β-hairpin, and β-sheet structures as stable structures and revealed pathways of conformational transitions among these structures from a free-energy landscape, as shown in Figure 1.

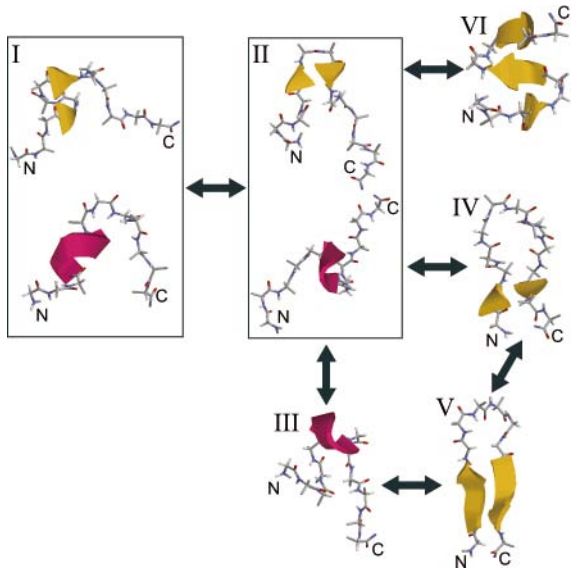

Figure 1. Folding pathways of amyloid-β peptide obtained from Coulomb replica-exchange MD simulations.

3. Replica Exchange Molecular Dynamics Simulation of Chitosan for Drug Delivery System Based on Carbon Nanotube

Chitosan is an important biopolymer in the medical applications because of its excellent biocompatibility. It has been recently highlighted in the targeted drug delivery system (DDS) by improvement of the carbon nanotube (CNT) solubility. To investigate the effect of chitosan length, the two targeted DDSs with 30 and 60 chitosan monomers were performed by replica-exchange molecular dynamics simulations at temperatures in the range of 300–455 K. Each DDS model contains the epidermal growth factor (EGF), chitosan (CS) of 30 (30CS) and 60 (60CS) monomers, single-wall CNT (SWCNT) and gemcitabine (Gemzar) as the model payload anticancer drug, called EGF/30CS/ SWCNT/Gemzar and EGF/60CS/SWCNT/Gemzar, respectively. The SWCNT confines gemcitabine inside its cavity, while the outer surface is wrapped by chitosan in which one end is linked to the EGF. The results showed that in the EGF/30CS/SWCNT/Gemzar DDS the 30CS chain was not long enough to wrap around the SWCNT, and consequently the EGF was located so close to the tube as to potentially cause steric inhibition of the binding of EGF to its receptor (EGFR), which is highly expressed on the surface of cancer cells. On the other hand, this phenomenon is not observed in the EGF/60CS/SWCNT/Gemzar DDS in which the 60CS was found to completely wrap over the CNT outer surface using only 50 chitosan units. Although an increase in the temperature is likely to influence the overall DDS structure, and especially the orbit of helical chitosan on the SWCNT and the EGF conformation, gemcitabine is still encapsulated inside the tube.

4. Monte Carlo Simulation for Isotropic–Nematic Phase Transition of Infinitely Thin Liquid Crystal Molecules

We are also interested in isotropic–nematic phase transition of liquid crystal molecules. We gave a criterion to test a non-biaxial behavior of infinitely thin hard platelets based upon the components of three order parameter tensors. We investigated the nematic behavior of monodisperse infinitely thin rectangular hard platelet systems by this criterion. Starting with a square platelet system, and we compared it with rectangular platelet systems of various aspect ratios. For each system, we performed equilibration runs by using isobaric Monte Carlo simulations. Each system did not show a biaxial nematic behavior but a uniaxial nematic one, despite of the shape anisotropy of those platelets. The relationship between effective diameters by simulations and theoretical effective diameters of these systems was also determined.

Reference

1) H. Okumura, *Proteins: Struct., Funct., Bioinf.* **80**, 2397–2416 (2012).

* carrying out graduate research on Cooperative Education Program of IMS with Yamagata University

Ultimate Quantum Measurements for Quantum Dynamics

Department of Theoretical and Computational Molecular Science
Division of Theoretical and Computational Molecular Science

SHIKANO, Yutaka — Research Associate Professor (Feb., 2012–)
NAKANE, Junko — Secretary

Due to great development on experimental technologies, it is possible to capture quantum dynamics in some physical and chemical systems. On the other hand, all experiments are in principle open and dissipative systems. Up to now, the well-explained experiments are approximated to the equilibrium situation. However, by recent technological development, some experiments reach to a transition from equilibrium to non-equilibrium situations. While there are the well-known tools on the non-equilibrium situations; the linear response theory and the Keldysh Green function method, this analysis cannot basically catch dynamical situations. Our goal is to construct the time-resolved theoretical models included the non-equilibrium situations. However, the quantum measurement theory is needed on measuring quantum dynamics, especially considering the measurement backaction. Our current activities are to resolve how sensitive (quantum) measurement can we carry out in principle, to build up some toy models on quantum dynamic, and to explain photo-luminescence phenomenon in nitrogen vacancy center in diamond.

1. Quantum Measurement Sensitivity without Squeezing Technique[1)]

As alluded before, our aim is to capture quantum dynamical phenomena. Capturing some phenomena needs to carry out the measurement. The conventional quantum measurement technique has huge measurement backaction. The measurement backaction prevents us chasing quantum dynamics like the classical trajectory. On the other hand, reducing the measurement backaction needs the tiny coupling between the target and probe quantum systems. However, under this situation, the signal in the probe system is also tiny small, that is, it is difficult to capture information. To resolve this problem, the squeezing technique was proposed and was experimentally implemented. However, this technique is practically difficult to be implemented. Our proposal is to use the weak measurement initiated by Aharonov, Albert, and Vaidman without squeezing technique. The profound meaning and interpretation of the weak measurement is seen in the review paper.[2)] The key of this method is to take the post-selection of the target system. Due to this effect, tiny probe signal can be amplified. In the original proposal by Aharonov, Albert, and Vaidman, the amplification factor is infinite by the approximation method. However, the effect measurement backaction is simultaneously amplified. When the probe state is Gaussian to be used in the original proposal, we have analytically shown the upper bound of the amplification factor. We have analytically derived the probe state to maximally amplify the signal by the variational method.[1)] By this optimal probe state, the amplification factor has no upper bound. Our result tells us the infinitely amplified single under the known coupling between the target and the probe. However, this result is ignored to consider the noise. We will extend our result to the signal-to-noise ratio optimization. Also, we are collaborating with the experiments to amplify the signal and consider the applications; the gravitational wave detector.

2. Discrete Time Quantum Walk as Quantum Dynamical Simulator[3)]

The discrete time quantum walk is defined as a quantum mechanical analogue of the classical random walk but is not the quantization of the classical random walk. This mathemati-

cal description is very simple but leads to many quantum dynamical phenomena. This is a toy model to better understand the quantum dynamics. Also, this has recently been various experimental demonstrations in the ultracold atoms in the optical lattice, trapped ions, and optical systems. We have analytically shown that the one- and two-dimensional discrete time quantum walks can be taken as the quantum dynamical simulator,[3] which concept is to emulate some classes of the differential equations, for example, the Dirac equation. Our approximation is used from the discrete lattice to continuous line for the large time steps of the discrete time quantum walk. This mathematical treatment is so powerful like the relationship between the cellular automaton and the integrable system.

3. Photoluminescence Phenomenon from Solid-State System[4]

A method to measure some physical properties by light is widely used in physical, chemical, and biological systems. Therefore, laser science has been developed along with our demands from science and technology. A single photon source is expected as the low power laser source and the quantum communication tool. A nitrogen vacancy center in diamond and a quantum dot in a semiconductor system are the promising candidate of the single photon source. Especially, a nitrogen vacancy center in diamond has been attracted since this is run at room temperature. For an application as the highly controlled photon source, the photoluminescence process in the nitrogen vacancy center in diamond needs to be well understood. This system has the $S = 1$ electronic spin with the hyperfine structure 2.87 GHz. Furthermore, inserting a magnetic field, the different magnetic states are separated due to the Zeeman shift. Since this electronic spin is highly localized, the local magnetic field evaluation is needed. We have shown the method to evaluate the local magnetic field from the conventional confocal microscopy.[4] Also, the nitrogen vacancy center in diamond is a candidate of the quantum memory. Since a lifetime of the nuclear spin of a ^{13}C atom nearly located in the nitrogen vacancy spot is long (~ sec order), the perfect quantum state transfer is needed. However, it is difficult to evaluate the location of the ^{13}C atom. On the other word, it is difficult to evaluate the coupling constant between the electronic spin of the nitrogen vacancy center and the nuclear spin of the ^{13}C atom. We have proposed the simple scheme to evaluate the coupling constant between the two spins system under the dissipative situation.[5] As the next step, we will study the photoluminescence process from the nitrogen vacancy center in diamond.

As the current activities of our laboratory, we are studying the photoluminescence processes of the quantum dots and the exciton-polariton Bose-Einstein condensations in the two dimensional electronic gas of the semiconductor. These materials are expected to be used as the classical optical devices; the optical switching, collaborated with the various experimentalists.

References

1) Y. Susa, Y. Shikano and A. Hosoya, *Phys. Rev. A* **85**. 052110 (2012).

2) Y. Shikano, *Time in Weak Value and Discrete Time Quantum Walk*, LAP Lambert; Germany (2012).

3) K. Chisaki, N. Konno, E. Segawa and Y. Shikano, *Quant. Infor. Comput.* **11**, 0741–0760 (2011).

4) S. Kagami, Y. Shikano and K. Asahi, *Phys. E* **43**, 761–765 (2011).

5) Y. Shikano and S. Tanaka, *Europhys. Lett.* **96**, 40002 (2011).

Theoretical Studies of Chemical Dynamics in Condensed and Biomolecular Systems

Department of Theoretical and Computational Molecular Science
Division of Theoretical and Computational Molecular Science

ISHIZAKI, Akihito — Research Associate Professor (March, 2012–)
YAMADA, Mariko — Secretary

Photosynthesis provides the energy source for essentially all living things on Earth, and its functionality has been one of the most fascinating mysteries of life. Photosynthetic conversion of the energy of sunlight into its chemical form suitable for cellular processes involves a variety of physicochemical mechanisms. The conversion starts with the absorption of a photon of sunlight by one of the light-harvesting pigments, followed by transfer of electronic excitation energy to the reaction center, where charge separation is initiated. At low light intensities, surprisingly, the quantum efficiency of the transfer is near unity. A longstanding question in photosynthesis has been the following: *How does light harvesting deliver such high efficiency in the presence of disordered and fluctuating dissipative environments? Why does not energy get lost?* At high light intensities, on the other hand, the reaction center is protected by regulation mechanisms that lead to quenching of excess excitation energy in light harvesting proteins. The precise mechanisms of these initial steps of photosynthesis are not yet fully elucidated from the standpoint of molecular science.

1. Electronic Excitation Transfer Dynamics in Light Harvesting Systems

Recently, the technique of two-dimensional electronic spectroscopy has been applied to explore photosynthetic light harvesting complexes. The observation of long-lived quantum superposition or coherence between eigenstates of electronic excitations (excitons) in a pigment-protein complex stimulated a huge burst of activity among experimentalists and theorists. Much of the interest arose because the finding of electronic quantum coherence is a “warm, wet, and noisy” biological system was considered very surprising. The initial experiments were carried out at 77 K, but more recent studies have detected coherence lasting at least 300 fs at physiological temperatures. These observations have led to the suggestion that electronic quantum coherence might play a role in achieving the remarkable efficiency of photosynthetic light harvesting. At the same time, the observations have raised questions regarding the role of the surrounding protein in protecting the coherence. In order to elucidate origins of the long-lived electronic coherence and its interplay with the protein environment, we have investigated appropriate theoretical frameworks and concepts with the use of statistical mechanics[1)] and in cooperation with experiment.[2)]

In particular, we have discussed significance of the finite timescale site-dependent reorganization dynamics of the protein environment surrounding (bacterio)chlorophyll molecules. The electronic coupling $\hbar J$ between pigments and the excitation-environment coupling characterized by the reorganization energy $\hbar\lambda$ are two fundamental interaction mechanisms determining the nature of electronic energy transfer (EET) in photosynthetic complexes. Ordinarily, photosynthetic EET is discussed only in terms of the mutual relation between magnitudes of the two couplings, as just described. However, the nature of EET also depends on the mutual relation between two timescales, the characteristic timescale of the environmental reorganization, τ (Figure 1), and the inverse of the electronic coupling, J^{-1}, that is the time the excitation needs to move from one pigment to another neglecting any additional perturbations. We showed that even in the region of reorganization energy much larger than that of a typical situation of photosynthetic light harvesting the sluggish reorganization

dynamics allows the excitation to stay above an energy barrier separating two local minima, which correspond to the two sites in the adiabatic potential surface, for a prolonged time (Figure 2). This is an essential origin of the experimentally observed long-lived electronic coherence.

Further, we showed this energy barrier is much small in comparison with the thermal energy k_BT (almost activationless) in the parameter regime corresponding to natural light harvesting systems. It can be considered that natural photosynthetic light harvesting systems avoid local trapping of electronic excitations, which yields a situation that electronic excitation energy gets lost in in the presence of disordered and fluctuating dissipative environments. By extending this argument, we are now tackling the above questions regarding the remarkable quantum efficiency and smart regulation mechanism that photosynthetic light harvesting systems exhibit.

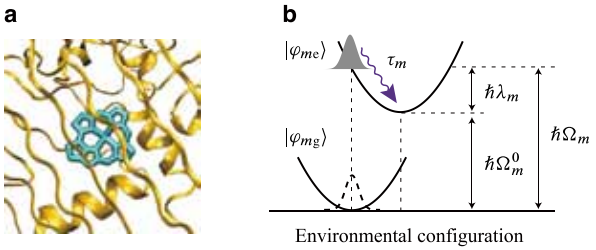

Figure 1. Schematic illustration of the *m*th pigment embedded in a protein (*a*) and the electronic ground and excited states of the *m*th pigment, $|\varphi_{mg}\rangle$ and $|\varphi_{me}\rangle$, affected by nuclear motion of the protein environment (*b*). After electronic excitation in accordance with the vertical Franck-Condon transition, reorganization takes place from the equilibrium nuclear configuration with respect to the electronic ground state $|\varphi_{mg}\rangle$ to the actual equilibrium configuration in the excited state $|\varphi_{me}\rangle$ with dissipation of the reorganization energy, $\hbar\lambda_m$. This reorganization of the protein environment proceeds on a characteristic timescale, τ_m.

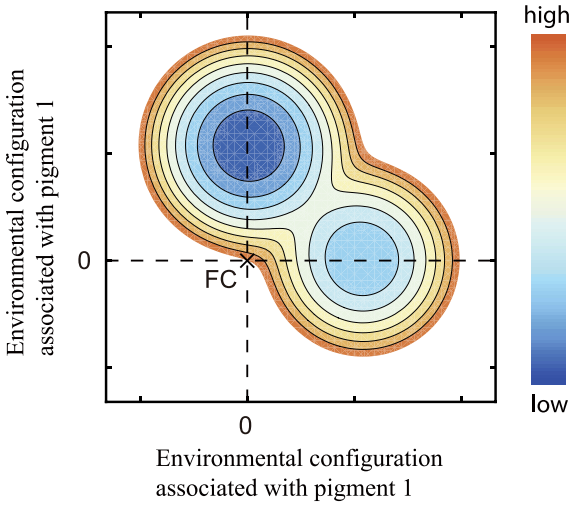

Figure 2. Schematic illustration of adiabatic excitonic potential surface of coupled two pigments. The point of origin corresponds to the Franck-Condon state. The energy of the point is higher than the barrier between the minima; therefore, we find that the electronic excited state is delocalized just after the excitation. As time increases, the dissipation of reorganization energy proceeds and the excitation will fall off into one of the minima and become localized. Namely, sluggish dissipation of reorganization energy increases the time an electronic excitation stays above an energy barrier separating pigments and thus prolongs delocalization over the pigments.

References

1) A. Ishizaki and G. R. Fleming, *Annu. Rev. Condens. Matter Phys.* **3**. 333–361 (2012).

2) G. S. Schlau-Cohen, A. Ishizaki, T. R Calhoun, N. S. Ginsberg, M. Ballottari, R. Bassi and G. R. Fleming, *Nat. Chem.* **4**, 389–395 (2012).

3) Y.-C. Cheng and A. Ishizaki, *J. Chem. Phys.* (invited), to appear.

Award

ISHIZAKI, Akihito; Short-term Fellowship at Wissenschaftskolleg zu Berlin, 2012/2013.

Theory and Computation of Reactions and Properties in Solutions and Liquids

Department of Theoretical and Computational Molecular Science
Division of Computational Molecular Science

ISHIDA, Tateki Assistant Professor

We focus on the projects both on ultrafast photoinduced electron energy transfer in the excited state in solution and on ionic liquids (ILs). The project on photoinduced electron energy transfer processes in the excited state in solution focuses on the development of a theoretical method to describe electron energy transfer including solvent motion and dynamics with the theoretical treatment we have developed. On the other hand, ILs' projects concentrate the study of specific interionic dynamics in ILs and the investigation of a new perspective on the physically and chemically unique characteristics of ILs.

1. The Theoretical Study of Photoinduced Electron Energy Transfer Processes in the Excited State in Solution

We have developed a procedure for describing the time-dependent evolution of the electronic structure of a solute molecule in solution, coupling an electronic structure theory with solvent motion in the formalism of an interaction site model. We extend this prescription for studying electron energy transfer processes in the excited state in solution. It is indicated that the coupling between solvation dynamics and a fast intramolecular electron energy transfer is likely to play an important role in the emergence of photoinduced unique functionalities in biochemical and metal complex systems.

2. The Unique Physical and Chemical Properties of Ionic Liquids through Interionic Interactions: Theoretical Investigation with Molecular Dynamics Simulations[1)]

Ionic liquids (ILs) have been found to possess a wide potential variety of interesting physical and chemical properties. We consider the unique properties of ILs which owe to the specific interionic interaction between ionic species. In particular, we study the importance of both the cross-correlation between cation and anion species, and the effect of polarization in ILs. On the basis of recent theoretical studies on ILs employing molecular dynamics simulations, how the collective dynamics through interionic interactions cause the unique physical and chemical properties of ILs and how electronic polarizability effects modify interionic dynamics have been investigated. Those include the investigation of the contribution of ionic motions with velocity cross-correlation functions and the study of many-body polarization effects on the cage effect in ILs.

3. Investigations of New Perspectives on the Characteristics of Ionic Liquids: Microscopic Aspects in Dicationic Ionic Liquids[2)]

The interionic vibrations in imidazolium-based dicationic ionic liquids (ILs) containing the bis(trifluoromethylsulfonyl)-amide ($[NTf_2]^-$) counteranion were investigated using femtosecond optical-heterodyne-detected Raman-induced Kerr effect spectroscopy. The microscopic nature of the dicationic ILs ($[C_n(MIm)_2][NTf_2]_2$, where n = 6, 10, and 12; MIm = *N*-methylimidazolium) was compared with that of the corresponding monocationic ILs ($[C_nMIm][NTf_2]$, where n = 3, 5, and 6) used as reference samples. Low-frequency Kerr spectra within the frequency range 0–200 cm^{-1} of the ILs revealed that the spectral profile of the dicationic ILs as well as that of the corresponding monocationic ILs is bimodal. The distinguished line-shape of the low-frequency Kerr spectrum of $[C_3MIm][NTf_2]$ from the other ILs can be accounted for by the homogeneous nature in the microstructure of the IL, but the other ILs indicate microsegregation structures due to the longer nonpolar alkylene linker or alkyl group in the cations.

References

1) T. Ishida, in *Handbook of Ionic Liquids: Properties, Applications and Hazards*, J. Mun and H.Sim, Eds., Nova Science Publishers Inc.; Hauppauge, NY, pp. 395–417 (2012).
2) H. Shirota and T. Ishida, *J. Phys. Chem. B* **115**, 10860–10870 (2011).

Visiting Professors

Visiting Associate Professor
HASEGAWA, Jun-ya *(from Kyoto University)*

Quantum Chemistry for the Excited States of Functional Molecules in Proteins and Solutions

Molecular interactions between chromophore and environment are the essential to furnish a protein with the photo-functionality. I am interested in the machinery of the photo-functions such as photo-synthesis, vision, and bioluminescence. To understand the mechanism and to develop chemical concept behind the photo-functions, we develop electronic structure theories for excited state, analytical method for excitation-energy transfer pathway, and a hybrid quantum-mechanics/molecular mechanics method. In recent studies, we have clarified color-tuning mechanism of photo-functional proteins and excitation transfer mechanism of bridge-mediated donor-acceptor systems. We are also interested in developing a configuration interaction picture for the solvatochromic response of the molecular environment.

Visiting Associate Professor
ANDO, Koji *(from Kyoto University)*

Quantum Transfer Processes in Chemical and Biological Systems

At the core of chemistry and biochemistry are reduction-oxidation and acid-base reactions, whose elementary processes are electron and proton transfers. Our research group has been working on theoretical and computational modeling of these inherently quantum dynamical processes. One recent achievement is a development of electron transfer (ET) pathway analysis method with use of fragment molecular orbital calculations, by which the ETs in a bacterial photosynthetic reaction center have been studied. Another is a development of nuclear wave packet molecular dynamics simulation method and its applications to hydrogen-bond exchange dynamics in water. It has been also discovered that the latter can be extended to electron wave packet simulations by exploiting the non-orthogonal valence-bond theory, which anticipates a non-Born-Oppenheimer electron–nuclear dynamical treatment.

Visiting Associate Professor
MORISHITA, Tetsuya *(from AIST)*

First-Principles Molecular-Dynamics Simulations of Liquids and Glassy Materials

I have been interested in structural and dynamical properties of non-crystalline materials including nanoscale materials. In 2011, I have found that liquid silicon exhibits compressed exponential relaxation over a wide temperature range including the supercooled regime, in contrast to water and other glass-forming liquids, using first-principles molecular-dynamics simulations.

I have also developed a new method for free-energy calculation, Logarithmic Mean-Force Dynamics (LogMFD). This method was successfully applied to reconstruction of the free-energy profile of a dipeptide molecule, showing that LogMFD considerably outperforms conventional free-energy calculation methods such as thermodynamics integration.

RESEARCH ACTIVITIES

RESEARCH ACTIVITIES

Photo-Molecular Science

We study the interaction between molecules and optical fields with its possible applications to active control of molecular functionality and reactivity. We also develop novel light sources to promote those studies. Two research facilities, the Laser Research Center for Molecular Science and the UVSOR, closely collaborate with the Department.

The core topics of the Department include ultrahigh-precision coherent control of gas- and condensed-phase molecules, high-resolution optical microscopy applied to nanomaterials, synchrotron-based spectroscopy of core-excited molecules and solid-state materials, vacuum-UV photochemistry, and the development of novel laser- and synchrotron-radiation sources.

Development of Advanced Near-Field Spectroscopy and Application to Nanometric Systems

Department of Photo-Molecular Science
Division of Photo-Molecular Science I

OKAMOTO, Hiromi	Professor
NARUSHIMA, Tetsuya	Assistant Professor
NISHIYAMA, Yoshio	IMS Research Assistant Professor
KOWAKA, Yasuyuki	Post-Doctoral Fellow
WU, Huijun	Graduate Student (–March, 2012) Technical Fellow (April, 2012–)
HASHIYADA, Shun	Graduate Student
OCHIAI, Takao	Graduate Student*
ISHIKAWA, Akiko	Technical Fellow
NOMURA, Emiko	Secretary
YAMASAKI, Yumi	Secretary

There is much demand for the study of local optical properties of molecular assemblies and materials, to understand nanoscale physical and chemical phenomena and/or to construct nanoscale optoelectronic devices. Scanning near-field optical microscopy (SNOM) is an imaging method that enables spatial resolution beyond the diffraction limit of light. Combination of this technique with various advanced spectroscopic methods may offer a direct probe for dynamics in nanomaterials and nanoscale functionalities. It may provide essential and basic knowledge to analyze origins of characteristic features of the nanomaterial systems. We have constructed apparatuses of near-field spectroscopy and microscopy for excited-state studies of nanomaterials, with the feasibilities of nonlinear and time-resolved measurements. The developed apparatuses enable near-field measurements of two-photon induced emission and femtosecond time-resolved signals, in addition to conventional transmission, emission, and Raman scattering. Based on these methods, we are investigating the characteristic spatiotemporal behaviors of various metal-nanoparticle systems and molecular assemblies.

1. Visualization of Localized Optical Fields and Plasmon Wavefunctions in Metal Nanostructures

We recently reported that wavefunctions of localized plasmon resonances of chemically synthesized metal (Au and Ag) nanoparticles are visualized by near-field transmission or two-photon excitation measurements.[1)] The same methods were also applied to Au nanoparticle assemblies to visualize confined optical fields.[1)] It was revealed for the Au nanoparticle dimers that highly localized optical field is generated at the interstitial sites between the particles. In many-particle assemblies, the localized fields were especially intensified at the rim parts of the assemblies, and such a characteristic field distribution has been attributed to interaction between plasmon excitations induced on the particles. We also observed confined optical fields in gaps between circular apertures opened on thin gold films.

We are extending the studies to various two-dimensional metal nanostructures manufactured by the electron-beam lithography technique, in part as collaboration with researchers of other institution, with which structures that are difficult to obtain with the chemical methods can be available. The nanostructures now under study are circular Au nanodisks, assembled Au nanodisks with designed arrangements, elongated rectangular nanoapertures opened on Au thin films, and so forth. Such a study is essential as a basis for designing unique optical properties and functions of metal nanostructures.

2. Studies of Metal-Nanostructure Modified Photovoltaic Cells by Near-Field Excited Site-Specific Photocurrent Detection

Metal nanoparticles and their assemblies collect photon energies to yield confined and enhanced optical fields in the vicinities of the particles due to plasmon resonances. Recently, it has been reported that efficiencies of photoenergy conversion can be improved by the use of noble metal nanostructures. The photoenergy conversion system ranges from wet-type and solid-state photo-current conversion cells to photo-chemical conversion systems. To reveal the mechanism of the enhanced photoenergy conversion process, studies of detailed nanostructures and site-dependent photocurrent measurements are essential.

We applied SNOM to clarify effects of surface plasmon resonance on photo-current conversion in GaAs semiconductor cells modified with Au nanoparticles, by photocurrent imaging measurements with localized near-field photoirradiation (Figure 1).[2)] Isolated nanospheres caused local photocurrent sup-

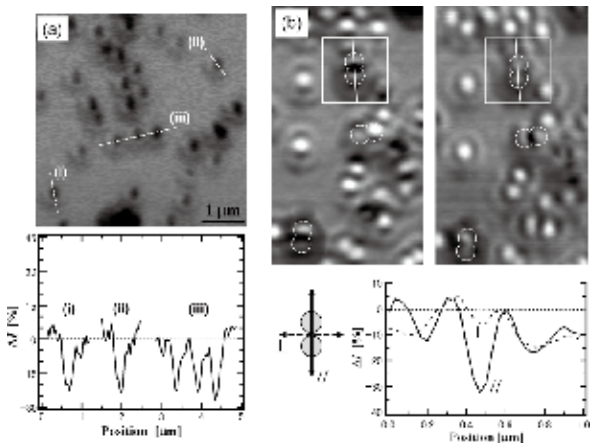

Figure 1. Near-field photocurrent images for GaAs photodiode modified with Au spherical nanoparticles. (a) Phorocurrent image at 532 nm for isolated particles (top) and line profiles along the dashed lines in the image (bottom). (b) Photocurrent images at 785 nm for dimeric particles (top; dimers are indicated with white circles; vertical and horizontal polarizations for left and right images, respectively) and line profiles along the white lines in the image for respective polarization directions (bottom).

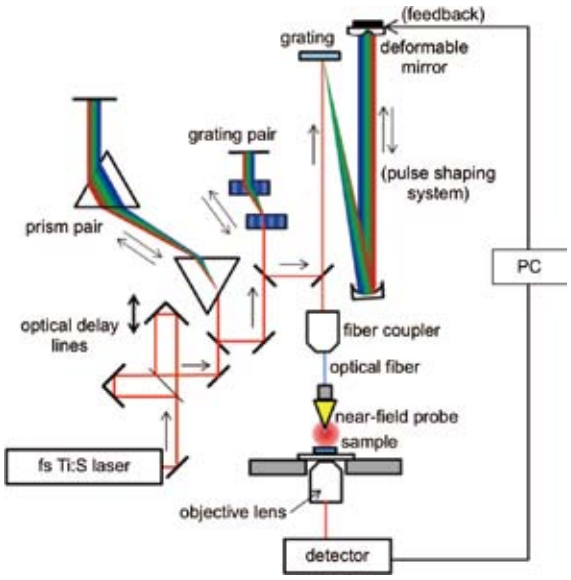

Figure 2. Experimental setup of sub-20-fs ultrafast near-field measurement.

pressions at the plasmon resonance wavelengths (~530 nm). In assemblies (dimers and trimers) of the spheres, a remarkable decrease of photocurrent at the gap site between the spheres was observed at ~800 nm near the dimer plasmon resonance, despite anticipated field enhancements in the gap sites. From the results, it is concluded that the enhanced optical fields induced by the plasmons do not improve the photovoltaic efficiency. The far-field forward scattering of photons by the gold nanoparticles may be more important than the enhanced field effects for the GaAs photovoltaic device studied.

3. Construction of Apparatuses for Sub-20-fs Ultrafast Near-Field Spectroscopy

Surface plasmons of noble metal nanoparticles have very short lifetimes in the range of ~2–20 fs. To achieve a SNOM observation of such fast dynamics in the individual nanoparticles, we have to overcome serious dispersion effects arising from the optical components involved, especially from the optical fiber. We achieved that by combining the conventional dispersion compensation devices composed of prism and grating pairs with adaptive pulse shaping technique, and succeeded in delivering 17-fs pulses to the the near-field aperture with a spatial resolution of ~100 nm.[3)]

The layout of the experimental setup is shown in Figure 2. A pair of transmission gratings and an SF14 prism pair were adopted to precompensate for the second- and third-order group velocity dispersion effects. The beam was then sent to adaptive pulse shaping system equipped with a deformable mirror, whose surface shape was adjusted to yield a shortest pulse duration at the probe tip using a genetic algorithm. The laser beam was then coupled to a 150-mm-long optical fiber to introduce the light into the apertured near-field probe tip. We used time-correlated two-photon-induced photoluminescence (TPI-PL) measurements to demonstrate the performance of the system. The light pulses were incident on a gold nanostructure sample through the near-field probe to excite the TPI-PL from Au, whose intensity was recorded as a function of the pump–probe delay time. With this setup we succeeded in measuring dephasing of ~10 fs in Au nanostructures. Position dependent dephasing measurements for Au nanostructures are now under way.

4. Near-Field Circular Dichroism Microscopy of Nanomaterials

Circular dichroism (CD) spectroscopy is widely used in the studies of chiral materials and magnetism. Some of nanomaterials composed of achiral molecules are reported to show CD activities arising from the nanoscale chirality. Two-dimensionally chiral metal nanostructures also show CD activities. Investigation of nanoscale local CD may provide valuable information on the origins of CD activities of such materials. For this purpose, we are developing an apparatus for near-field CD microscopy and measuring CD images of nanoscale chiral materials.

References

1) H. Okamoto and K. Imura, *Prog. Surf. Sci.* **84**, 199–229 (2009).
2) Y. Harada, K. Imura, H. Okamoto, Y. Nishijima, K. Ueno and H. Misawa, *J. Appl. Phys.* **110**, 104306 (2011).
3) H. J. Wu, Y. Nishiyama, T. Narushima, K. Imura and H. Okamoto *Appl. Phys. Express* **5**, 062002 (2012).

* carrying out graduate research on Cooperative Education Program of IMS with University of Tsukuba

Design and Reconstruction of Molecular Quantum States of Motion

Department of Photo-Molecular Science
Division of Photo-Molecular Science I

OHSHIMA, Yasuhiro	Professor
MIZUSE, Kenta	Assistant Professor
FUJIWARA, Masanori	IMS Research Assistant Professor
HAYASHI, Masato	Post-Doctoral Fellow
MIYAKE, Shinichiro	Graduate Student
INAGAKI, Itsuko	Secretary

Molecules are vital existence. In a gas-phase ensemble at room temperature, they are, in an average, flying away by a few hundred meters, making turns almost reaching to 10^{11} times, and shaking themselves more than 10^{13} times within the duration of only one second. The ultimate goal this research group has been aiming to is to capture the lively figures of molecules moving in such a dynamic manner and to have a perfect command over the molecular motions. Here lasers with ultimate resolution in time and energy domains are employed complementally and cooperatively for this purpose.

1. Nonadiabatic Excitation of Molecular Rotation Induced by Intense Ultrashort Laser Fields

When a gaseous molecular sample is irradiated by an intense nonresonant ultrashort laser pulse, the laser field exerts a torque that aligns the molecular axis along the laser polarization vector, due to the interaction with the molecular anisotropic polarizability. Here the field–matter interaction only remains in much shorter duration than the characteristic time for molecular rotation, and thus the rotation of the molecules is coherently excited to create a rotational quantum wave packet (WP). We have developed a method to explore the nonadiabatic excitation in a quantum-state resolved manner and applied it to diatomic and symmetric-top molecules.[1)] It has been shown that the state distribution is a useful experimental source for verifying the excitation process.[2,3)] When a pair of excitation pulses is implemented with appropriate time delay between them, partial control of rotational-state distribution has been achieved.[1,4)] In a favorable case, the double-pulse excitation coupled with the state-selective probe has enabled us to reconstruct experimentally a rotational WP thus created.[5)] If the mutual polarization direction and time delay between the two pulses are adjusted, the sense of rotation around the laser propagation direction can also be controlled, yielding to a rotational WP exhibiting angular-momentum orientation.[6,7)]

2. Coherent Excitation of Intermolecular Vibrations in Molecular Clusters by Nonresonant Intense Ultrashort Laser Fields

Nonadiabatic interaction with a nonresonant intense ultrashort laser field can also coherently excite vibration of molecule through the structural dependence of the molecular polarizability. We have recently succeeded in creating and observing WPs pertinent to intermolecular vibrations of several molecular clusters in their electronic ground states. So far, NO–Ar, benzene dimer and trimer have been studied. Here, vibrational distribution after nonadiabatic vibrational excitation (NAVEX) is probed in a quantum-state resolved manner. By monitoring the resonant two-photon ionization (R2PI) spectra, substantial decrease of the transition from the vibrationally ground state has been clearly observed when the femtosecond (fs) pump pulse was applied, and in the case of NO–Ar, the observation was accompanied with the emergence of several hot bands, assigned to those from vibrationally excited states pertinent to intermolecular modes. The double fs pulse excitation has also been implemented for examining the real-time quantum interference of the WPs. The observed time-domain signals for NO–Ar were directly compared with the calculation on the WP propagation by numerically solving the time-dependent Schrödinger equation on the intermolecular potential energy surface. For more detailed examination of the NAVEX process and further application to various molecular cluster systems, we are now renovating the experimental setup, in particular, the molecular beam time-of-flight mass spectrometry (TOF-MS) apparatus. The modification includes: Improvement of mass resolution by extending the TOF flight tube, rejection of the interference of strong monomer signals by implementing a mass gate, and realization of more extensive cooling by enlarging the vacuum pumping capabilities.

3. High-Resolution Laser Spectroscopy of Benzene Clusters with Atoms and Small Molecules

Molecular clusters containing benzene are prototypical systems for elucidating the intermolecular interaction pertinent to aromatic rings. The information on the precise cluster geometry and energy-level structure pertinent to the intermolecular vibration are useful experimental input to reconstruct the intermolecular potential energy surface. We are now focusing on clusters of benzene attached by small numbers of atoms and molecules. So far, electronic spectra of C_6H_6 complexed with one and two He atom(s), two Ar atoms, up to three H_2 molecules, and one H_2O molecule have been examined via two-color R2PI in the vicinity of the monomer S_1–S_0 6_0^1 band. We employed a tripled output from a ns pulsed dye amplifier, which was injection-seeded by the CW output from a Ti:Sapphire laser, as an excitation source. Owing to the narrow band width (~250 MHz) of the laser system and the efficient rotational cooling down to 0.3 K by implementing a high-pressure pulsed valve, rotational structures have been greatly simplified.

Structural parameters of the clusters with He have been substantially refined than those reported previously.[8] The distances of He above the plane are set to be: 3.602 (+0.063) Å and 3.596 (+0.057) Å, respectively, for the clusters with one and two He atoms, where values in parentheses represent the change by the excitation from S_0 to S_1. Several vibronic bands with excitation of intermolecular vibrations have also been observed. The vibrational frequencies of benzene(S_1)–He are derived as: 17 and 13 cm^{-1} for the intermolecular stretch and bend modes, respectively. The intermolecular stretch of the cluster with two He is 15.72 cm^{-1}, while no experimental information has been obtained for the bend modes. The vibronic bands of benzene–He exhibit tunneling splitting due to a large-amplitude migration of He above and below the benzene molecular plane. This finding is matched with the prediction based on a high-level *ab initio* calculation. We have also recorded the R2PI spectrum of mono ^{13}C substituted species of benzene–He.

For the clusters with H_2, two distinguished isomers, correlating to *para* and *ortho* H_2, are identified. This finding shows that the permutation of the two H atoms in H_2 is feasible in the clusters. When the *normal* H_2 was used as a sample gas, only the clusters of *ortho* H_2 were observed, and thus we had to use a gas sample of pure *para* H_2 to record the clusters with *para* H_2 (see Figure 1). This observation indicates the smaller effective binding energy for benzene–*para* H_2 than that of the *ortho* H_2 cluster. This energy relation has been well known for the clusters with smaller molecules (*e.g.*, HF, HCl, and OCS) attached by H_2. It is noted the present study is the first experimental report on the coexistence of *para* and *ortho* H_2 isomers in the clusters of aromatic molecules. Rotationally resolved spectra allowed us to fix the cluster geometry unambiguously, as shown in Figure 2. It has shown that the effective intermolecular distances are substantially different from each other between the clusters with *para* and *ortho* H_2, indicating the change in the average H_2 orientation relative to the benzene plane in the two isomers.

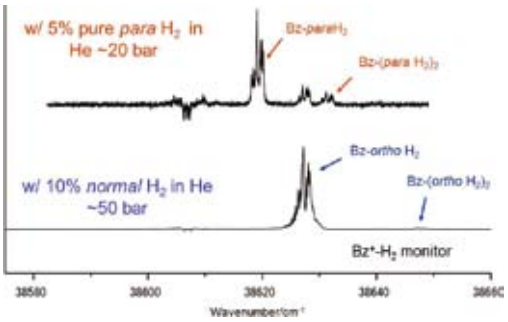

Figure 1. Excitation spectra of C_6H_6–$(H_2)_n$ recorded with the *normal* H_2 sample (bottom) and the pure *para* H_2 sample (top).

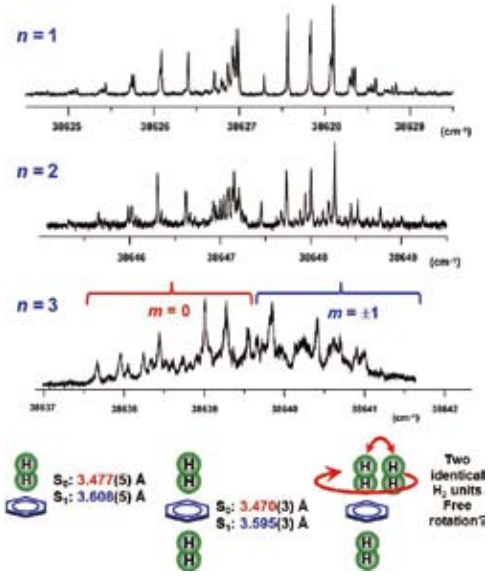

Figure 2. High-resolution excitation spectra and the experimentally derived cluster geometry of C_6H_6–(ortho $H_2)_n$.

We also recorded for the first time rotationally resolved excitation spectrum of the cluster with two Ar atoms lying on the same side of the benzene plane.

References

1) Y. Ohshima and H. Hasegawa, *Int. Rev. Chem. Phys.* **29**, 619–663 (2010).
2) H. Hasegawa and Y. Ohshima, *Phys. Rev. A* **74**, 061401 (4 pages) (2006).
3) H. Hasegawa and Y. Ohshima, *Chem. Phys. Lett.* **454**, 148–152 (2008).
4) D. Baek, H. Hasegawa and Y. Ohshima, *J. Chem. Phys.* **134**, 224302 (10 pages) (2011).
5) H. Hasegawa and Y. Ohshima, *Phys. Rev. Lett.* **101**, 053002 (4 pages) (2008).
6) K. Kitano, H. Hasegawa and Y. Ohshima, *Phys. Rev. Lett.* **103**, 223002 (4 pages) (2009).
7) Y. Khodorkovsky, K. Kitano, H. Hasegawa, Y. Ohshima and I. Sh. Averbukh, *Phys. Rev. A* **83**, 023423 (10 pages) (2011).
8) S, M. Beck, M. G. Liverman, D. L. Monts and R. E. Smalley, *J. Chem. Phys.* **70**, 232–237 (1979).

Development of High-Precision Coherent Control and Its Applications

Department of Photo-Molecular Science
Division of Photo-Molecular Science II

OHMORI, Kenji	Professor
KATSUKI, Hiroyuki	Assistant Professor
TAKEI, Nobuyuki	Assistant Professor
GOTO, Haruka	Post-Doctoral Fellow
SOMMER, Christian	Post-Doctoral Fellow
NAKAGAWA, Yoshihiro	Graduate Student
KOYASU, Kuniaki	Graduate Student
INAGAKI, Itsuko	Secretary
YAMAGAMI, Yukiko	Secretary

Coherent control is based on manipulation of quantum phases of wave functions. It is a basic scheme of controlling a variety of quantum systems from simple atoms to nanostructures with possible applications to novel quantum technologies such as bond-selective chemistry and quantum computation. Coherent control is thus currently one of the principal subjects of various fields of science and technology such as atomic and molecular physics, solid-state physics, quantum electronics, and information science and technology. One promising strategy to carry out coherent control is to use coherent light to modulate a matter wave with its optical phase. We have so far developed a high-precision wave-packet interferometry by stabilizing the relative quantum phase of the two molecular wave packets generated by a pair of femtosecond laser pulses on the attosecond time scale. We will apply our high-precision quantum interferometry to gas, liquid, solid, and surface systems to explore and control various quantum phenomena.

Award

OHMORI, Kenji; Humboldt Research Award (Germany).

Molecular Inner-Shell Spectroscopy: Local Electronic Structure and Intermolecular Interaction

Department of Photo-Molecular Science
Division of Photo-Molecular Science III

KOSUGI, Nobuhiro	Professor
YAMANE, Hiroyuki	Assistant Professor
NAGASAKA, Masanari	Assistant Professor
YUZAWA, Hayato	IMS Fellow
MOCHIZUKI, Kenji	Graduate Student
LELOUP, Valentin	Graduate Student*
NAKANE, Junko	Secretary

In order to reveal local electronic structures and weak intermolecular interactions in molecular systems such as organic solids, liquids, aqueous solutions, and molecular clusters, we are developing and improving several kinds of soft X-ray spectroscopic techniques, such as X-ray photoelectron spectroscopy (X-ray PES, XPS), X-ray absorption spectroscopy (XAS), resonant Auger electron spectroscopy (RAS), X-ray emission spectroscopy (XES), resonant XES (RXES), and resonant inelastic X-ray scattering (RIXS), at UVSOR in-vacuum undulator beamlines BL-3U and BL-6U with some international collaboration programs, and also an original *ab initio* quantum chemical program package GSCF, which is optimized to calculation of molecular inner-shell processes.

1. Concentration Dependence of Local Structure in Methanol-Water Binary Liquid

A water molecule has two H(hydrogen)-accepting ('acceptor') and H-donating ('donor') sites, and the water liquid forms three dimensional (3D) hydrogen bonding (HB) networks. On the other hand, a methanol molecule with a hydrophobic methyl group has one H-donor and one or two H-acceptor sites, and the methanol liquid forms one and two dimensional (1D, 2D) HB networks, such as chains and rings of 6–8 methanol molecules. It is known that the methanol–water binary liquid has 3D cluster structures. However, the local structures of the methanol–water mixtures are still unknown. In this work, the local structure of the methanol–water binary liquid at different concentrations is studied by using carbon K-edge XAS.

The experiments were performed at soft X-ray undulator beam line BL3U at UVSOR-II facility. The liquid thin layer was sandwiched between two 100 nm-thick Si_3N_4 membranes. The photon energy was calibrated by the first peak (287.96 eV) of methanol gas filled in a He buffer space between the Si_3N_4 membrane and the detector in the liquid cell.

Figure 1 shows the carbon K-edge XAS spectra of the methanol–water binary liquids. The peak around 288.5 eV arises from the molecular orbital with a component of the hydroxyl group in the methanol molecule, and has a HB effect. On the other hand, the peak around 290 eV is mainly distributed at the methyl group. This peak is shifted to the higher photon energy by increasing the mixing ratio of water. It means that the methyl groups approach with each other in a dilute aqueous solution and the interaction between the methyl groups increase, contrary to liquid methanol, where the methyl groups are apart from each other.

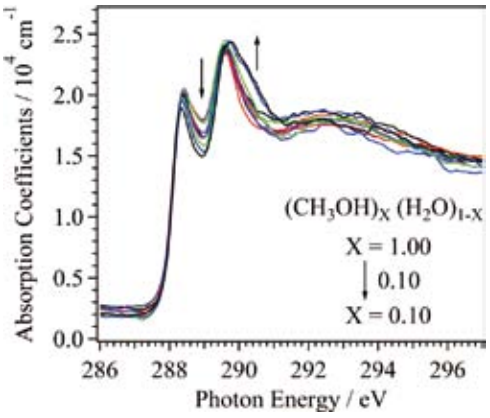

Figure 1. Carbon K-edge XAS spectra of the methanol-water binary liquid at different concentrations at 25 °C. The mixing ratio of water is increased along indicated arrows.

Figure 2 shows the intensities of the 289 eV region at different mixing ratios. The intensities are changed non-linearly, and indicate three different regions. The intensities are not changed so much in the methanol-rich region (I), indicating the local structure of pure methanol chain and ring clusters is preserved. On the other hand, in the region (II), the intensity is suddenly decreased at the methanol molar fraction $X \approx 0.7$, indicating a 1D/2D methanol–water mixed cluster is suddenly formed and this local structure is preserved down to $X \approx 0.3$. When $X <$ ~0.3 (III), the intensity is going down, indicating a 3D methanol–water mixed cluster is almost proportionally formed.

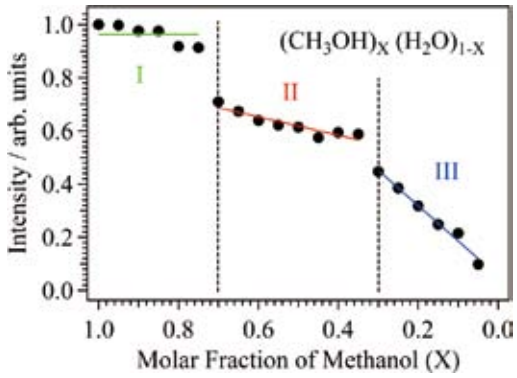

Figure 2. Intensities of the 289 eV region as a function of molar fraction of methanol in the methanol–water mixtures. The intensities of methanol and water are normalized to one and zero, respectively

2. Intramolecular and Intermolecular Interactions in Crystalline Films of Zinc Phthalocyanine (ZnPc)

It has been theoretically predicted that local and nonlocal electron–phonon (e–ph) interactions play a crucial role in the charge transport mechanism in organic solids. Recently, we have succeeded in observation of a small energy *versus* wave-vector [$E(\boldsymbol{k})$] relation for the crystalline film of an archetypal organic semiconductor of ZnPc on Au(111) by using the high-resolution angle-resolved UV photoemission spectroscopy (ARPES). Based on the precise $E(\boldsymbol{k})$ data, we have evaluated the e–ph interaction on the charge transport mechanism of the ZnPc crystalline film.

Figure 3(a) shows the $E(\boldsymbol{k})$ relation of the ZnPc crystalline film on Au(111), which is obtained from the photon energy dependence of the normal-emission ARPES spectra at 15 K. The highest occupied molecular orbital [HOMO (π, a_{1u})], Zn 3d (b_{1g}), and π's derived peaks show a dispersive shift with the same periodicity. This periodicity corresponds well with the highly symmetric Γ and Y points, estimated from the lattice constant of 3.32 Å determined by the specular X-ray diffraction [Figure 3(b)].

In order to examine the e–ph coupling in crystalline ZnPc film, we measured the temperature dependence of ARPES at the Γ and Y points with the 60 and 90 eV incident photons, respectively. As seen in Figure 3(c), the Γ-point HOMO energy shifts depending on the temperature, while the Y-point HOMO energy seems independent on the temperature. From the lineshape analysis, we found that both the HOMO bandwidth (*i.e.*, energy difference between the Γ-HOMO and Y-HOMO) and the Γ-HOMO peakwidth are narrowed with increasing the temperature, which is an opposite behavior to the remanent Au(111) Fermi edge. This is distinct indication of the local/nonlocal e–ph interaction; that is, band narrowing due to the interaction with local phonons (*intra*molecular vibrations) and band widening due to the interaction with nonlocal phonons (*inter*molecular lattice vibrations). Judging from the temperature dependence of the HOMO bandwidth and peakwidth, it is considered that the temperature-dependent transition between the incoherent hopping transport associated with the local e–ph coupling and the coherent band transport associated with the nonlocal e–ph coupling occurs within the energy scale of 100 meV in the ZnPc crystalline film.

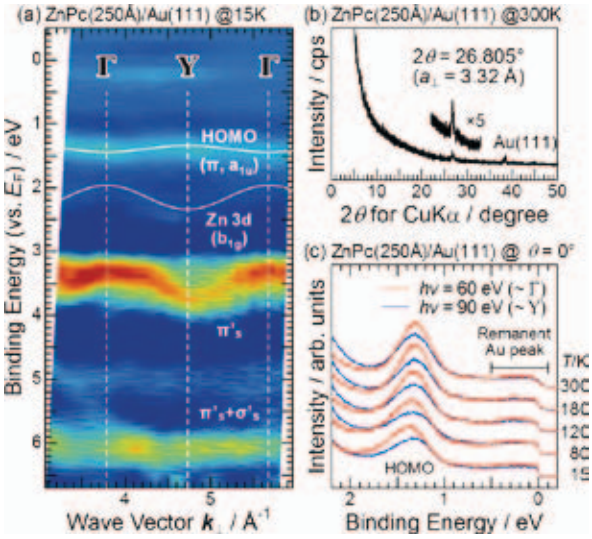

Figure 3. (a) Intermolecular $E(\boldsymbol{k})$ relation of the crystalline ZnPc film on Au(111) at 15 K, wherein the second derivative of the ARPES spectra were used for mapping out. White curves for the HOMO and Zn 3d derived bands are the best-fit results in the tight-binding model. (b) CuKα X-ray diffraction of the crystalline ZnPc film on Au(111) at 300 K. (c) Temperature dependence of ARPES in the HOMO-band region at the Γ and Y points, measured with 60 and 90 eV incident photons, respectively.

* carrying out graduate research on Cooperative Education Program of IMS with Ecole Nationale Superieure de Chimie de Paris

Photoabsorption and Photoionization Studies of Fullerenes and Development of High-Efficiency Organic Solar Cells

Department of Photo-Molecular Science
Division of Photo-Molecular Science III

MITSUKE, Koichiro	Associate Professor (–March, 2012)*
KATAYANAGI, Hideki	Assistant Professor
PRAJONGTAT, Pongthep	Research Fellow
MORENOS, Lei Angeli S.	Visiting Scientist
VAILIKHIT, Veeramol	Visiting Scientist
BASHYAL, Deepak	Graduate Student
ASARI, Chie	Technical Fellow
SHIMIZU, Atsuko	Secretary

We have observed the formation of multiply-charged photoions from gaseous fullerenes or aromatic hydrocarbons irradiated with synchrotron radiation at $h\nu$ = 25 to 200 eV. We thus studied the mechanisms and kinetics of consecutive C_2-release reactions on the basis of (i) the yield curves for the fragments $C_{60(70)-2n}^{z+}$ ($n \geq 1$, z = 1–3) as a function of the primary internal energy and (ii) the three dimensional velocity distributions of the fragments. The velocity distributions of C_{60-2n}^{z+} and C_{70-2n}^{z+} were measured for the first time. Concepts of the microcanonical temperature and Arrhenius-type rate constants for individual C_2 ejection steps allowed us to compare the experimental total average kinetic energy with theoretical kinetic energy release predicted from the "model free approach" developed by Klots.

In the second topic, we have fabricated dye-sensitized solar cells (DSSCs) containing ruthenium dye, iodide electrolyte, and platinum or carbon nanotube catalysts. The incidence photon-to-current conversion efficiencies (IPCE) and photoabsorbance (ABS) were measured in the range of 300 nm to 1 μm. We also evaluated the quantum yield (APCE) of DSSCs for the electron injection from the excited orbital of Ru dye to the conduction band of mesoporous TiO_2 nanoparticles. Our final goal is to develop DSSCs with high performance by improving ABS and APCE.

1. Photodissociation Dynamics of Fullerenes by Velocity Map Imaging with Improved Mass Resolution

We observed images of three-dimensional scattering velocity distributions of fragments produced by the photodissociation of the fullerenes, C_{60} and C_{70}, using a mass-resolved velocity map imaging spectrometer.[1,2] From the images we successfully obtained translational temperatures of the fragments and kinetic energy releases. Still the peaks of the fragments were found to be partially overlapped in their time-of-flight (TOF) mass spectra. We tried to improve the mass resolution of the imaging spectrometer by adding a focusing electrode to the Eppink-Parker type imaging electrode assembly.[3] This focusing electrode was designed after the ion lens device presented by Peši.

After introducing the focusing electrode, vertical stripes involving the fragment ions are completely resolved in the velocity vs. TOF maps, or y–t maps, and their masses are unquestionably identified. The y–t maps with improved mass resolution were obtained for C_{70} with the excitation photon energy $h\nu$ range of 70–125 eV. The translational temperature T_{trans} of each fragment was extracted from the map. The $h\nu$ dependence of T_{trans} exhibits the same propensity as that obtained previously[2] at low mass resolution. For C_{60}^{2+} from C_{70} singularity in T_{trans} remains also in the present measurements. Probably the C_{60}^{2+} formation mechanism is quite different from the stepwise C_2 emission from C_{70} that has widely been accepted for the other fragments.

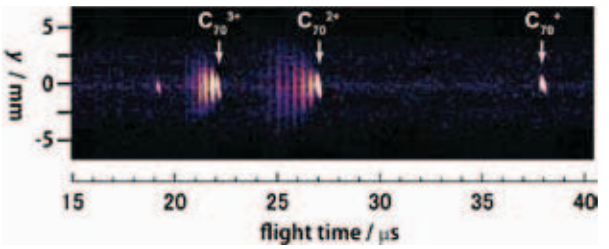

Figure 1. Y–t map of parent and fragment ions produced from C_{70} with the excitation $h\nu$ of 110 eV. The y coordinate is proportional to the y component of the ion velocity.

2. Estimation of the Translational Temperatures of High-Speed Fragment Ions Released from Sumanene and Coronene

Dissociative photoionization processes of polycyclic aromatic hydrocarbons (PAHs), sumanene $C_{21}H_{12}$ and coronene

$C_{24}H_{12}$, were studied by a mass-resolved velocity map imaging (VMI) technique. Since PAHs constitute the substructures of C_{60}, their behaviors in fragmentation are expected to have some analogies with those of fullerenes. Nevertheless, the *y*–*t* maps revealed a large difference in fragmentation mechanisms between PAHs and C_{60}. Main species produced from $C_{21}H_{12}$ and $C_{24}H_{12}$ were singly–charged ions with very high speed: CH^+, $C_2H_2^+$ and $C_nH_{n/2}^+$ ($2 < n < 13$). The translational energies of these fragments are so large that the scattering distributions extend beyond the coverage of our imaging apparatus. The peak profiles of the time-of-flight distributions were computer simulated on the basis of the ion trajectories calculated by the Simion–3D software. The translational temperatures of fragments from $C_{21}H_{12}$ were thus estimated to be 3000 to 30000 K (see Figure 2), depending on the number of carbon atoms in the fragments. A similar trend was observed for dissociation of $C_{24}H_{12}$. Our results suggest that dissociation of PAHs proceeds through the fission mechanism, which is not dominant in the fullerene cases.

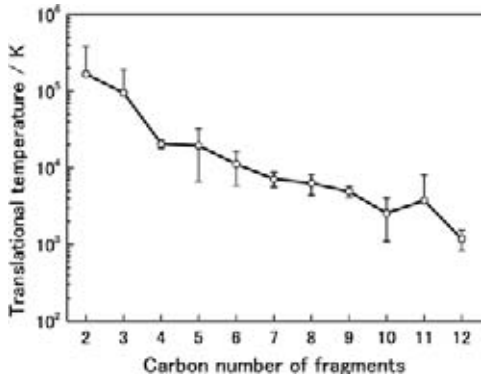

Figure 2. Translational temperatures of the fragment ions from coronene at *h*ν = 100 eV. Error bars show the standard deviations of repeated experimental runs.

3. Enhancement of the Solubility, Thermal Stability, and Electronic Properties of Carbon Nanotubes Functionalized by MEH-PPV

Multi-walled carbon nanotubes functionalized with poly [2-methoxy-5-(2'-ethylhexyloxy)-1,4-phenylenevinylene] (MWCNT-f-MEH-PPV) nanocomposites were successfully prepared by employing a "grafting from" approach.[4] The content of the functionalizing MEH-PPV in the composites was observed as 76%wt. Compared with pristine MWCNT, p-MWCNT, the aqueous solubility and thermal stability of the former are significantly enhanced. The effect of covalently and non-covalently functionalized nanotubes on the performances of the DSSCs has been investigated. The cells having the counter electrodes coated with isolated MEH-PPV, p-MWCNT/MEH-PPV, and MWCNT-f-MEH-PPV/MEH- PPV were fabricated. The cells based on a MWCNT- f-MEH-PPV/MEH-PPV counter electrode demonstrate the best photovoltaic performance as observed by higher J_{SC}, V_{OC}, and *FF* values. The experimental phenomena can be explained by quantum chemical calculations: Charge transfer from MEH-PPV oligomers to nanotubes is greater when covalently functionalized than when non-covalently functionalized. These suggest that the improvement in the photovoltaic parameters of the cells containing covalently functionalized nanotubes results not only from the higher concentration present in the nanotube films of the counter electrode, but also from the greater electron delocalization between the oligomers and nanotubes. The obtained results are very useful for enhancement of functionalized nanotubes applied to DSSCs.

4. Gas Phase Spectroscopy of Carbon Nanotubes

Our efforts have been concentrated on elucidation of the electronic and optical properties of fullerenes as well as their reaction dynamics in the gas phase. Such knowledge is critical in applying fullerenes to molecular functional devices. Recently, we started to investigate the properties of gaseous carbon nanotubes (CNTs) which of course form another group of promising carbon material.

CNTs are vaporized by matrix assisted laser desorption ionization (MALDI) and analyzed by time-of-flight (TOF) mass spectrometry. Commercially available multiwall CNT powder and single-wall CNT aqueous dispersion were used as samples. We have checked several solvents and matrices to optimize the MALDI conditions. The images of electron microscope prove that the laser irradiation certainly gives rise to vaporization of the sample. A temporal increase in the pressure of the sample chamber also supports the vaporization during the laser irradiation. Nevertheless, the signal of whole CNTs has not been observed yet. Smaller fragment ions C_n ($n < 200$) were only detected. Interaction between matrices and dispersants may prevent effective ionization.

We will continue to seek for the suitable vaporization method and construct a new vacuum chamber for the gas phase CNT experiment. The chamber will be connected to the beamline 4B in the UVSOR facility. Photoabsorption and photoionization experiments will be performed using the same chamber at the outset.

References

1) H. Katayanagi and K. Mitsuke, *J. Chem. Phys. (Communication)* **133**, 081101 (4 pages) (2010).
2) H. Katayanagi and K. Mitsuke, *J. Chem. Phys.* **135**, 144307 (8 pages) (2011).
3) K. Mitsuke, H. Katayanagi, B. Kafle and Md S. Prodhan, *ISRN Phys. Chem.* **2012**, 959074 (9 pages) (2012).
4) P. Prajongtat, S. Suramitr, M. P. Gleeson, K. Mitsuke and S. Hannongbua, *J. Mater. Sci.*, submitted.

* Present Position; Professor, Department of Chemistry, Faculty of Science, Josai University

Light Source Developments by Using Relativistic Electron Beams

UVSOR Facility
Division of Advanced Accelerator Research

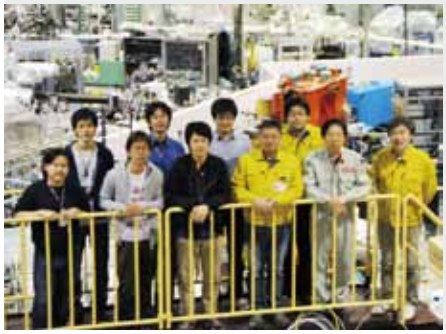

KATOH, Masahiro	Professor
ADACHI, Masahiro	Assistant Professor
KONOMI, Taro	Assistant Professor
OHIGASHI, Takuji	Assistant Professor
TANAKA, Seiichi	Post-Doctoral Fellow
ARAI, Hidemi	Post-Doctoral Fellow
TAIRA, Yoshitaka	Graduate Student*
GOTO, Yoshiaki	Graduate Student*
WASA, Naoki	Graduate Student*
HIDA, Yohei	Graduate Student*
UEMATSU, Youhei	Graduate Student*
NIWA, Takahiro	Graduate Student*

This project involves researches and developments on synchrotron light source, free electron laser, beam physics and their related technologies, including application of the light sources.

1. Developments on UVSOR Accelerators

The magnetic lattice of UVSOR was modified in 2012. This was the second major upgrade of the lattice, following the first one in 2003. This time all the bending (dipole) magnets were replaced with newly designed combined function ones. They have specially designed pole shapes and edge shapes as shown in Figure 1, to produce dipole, quadrupole and sextupole fields at the same time. By this modification, the emittance was reduced from 27 nm-rad to around 15 nm-rad, which would results in higher brightness of the synchrotron radiation. The magnetic lattice function changed, as shown in Figure 2. The storage ring was successfully commissioned in July with the new lattice. Fine machine tuning is in progress. After this upgrade, the ring is called UVSOR-III.

Figure 1. New combined function bending magnet (a lower half is shown).

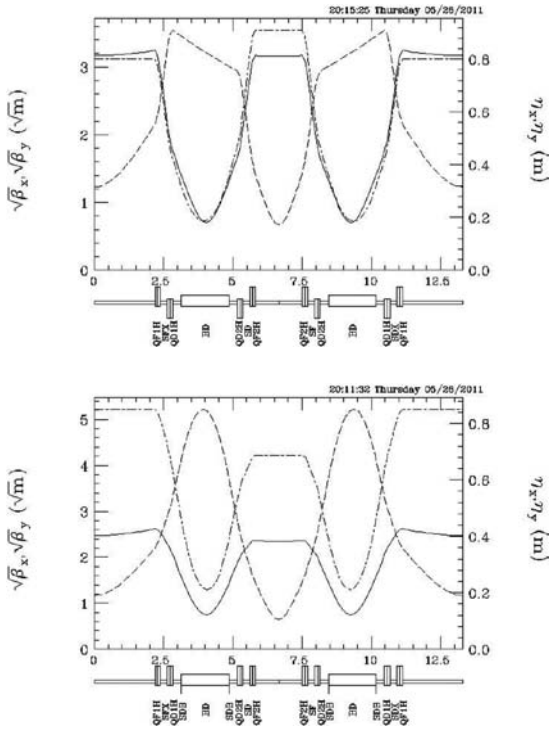

Figure 2. Lattice functions of UVSOR-II (upper) and UVSOR-III (lower). One quadrant of the ring is shown. The emittance is 27nm-rad and ~15nm-rad, respectively.

2. Construction of STXM Beam-Line

A new in-vacuum undulator was constructed and, in May 2012, it was installed at the last straight section in the ring reserved for insertion devices. This is the sixth undulator at UVSOR. It would provide soft X-rays to a scanning transmission X-ray microscope (STXM) beam-line.

Since April in 2012, the STXM beam-line, BL4U, has been constructed. Recently, its construction and installation of the STXM system were finished and their commissioning is due to start in October, 2012. We have been preparing the facilities of the beam-line, such as microscopes for pre-observations, a glove-box, an experimental hutch and infra-structures, for stating the operation in next April.

3. Light Source Developments

We have demonstrated that coherent synchrotron radiation of various properties could be generated in an electron storage ring by using an external laser source.[1–3] This research is supported by the Quantum Beam Technology Program of JST/MEXT. Under this support, a new experimental station has been constructed.[4] A new optical klystron/undulator was installed as shown in Figure 3. The magnetic field properties were verified by observing the spontaneous synchrotron radiation. The upgrade of the laser system was completed. The laser transport line, which was carefully designed as considering the effects of the air fluctuation, was also constructed. Two new beam-lines dedicated to the coherent lights in the VUV range and in the THz range has been almost completed.[5] The generation of coherent synchrotron radiation at the new site was successfully demonstrated. Some applications will be demonstrated soon in this fiscal year.

Figure 3. Experimental ser-up of Coherent Harmonic Generation at UVSOR-II.

A tunable, quasi-monochromatic ultra-short pulse and polarization-variable gamma-ray source is under development, based on a technology called Laser Compton scattering. The laser photons are Compton back-scattered by the high energy electrons and are converted to gamma-rays. The electron beam circulating in the storage ring is very thin in the vertical direction, typically in the order of 10 microns. By injecting laser light from the vertical direction to the beam, it is possible to produce ultra-short, quasi-monochromatic, energy tunable, polarization variable gamma-ray pulses. The energy tunability was successfully demonstrated.[6] An application utilizing the short pulse property was successfully demonstrated.

4. Accelerator Technology Developments

A novel beam injection scheme using a pulse sextupole magnet has been studied, in which the perturbation to the stored beam could be minimized during the injection. This is beneficial to the users experiments in the top-up operation mode. A new pulse sextupole magnet was designed and has been constructed. The field measurement is in progress. This device will be installed in the ring in September 2012.

A turn-by-turn beam position measurement system has been constructed, collaborating with the Equipment Development Center. This system enables to measure the electron beam orbit turn-by-turn just after the injection. It was proved that this device was a powerful tool for the commissioning of the storage ring.

References

1) (in alphabetic order) S. Bielawski, C. Evain, T. Hara, M. Hosaka, M. Katoh, S. Kimura, A. Mochihashi, M. Shimada, C. Szwaj, T. Takahashi and Y. Takashima, *Nat. Phys.* **4**, 390–393 (2008).
2) M. Labat, M. Hosaka, M. Shimada, M. Katoh and M. E. Couprie, *Phys. Rev. Lett.* **101**, 164803 (2008).
3) M. Shimada, M. Katoh, M. Adachi, T. Tanikawa, S. Kimura, M. Hosaka, N. Yamamoto, Y. Takashima and T. Takahashi, *Phys. Rev. Lett.* **103**, 144802 (2009).
4) M. Adachi, M. Katoh, H. Zen, T. Tanikawa, M. Hosaka, Y. Takashima, N. Yamamoto and Y. Taira, *AIP Conf. Proc.* **1234**, 492 (2010).
5) S. Kimura, E. Nakamura, M. Hosaka, T. Takahashi and M. Katoh, *AIP Conf. Proc.* **1234**, 63 (2010).
6) Y. Taira, M. Adachi, H. Zen, T. Tanikawa, M. Hosaka, Y. Takashima, N. Yamamoto, K. Soda and M. Katoh, *Nucl. Instrum. Methods Phys. Res., Sect. A* **637**, 5116–5119 (2011).

* carrying out graduate research on Cooperative Education Program of IMS with Nagoya University

Synchrotron Radiation Spectroscopy on Strongly Correlated Electron Systems

UVSOR Facility
Division of Advanced Solid State Physics

KIMURA, Shin-ichi	Associate Professor
MATSUNAMI, Masaharu	Assistant Professor
IMURA, Keiichiro	Post-Doctoral Fellow*
IIZUKA, Takuya	Graduate Student†
HAJIRI, Tetsuya	Graduate Student‡
NIWA, Ryosuke	Graduate Student‡
SHIMURA, Yusuke	Graduate Student‡
HIRATE, Satoshi	Graduate Student‡

Solids with strong electron–electron interaction, namely strongly correlated electron systems (SCES), have various physical properties, such as non-BCS superconducting, colossal magneto-resistance, heavy fermion and so on, which cannot be predicted by first-principle band structure calculation. Due to the physical properties, the materials are the candidates of the next generation functional materials. We investigate the mechanism of the physical properties as well as the electronic structure of SCES, especially rare-earth compounds, organic superconductors and transition-metal compounds, by infrared/THz spectroscopy and angle-resolved photoemission spectroscopy based on synchrotron radiation. Since experimental techniques using synchrotron radiation are evolved rapidly, the development of the synchrotron radiation instruments is also one of our research subjects.

1. Existence of Heavy Fermions in the Antiferromagnetic Phase of $CeIn_3$[1)]

Recently, physics at the quantum critical point (QCP), which is the border between local magnetism and itinerant paramagnetism at zero temperature, has become one of the main topics in the condensed-matter field because new quantum properties such as non-BCS superconductivity appear in the vicinity of the QCP. The ground state of rare-earth intermetallic compounds, namely, heavy-fermion (HF) materials, changes between the local magnetic and itinerant nonmagnetic states through external perturbation by such factors as pressure and magnetic field. The QCP appears owing to the energy balance between the local magnetic state based on the Ruderman–Kittel–Kasuya–Yoshida (RKKY) interaction and the itinerant HF state due to the Kondo effect. In the itinerant HF regime, the conduction band hybridizes with the nearly local 4*f* state, so that a large Fermi surface as well as the hybridization band between them, namely, the *c*–*f* hybridization band, is realized. In the case of a magnetic regime, on the other hand, two theoretical scenarios have been proposed. One is the spin-density wave (SDW) scenario based on spin fluctuation, in which large Fermi surfaces due to *c*–*f* hybridization remain even in magnetically ordered states. The other is the Kondo breakdown (KBD) scenario, in which the *c*–*f* hybridization state disappears in the magnetic state and only small Fermi surfaces due to conduction electrons appear. Many controversies for these scenarios have been performed so far, but the conclusion has not been obtained yet.

Here, we report the pressure-dependent electronic structure as well as the *c*–*f* hybridization state obtained by far-infrared reflectivity [$R(\omega)$] and optical conductivity [$\sigma(\omega)$] measurements of $CeIn_3$ under pressure. $CeIn_3$ has an AFM ground state with a Néel temperature T_N of 10 K. With the

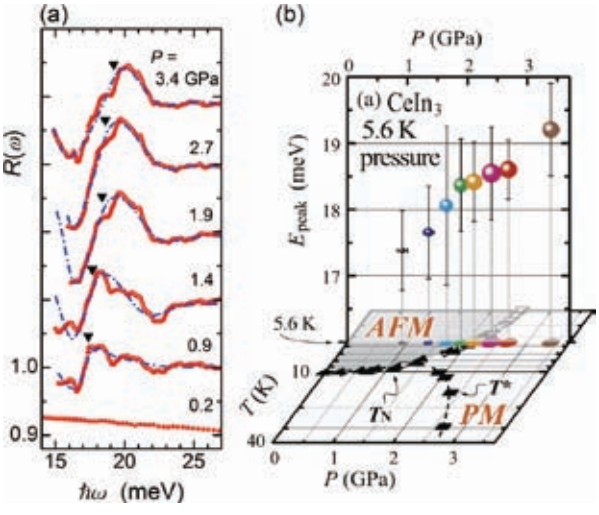

Figure 1. (a) Pressure dependence of the reflectivity [$R(\omega)$] spectrum (solid circles) of $CeIn_3$ and Drude-Lorentz fitting results (dotted-dashed lines) in the photon energy range of 14–27 meV at 5.6 K. The spectra are shifted by 0.1 for clarity. (b) The edges of $R(\omega)$ spectra as functions of pressure. The size of the marks denotes the intensity of the corresponding edge in the $R(\omega)$ spectra. The pressure-dependent Néel temperature (solid and open triangles, T_N) and valence transition temperature (solid squares, T^*) are also plotted at the bottom.

application of pressure, T_N monotonically decreases and disappears at a critical pressure of approximately 2.6 GPa. We observed that the *c–f* hybridization gap appears not only in the HF state but also in the AFM state, and both the energy and intensity of the σ(ω) peak due to the *c–f* hybridization band continuously increase with the application of pressure as shown in Figure 1. Our observations suggest that the electronic structure of $CeIn_3$ in the AFM phase can be explained by the SDW scenario because the *c–f* hybridization state exists even in the AFM phase.

2. Three-Dimensional Electronic Structure and Interband Nesting in the Stoichiometric Superconductor LiFeAs[2)]

Recently discovered iron pnictide superconductors have two-dimensional (2D) Fe–As layers that are similar to the Cu–O planes in high-T_c superconducting cuprates. In high-T_c cuprates, 2D magnetic interaction is important for the origin of the high T_c because of their 2D electronic structure. Such 2D interaction as well as the 2D nesting condition in iron pnictides has long been a focus of discussions. However, the crystal structures of iron pnictides are more three dimensional (3D) than those of cuprates. It is therefore important to clarify the 3D electronic structure of iron pnictides in order to understand the effective interaction of Cooper pair formation.

We reported the electronic structure as well as the orbital characters of a stoichiometric iron-based superconductor LiFeAs (T_c = 18 K) using polarization-dependent 3D angle-resolved photoemission spectroscopy (ARPES) as shown in Figure 2. The obtained band dispersions and orbital characters are qualitatively in good agreement with those derived from local density approximation (LDA) band calculations. Considering a 3D nesting condition, we find that each 2D hole and electron Fermi surface (FS) of d_{xy} orbital character is weakly nested. This weak nesting suggests that (π,π,π) interband scattering is important for the superconducting behavior of LiFeAs.

3. Momentum-Dependent Hybridization Gap and Dispersive In-Gap State of the Kondo Semiconductor SmB_6[3)]

Materials with strong electron correlation have exotic physical properties that cannot be predicted from first-principle band calculations. One example may be seen in a semiconductor with a very small energy gap, which appears in rare-earth compounds such as the Kondo semiconductor or insulator (KI). At high temperatures, KI behaves as a dense Kondo metal, while an energy gap with activation energy of several 10 meV appears at low temperature. The energy gap is believed to originate from hybridization between the nearly localized 4*f* state near the Fermi level (E_F) and the conduction band (*c–f* hybridization).

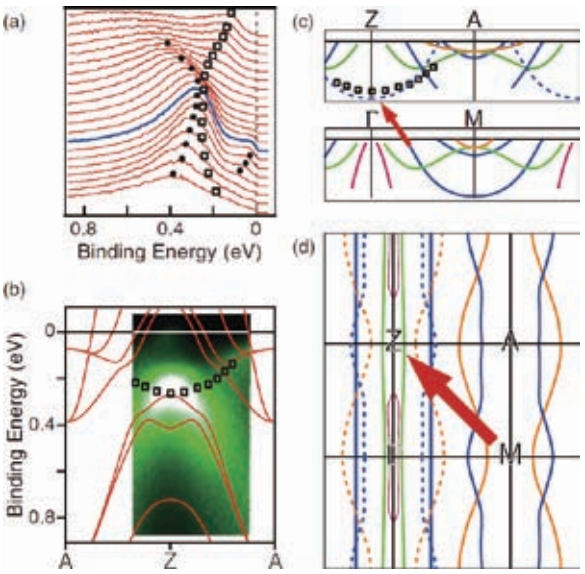

Figure 2. (a)ARPES spectra at the Z point. The solid circles are values that are expected and the open squares are those that are not expected by the band calculation. (b) ARPES image with the band calculation at the Z point. (c) Schematic band dispersions obtained from the experiments. The open squares used in (c) have the same meaning as in (a) and (b). (d) Schematic figure of the 3D FS nesting conditions. The solid and dashed lines indicate the original and nested FSs, respectively. The bold arrow indicates the expected nesting wave vector of (π,π,π).

We reported the temperature dependence of the dispersion curve of the hybridization state using temperature-dependent 3D-ARPES, in order to determine the electronic structure and the reason for the different temperature dependences of the valence transition and magnetic excitation. We found that the hybridization band with a peak at a binding energy of 15 meV near the X point gradually appears on cooling from 150 to 40 K, which has the same temperature dependence as the valence transition. At the Γ point, on the other hand, the peak at E_B ~ 20 meV has the same temperature dependence as the magnetic excitation at Q = (0.5,0.5,0.5), which differs from the 15-meV peak at the X point. This suggests that the magnetic excitation originates from the hybridization band at the Γ point.

References

1) T. Iizuka, T. Mizuno, B. H. Min, Y. S. Kwon and S. Kimura, *J. Phys. Soc. Jpn.* **81**, 043703 (2012). (Papers of Editors' Choice)
2) T. Hajiri, T. Ito, R. Niwa, M. Matsunami, B. H. Min, Y. S. Kwon and S. Kimura, *Phys. Rev. B* **85**, 094509 (2012).
3) H. Miyazaki, T. Hajiri, T. Ito, S. Kunii and S. Kimura, *Phys. Rev. B* **86**, 075105 (2012).

* Present Address; Graduate School of Science, Nagoya University
† Present Address; Physikalisches Institut, Universität Stuttgart, Germany
‡ carrying out graduate research on Cooperative Education Program of IMS with Nagoya University

Electronic Structure and Decay Dynamics in Atoms and Molecules Following Core Hole Creation

UVSOR Facility
Division of Advanced Photochemistry

SHIGEMASA, Eiji — Associate Professor
IWAYAMA, Hiroshi — Assistant Professor
ISHIKAWA, Lisa — Post-Doctoral Fellow

The dynamics of the inner-shell photoexcitation, photo-ionization, and subsequent decay processes is much more complex, in comparison to outer-shell photo-processes. For instance, the inner-shell photoionization is concomitant with the excitation and ionization of valence electrons, which reveal themselves as shake-up and shake-off satellite structures in the corresponding photoelectron spectrum. The one-photon multi-electron processes, which are entirely due to the electron correlation in the system, are known to happen not only in the primary inner-shell hole creation processes, but also in their relaxation processes. Our research project is focused on elucidating the electronic structures and decay dynamics in core-excited atoms and molecules, by utilizing various spectroscopic techniques together with monochromatized synchrotron radiation in the soft x-ray region.

1. Ultrafast Molecular Dissociation of Core-Excited HBr Studied by High-Resolution Electron Spectroscopy

Soft X-ray absorption spectra of molecules exhibit rich structures in the region below the ionization thresholds, which are due to the excitations of a core electron to unoccupied valence or Rydberg orbitals. The core excited states are predominantly relaxed via Auger electron emission, in the case of the molecules composed of light elements, and subsequently fragmentation follows. As demonstrated by Morin and Nenner, however, a fast neutral dissociation could precede the resonant Auger decay.[1)] In other words, the electronic decay of the core hole takes place after the constituent atoms come apart. Since then, many research works have been conducted to identify such ultrafast dissociation processes in various different systems. Recent works on high-resolution resonant Auger electron spectroscopy have revealed that the nuclear motion of the molecular core-excited states is promoted in competition with the Auger decay. Here, we revisit the first discovery of ultrafast dissociation following the Br 3d core excitation in HBr. High-resolution electron spectroscopy for the subsequent Auger decay has been applied.

The experiments were carried out on the soft X-ray beamline BL6U at UVSOR. The radiation from an undulator was monochromatized by a variable included angle varied line-spacing plane grazing monochromator. The exit slit opening was set to 300 μm, which corresponds to the photon energy resolution $E/\Delta E$ of ~1500 at 70 eV. The monochromatized radiation was introduced into a gas cell with sample gases. Kinetic energies of the emitted electrons were measured by a hemispherical electron energy analyzer (MBS-A1) placed at a right angle relative to the photon beam direction. The degree of the linear polarization of the incident light was essentially 100%, and the direction of the electric vector was set to be parallel to the axis of the electrostatic lens of the analyzer. The energy resolution of the analyzer was set to ~12 meV. Under these experimental conditions, the full width at half maximum of the vibrational fine structure for the X state of HBr^+ was measured to be ~50 meV.

Figure 1 represents a resonant Auger spectrum taken at 70.4 eV, where the $3d_{5/2}$ core-hole states are mainly populated. The vertical scale of the red line spectrum is magnified by the five times. The most marked feature in Figure 1 is the numerous sharp peaks, due to the vibrational structures for the HBr^+ states and the atomic Auger lines from the Br fragments with a 3d core-hole. In the previous work,[1)] only five atomic lines indicated by the blue arrows in Figure 1 have been identified, owing to the limited resolution. In contrast, at least ten more

atomic Auger peaks and some molecular peaks with vibrational structures are clearly resolved in the present work. The detailed analyses for the spectral features observed are just beginning to be performed.

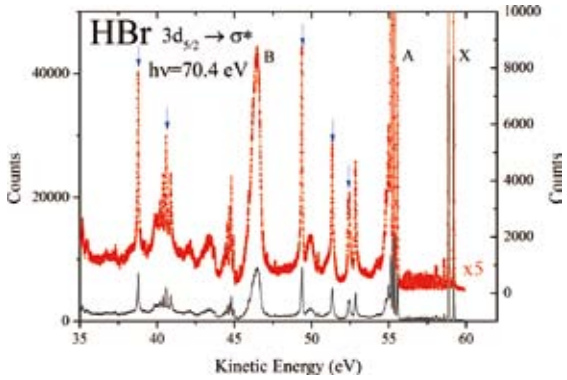

Figure 1. Resonant Auger spectrum taken at the Br $3d_{5/2} \rightarrow \sigma^*$ resonance of HBr.

2. Angle-Resolved Metastable Fragment Yields Spectra

Multi-electron processes, where more than two electrons are excited simultaneously, have usually been observed in absorption and photoelectron spectra of inner-shell excited molecules. Double excitations, one of the typical multielectron processes involving two electrons, are often observed above the ionization threshold energy region in photoabsorption spectra. Shake-up excitations in ions, where one of two electrons is excited into the continuum, are often observed in the energy region close to resonance features in photoelectron spectra. These processes occur mainly due to correlation effects among the electrons in a system and are fundamental aspects of atomic and molecular physics.

Recently, we demonstrated that "metastable" fragments spectroscopy, in which highly excited neutral fragments are observed, is quite useful as a spectroscopic technique for the investigation of multi-electron processes.[2)] Metastable photofragment spectroscopy can also be used for investigating shake-up satellites at the threshold excitation energy, because neutral photofragments can be detected wherever the scanning photon energies match the threshold energies of the ionic states. In addition, if one measures the angular distribution of the fragment emission with respect to the polarization direction of the synchrotron radiation, the symmetries of the inner-shell excited states can be deduced from this information. The angular distribution of fragments emitted after core-hole creation is related to the molecular orientation upon photoabsorption, because the lifetime of the core-hole ($\tau \sim 10^{-14}$ s) is dominated by Auger decay leading to dissociative states and is much shorter than the molecular rotational period ($\tau \sim 10^{-10}$ s). Thus, symmetry-resolved, namely, angle-resolved metastable spectroscopy provides complete symmetry resolution between the $\Delta\Lambda = 0$ (parallel) and $\Delta\Lambda = \pm 1$ (perpendicular) transitions in the *K*-shell photoabsorption of diatomic molecules. As a result, the Σ- or Π-symmetry character of transition states can be detected.[3)]

Figure 2 demonstrates a zero kinetic energy electron (ZEKE) spectrum, and angle-resolved metastable yield spectra of CO in the C *K*-edge region, measured at 0° (Σ-symmetry) and 90° (Π-symmetry), respectively, as an example of successful measurements. The photon energy range shown in Figure 2 corresponds to double and triple excitation regions, where shake-up satellite states also lie. Several peaks are clearly separated by Π-symmetry and Σ-symmetry spectra. We observed new peaks at 310.2 eV, 313.2 eV, and 313.9 eV. These should be double/triple excitation peaks since angle-resolved photoion yield spectra show small peaks at the same energy positions and these peaks have not been observed by conventional photoelectron spectroscopy. We successfully showed that all peaks in angle-resolved metastable fragment yields spectra of CO in the C 1*s* ionization threshold region can be assigned as either satellite states or double/triple excitation states.

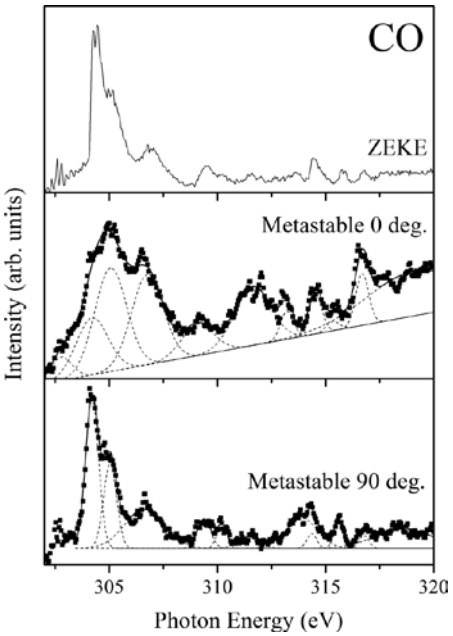

Figure 2. ZEKE spectrum, and angle-resolved metastable yield spectra, measured at 0° (Σ-symmetry) and 90° (Π-symmetry), in the satellite and double/triple excitation regions of CO in the C *K*-edge region.

References

1) P. Morin and I. Nenner, *Phys. Rev. Lett.* **56**, 1913–1916 (1986).
2) Y. Hikosaka *et al.*, *J. Phys. B* **40**, 2091–2097 (2007).
3) E. Shigemasa and N. Kosugi, *Adv. Chem. Phys*. **147**, 75–126 (2012).

Micro Solid-State Photonics

Laser Research Center for Molecular Science
Division of Advanced Laser Development

TAIRA, Takunori	Associate Professor
ISHIZUKI, Hideki	Assistant Professor
AKIYAMA, Jun	IMS Research Assistant Professor
TSUNEKANE, Masaki	Post-Doctoral Fellow
SATO, Yoichi	Post-Doctoral Fellow
KAUSAS, Arvydas	Post-Doctoral Fellow
KONG, Weipeng	Graduate Student
ONO, Yoko	Secretary
INAGAKI, Yayoi	Secretary

The artistic optical devices should be compact, reliable, efficient and high power light sources. With the approaches of domain structures and boundaries engineering, it is possible to bring the new interaction in their coherent radiation. The high-brightness nature of Yb or Nd doped single crystal or ceramic microchip lasers can realize efficient nonlinear wavelength conversion. In addition, designed nonlinear polarization under coherent length level allows us new function, such as the quasi phase matching (QPM). The development of "***Micro Solid-State Photonics***," which is based on the micro domain structure and boundary controlled materials, opens new horizon in the laser science.

1. High Brightness, Passively Q-Switched Yb:YAG/Cr:YAG Micro-Laser

A QCW diode end-pumped, high peak power passively Q-switched Yb:YAG/Cr:YAG micro-laser was demonstrated as shown in Figure 1. An output pulse energy of 3.6 mJ was obtained with a duration of 1.3 ns. The peak power is 2.8 MW. An M^2 value was nearly 1.

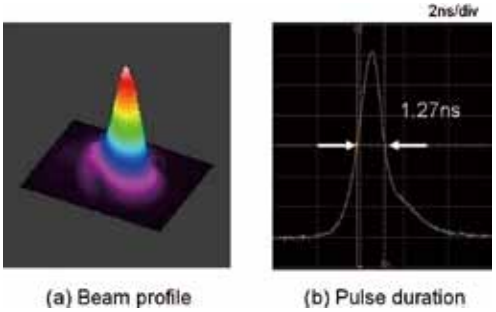

Figure 1. Beam profile and pulse duration at 3.6 mJ.

2. 60% FHG Efficiency from Fluxless-Grown BBO Using Nd:YAG/Cr^{4+}:YAG Microchip Laser

High-efficiency, compact ultra-violet (UV) sources are desirable for many applications, such as, ultrafast UV spectroscopy, photolithography, micromachining, *etc*.

We have developed a Nd:YAG/Cr^{4+}:YAG microchip laser which gives > 8 MW peak power at 100 Hz. We used LBO crystal to obtain 85% second harmonic generation (SHG) and a BBO crystal, grown by a new fluxless method, to obtain 60% fourth harmonic generation (FHG) as shown in Figure 2. A BBO crystal grown by the conventional flux technique can give only 40% FHG under identical conditions. We can obtain a stable pulse train having 3.4 MW peak power with 250 ps pulse width and 100 Hz repetition rate at 266 nm wavelength. We believe that this is the highest conversion efficiency reported so far for the BBO crystal in the generation of deep ultraviolet light.

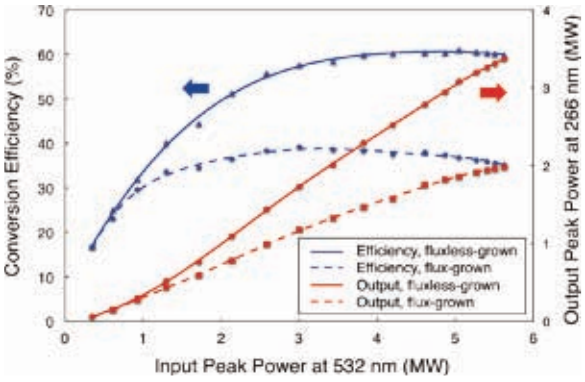

Figure 2. FHG conversion characteristics by different BBO crystal.

3. Lens-Less Edge-Pumped High Power Microchip Laser

A lens-less edge-pumped microchip laser was realized, which is directly pumped by single-emitter diode chips from multiple directions. Figure 3 shows the scheme of this laser head. The lens-less design makes the microchip laser more compact; the multi-direction designable pump schemes can realize desired pump shape. As a preliminary result, continuous wave output power of 32.5 W and slope efficiency of 45% was obtained by 9-direction pumped Yb:YAG ceramic

microchip. Further, 27.2 W single peak Gaussian beam was obtained by a small adjustment of the output mirror. Besides, watt-level high-order Hermite–Gaussian mode, doughnut-shape mode and vortex arrays were demonstrated as an evidence of designable pump scheme. Power scalability is easy by increasing the number of pump diodes to achieve hundred-watt-level high power microchip laser.

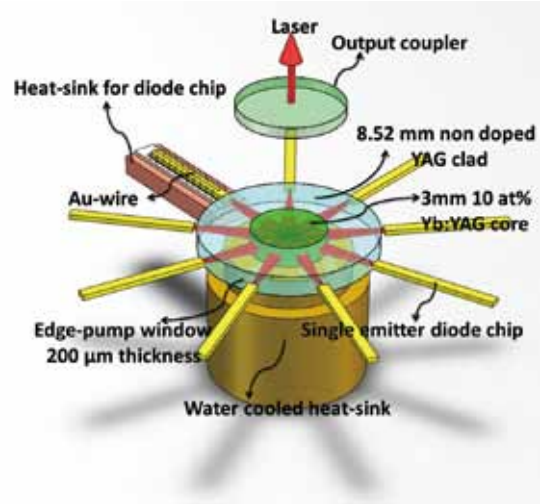

Figure 3. The scheme of lens-less edge-pumped microchip laser.

4. Temperature Dependencies of Stimulated Emission Cross Section for Nd-Doped Solid-State Laser Materials

Temperature dependencies of stimulated emission cross section for Nd:YAG, Nd:YVO_4, and Nd:$GdVO_4$ were carefully evaluated. Our spectral evaluations with fine spectral resolution were carried out under the condition that the population inversion was induced into samples by a weak pumping field. Within the temperature range from 15 °C to 65 °C, the variation of emission cross section at 1.06 μm in Nd:YAG was –0.20%/°C, while those in Nd:YVO_4 and Nd:$GdVO_4$ for π-polarization were –0.50%/°C and –0.48%/°C, respectively. Consideration of measured temperature dependence gave the numerical model for temperature dependent emission cross sections of Nd-doped solid-state laser materials. We have also presented numerical approximations of this model for our samples by a simple polynomial, which can be applicable as shown in Figure 4.

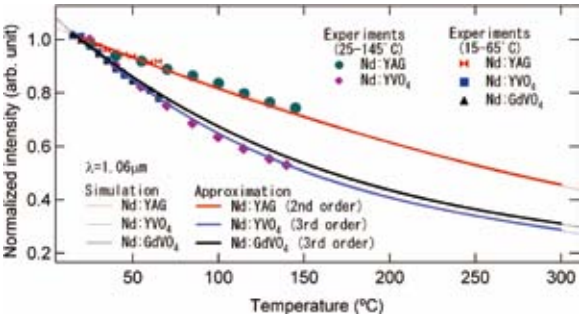

Figure 4. Temperature dependence of emission intensity of various Nd-doped laser media.

5. Fabrication of 10-mm-Thick Periodically Poled Mg-Doped Congruent $LiNbO_3$ Device for High-Energy Wavelength Conversion

Periodically poled Mg-doped congruent $LiNbO_3$ device with 10mm thickness of 32.2 μm period was fabricated by 33 kV pulse application. High-energy optical-parametric oscillation with half-joule-class output energy can be expected by joule-class pumping source in 10 ns pulse region.

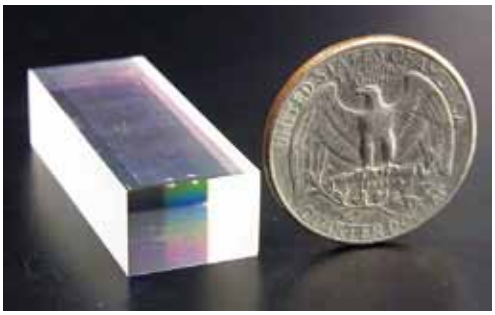

Figure 5. 10-mm-thick PPMgLN device with QPM period Λ = 32.2 μm.

References

1) M. Tsunekane and T. Taira, *The 59th Spring Meeting of the Japan Society of Applied Physics*, 15p-GP6-2 (2012).
2) R. Bhandari and T. Taira, *Opt. Mater. Express* **2**, 914–919 (2012).
3) W. Kong and T. Taira, *Appl. Phys. Lett.* **100**, 141105 (2012).
4) Y. Sato and T. Taira, *Opt. Mater. Express* **2**, 1076 (2012).
5) H. Ishizuki and T. Taira, *Technical Digest of CLEO2012*, CTh1B.1, San Jose, California, USA (May 16–21, 2012).

Ultrafast Laser Science

Laser Research Center for Molecular Science
Division of Advanced Laser Development

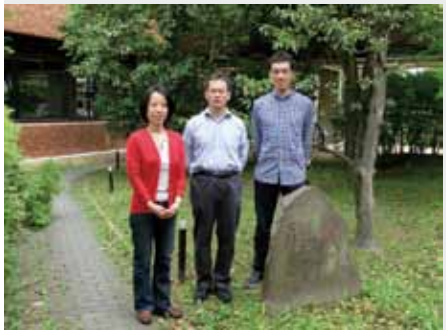

FUJI, Takao — Associate Professor
NOMURA, Yutaka — Assistant Professor
KAWAI, Shigeko — Secretary

Speed of ultrafast energy transfer from light to molecules (*i.e.* primary processes of photosynthesis, photoisomerization in visual pigments, *etc.*) is on the order of femtosecond (10^{-15} s). In our laboratory, we develop cutting edge lasers for such ultrafast molecular science, namely, femtosecond or attosecond (10^{-18} s) ultrashort pulse lasers.

For example, arbitrary waveform synthesis can be perf-ormed with simultaneous generation of femtosecond light pulses in various wavelength regions and superimposition of them with precisely controlled phases.

We would like to develop such advanced light control technology, which can push forward the research on ultrafast photochemical reactions.

1. Generation of Phase-Stable Half-Cycle Mid-Infrared Pulses through Filamentation in Gases[1)]

Filamentation of powerful ultrashort laser pulses in gases is one of the most interesting phenomena in nonlinear optics. The balance between self-focusing and plasma self-defocusing makes the pulse propagate much longer than the Rayleigh range with a very high intensity. It results in a dramatic enhancement of nonlinear processes occurring in the fila-mentation zone. This phenomenon enables high intensity pulse compression and efficient nonlinear wavelength conversion with gas media.

Enhanced nonlinear-optical processes in laser-induced filaments suggest a new strategy for the generation of ultra-short pulses of long-wavelength radiation. Ultrabroadband mid-infrared (MIR, 3–20 μm) pulse generation through fila-mentation in air was firstly demonstrated in 2007,[2)] and the technique was followed by several groups. Such MIR pulses with more than one octave at full width at half maximum are very attractive to be applied for molecular spectroscopy, *e.g.* two-dimensional infrared spectroscopy.

Here we report the latest progress of the ultrabroadband MIR pulse generation through filamentation. By using argon gas as the nonlinear medium and purging the optical path for the MIR pulse with the argon gas, a long tail of the pulse due to free induction decay of atmospheric carbon dioxide and water vapor disappeared, and it was possible to achieve gen-eration of high contrast MIR pulses. Full characterization of the pulse shape of the MIR field indicates that its pulse duration was 7.4 fs, which is about half-cycle period of the center wavelength (3.9 μm) of the pulse.

The experimental setup is shown in Figure 1. The light source was based on a Ti:Sapphire multi-pass amplifier system (Femtolasers, 800 nm, 25 fs, 0.9 mJ at 1 kHz). The second harmonic (ω_2, 25 μJ) and fundamental (ω_1, 675 μJ) pulses were spatially and temporally overlapped and focused into argon by a concave mirror (r = –1000 mm), generating a bright filament with a length of ~3 cm around the beam focus. This filament generated an MIR pulse (ω_0) through an ioni-zation-assisted wave mixing process ($\omega_1 + \omega_1 - \omega_2 \rightarrow \omega_0$). The energy of this MIR pulse was measured as ~250 nJ by using a pyroelectric detector (J-10MB-LE, Coherent). With this energy level, it is possible to apply the pulses for the nonlinear spectroscopy of condensed matter. The pulse-to-pulse intensity fluctuation was about 2.5% rms.

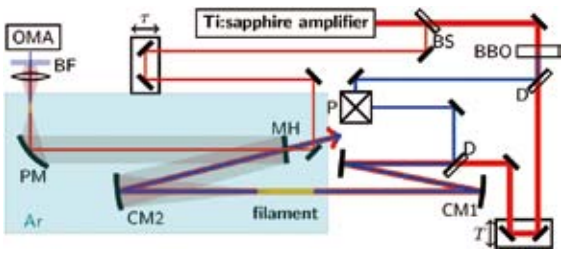

Figure 1. Schematic of the system. The shaded area was purged with argon. BS: beam splitter (5% reflection), BBO: β-BaB_2O_4 crystal (Type 1, θ = 29 deg, t = 0.1 mm), D: Dichroic mirror, P: Periscope, CM1: r = 1 m concave mirror, CM2: r = 0.5 m concave mirror, MH: Aluminium-coated mirror with a hole (ϕ = 7 mm), PM: Aluminium-coated parabolic mirror, BF: Bandpass filter for 335–610 nm (FGB37, Thorlabs), OMA: Spectrometer for ultraviolet region (USB2000+, OceanOptics).

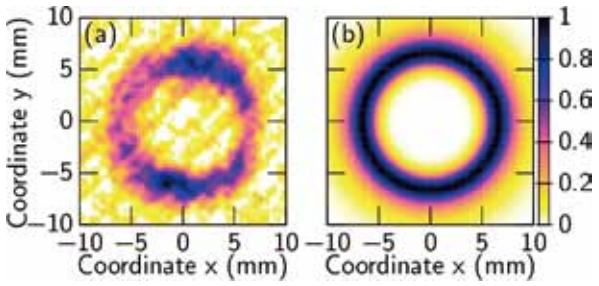

Figure 2. (a) Experimental and (b) simulated radial intensity distributions of the mid-infrared pulses.

The beam profile of the MIR beam after ZnSe and Si filters measured with a pyroelectric camera (Pyrocam III, Spiricon) is shown in Figure 2(a). The shape of the beam was ring and the angle of the cone was estimated to be about 3 deg. Some asymmetric shape and distortion from ideal ring pattern comes from residual pulse front tilt and/or astigmatism of the light source. The generated MIR pulse has basically pure one-direction linear polarization (>40:1) in the entire cross-section of the beam as the input pulses, which fact was confirmed with a wire grid polarizer (NT62-774, Edmund).

We compare the experimental result with FWM-beam analysis based on a straightforward integration of the FWM response over the beam overlap region. As can be seen from Figure 2(b), the simple approach provides an accurate agreement with the experimental result. It confirms that the ring-shaped beam profile originates from a dramatic confocal-parameter mismatch between the MIR field and the laser beams.

Additionally, the ~12 mm diameter beam was focused down to 1.0 mm with a r = 2 m concave mirror, indicating a reasonable focusability for a ring shaped spatial mode. The beam profile at the focal point. Although the beam may contain some angular dispersion, the dispersion is basically radially symmetric, and thus does not significantly deteriorate the good focusability of our MIR beam.

In order to quantitatively evaluate the temporal shape of the generated MIR pulse, we measured cross-correlation frequency-resolved optical gating (XFROG) We used argon again as a nonlinear medium and used four-wave mixing process ($\omega_1 + \omega_1 - \omega_0 \rightarrow \omega_2$) as a nonlinear interaction between the test pulse (MIR pulse) and the reference pulse. The scheme is free from spectral filtering caused by phase matching condition in the nonlinear interaction.

The system for the XFROG measurement is also shown in Figure 1. Small portion (~2 μJ) of the fundamental 25-fs pulse was used as a reference pulse. The reference pulse and the MIR pulse (test pulse) were combined through a mirror with a hole and focused into argon with an aluminium-coated parabolic mirror (f = 150 mm). Generated blue spectra (centered around 440 nm) were measured with a spectrometer (USB 2000+, OceanOptics) by scanning the delay time (τ in Figure 1) between the reference pulse and the MIR test pulse.

The measured and the retrieved XFROG traces are shown

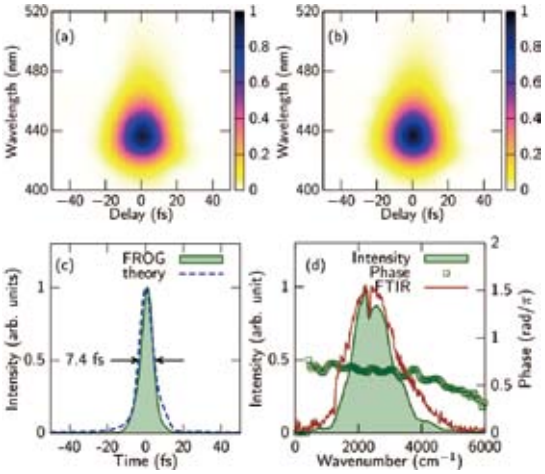

Figure 3. (a) Experimental and (b) retrieved XFROG traces. The retrieved pulse in (c) time and (d) frequency domain. The temporal profile from the 3D numerical simulation and the spectrum measured with Fourier transform spectrometer are also shown. Measured XFROG trace.

in Figure 2(a) and (b). The main feature of the trace indicates that the residual chirp of the test pulse is very small. The FROG error was 0.0009 with 256 × 256 grid. The retrieved time and frequency domain pictures are shown in Figure 2(c) and (d), respectively. The pulse width is estimated to be 7.4 fs, which is 0.57 cycles for 3.9 μm carrier wavelength. The retrieved spectrum is spread over whole MIR region (500–5000 cm^{-1}). The broadness of the spectrum was due to the weak dispersion of the medium, with the phase-matching length exceeding the length of the filament for all the MIR spectral components observed in the experiments.

In conclusion, ultrabroadband coherent MIR spectrum which covers the entire MIR region was generated through two-color filamentation. Due to the spatial and temporal quality, ultrashort MIR pulses generated in two-color filaments are ideal for numerous applications. In our experiments, MIR pulses as short as 7.4 fs were generated, which corresponds to about a half-cycle of 3.9 μm center wavelength.

The light source has a potential to change the situation of traditional MIR spectroscopy dramatically. For example, the coherent broadband MIR light source enables us to obtain absorption spectra through entire MIR region by single-shot with chirped pulse up-conversion technique. The reasonable quality of the spatial mode can be useful for efficient MIR microscope imaging combined with the up-conversion technique. Multi-dimensional spectroscopy for entire MIR region to monitor vibrational coupling among very different vibrational modes can be realized with the light source.

References

1) T. Fuji and Y. Nomura, *21th International Laser Physics Workshop (LPHYS'12)*, 5.2.1 Calgary, July 23–27 (2012). (invited talk)

2) T. Fuji and T. Suzuki, *Opt. Lett.* **32**, 3330–3332 (2007).

Visiting Professors

Visiting Professor
KONDOH, Hiroshi *(from Keio University)*

Surface Dynamic Processes Studied by Soft X-Ray Spectroscopy

Surface physics and surface chemistry have made significant progress in understanding of surface static structures but much less progress has been made with respect to understanding of surface dynamic processes. We have been interested in surface dynamic processes such as catalytic reactions at surfaces of metals and oxides. Recently we have been working on oxide photocatalysts using synchrotron radiation in a soft-x-ray region. In particular, we studied the geometric and electronic structures of N-doped TiO_2 at BL3U and BL6U in the UVSORII and determined the local structure of the doped nitrogen that induces the visible-light response of the photocatalyst. Another research subject concerns understanding of catalytic reactions on metal nanoparticles which proceed under practical working conditions. A soft x-ray absorption spectroscopy with the transmission mode has been developed at BL3U in such a way that real-time observations of catalytic processes under gas flow with ambient-pressure conditions can be conducted. Catalytic reactions over metal nanoparticles that are enhanced by absorption of the gas molecules inside the particles will be studied with this technique.

Visiting Professor
NODA, Susumu *(from Kyoto University)*

Strong Coupling of Single Atoms to Photonic Crystal Cavity Field

We have investigated photonic crystal structures which enable modification of propagation properties of an electromagnetic field and also tight confinement of the field to a tiny resonator. Accordingly the field strength inside the resonator is much enhanced and therefore the field can be strongly coupled to a quantum emitter such as a quantum dot even at a single photon level. Such a nanostructure device would be suitable for applications in optical communication and future quantum information processing in terms of its scalability. We have studied the strong coupling of the cavity field with a quantum dot and also the Purcell effect. Recently we have been interested in adopting a single cold atom as a quantum emitter, which shows much longer coherence time and therefore would be desirable for future application. Cold atoms are first loaded into a magneto-optical trap and then one of them is captured in tightly-focused optical tweezers. A movable lens-positioner can translate the position of the focal point, thereby transferring the trapped atom to the vicinity of the photonic crystal cavity. With this technique, the strong coupling of the single atom with the cavity field will be studied.

Visiting Professor
ITO, Atsushi *(from Tokai University)*

X-Ray Spectromicroscopy of Biomedical Specimens

Soft X-ray microscopy has a great advantage over other microscopies in the mapping of light elements or molecules containing such elements at high resolution. The mapping is realized by X-ray spectromicroscopy which utilizes unique spectral features of elements and molecules, that is, absorption edges and XANES profiles observed in the vicinity of the absorption edge. Our effort to apply spectromicroscopy to biomedical specimens has been focused on the mapping of sulfur oxidation state in human hair, because hair consists of mainly cystine, a sulfur-rich amino acid. Cystine is oxidized to cysteic acid by oxidative damage. Both products were found to have significantly different XANES peaks at the S-K absorption edge. Spectromicroscopy in combination with an electronic zooming tube as a two dimensional detector revealed that the oxidative damage was preferentially generated in the outer part of hair called cuticle. Furthermore a bleaching treatment of hair also increased the content of cysteic acid.

Visiting Associate Professor
TSUBOUCHI, Masaaki *(from Japan Atomic Energy Agency)*

Development of THz Tomography of Photo-Induced Carrier

We are developing a new technique for the THz tomography of photo-induced carriers in a semi-conductor based on the optical-pump THz-probe reflection spectroscopy. Since the photo-induced carrier strongly interacts with the THz light, the measurement and control of the carrier distribution and dynamics are significantly important to design THz optics using semi-conductors. Our THz tomography is a noncontact technique which determines both the dynamics and the spatial distribution of photo-induced carrier, simultaneously. We are demonstrating the THz tomography using photo-excited silicon (Si), and comparing the experimental results with the exact solutions of Maxwell's equations.

RESEARCH ACTIVITIES

Materials Molecular Science

Extensive developments of new molecules, molecular systems, and their higher-order assemblies are being conducted in three Divisions of Electronic Structures, Electronic Properties, and Molecular Functions, one division for visiting professors, and Research Center for Molecular Scale Nanoscience, in an attempt to discover new phenomena and useful functions. The physical properties of electronic, optical and magnetic properties on new functional materials are investigated, and moreover, the chemical properties like catalysis and photochemistry and technological applications like solar cells are also examined in this department.

Novel Properties of Magnetic Ultrathin Films Studied by *In Situ* Spectroscopic Methods

Department of Materials Molecular Science
Division of Electronic Structure

YOKOYAMA, Toshihiko	Professor
NAKAGAWA, Takeshi	Assistant Professor
TAKAGI, Yasumasa	Assistant Professor
EGUCHI, Keitaro	Graduate Student
NAKANO, Hirohito	Graduate Student*
FUNAKI, Yumiko	Secretary
TOYAMA, Yu	Secretary (Nanotechnology Platform project)
YASUI, Yuco	Secretary (Graduate school affairs)

Novel properties of magnetic metal ultrathin films have been attractive both from fundamental interest and from technological requirements. We are especially interested in drastic modification of metal thin films through the film–substrate interaction and/or a surface chemical treatment. The magnetic properties are characterized by means of several kinds of *in situ* spectroscopic methods like MOKE (Magneto-Optical Kerr Effect) using UV-visible lasers and XMCD (X-ray Magnetic Circular Dichroism) using synchrotron radiation soft X-rays, and UV magnetic circular dichroism photoelectron emission microscopy (UV MCD PEEM) using such ultrashort pulsed UV lasers.

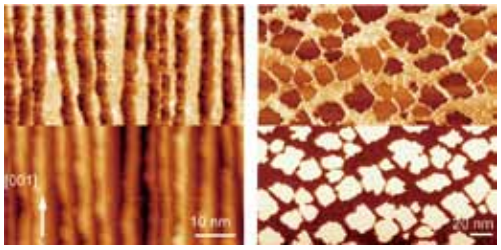

Figure 1. STM images of nanowires for Fe 0.3 ML (~6 atom width) (left) and nanodots for Fe 0.4 ML. The top and bottom panels correspond to the spin-polarized *dI*/*dV* and topographic images, respectively. The right-top panel clearly shows magnetically single domain dots (arrows denote the magnetization directions along [1-10]).

1. Giant Magnetic Anisotropy and Coercivity in Fe Island and Atomic Wire on W(110)[1)]

Hard magnets is an important industrial material both for data storage and power applications like electromotive actuators and power generators. Although the magnetic energy product (BH_{max}) that characterizes hard magnets has improved in the last century, rare earth (RE) magnets like $Nd_2Fe_{14}B$ have marked a saturation of the maximum available value of BH_{max} = 500 kJ/m^3 since 1990. Moreover, the replacement of the RE has been demanded due to the scarcity of RE, and novel approaches to improve hard magnets have attracted interests. Magnetic nanostructures with single atomic layers have a possibility to manifest prominent magnetic properties such as magnetocrystalline anisotropy energy (MAE) and coercivity (H_c) that remarkably differ from the properties of bulk materials. The Fe monolayer on W(110) has been extensively studied as an ideal two-dimensional ferromagnetic system with a pseudomorphic growth mode and an extremely large strain due to a large difference in the lattice constants between Fe and W. Owing to its extreme hard magnet character, the anisotropy energy or the coercivity has not been directly determined from the hard axis magnetization curve measurements. In this work, we directly measure the giant MAE as well as large coercivity in Fe nanodots and nanowires grown on W(110) by using our ultrahigh vacuum superconducting magnet XMCD system installed in UVSOR-II. A remarkable difference between the dots and the stripes is found in the coercivity, although the MAE is similar for both systems.

Figure 1 shows the spin-polarized and topographic STM (scanning tunnel microscopy) images of Fe nanowires and nanodots. The measurements were performed in Johannes Gutenberg Mainz University through the collaboration with Prof. H. J. Elmers group. In the spin-polarized STM image of the nanodots, a clear contrast (darker and brighter islands) can be seen, implying that the nanodots are magnetically ordered as single domains with the magnetization easy axis of the [1-10] crystal axis.

Figure 2 shows the anisotropic magnetization curves of Fe 0.25 ML nanodots and nanowires at 5 K taken by measuring the Fe L_3-edge circularly polarized X-ray absorption intensities using Beamline 4B at UVSOR-II. The G.I.[1-10] and G.I.[001] directions imply that the magnetization direction is tilted by 35° toward the surface normal with respect to the given crystal axis direction. The apparent coercivities are found to be larger than ~4 T for both the nanodots and nanowires. The anisotropic magnetic field, which is obtained by the extrapolation of the hard-axis magnetization curve (green lines in Figure 2) up to the saturated magnetization, can be esti-

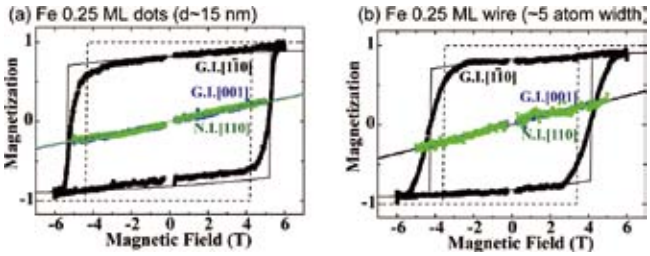

Figure 2. Anisotropic magnetization curves of 0.25 ML Fe nanodots (a) and nanowires (b) at 5 K. The data were recorded by measuring the Fe L_3-edge circularly polarized X-ray absorption intensities. Huge coercivities along the [1-10] easy axis (black lines) and anisotropic magnetic fields along the hard axes (green) were observed for both nanodots and nanowires.

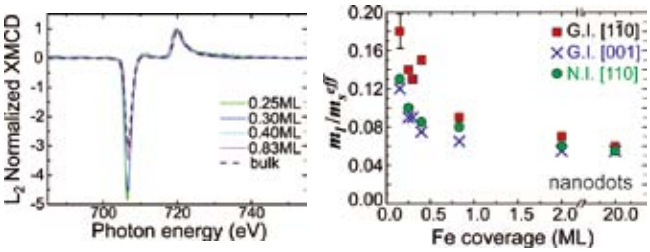

Figure 3. (left) Fe L-edge XMCD spectra of Fe nanodots on W(110) at 5 K along the G.I.[1-10] axis. (right) Ratio of the orbital magnetic moment (m_l) relative to the effective spin magnetic moment (m_s^{eff}). Smaller nanodots (lower Fe coverage) show larger orbital magnetic moments.

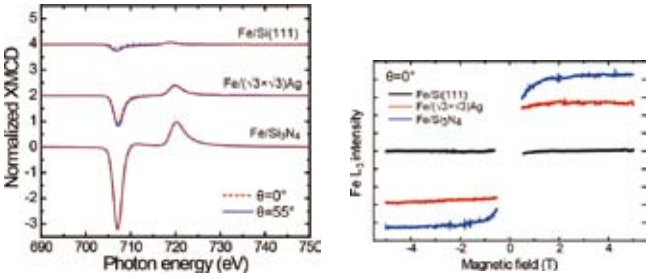

Figure 4. (left) Fe L-edge XMCD of Fe on clean Si(111) (1.6 ML), Ag/Si(111) (2.0 ML) and Si_3N_4 (1.6 ML) at H = ±5 T and T = 5 K. The X-ray incidence angles θ are 0° (normal incidence) and 55° (grazing). (right) Magnetization curves of Fe on clean Si(111) (1.6 ML, black), Ag/Si(111) (2.0 ML, red) and Si_3N_4 (1.6 ML, blue), taken at T = 5 K and θ = 0°.

mated to be >15 T. Huge magnetic anisotropy can be concluded both for the nanodots and nanowires. By fitting the experimental data with a simple anisotropic magnetic energy model, the magnetic anisotropic constants were determined to be ~1 meV for both the in-plane and out-of-plane directions, which is a few hundred times larger than that of bulk *bcc* Fe.

Figure 3 shows the Fe L-edge XMCD spectra of the nanodots at 5 K. The spectra were normalized with the L_2-edge peak tops. As the Fe coverage (nanodot size) decreases, the L_3-edge negative peak intensity increases drastically, implying a larger orbital magnetic moment as shown in the right panel of Figure 3. The orbital magnetic moment of the edge Fe atoms may be enhanced.

2. Magnetic Properties of Fe Nanostructures on Si_3N_4/Si(111)-(8×8) and Ag/Si(111)-(√3×√3)R30°[2)]

The magnetic properties of ferromagnetic transition metals on Si substrates have been widely investigated for the exploitation of new magnetic devices. Since clean Si surfaces react with transition metals very easily to form usually non-magnetic transition-metal silicides, it is essential to insert some inert film between transition metals and Si substrate. No reports have been however published for epitaxially ordered substrates on Si(111). In the present study, we investigated growth processes and magnetic properties of Fe deposited on well-defined Si_3N_4/Si(111)-(8×8) and Ag/Si(111)-(√3×√3) R30° by using STM and XMCD.

Figure 4 show the Fe L-edge XMCD spectra and the corresponding magnetization curves of Fe deposited on Si_3N_4/Si(111)-(8×8), Ag/Si(111)-(√3×√3)R30° and clean Si(111)-(7×7). It is clearly found that the Fe XMCD signals is enhanced in the sequence of Si(111) < Ag/Si(111) < Si_3N_4/Si(111). The XMCD sum-rule analysis yields the spin magnetic moments as m_s = 0.17 μ_B (clean), 1.25 μ_B (Ag), and 2.62 μ_B (Si_3N_4). On clean Si(111)-(7×7), the spin magnetic moment is almost quenched. On the contrary, Fe/Si_3N_4 has a much larger spin magnetic moment, which is even larger than that of *bcc* bulk Fe (2.2 μ_B). Fe/Ag/Si(111) shows a intermediate property. Such a drastic difference among the three substrates is caused by the fact that the Si_3N_4 substrate most effectively suppresses the silicide formation. Moreover, it is also found that the magnetic moment of Fe on Ag/Si(111) is lost quite easily by annealing at 500 K (m_s = 0.32 μ_B), while that of Fe on Si_3N_4 is sufficiently kept even when the sample is annealed at 500 K (m_s = 2.19 μ_B).

References

1) T. Nakagawa, Y. Takagi, T. Yokoyama, T. Methfessel, S. Diehl and H.-J. Elmers, *Phys. Rev. B* **86**, 144418 (2012).
2) K. Eguchi, Y. Takagi, T. Nakagawa and T. Yokoyama, *Phys. Rev. B* **85**, 174415 (2012).

* carrying out graduate research on Cooperative Education Program of IMS with Kyoto University

Design and In-Situ Characterization of Catalyst Surfaces

Department of Materials Molecular Science
Division of Electronic Structure

TADA, Mizuki	Associate Professor
MURATSUGU, Satoshi	Assistant Professor
MAITY, Niladri	Post-Doctoral Fellow
ZHANG, Shenghong	Post-Doctoral Fellow
SAIDA, Takahiro	Post-Doctoral Fellow
WAKI, Minoru	Post-Doctoral Fellow
SODE, Aya	Post-Doctoral Fellow
THUMRONGPATANARAKS, Wipavee	JENESYS Program Visiting Scientist
GAN, Raymond	Visiting Scientist*
JIANG, Lu	Visiting Scientist*
LIM, Min Hwee	Visiting Scientist*
WANG, Fei	Graduate Student
ISHIGURO, Nozomu	Graduate Student†
FUNAKI, Yukino	Technical Fellow
USUI, Chika	Technical Fellow
GONDO, Makiko	Technical Fellow
FUKUTOMI, Yukiyo	Secretary

1. Preparation and Catalytic Performances of a Molecularly Imprinted Ru-Complex Catalyst with an NH_2 Binding Site on SiO_2

The potential of immobilized metal-complex catalysts remarkably interplays with the nature of support surfaces, resulting in significant rate enhancements and unique catalytic performances that their homogeneous counterparts do not exhibit. We proposed the design of molecularly imprinted metal-complex catalysts on SiO_2 surfaces, whose ligand was used as a template, and molecularly imprinted metal-complex catalysts have been applied for selective catalysis.

Natural enzymes, which are quite selective catalysts for particular reactants, possess highly sophisticated catalytic systems with active metal species, shape-selective reaction space, and molecular recognition sites spatially arranged for the particular reactants. Artificial design of such a sophisticated catalytic system is still difficult and the preparation of both catalytically active site and shape-selective reaction space with spatially arranged molecular binding sites. We have prepared a molecularly imprinted Ru-complex catalyst with NH_2 binding site on the wall of a molecularly imprinted cavity toward the shape-selective transfer hydrogenation catalysis.[1)]

A template alcohol, which was the template for *o*-fluorobenzophenone hydrogenation, was coordinated to a SiO_2-supported Ru complex (Ru-*N*-*p*-styrenesulfonyl- 1,2-diphenylethylenediamine) and the hydrolysis polymerization of tetramethoxysilane produced SiO_2-matrix overlayers surrounding the supported Ru complex on the surface. A carbamate group (-NHCOO-) connected to a silane-coupling moiety (-Si$(OC_2H_5)_3$) was tethered to the alcohol template and the cleavage of the carbamate moiety after hanging the silane-coupling branch on the wall of a molecularly imprinted cavity produced a spatially arranged NH_2 binding site for the hydrogenation of *o*-fluorobenzophenone as shown in Figure 1.

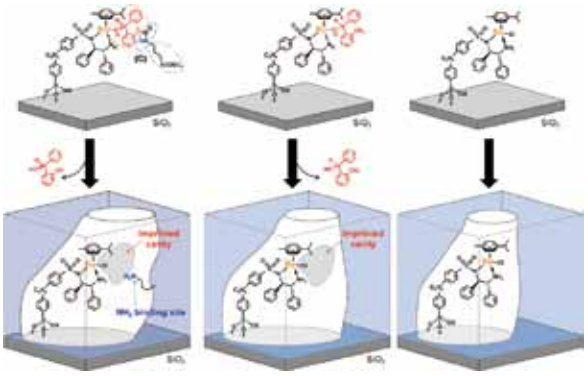

Figure 1. Preparation of molecularly imprinted Ru catalysts with an imprinted cavity with an NH_2 binding site on the wall of the cavity, with an imprinted cavity without an NH_2 binding site, and without an imprinted cavity.

We prepared three catalysts with a molecularly imprinted cavity with an NH_2 binding site, with a molecularly imprinted cavity without an NH_2 binding site, and without a cavity of the template illustrated in Figure 1. The catalytic performances of the transfer hydrogenation of *o*-fluorobenzophenone were significantly different between these three catalysts under identical reaction conditions. The transfer hydrogenation did not proceed at all on the catalyst prepared without the template. On the other hand, other two catalysts prepared with the templates exhibited activity for the hydrogenation, but we

found differences in the hydrogenation rates of *o*-fluorobenzophenone and *o*-methylbenzophenone. These two reactants have similar shapes to each other, but *o*-fluorobenzophenone with F group, which can interact to the NH_2 binding site by hydrogen bonding, was preferably hydrogenated on the molecularly imprinted catalyst with the NH_2 binding site. Such differences in the hydrogenation activity were not observed on the imprinted catalyst without the NH_2 binding site. The NH_2 binding site promoted the preferable adsorption of the specific molecule that can interact with the molecular binding site, resulting in increase in the transfer hydrogenation activity. The strategy is promising to create an artificial enzymatic catalyst surfaces in the future.

2. Operando Time-Resolved XAFS for Surface Events on Pt_3Co/C and Pt/C Cathode Catalysts in Practical PEFCs during Voltage-Operating Processes

Polymer electrolyte fuel cells (PEFCs) are among the most efficient clean energy technologies, but practical application in automobiles remains challenging because of the high cost and insufficient durability of cathode catalysts. To improve fuel-cell performance and cathode catalyst durability, alloying of Pt with 3*d* transition metal elements is a promising approach. Pt-Co alloy is a representative of the Pt-alloy cathode catalysts and has been reported to be more active and durable than Pt/C catalysts. Although electrochemical surface events have been extensively investigated, the structural kinetics of the transformations of catalyst themselves and the ORR reaction mechanism on practical Pt-Co catalysts have not been established. *In situ* time-resolved QXAFS spectra at the Pt L_{III}-edge and Co *K*-edge were measured at 500 ms intervals, and the analysis of the series of the operando QXAFS spectra for the PEFC bimetal cathode catalyst revealed the rate constants of electron transfer, changes in the charge density of Pt_3Co nanoparticles, and changes in the local coordination structures with Pt–Pt, Pt–Co, Co–Co, and Pt–O bonds for the first time (Table 1).[2)]

We compared the reaction mechanism and structural kinetics on the Pt_3Co/C and Pt/C catalysts under similar fuel-cell operating conditions. It is to be noted that all the rate constants on the Pt_3Co/C catalyst were larger than the corresponding rate constants on the Pt/C catalysts. During the 1.0 V → 0.4 V process, for example, Pt–Pt bond breaking on the Pt_3Co/C catalyst was 1.5-fold to that on the Pt/C catalyst. The rate constant of Pt–O bond breaking (k'_{Pt-O}), which is highly related to the ORR activity of the cathode catalyst, was about 4 times higher on Pt-Co/C (0.4 s^{-1}) than on Pt/C (0.11 s^{-1}). There were also a significant difference in the rate constant of Pt–Pt bond re-formation (k'_{Pt-Pt}), on Pt_3Co/C (0.3 s^{-1}) and Pt/C (0.078 s^{-1}), which may be relevant for realizing better catalyst durability of the Pt_3Co/C catalyst.

The irreversible oxidation of the Pt catalysts depends on the difference in rate between oxidation and reduction of the Pt catalysts during voltage cycling. The repeated cycling on oxidized Pt species which could not be recovered causes extensive dissolution of the Pt cathode catalyst. Pt_3Co alloy systems facilitate reversible oxidation/reduction in the voltage-cycling processes. The structural kinetics determined from the *in situ* time-resolved XAFS revealed that all the rate constants of the surface events on the Pt_3Co/C cathode catalyst were higher than those on Pt/C, particularly the reduction steps involving Pt–O bond breaking. Reversible redox cycles on Pt_3Co alloys are suggested as a key factor in the superior performance of Pt_3Co alloy cathode catalysts in PEFCs. Understanding of the fundamental issues of the structural kinetics of the catalyst surface events by *in situ* time-resolved XAFS establishes new boundaries for the regulation and operation of fuel cells.

Table 1. Rate constants for Pt_3Co/C and Pt/C MEAs in voltage-cycling processes by operando time-resolved XAFS.

Process		Rate constant /s^{-1}	
		Pt_3Co/C	Pt/C
0.4 → 1.0 V	XANES white-line height	0.12 ± 0.02	0.073 ± 0.001
	CN (Pt–Pt)	0.13 ± 0.03	0.088 ± 0.008
	CN (Pt–Co)	No change	–
	CN (Pt–O)	0.10 ± 0.03	0.076 ± 0.009
	charge in the fuel cell	2.86 ± 0.04	1.84 ± 0.02
		0.258 ± 0.003	0.167 ± 0.001
1.0 → 0.4 V	XANES white-line height	0.24 ± 0.05	0.14 ± 0.03
	CN (Pt–Pt)	0.3 ± 0.1	0.078 ± 0.009
	CN (Pt–Co)	No change	–
	CN (Pt–O)	0.4 ± 0.2	0.11 ± 0.02
	charge in the fuel cell	3.68 ± 0.03	2.16 ± 0.01
		0.484 ± 0.002	0.259 ± 0.001

References

1) Y. Yang, Z. Weng, S. Muratsugu, N. Ishiguro, S. Ohkoshi and M. Tada, *Chem. –Eur. J.* **18**, 1142–1153 (2012).
2) N. Ishiguro, T. Saida, T. Uruga, O. Sekizawa, S. Nagamatsu, K. Nitta, T. Yamamoto, S. Ohkoshi, Y. Iwasawa, T. Yokoyama and M. Tada, *ACS Catal.* **2**, 1319–1330 (2012).

Award

ISHIGURO, Nozomu; Student Presentation Award (JXAFS 14).

* IMS International Collaboration Program

† carrying out graduate research on Cooperative Education Program of IMS with The University of Tokyo

Studies of Field-Effect-Transistor Based on Highly-Correlated Molecular Materials

Department of Materials Molecular Science
Division of Electronic Properties

YAMAMOTO, Hiroshi — Professor (April, 2012–)
URUICHI, Mikio — Technical Associate
SHIMIZU, Atsuko — Secretary

Field effect transistor (FET) with organic molecules as a channel material is under intense studies because of its application possibilities such as flexible, printable, and large-area electronic devices. Despite such a thorough investigation on single-component neutral molecules to pursuit high performance (say, high mobility *etc*.) in FET uses, few studies are known for compound organic semiconductor- based transistors. We have been exploiting FET devices with charged molecular materials, namely cation-radical salts of electron-donating molecules (donors) such as BEDT-TTF and anion-radical salts of electron accepting molecules (acceptors) such as $Ni(dmit)_2$. Among these materials, our focus concentrates in Mott-insulators in which Coulomb interaction among carriers blocks metallic transport. In this highly correlated situation of charge carriers, Mott insulator stays in a fragile semiconducting state, where carrier injection, chemical and/or physical pressure (or strain), and thermal fluctuation can drive it into a metallic state by phase transition (*i.e.* Mott transition: Figure 1). Since the carrier density (band-filling) of a FET interface can be finely modulated by an electrostatic field from the gate electrode, it is anticipated that the Mott-insulating state can be switched to a metallic state by a field effect. Indeed, our previous work showed such an insulator-to-metal transition in terms of the band structure, and these results provide not only a possibility of application use of organic Mott-FET but also a significant insight into the mechanism of Mott transition itself. We are now expanding our research target both to the superconducting transition of Mott-FET and to its room-temperature operation.
(BEDT-TTF = bis(ethylenedithio)tetrathiafulvalene,
dmit = 1,3-dithiole-2-thione-4,5-dithiolate)

1. Field-Induced Superconductivity in an Organic Mott-FET

κ-(BEDT-TTF)$Cu[N(CN)_2]Br$ (κ-Br) is an organic superconductor whose electronic state is Mott-insulating at room-temperature but turns into metallic at low temperature through a crossover around 50–100 K, possibly because of an increase of bandwidth upon thermal contraction. In our previous works, a tensile strain altered its ground state into a Mott-insulating state, when its thin (100–300 nm) crystal is laminated on top of SiO_2/Si^{++} substrate and cooled down to low temperature.

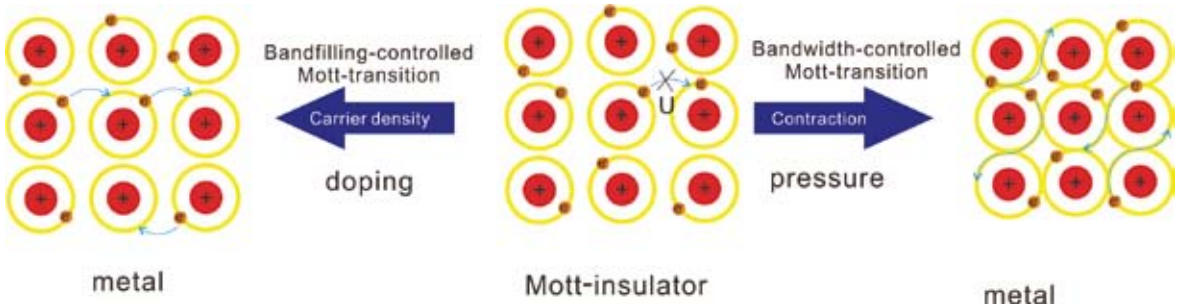

Figure 1. Concept of a Mott-insulator (center) along with its bandfilling-controlled (left) and bandwidth-controlled (right) Mott transitions. When the band is half-filled and band energy is small, the carriers are localized because of on-site Coulomb interaction (*U*). This situation is broken down either by changing the carrier concentration or by compressing the lattice. In many cases, the Mott transitions are associated with superconductivity at the boundary between metallic and insulating phases.

Although the electronic state at low temperature became completely insulating in this experiment because of the very small thermal expansion coefficient of Si substrate (2 ppm/K), one can anticipate from the *T–P* (temperature *vs.* pressure) phase diagram that somehow mixed electronic state between superconducting and Mott-insulating states can be realized when the tensile strain is much weaker. To achieve such a mixed state in the device, where phase-separation occurs between superconducting and Mott-insulating states, we have chosen Nb-doped $SrTiO_3$ as a back-gate substrate because of its larger thermal expansion coefficient (*ca.* 10 ppm/K) than Si. An aluminum oxide layer was grown by atomic layer deposition technique to form a gate dielectric on the substrate. After lamination process of κ-Br on the substrate, the Mott-FET device which showed a weakly insulating behavior at low temperature was fabricated (Figure 2). Upon applying a positive gate voltage, however, the resistivity goes down and weakly metallic behavior was observed at $V_G > 2$ V. By further increasing the gate voltage up to 8 V, the device showed a sudden drop of resistivity around 5 K, which can be attributed to superconductivity. Taking account of bistable IV characteristics observed in the low resistance region, the above transition can be understood as a percolation transition of superconducting islands that is induced by the electrostatic doping of electrons. The transition temperature increases as the gate voltage rises and saturates around $V_G = 11$ V. The above result is the first example of field-induced superconductivity in organic materials, and can be utilized for uncovering a phase diagram of organic Mott system in the band filling controlled regime.

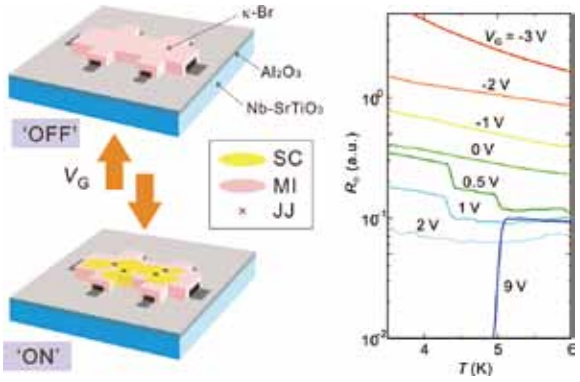

Figure 2. The device structure and temperature dependency of device resistance under various gate voltages. The device comprises κ-Br thin-layer single crystal and $Al_2O_3/SrTiO_3$ substrate. By applying a positive gate voltage, the resistance of the device starts decreasing, while a negative gate voltage results in an increase of the resistance. Although superconducting (SC) and Mott-insulating (MI) phases are separated in the device, the four-terminal resistance drops to zero when the Josephson junction (JJ) network forms a pathway to shunt the voltage terminals. This kind of percolation transition is clearly observed in the right panel, where the resistance drops at 5 K with a gate voltage of 9 V.

2. Operation of Organic Mott-FET at Higher Temperature

In order to operate the organic Mott-FET at higher temperature, hopefully at room temperature, it is necessary to realize much larger Mott gap energy and thinner crystal thickness. For this purpose, we are examining several strategies in parallel.

κ-(BEDT-TTF)$Cu[N(CN)_2]Cl$ (κ-Cl) is a Mott-insulator with larger Mott gap than κ-Br and is therefore suitable for examining the influence of an increase in Mott-gap energy on the device performance. For example, it has higher resistance than κ-Br and exhibit better ON/OFF ratio. In addition, it always shows ambipolar behavior, probably because of its clean surface (Figure 3). This situation allows us to analyze the critical exponents of filling-controlled Mott transition, which will give us important information about ON/OFF efficiency of the device. Because it is also possible to control the Mott gap energy by applying a mechanical strain, κ-Cl device provides an ideal platform to expand Mott-FET strategy to higher temperature.

Another candidate of the channel material for Mott-FET that can be used at room temperature is (BEDT-TTF)(TCNQ). We are exploiting this material both in a crystalline and amorphous form to find a better FET setup for simple but highly efficient device at room temperature. (TCNQ = tetracyanoquinonedimethane)

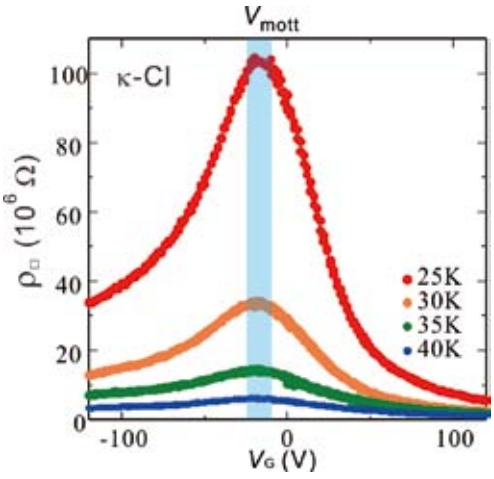

Figure 3. Gate voltage dependence of the resistance for κ-Cl based Mott-FET. Because this device clearly shows ambipolar behavior due to a smaller number of mid-gap trap states, it is possible to exactly define the gate voltage for charge neutrality point (V_{Mott}). This fact helps determining the critical exponent for Mott transition, which is important both for theoretical investigation and for analyzing device parameters such as subthreshold swing.

Reference

1) Y. Kawasugi, H. M. Yamamoto, N. Tajima, T. Fukunaga, K. Tsukagoshi and R. Kato, *Phys. Rev. B* **84**, 125129 (9 pages) (2011).

Magnetic Resonance Studies for Molecular-Based Conductors

Department of Materials Molecular Science
Division of Electronic Properties

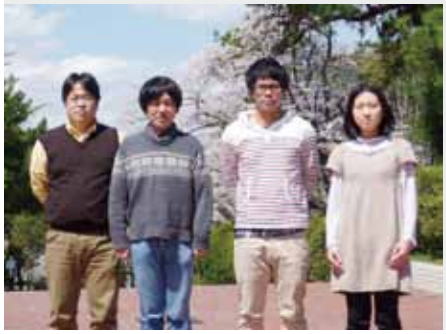

NAKAMURA, Toshikazu	Associate Professor
FURUKAWA, Ko	Assistant Professor
TAKAHASHI, Seiya	Graduate Student*
ABE, Hitomi	Secretary

Magnetic resonance measurements are advantageous for studying fundamental electronic properties and for understanding the detailed electronic structures of molecular based compounds. Developing an understanding of the electronic phases and functionality of these materials enables us to perform systematic investigations of low-dimensional, highly-correlated electron systems and functional materials. Competition between the electronic phases in molecular-based conductors has attracted much attention. The investigations of such electronic phases by magnetic resonance measurements are important to understanding unsolved fundamental problems in the field of solid state physics, and to explore novel functionalities in the field of material science.

In this study, we performed broad-line NMR and ESR measurements on molecular-based conductors to understand electron spin dynamics and functionality in low-temperature electronic phases.

1. ^{13}C NMR Study of the Magnetic Properties of the Quasi-One-Dimensional Conductor, $(TMTTF)_2SbF_6$

Magnetic properties in the quasi-one-dimensional organic salt, $(TMTTF)_2SbF_6$, where TMTTF is tetramethyltetrathiafulvalene, are investigated by ^{13}C NMR under pressures. Antiferromagnetic phase transition at ambient pressure (AFI) is confirmed. Charge ordering is suppressed by pressure and is not observed under 8 kbar. For $5 < P < 20$ kbar, a sharp spectrum and the rapid decrease of the spin-lattice relaxation rate $1/T_1$ were observed below about 4 K, which is attributed to a spin-gap transition. Above 20 kbar, an extremely broadened spectrum and a critical increase of $1/T_1$ were observed. This indicates that the system enters into another antiferromagnetic phase (AFII) under pressure. The slope of the antiferromagnetic phase transition temperature T_{AFII}, dT_{AFII}/dP, is positive, while T_{AFI} decreases with pressure. The magnetic moment is weakly incommensurate with the lattice at 30 kbar.

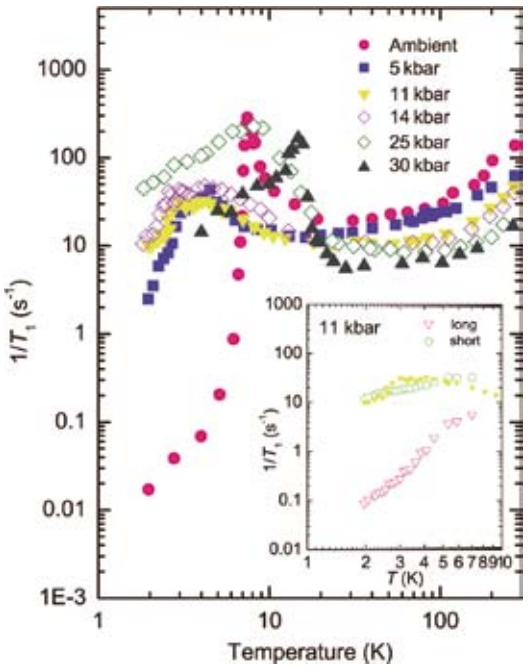

Figure 1. Temperature dependence of the ^{13}C-NMR spin-lattice relaxation rate, $1/T_1$, at six different pressures.

2. Time-Resolved ESR Study for Photoconductive Mechanism of Photoconductive TTF-Derivatives

The spin dynamics of photoconductive ethylene-dithiolo-tetrathiafulvalene (EDT-TTF) containing 1,3-benzothiazole (BTA) was examined for froze solution and powdered samples using time-resolved electron spin resonance (TR-ESR) spectroscopy. While the TR-ESR signal of a frozen solution sample under visible excitation were attributed to the excited triplet state $\mathbf{T_1}$, that of the powdered indicates a charge-separated state. It is a characteristic feature of molecular assembled system.

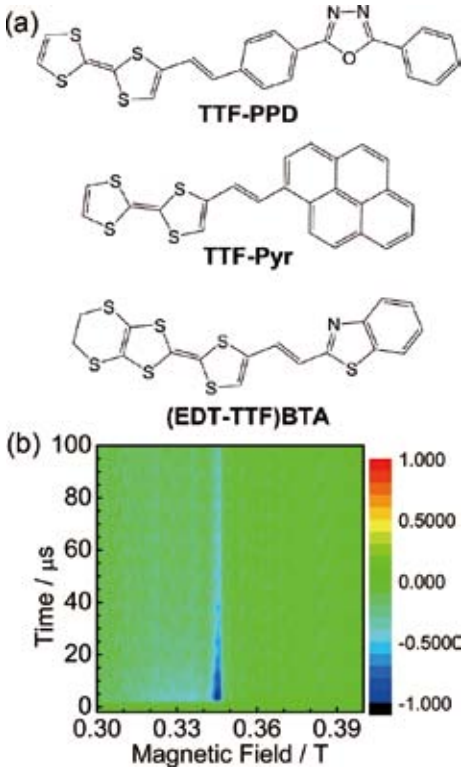

Figure 2. (a) Molecular structure of single-molecule-type photoconductive materials, TTF and EDT-TTF derivatives. (b) 2D pulsed TR-ESR spectra for powder sample of photoconductive EDT-TTF containing BTA. The normal axis represents the ESR signal intensity. The color scale denotes the signal intensity. Positive and negative values indicate the absorption and emission of microwaves, respectively.

3. Physical Properties of a Molecular Conductor $(BEDT\text{-}TTF)_2I_3$ Nanohybridized with Silica Nanoparticles by Dry Grinding

The dry grinding of a mixture of bis(ethylenedithio)tetrathiafulvalene (BEDT-TTF) and silica nanoparticles has produced powdery (BEDT-TTF)–silica nanocomposites. The (BEDT-TTF)–silica nanocomposites are readily doped with iodine in hexane dispersion to give powdery nanocomposites of $(BEDT\text{-}TTF)_2I_3$–silica. XRD and TEM measurements suggest that $(BEDT\text{-}TTF)_2I_3$ in the nanocomposite exists as shell layers of core-shell-type nanoparticles and as nanometre-sized crystals incorporated into hollow sites of aggregated silica nanoparticles. Magnetic susceptibility measurements reveal that the nanocomposites accompanied a large number of Curie spins attributable to surface molecules of the core-shell-type nanoparticles. The nanocomposites show a magnetic susceptibility change corresponding to the metal–insulator transition of α-$(BEDT\text{-}TTF)_2I_3$ in a broad temperature range of 110–140 K, which is attributed to the properties of the nanocrystalline components. Doping in diethyl ether dispersion leads to higher amounts of the nanocrystalline component being obtained. The doping of (BEDT-TTF)–silica nanocomposites by dry grinding produces a paramagnetic powder containing amorphous $(BEDT\text{-}TTF)_2I_3$, which possesses a Curie spin concentration of 50%. The effects of annealing on these nanocomposites are investigated. The electrical conductivity of the compaction pellets of (BEDT-TTF)–silica nanocomposites is enhanced by iodine doping to reach approximately 10^{-6} S cm^{-1}, but the value is much lower than that of the bulk crystals (10^1 S cm^{-1}).

4. Electronic Properties and ^1H Dynamics in Self-Doped Organic Conductor $(TTFCOO)[(NH_4^{+1})_{1-x}(NH_3)_x]$

^1H-NMR and High-Field ESR measurements were carried out for self-doped type organic conductor, $(TTFCOO)[(NH_4^{+1})_{1-x}(NH_3)_x]$ and its deuterated salt. $(TTFCOO)[(NH_4^{+1})_{1-x}(NH_3)_x]$ and related salts are TTF-based self-doped hydrogen-bonding conductor developed by NIMS group. The TTF-skeleton stacks to form a one-dimensional column. The pristine $TTFCOONH_4$ molecule is closed-shell. Self-doped type carrier is generated by substitution of the end group of (NH_3^0) with (NH_4^{+1}), which is regarded as a charge-reservoir. Actually, a considerable concentration of NH_3 molecules has been confirmed by X-ray photoelectron spectroscopy data. According to the static magnetic susceptibility and high-field ESR measurements, we found that the observed spin was distributed on quasi-hole-like TTF skeletons, and that the TTFCOO mainframe partially becomes a neutral radical. The spin susceptibility was well fitted with a Curie-Weiss term and an activation-type term. The activation-type term was dominant at high temperatures.

In order to clarify the ^1H dynamics, we carried out ^1H-NMR measurements for pristine and deuterated salts. The ^1H-NMR spin-lattice relaxation rate, $^1H\text{-}T_1^{-1}$, of indicates a characteristic temperature and frequency dependence. A pronounced peak observed at around 200 K is possibly due to molecular motion. Since the relaxation curve is not single component below 200 K, we assumed the $^1H\text{-}T_1^{-1}$ from initial slope (weighted average). Below 100 K $^1H\text{-}T_1^{-1}$ follows $T^{0.5}$, and remains frequency dependence, indicating a 1D spin-diffusion type relaxation. However, the Fermi surface of $(TTFCOO)[(NH_4^{+1})_{1-x}(NH_3)_x]$ is considered to be 2D, according to the tight-binding band calculation. This discrepancy is an open question at present.

References

1) F. Iwase, K. Sugiura, K. Furukawa and T. Nakamura, *Phys. Rev. B* **84**, 115140 (7 pages) (2011).
2) K. Furukawa, Y. Sugishima, H. Fujiwara and T. Nakamura, *Chem. Lett.* **40**, 292–294 (2011).
3) A. Funabiki, H. Sugiyama, T. Mochida, K. Ichimura, T. Okubo, K. Furukawa and T. Nakamura, *RSC Adv.* **2**, 1055–1060 (2012).

* carrying out graduate research on Cooperative Education Program of IMS with Yokohama National University

Design of Porous Polymer Frameworks

Department of Materials Molecular Science
Division of Molecular Functions

JIANG, Donglin	Associate Professor
NAGAI, Atsushi	Assistant Professor
LIU, Xiaoming	Post-Doctoral Fellow
GUO, Zhaoqi	Post-Doctoral Fellow
LIN, Jianbin	Post-Doctoral Fellow
XU, Yanhong	Graduate Student
DING, Xuesong	Graduate Student
JIN, Shangbin	Graduate Student
CHEN, Xiong	Graduate Student
FENG, Xiao	Graduate Student
CHEN, Long	Graduate Student
XU, Hong	Graduate Student
WU, Yang	Graduate Student
SUZUKI, Hiroko	Secretary

Covalent organic frameworks (COFs) are crystalline porous polymers that allow organizaiton of organic units into long-range-ordered two and three-dimensional periodicities.[1)] COFs are intriguing frameworks because they allow a new degree of control of porosity, composition and component positions. In our group, we have pioneered the synthesis of π-electronic 2D COFs with various π-units.[1–6)]

Conjugated microporous polymers (CMPs) are a class of porous organic frameworks consisting of extended π-conjugation and inherent nanopores. The π-conjugation skeletons together with the well-defined nanopores enable the development of novel materials that are completely different from traditional linear conjugated polymers and conventional porous polymeric materials lacking of strong π correlations among the building blocks. We have developed CMPs as a new platform to achieve light-emitting, light-harvesting, catalysis, energy storage, and sensing functions.[7,8)]

1. Pore Surface Engineering of COFs

COFs are a class of important porous materials that enable pre-designable pore size and geometry; however, pore surface engineering in COFs remains challenging. COFs, which offers precise control over the composition, density, and functionalities of organic groups anchored onto the pore walls.[2)] For this purpose, an azide-appended phenylene block was synthesized and utilized as the wall component in a two-component condensation system for the construction of COFs with azide-integrated walls. The two-component system was further developed to a three-component system that consists of azide-appended phenylene and 'naked' phenylene walls, and corner blocks, thereby enabling the synthesis of COFs bearing a tunable content of azide units on the walls. The azide units on the COF walls were found to undergo quantitative click reaction with alkynes to form triazole-linked groups on the wall surfaces. Consequently, the combination of a three-component condensation system with click reaction led to the establishment of a protocol that allowed control of both the composition and density of organic groups in the pores (Figure 1). This methodology was widely useful for the creation of various specific surfaces in COF pores.[2)]

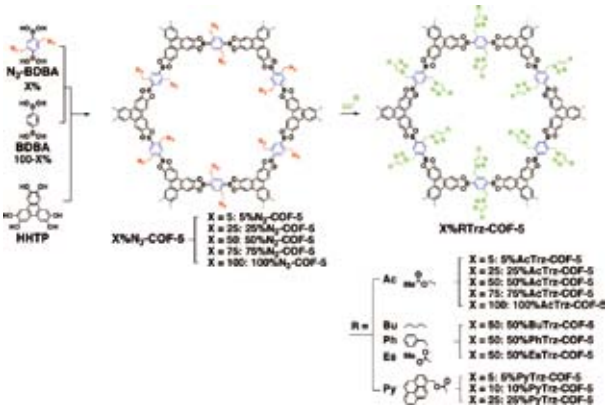

Figure 1. A general strategy for the surface engineering of COFs through the combination of condensation reaction and click chemistry. COFs bearing azide units on the walls are synthesized by the condensation reaction of hexahydroxytriphenylene (HHTP) with azide-appended benzene diboronic acid (N_3-BDBA) and benzene diboronic acid (BDBA) in a designated molar ratio (X = 0–100%). The azide groups on the COF walls are clicked with alkynes to anchor various organic groups onto the walls of COFs (X%RTrz-COF-5). The density of R surface groups on the walls is determined by the azide content in X%N_3-COF-5.

COF-5 is a typical mesoporous COF that consists of triphenylene at the corners and phenylene on the walls of a boronate ester-linked 2D hexagonal skeleton.1 We introduced azide groups to the 2 and 5 positions of the phenylene unit of 1,4-benzenediboronic acid and utilized the azide-appended benzenediboronic acid (N_3-BDBA) as wall blocks for the condensation reaction with hexahydroxytriphenylene (HHTP) (Figure 1). The resulting hexagonal skeleton is identical to that of COF-5, with triphenylene corners but azide-appended phenylene walls. Such a strategy allows the growth of various specific groups on the surface because the azide units in the

skeletons are reactive groups that can click with various alkynes for pre-designable functionalization. The content of azide units on the pore walls can be tuned using a three-component condensation system using HHTP as the corners and a mixture of N_3-BDAB and BDBA as the walls, because the azide units in N_3-BDAB did not affect the reactivity of BDBA in the condensation.

Azide units are well established for click reactions with alkynes to introduce functional groups via 1,2,3-triazole rings (Trz). Reaction of azide units on the walls of *X*%N_3-COF-5 (*X* = 5, 25, 50, 75, and 100) in a typical click reaction with 2-propynyl acetate in anhydrous N,N-dimethylacetamide (DMAc) at 50 °C with CuI present as a catalyst gives the corresponding *X*%AcTrz-COF-5 in quantitative yields. The present strategy can be further extended to the introduction of various specific groups onto the walls of COFs. We selected a paraffinic unit, aromatic hydrocarbon, and ester groups as typical examples to react with 50%N_3-COF-5. The click reactions of 50%N_3-COF-5 with 1-hexyne, 3-phenyl-1-propyne, and methyl propiolate were quantitatively achieved and led to the integration of *n*-butyl, benzyl, and methyl ester units to the walls of COF-5.

The present method for the pore surface engineering of COFs is simple and universal. This approach is high throughput due to the high efficiency condensation reaction and the quantitative click reaction. The most significant feature is that the combination of condensation and click reactions enables the molecular design of pore surface with controlled composition, component, and density. Therefore, this approach provides a new aspect in the chemistry of these well-defined porous materials, and provides a means to tailor pores for specific purposes and applications.

2. Highly Luminescent CMPs with Facilitated Exciton Migration and Improved Light-Emitting Activity

Conjugated polymers play a vital role in lasing, light-emitting diodes, flexible transistors, and solar cells. Owing to their rigid conformation, they have a high tendency to aggregate in solution and the solid state. Such aggregation leads to the dissipation of excitation energy and ultimately limits their utility as light-emitting motifs.

Herein we report a new strategy for the construction of light-emitting conjugated polymers based on conjugated microporous architectures.[7] We have developed a highly luminescent CMP with tetrakisphenylethene(TPE) as building block (Figure 2, TPE-CMP). Owing to the crosslinking nature of CMP, TPE-CMP can suppress the rotation of TPE units, thus allowing the high luminescence in both solution and solid states. As a result, a positive "CMP effect" was observed, *i.e.* the interweaving CMP architecture can promote π conjugation, facilitates excitation migration, and improves luminescence activity. Changing the reaction time allows for the synthesis of a series of CMPs with different size and absorption band. As the reaction time increased, the TPE-CMP particles become larger to give an increased surface area and display red-shifted electronic absorption band accordingly.

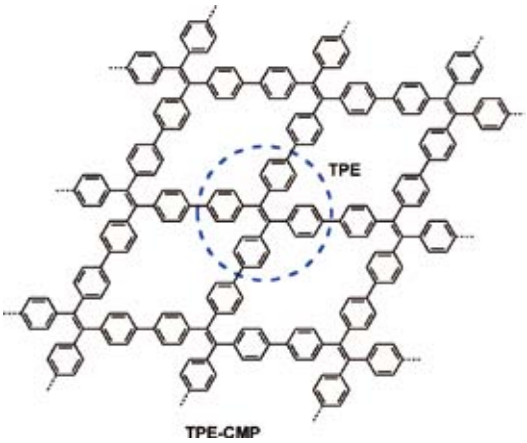

Figure 2. Structure of TPE-CMP.

These results the propagation of network structure takes place with the reaction time. The fluorescence quantum yield could reach 40%. In contrast, linear TPE polymer showed a low quantum yield of only 0.65% at otherwise identical condition. Interesting, owing to the crosslinking nature of the network, TPE-CMP is highly luminescent in various solvents such as methanol, dioxane, tetrohydorfuran, dichloromethane, chloroform, hexane, dimethylforamide, benzene, and water while the linear polymer analogue is almost nonemissive in solvents such as dichloromethane, chloroform, and tetrehydrofuran. Furthermore, TPE-CMP emits strong luminescence at solid state with a similar emission band as that in solutions. Fluorescence anisotropy measurements suggest that the exciton can migrate over the three-dimensional CMP skeletons. These positive CMP effects suggest that the CMP architecture provides a new platform for the design of highly luminescent materials

References

1) X. Feng, X. Ding and D. Jiang, *Chem. Soc. Rev.* **41**, 6102 (2012).
2) A. Nagai, Z. Guo, X. Feng, S. Jin, X. Chen, X. Ding and D. Jiang, *Nat. Commun.* 2:536 doi: 10.1038/ncomms1542 (2011).
3) X. Ding, X. Feng, A. Saeki, S. Seki, A. Nagai and D. Jiang, *Chem. Commun.* **48**, 8952–8954 (2012).
4) X. Feng, L. Chen, Y. Honsho, O. Saengsawang, L. Liu, L. Wang, A. Saeki, S. Irle, S. Seki, Y. Dong and D. Jiang, *Adv. Mater.* **24**, 3026–3031 (2012).
5) X. Feng, L. Liu, Y. Honsho, A. Saeki, S. Seki, S. Irle, Y. Dong, A. Nagai and D. Jiang, *Angew. Chem., Int. Ed.* **51**, 2618–2622 (2012).
6) X. Ding, L. Chen, Y. Honsho, X. Feng, O. Saengsawang, J. Guo, A. Saeki, S. Seki, S. Irle, S. Nagase, P. Vudhichai and D. Jiang, *J. Am. Chem. Soc.* **133**, 14510–14513 (2011).
7) Y. Xu, L. Chen, Z. Guo, A. Nagai and D. Jiang, *J. Am. Chem. Soc.* **133**, 17622–17625 (2011).
8) X. Liu, Y. Xu and D. Jiang, *J. Am. Chem. Soc.* **134**, 8738–8742 (2012).

Solid State NMR for Molecular Science

Department of Materials Molecular Science
Division of Molecular Functions

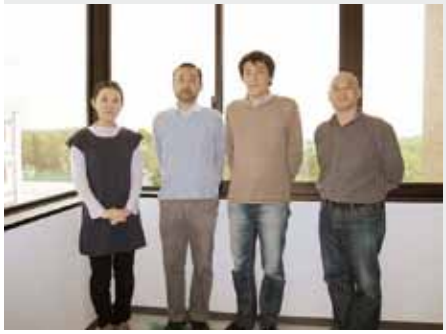

NISHIMURA, Katsuyuki — Associate Professor
IIJIMA, Takahiro — Assistant Professor
TANIO, Michikazu — IMS Research Assistant Professor

We are working on methodology and hardware developments of solid state NMR and structural biology and materials molecular science. In the following, we show studies of peripheral membrane proteins and inorganic compounds based on NMR.

1. NMR and Native-PAGE Analyses of the Phospholipase C-δ1 Pleckstrin Homology Domain

Phospholipase C (PLC) binds to phosphatidylinositol 4,5-bisphosphate (PIP_2) in the cell membrane through the pleckstrin homology (PH) domain, and hydrolyzes PIP_2 to produce two second messengers, diacylglycerol and inositol 1,4,5-triphosphate (IP_3), by the catalytic domain. The PLC-δ1 PH domain has a characteristic short α-helix (α2) from residues 82-87 (Figure 1). Solid-state ^{13}C NMR studies of the PLC-δ1 PH domain suggested that the α2-helix non-specifically interacts with the hydrophobic layer of the membrane due to the membrane localization of the protein.[1)]

In this study, the contributions of the α2-helix toward the IP_3 binding activity and thermal stability of the PLC-δ1 PH domain were therefore investigated by using NMR and Native-PAGE methods.

Native-PAGE analyses indicated that IP_3 binding to the PLC-δ1 PH domain results in a drastic migration shift on the gel and in an increased thermal stability. In addition, we found that disruption of the α-helical conformation by replacement of Lys-86 with proline resulted in reduced affinity for IP_3 and in thermal destabilization of the IP_3-binding state. Although the mutant protein with replacement of Lys-86 with alanine showed a slight reduction in thermal stability, the IP_3-binding affinity was similar to that of the wild-type protein. Replacement of Phe-87 with alanine, but not with tyrosine, also resulted in reduced affinity for IP_3 and in thermal instability. These results indicated that the helical conformation of the α2-helix and the phenyl ring of Phe-87 play important roles in the IP_3-binding activity and thermal stability of the PLC-δ1 PH domain.[2)] The ^{1}H-^{15}N HSQC NMR study of the selectively [α-^{15}N]Lys-labeled PLC-δ1 PH domain indicated that

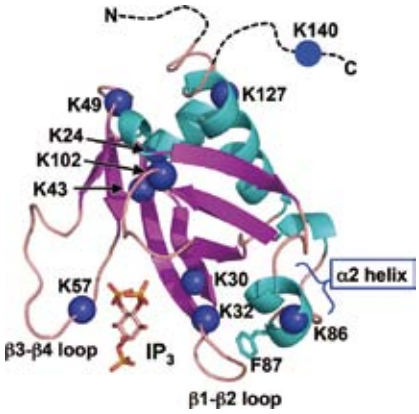

Figure 1. Crystal structure of the PLC-δ1 PH domain complexed with IP_3 (PDB ID, 1MAI).

IP_3 binding induces chemical shift displacement of all lysine signals (Figure 2). Interestingly, among those signals, only line width of α-^{15}N signal from Lys-86 located on the α2-helix markedly changed due to IP_3 binding (Figure 2, inset): in the ligand-free form, the α-^{15}N signal line width of Lys-86 was about two-fold broader than those of the other lysine signals in the one-dimensional ^{15}N projection of the ^{1}H-^{15}N HSQC NMR spectrum, and the addition of IP_3 resulted in line narrowing, and that the broad line width of the [α-^{15}N]Lys-86 signal converts to a narrow line width with addition of IP_3 (Figure 2). These findings provide evidence that the conformation and/or dynamics of the α2-helix couple with the ligand-binding activity of the PLC-δ1 PH domain. These findings suggested that the conformational changes of the α2-helix induced by membrane binding result in conversion of the stereospecific ligand-binding site to a weak-affinity site and in protein instability. Based on these results, we propose a new affinity regulation mechanism in which the ligand stereospecificity of the PLC-δ1 PH domain is significantly reduced due to protein structural changes by the membrane binding, and non-specific membrane binding or insertion is therefore important for stable anchoring to the lipid membrane. These findings also suggest that the ligand stereospecificity of the protein mainly contributes to searching the membrane contain-

ing PIP_2 and that stable anchoring to the lipid membrane is mainly achieved by non-specific membrane binding or insertion rather than PIP_2 binding. This mechanism also explains the lower affinity of the protein to lipid bilayers than IP_3, which is an essential property for feedback control of catalytic reaction of PLC-δ1 with respect to PIP_2.

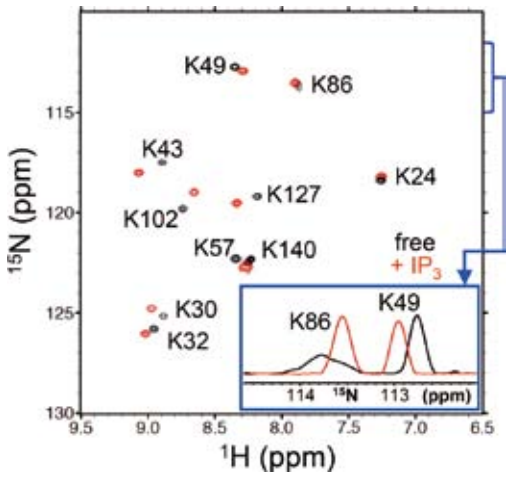

Figure 2. Solution NMR analyses of the [α-^{15}N]Lys-labeled PLC-δ1 PH domain. The ^{1}H-^{15}N HSQC NMR spectra without (black) and with (red) IP_3. (inset) The one-dimensional ^{15}N projections of the HSQC NMR spectra around the Lys-86 signal under the absence (black) and presence (red) of IP_3.

2. Solid State ^{95}Mo NMR of Paramagnetic Crystals of Polyoxomolybdates

For a group 6 element of molybdenum, there exist stable compounds with all valences from Mo(0) to Mo(VI). Among them, Mo(V) species are included in materials such as ε-Keggin anion and nanosized oxides with ring-, tube- and ball-structure. Localization of the d^1 electron in Mo(V) has attracted attention in terms of molecular design and solid state physics like optic, electric and magnetic properties. Since ^{95}Mo is a quadrupole nuclei of spin $I = 5/2$ with the small gyromagnetic ratio $\gamma = -1.743 \times 10^7$ rad s^{-1} T^{-1}, it is difficult to measure ^{95}Mo NMR spectra in solid state in general. Recently, we have reported solid-state ^{95}Mo NMR spectra of mixed balanced polyoxomolybdates(V, VI) with the localized or delocalized d^1 electrons measured by enhancing sensitivity and resolution using a high-field magnet.[3] Furthermore, we clarified a disorder structure of $[PMo_{12}O_{36}(OH)_4\{La(H_2O)_{2.75}Cl_{1.25}\}_4]27H_2O$ with the ε-Keggin $\{Mo_{12}\}$ core by ^{95}Mo NMR in solids.

In this study, we investigated a paramagnetic polyoxomolybdate of $[Mo_{12}O_{30}(OH)_{10}H_2\{Ni(H_2O)_3\}_4]$ (hereafter, abbreviated as $\{Mo_{12}\}$(Ni)). Although the core of this crystal is also ε-Keggin $\{Mo_{12}\}$, it is caped with four paramagnetic $Ni(II)(H_2O)_3$. In order to examine coupling constants appearing in solid state NMR, we measured high-field ^{95}Mo NMR in solids, simulated the obtained spectra numerically, and performed DFT calculation.

Figures 3(i-a) and 3(ii-a) show the ^{95}Mo NMR static spectra of $\{Mo_{12}\}$(Ni) measured under 21.8 and 11.7 T, respectively. Considerably broadened spectra with breadth of several thousands of ppm were obtained under both magnetic fields. In the spectral simulation, in addition to the quadrupole and chemical shift interactions, the hyperfine interaction between ^{95}Mo nuclei and unpaired electron spins in paramagnetic Ni(II) ions were considered as internal interactions. The simulated spectra shown in Figures 3(ii-a) and 3(ii-b) represented experimental spectra well. Since the broadening due to the quadrupole and anisotropic chemical shift interactions were quite large, the effect of the anisotropic hyperfine interaction on the spectral lineshape was small. In order to investigate the contribution from the isotropic hyperfine interaction, the ^{95}Mo NMR spectrum was measured at 173 K under 11.7 T (Figure 3(i-c)). Notable difference of the spectra between 301 and 173 K was not found. By lowering of temperature, although the line width was slightly broadened owing to the increase of magnetization of the electron spins, we needed not consider temperature dependence of the isotropic shift in the simulation.

The coupling constants for the internal spin interactions were also obtained from DFT calculation. Although the chemical shift estimated by DFT was larger than that by the spectral simulation, the trend such as a considerably large anisotropic chemical shift agreed between DFT and spectral simulation. Also, a spin density localized around the Ni(II) ions was obtained by DFT calculation, which agreed with small temperature-dependence of the whole shift of the spectra.

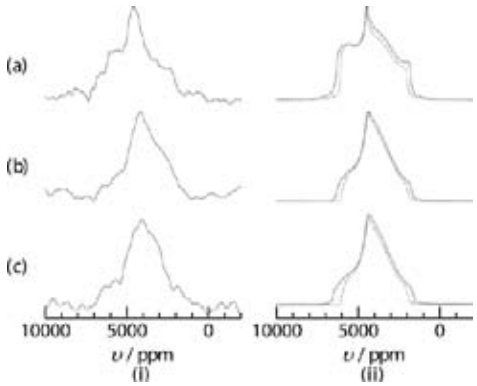

Figure 3. ^{95}Mo NMR static spectra of $\{Mo_{12}\}$(Ni) under the magnetic field of (a) 21.8 and (b, c) 11.7 T. (b) and (c) show the spectra at 301 and 173 K, respectively. (i) and (ii) show the observed and simulated spectra, respectively. The solid and broken lines in (ii) show the theoretical curves with and without considering the hyperfine interaction, respectively.

References

1) N. Uekama, T. Aoki, T. Maruoka, S. Kurisu, A. Hatakeyama, S. Yamaguchi, M. Okada, H. Yagisawa, K. Nishimura and S. Tuzi, *Biochim. Biophys. Acta* **1788**, 2575–258 (2009).
2) M.Tanio and K.Nishimura, *Anal. Biochem.* **431**, 106–114 (2012).
3) T. Iijima, T. Yamase, M. Tansho, T. Shimizu and K. Nishimura, *Chem. Phys. Lett.* **487**, 232–236 (2010).

Organic Solar Cells

Research Center for Molecular Scale Nanoscience
Division of Molecular Nanoscience

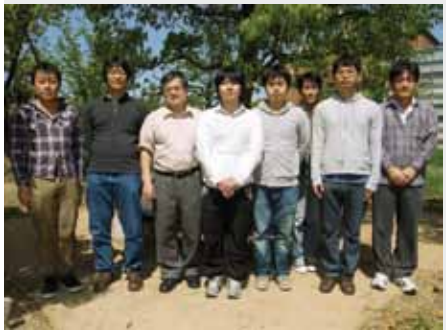

HIRAMOTO, Masahiro	Professor
KAJI, Toshihiko	Assistant Professor
NAKAO, Satoru	Post-Doctoral Fellow
SHINMURA, Yusuke	Research Fellow
KUBO, Masayuki	Research Fellow
YOKOYAMA, Kazuya	Research Fellow
YOSHIOKA, Tadashi	Research Fellow
ISHIYAMA, Norihiro	Graduate Student
SUGIHARA, Hidemi	Secretary

Organic solar cell is recognized as a next generation solar cell. In 2009, we started CREST Project; "Bandgap Science for Organic Solar Cells." Target of this project is 15% efficiency of organic solar cells by establishing bandgap science for organic semiconductors, which is equivalent to that for silicon semiconductor.

Recently, we have established *pn*-control technique for organic semiconductors (Topic 1) and applied to the fabrication of the ohmic organic/metal contacts (Topic 2) and of the tandem cell formed in the codeposited film only by doping (Topic 3).

1. *pn*-Control and *pn*-Homojunction Formation in Single C_{60} and H_2Pc Films[1–3)]

Fullerene (C_{60}) and phthalocyanines are typical components in small-molecular-type organic photovoltaic cells. Based on experience with inorganic solar cells, to create a built-in potential, *pn*-control of highly purified organic semiconductors by doping is required.

In this study, complete *pn*-control and *pn*-homojunction formation were demonstrated for single C_{60} films[1,2)] and for single metal-free phthalocyanine (H_2Pc) films.[3)] Cesium carbonate (Cs_2CO_3) and molybdenum oxide (MoO_3) were used as donor and acceptor dopants, respectively. Doping was performed by the coevaporation. Here, results on H_2Pc films are summarized.

The Fermi level (E_F) of H_2Pc, located at the center of the bandgap (4.4 eV), is shifted to 3.8 eV, close to the conduction band (3.5 eV), by Cs_2CO_3 doping (5,000 ppm) and shifted to 4.9 eV, close to the valence band (5.1 eV), by MoO_3 doping (5,000 ppm) under oxygen free conditions (Figure 1). Formation of *n*- and *p*-type Schottky junctions and *pn*-homojunctions in single H_2Pc films, confirmed by their photovoltaic properties, clearly demonstrates the formation of *n*- and *p*-type H_2Pc.

Moreover, the band bending can be also mapped in real scale based on the Kelvin probe measurements and the widths of depletion regions for *n*-type (Figure 2(a)), *p*-type (Figure 2(b)) Schottky junctions and *pn*-homojunction (Figure 2(c)) were determined to 23, 30, and 35 nm, respectively.

Conventionally, H_2Pc and C_{60} have been regarded as inherent *p*- and *n*-type semiconductors, respectively. However, *n*-H_2Pc and *p*-C_{60} can be formed by doping. So, it is reasonable that single organic semiconductors can, in general, be controlled to be *n*- or *p*-type, similar to inorganic semiconductors.

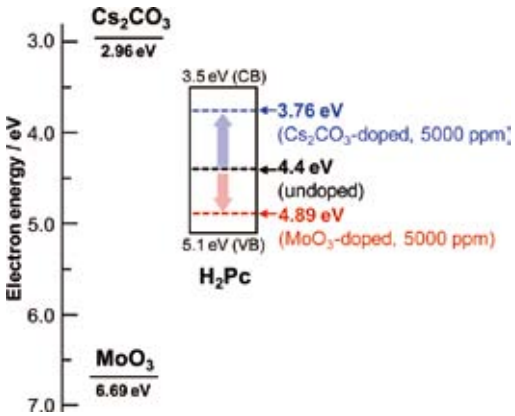

Figure 1. Energy diagram of a H_2Pc film. The broken lines show the energy levels of E_F for undoped (black), MoO_3-doped (red) and Cs_2CO_3-doped (blue) H_2Pc films.

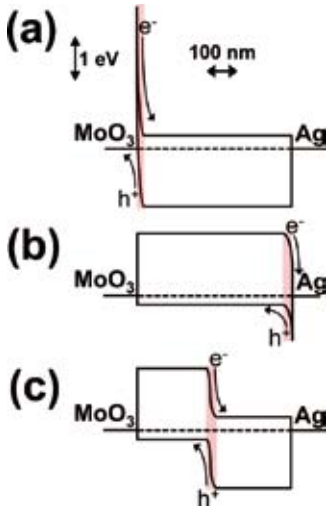

Figure 2. Energy structures for Cs_2CO_3-doped (a), MoO_3-doped (b), and Cs_2CO_3-/MoO_3-doped (c) cells in real scale based on the Kelvin probe measurements. Photocarrier generation occurs in the depletion regions (shaded).

2. Invertible Organic Photovoltaic Cells with Heavily Doped Organic/Metal Ohmic Contacts[4)]

In this study, we applied *pn*-control to make the two organic/metal contacts in a photovoltaic cell ohmic. Figure 3 shows the energetic structure for ITO/n^+-C_{60} contact depicted based on the Kelvin probe measurements. 10,000 ppm Cs_2CO_3 was heavily doped in the vicinity of ITO electrode and made C_{60} n^+-type. Though there is a distinct barrier to electrons with a height of 0.34 eV from the conduction band of C_{60} to the ITO, since the band bends down steeply within 5 nm of the interface, photogenerated electrons can tunnel through this barrier. Thus, an ohmic contact is formed.

Heavily doped 10-nm-thick p^+- and n^+-type regions of H_2Pc and C_{60} were formed to facilitate the formation of ohmic contacts at the organic/metal interfaces of two-layered organic photovoltaic cells [ITO/H_2Pc/C_{60}/Ag]. Formation of the ohmic contacts allowed the cells to be invertible [ITO/C_{60}/H_2Pc/Ag] and independent of the type of electrode material used.

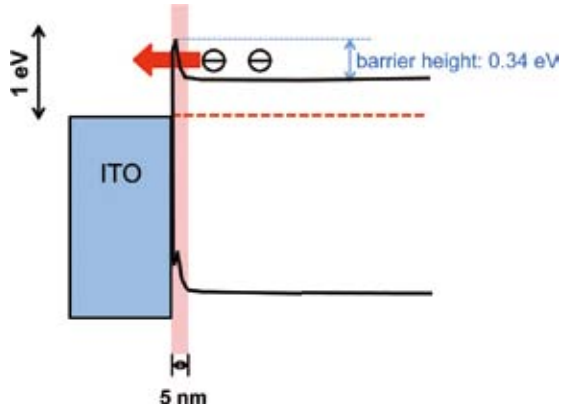

Figure 3. Energy structure for ITO/n^+-C_{60} contact in real scale. A tunneling ohmic junction for photogenerated electrons is formed.

3. Tandem Organic Photovoltaic Cells Formed in Codeposited Films by Doping[5)]

pn-control technique should be extended to co-deposited films since organic solar cells should use co-deposited films to generate significant photocurrent densities based on the dissociation of excitons by the photoinduced electron transfer process.

In this study, tandem organic solar cells connecting two single homojunctions were formed in C_{60}:6T (α-sexithiophene) co-deposited films only by doping with MoO_3 and Cs_2CO_3 (Figure 4). Doping were performed by "three component co-evaporation."[6)] The single and tandem cells showed the open-circuit voltage of 0.85 and 1.69 V and conversion efficiency of 1.6 and 2.4%, respectively.

Figure 5 shows the energetic structure of tandem cell. Photocurrent is generated in the intrinsic (i) layers in front and back cells. Two single cells are connected by heavily doped n^+p^+-homojunction. Since the depletion region width of the n^+p^+-homojunction is extremely thin, *i.e.*, 20 nm, it can act as ohmic interlayer due to the carrier tunneling. Thus, the photovoltage of tandem cell (1.69 V) is doubled compared to that of single cell (0.85 V).

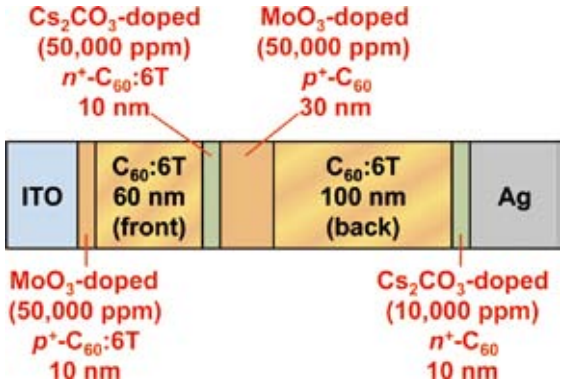

Figure 4. Structure of a tandem cell connecting two homojunction cells, which is made only by doping to C_{60}:6T codeposited film.

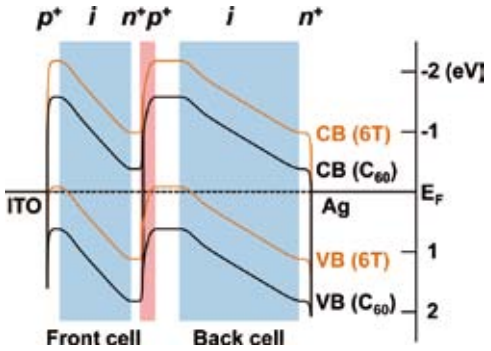

Figure 5. Energy structure of a tandem cell in real scale. n^+p^+-heavily doped homojunction acts as an ohmic interlayer connecting two single cells.

References

1) M. Kubo, K. Iketaki, T. Kaji and M. Hiramoto, *Appl. Phys. Lett.* **98**, 073311 (2011).
2) M. Kubo, T. Kaji and M. Hiramoto, *AIP Adv.* **1**, 032177 (2011).
3) Y. Shinmura, M. Kubo, N. Ishiyama, T. Kaji and M. Hiramoto, *AIP Adv.* **2**, 032145 (2012).
4) M. Kubo, Y. Shinmura, N. Ishiyama, T. Kaji and M. Hiramoto, *Appl. Phys. Express* **5**, (2012), in press.
5) N. Ishiyama, M. Kubo, T. Kaji and M. Hiramoto, *Appl. Phys. Lett.*, submitted.
6) N. Ishiyama, M. Kubo, T. Kaji and M. Hiramoto, *Appl. Phys. Lett.* **99**, 133301 (2011).

Award

KAJI, Toshihiko; Young Scientist Oral Presentation Award from Japan Society of Applied Physics (31st, 2011 Autumn Meeting).

Development of Organic Semiconductors for Molecular Thin-Film Devices

Research Center for Molecular Scale Nanoscience
Division of Molecular Nanoscience

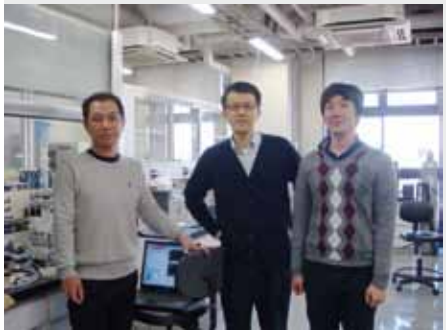

SUZUKI, Toshiyasu — Associate Professor
SAKAMOTO, Youichi — Assistant Professor
KURODA, Yasuhiro — Post-Doctoral Fellow
WATANABE, Yoko — Secretary

Organic light-emitting diodes (OLEDs) and organic field-effect transistors (OFETs) based on π-conjugated oligomers have been extensively studied as molecular thin-film devices. Organic semiconductors with low injection barriers and high mobilities are required for highly efficient OLEDs and OFETs. Radical cations or anions of an organic semiconductor have to be generated easily at the interface with an electrode (or a dielectric), and holes or electrons must move fast in the semiconducting layer. Compared with organic p-type semiconductors, organic n-type semiconductors for practical use are few and rather difficult to develop. Recently, we found that perfluorinated aromatic compounds are efficient n-type semiconductors for OLEDs and OFETs.

1. Selective Synthesis and Crystal Structure of [10]Cycloparaphenylene[1)]

[10]Cycloparaphenylene ([10]CPP) was selectively synthesized in four steps in 13% overall yield from commercially available 4,4'-diiodobiphenyl by using mono-I–Sn exchange, Sn–Pt transmetalation, I–Pd exchange, and subsequent oxidative coupling reactions. The structure of [10]CPP was determined by using single-crystal X-ray analysis. Suitable crystals were obtained by slow vapor diffusion of *n*-hexane into a solution of [10]CPP in CH_2Cl_2 at room temperature. In the solid state, [10]CPP is slightly distorted to an ellipsoidal structure with major and minor axes of 13.9 and 13.5 Å, respectively. The cavity of [10]CPP is occupied by a hexane molecule, which was highly disordered. Although the D_{5h} structure with a dihedral angle between two paraphenylene units of 32°–33° was calculated to be the most stable conformer, the structure is closer to a D_{2h} conformer with alternating triphenylene and biphenylene units. The dihedral angles between two paraphenylene units were approximately 20° and 45°, respectively. The average C_{ipso}–C_{ipso}, C_{ipso}–C_{ortho}, and C_{ortho}–C_{ortho} bond lengths are 1.484(1), 1.399(2), and 1.385(9) Å, respectively. [10]CPP molecules pack in a herringbone manner, and there are no significant π–π interactions among [10]CPP molecules. A tilted tubular channel structure was observed along the *b* axis. The crystal packing is similar to [9]- and [12]CPPs but different from [6]CPP. The size of the CPP may be important for determining the packing arrangement.

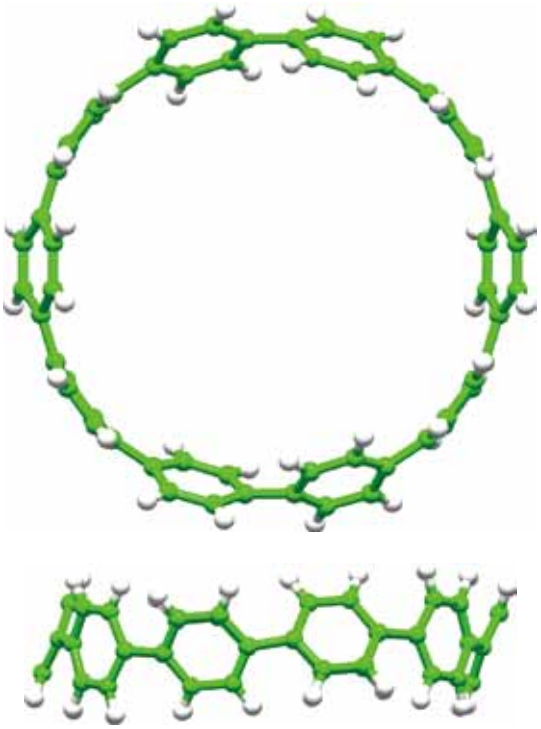

Figure 1. X-ray structure of [10]CPP.

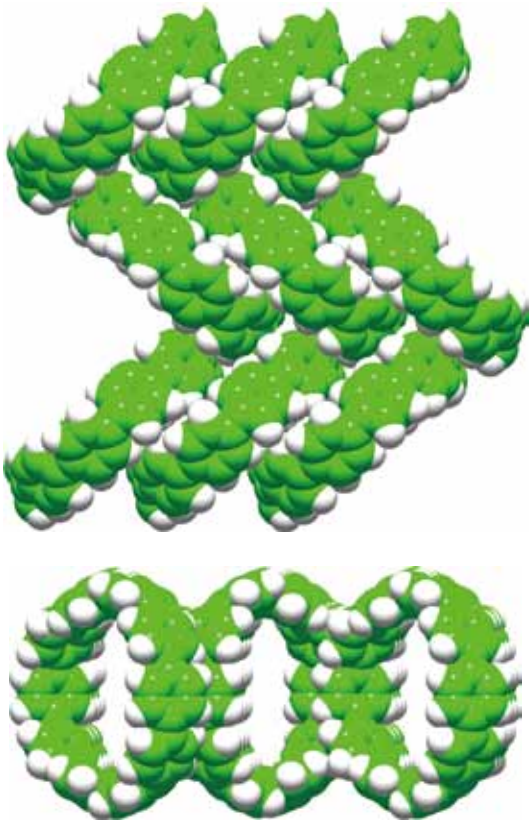

Figure 2. Packing structure of [10]CPP.

Reference

1) E. Kayahara, Y. Sakamoto, T. Suzuki and S. Yamago, *Org. Lett.* **14**, 3284–3287 (2012).

Building Photosynthesis by Artificial Molecules

Research Center for Molecular Scale Nanoscience
Division of Molecular Nanoscience

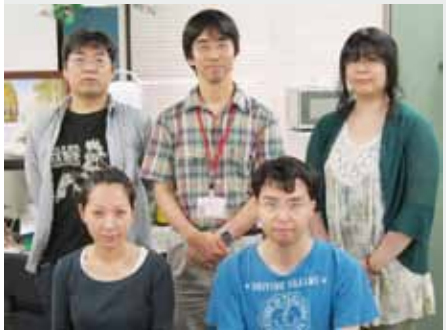

NAGATA, Toshi	Associate Professor
SAKURAI, Rie	IMS Fellow
YUSA, Masaaki	Graduate Student
MIURA, Takahiro	Technical Fellow
WANATABE, Yoko	Secretary

The purpose of this project is to build nanomolecular machinery for photosynthesis by use of artificial molecules. The world's most successful molecular machinery for photosynthesis is that of green plants—the two photosystems and related protein complexes. These are composed almost exclusively from organic molecules, plus a small amount of metal elements playing important roles. Inspired by these natural systems, we are trying to build up multimolecular systems that are capable of light-to-chemical energy conversion. At present, our interest is mainly focused on constructing necessary molecular parts and examining their redox and photochemical behavior.

1. Photoreduction of Quinones Sensitized by Soluble Phthalocyanines

Organic pigments are useful molecular parts for photosynthesis because of their ease of modification and high tunability. In particular, pigments for utilizing visible lights with long wavelength (>650 nm) are useful because they can complement the existing series of sensitizers for more efficient use of solar light. Phthalocyanines are good candidates as they have very strong absorption bands around 700 nm. However, studies on photochemistry of phthalocyanines are often hampered by the low solubility. To address this problem, we chose phthalocyanines (Pc) having 2,4-di-*t*-butylphenoxy substituents in the periphery. These phthalocyanines are so soluble in many organic solvents (even in hexanes!) that study of photoreactions in solutions can be easily carried out.

The target photoreaction is shown in Figure 1. The rate of reaction was dependent on the redox potentials of quinones, namely the reaction was faster for quinones with higher potential (*i.e.* more easily reduced). This indicates the reaction proceeds *via* photoinduced electron transfer from Pc to quinones. In particular, 2-*t*-butylanthraquinone and 2,6-dibutoxyanthraquinone did not react at all; these results suggest that the reaction proceeds *via* the triplet state of Pc (^{3}Pc) rather than the excited singlet state (^{1}Pc*), because ΔG's for the photoinduced electron transfer to these quinones were positive for ^{3}Pc but negative for ^{1}Pc*.

Figure 1. Photoreduction of quinones sensitized by soluble phthalocyanines with various central metals.

On the other hand, when different thiols were used as reductant, the rate of reaction was dependent on the acidity of thiols rather than the redox potential. Therefore, it is likely that the thiol works first as the proton donor to the anion radical of quinone, and then gives an electron to the cation radical of Pc (or to the neutral semiquinone radical).

When phthalocyanines with different central metal ions were employed, the rates of photoreaction were in the order Zn > Mg > Pd > 2H. Although the triplet quantum yield is higher for Pd than Zn, the photoreaction was very slow with Pd phthalocyanine. This is attributed to the high redox potential of PdPc, causing the photoinduced electron transfer unfavorable (ΔG = +0.17 eV for 2,5-di-*t*-butylbenzoquinone).

On the basis of these results, a plausible mechanism of this reaction is proposed as shown in Figure 2. Kinetic studies for important steps are currently underway. This study will lay an important cornerstone in utilization of low-energy photons for direct chemical conversions.

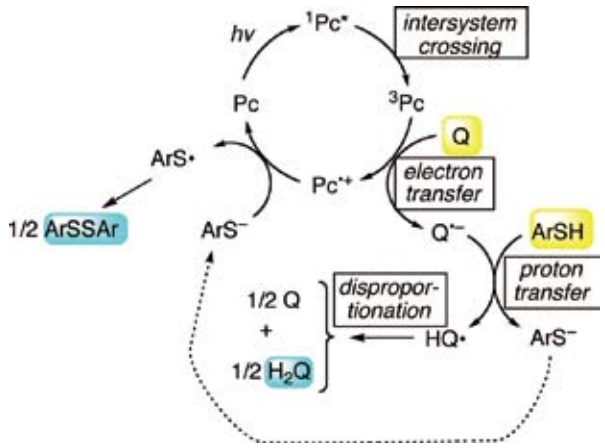

Figure 2. A plausible mechanism of photoreduction of quinones. Pc: phthalocyanine.

2. Synthesis of Dinuclear Metal Complexes with Ternary Binucleating Ligands

As we already reported,[1)] combination of photochemistry of organic pigments and redox chemistry of transition metal complexes is a promising approach to develop new photoredox chemistry. In particular, use of first transition metals (3d metals) is worth studying, because they can provide crucial bridge between one-electron (photochemical) and two-electron (common organic chemical) processes. Synthesis of 3d metal complexes, however, is not always straightforward, because many 3d metal ions exchange ligands so easily that there are only limited choices of isolable compounds. In this respect, we can learn from biological systems where 3d metal complexes are utilized with a wide structural variation. This is made possible by the surrounding organic ligands (proteins).

Along this context, we prepared two new "ternary" ligands **1** and **2**, which consist of two terpyridines and one "N4 bridge" (1,4-bis(2-pyridyl)phthalazine for **1** and 3,6-bis(2-pyridyl) pyridazine for **2**). They formed stable dinuclear complexes [(**1**)Co_2(μ-OH)]$^{3+}$, [(**1**)Ni_2(μ-Cl)]$^{3+}$ and [(**2**)Co_2(μ-OH)]$^{3+}$. The X-ray structures of the first two complexes revealed subtle but characteristic differences (Figure 4). The steric repulsion between the hydrogen atoms at the *peri*-positions of the phthalazine ring and the 3-positions of the neighboring pyridine rings (indicated by arrows in Figure 4) caused twisting of the pyridine rings resulting in local axial chirality, and the stereochemistry of the axes were different between the Co and Ni complexes. In the Co complex, the two axes have the opposite axial stereochemistry, whereas in the Ni complex, the two axes have the same stereochemistry. Such difference was caused by the different ionic radii of the metal centers and by the different bridging anions (OH^- and Cl^-).

The cyclic voltammogram of [(**1**)Co_2(μ-OH)]$^{3+}$ showed interesting behavior in the presence of acid (Figure 5). When triflic acid was added, the peaks of the Co_2 parts disappeared and new peaks corresponding to a mononuclear Co complex appeared instead. This change was attributed to the (reversible) release of one Co ion upon addition of acid.

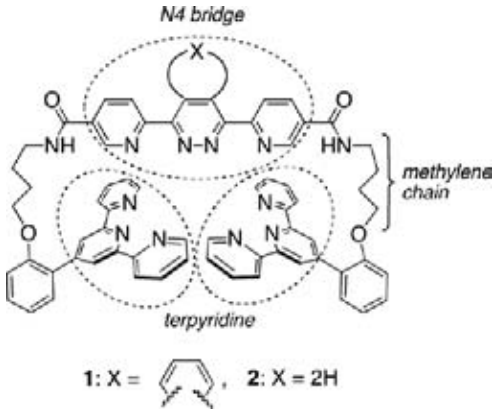

Figure 3. The ternary ligands consisting of two terpyridines and one "N4 bridge."

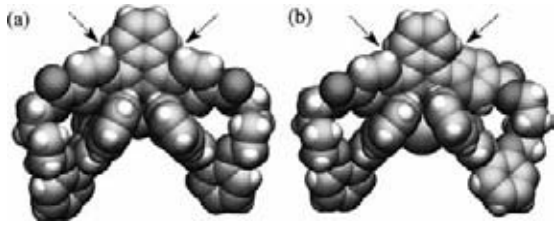

Figure 4. The space-filling drawing of the X-ray structures of (a) [(**1**)Co_2(μ-OH)]$^{3+}$ and (b) [(**1**)Ni_2(μ-Cl)]$^{3+}$.

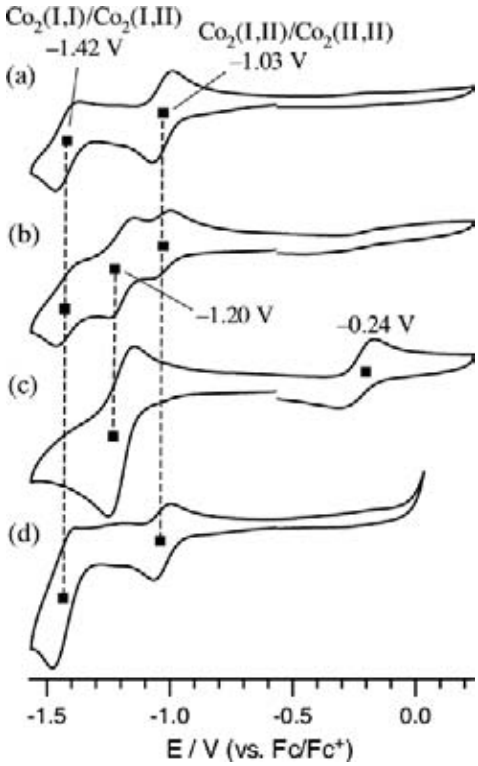

Figure 5. The changes of the CVs of [(**1**)Co_2(μ-OH)]$^{3+}$ with the addition of CF_3SO_3H (a) 0 eq., (b) 1.0 eq., (c) 2.0 eq. and (d) after the addition of 5 eq. *i*PrNEt_2.

Reference

1) H. Kon and T. Nagata, *Chem. –Eur. J.* **18**, 1781–1788 (2012).

Chemistry of Bowl-Shaped Aromatic Compounds and Metal Nanocluster Catalysts

Research Center for Molecular Scale Nanoscience
Division of Molecular Nanoscience

SAKURAI, Hidehiro	Associate Professor
HIGASHIBAYASHI, Shuhei	Assistant Professor
PANDA, Gautam	Visiting Scientist; JSPS Invited Fellow
MURUGADOSS, Arumugam	Visiting Scientist; JSPS Post-Doctoral Fellow
TAN, Qi-Tao	Visiting Scientist; JSPS Post-Doctoral Fellow
MORITA, Yuki	Post-Doctoral Fellow
SUGIISHI, Tsuyuka	Post-Doctoral Fellow
REZA, A. F. G. Masud	Visiting Scientist (JASSO Follow-up Research Fellow)
ANWER, Muslih	Visiting Scientist
SOPHIPHUN, Onsulang	Visiting Scientist
KAMONSATIKUL, Choavarit	Visiting Scientist
KOO, Jin Young	Visiting Scientist
ONOGI, Satoru	Graduate Student
DHITAL, Raghu Nath	Graduate Student
KARANJIT, Sangita	Graduate Student
SHRESTHA, Binod Babu	Graduate Student
KAEWMATI, Patcharin	Graduate Student
HAESUWANNAKIJ, Setsiri	Graduate Student
OKABE, Yuki	Graduate Student
SCHMIDT, Bernd	Graduate Student*
TOPOLINSKI, Berit	Graduate Student*
NAKANO, Sachiko	Technical Fellow
KIM, Yukimi	Technical Fellow
SASAKI, Tokiyo	Secretary
TANIWAKE, Mayuko	Secretary
HAZAMA, Kozue	Secretary

Bowl-shaped π-conjugated compounds including partial structures of the fullerenes, which are called “buckybowls,” are of importance not only as model compounds of fullerenes but also as their own chemical and physical properties. For example, in solution they show the characteristic dynamic behavior such as bowl-to-bowl inversion. On the other hand, they sometimes favor stacking structure in a concave-convex fashion in the solid state, giving excellent electron conductivity. Furthermore, some buckybowls are conceivable to possess the bowl-chirality if the racemization process, as equal as bowl-to-bowl inversion, is slow enough to be isolated. Very few buckybowls has been achieved for preparation mainly due to their strained structure, and no report on the preparation of chiral bowls has appeared. In this project, we develop the rational route to the various buckybowls with perfect chirality control using the organic synthesis approach.

We also investigate to develop novel catalytic properties of metal nanoclusters. We focus on the following projects: Preparation of size-selective gold nanoclusters supported by hydrophilic polymers and its application to aerobic oxidation catalysts: Synthetic application using metal nanocluster catalyst: Development of designer metal nanocluster catalyst using the highly-functionalized protective polymers.

1. Enantioselective Synthesis of a Chiral Nitrogen-Doped Buckybowl[1)]

Bowl-shaped aromatic compounds, buckybowls, constitute a family of curved polycyclic aromatic carbons along with fullerenes and carbon nanotubes (CNTs). Doping of heteroatoms to the carbon frameworks of such aromatic compounds drastically modulates their physical and chemical properties. In contrast to nitrogen-doped azafullerenes or CNTs, synthesis of azabuckybowls, nitrogen-doped buckybowls, remains an unsolved challenging task. Accordingly, we have achieved the first enantioselective synthesis of a chiral azabuckybowl, triazasumanene. X-ray crystallographic analysis confirmed that the doping of nitrogen induces a more curved and deeper bowl structure than in all-carbon buckybowls. As a result of the deeper bowl structure, the activation energy for the bowl inversion (thermal flipping of the bowl structure) reaches an extraordinarily high value (42.2 kcal/mol). Since the bowl inversion corresponds to the racemization process for chiral buckybowls, this high bowl inversion energy leads to very stable chirality of triazasumanene.

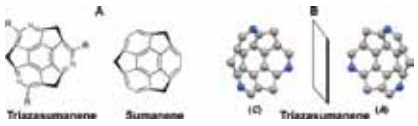

Figure 1. (A) Triazasumanene and sumanene; (B) Enantiomers of triazasumanene.

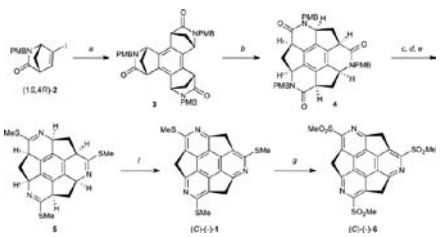

Figure 2. Conditions: (a) $Pd(OAc)_2$, PPh_3, Bu_4NOAc, Na_2CO_3, molecular sieve 4 Å, 1,4-dioxane, 100 °C, 2 h, 57%; (b) i) 12 M HCl, AcOH, 60 °C, 3 h; ii) $C_6F_5OP(=O)Ph_2$, DIPEA, DMF, 0 °C to 60 °C, 59% (two steps); (c) Lawesson’s reagent, dichloroethanene, microwave, 160 °C, 40 min, 92%; (d) Trifluoroacetic acid, microwave, 100 °C, 2 h, 88%; (e) MeI, K_2CO_3, DMF, 30 °C, 3 h, 79%; (f) Ph_3CBF_4, DTBMP, CH_2Cl_2, 25 °C, 3 d, 73%; (g) *m*-CPBA, CH_2Cl_2, 25 °C, 5 h, 90%.

2. Trimethylsumanene: Enantioselective Synthesis, Substituent Effect on Bowl Structure, Inversion Energy, and Electron Conductivity[2)]

C_3 symmetric chiral trimethylsumanene was enantioselectively synthesized through Pd-catalyzed *syn*-selective cyclotrimerization of an enantiomerically pure iodonorbornenone, ring-opening/closing olefin metathesis, and oxidative aromatization where the sp^3 stereogenic center was transmitted to the bowl chirality. Chiral HPLC analysis/resolution of the derivatives were also achieved. Based on theoretical calculations, the columnar crystal packing structure of sumanene and trimethylsumanene was interpreted as due to attractive electrostatic or CH–π interaction. According to the experimental and theoretical studies, the bowl depth and inversion energy were found to increase on methylation for sumanene in contrast to corannulene. Dissimilarities of the effect of methylation on the bowl structure and inversion energy of sumanene and corannulene were ascribed to differences in steric repulsion. A double-well potential model was fitted to the bowl structure-inversion energy correlation of substituted sumanenes, with a small deviation. The effects of various substituents on the sumanene structure and bowl inversion energy were analyzed by density functional theory calculations, and it was shown that the bowl rigidity is controlled by a combination of electronic and steric effects of the substituents. The electron conductivity of trimethylsumanene was investigated by time-resolved microwave conductivity method, compared with that of sumanene.

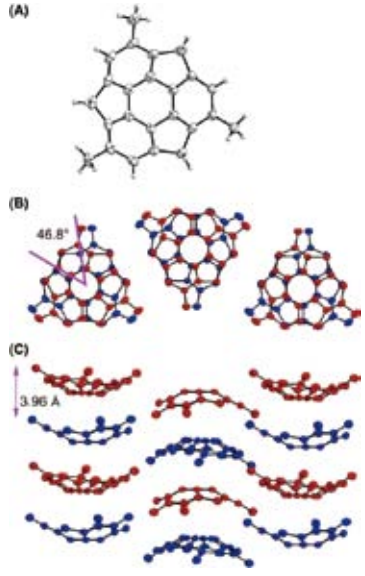

Figure 3. (A) ORTEP drawings of X-ray crystallographic analysis of (±)-**3**, (B) top view, (C) side view, shown at the 50% probability level.

3. Dual Roles of Polyhydroxy Matrices for Homocoupling of Arylboronic Acid Catalysed by Gold Nanoclusters Under Acidic Conditions[3)]

Polyhydroxy biopolymers including chitosan and starch play the dual roles of stabilization of gold clusters as well as activation of arylboronic acids through reversible binding. In acidic pH of 4.57 the electronic state of boron is changed to the corresponding to that at pH 9 inside the vicinity of Au:chit or Au:starch which favours the transmetallation process *i.e.* why homo-coupling product was observed even under acidic solutions.

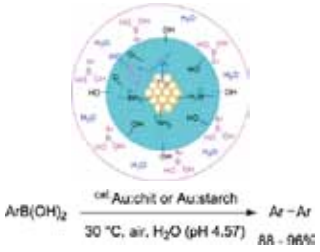

4. Anomalous Efficacy of Bimetallic Au/Pd Nanoclusters in C–Cl Bond Activation and Formal Metathesis-Type C–B Bond Activation at Room Temperature[4)]

Au/Pd alloy nanoclusters stabilized by poly (N-vinylpyrrolidone) catalyze two different reactions of phenylboronic acid with 4-chlorobenzoic acid at room temperature in a single reaction cycle, cross coupling and metathesis-type homocoupling that is normally inaccessible through conventional catalysis.

References

1) Q.-T. Tan, S. Higashibayashi, S. Karanjit and H. Sakurai, *Nat. Commun.* 3:891 doi: 10.1038/ncomms1896 (2012).
2) S. Higashibayashi, R. Tsuruoka, Y. Soujanya, U. Purushotham, G. N. Sastry, S. Seki, T. Ishikawa, S. Toyota and H. Sakurai, *Bull. Chem. Soc. Jpn.* **85**, 450–467 (2012).
3) R. N. Dhital, A. Murugadoss and H. Sakurai, *Chem. –Asian J.* **7**, 55–59 (2012).
4) R. N. Dhital and H. Sakurai, *Chem. Lett.* **41**, 630–632 (2012).

Awards

DHITAL, Raghu Nath; Young Scientist Award, International Conference on Advanced Materials and Nanotechnology (2011).
DHITAL, Raghu Nath; Young Oral Presentation Award, International Symposium on Catalysis and Fine Chemicals 2011 (2011).
TAN, Qi Tao; Outstanding Poster Presentation, International Symposium on Catalysis and Fine Chemicals 2011 (2011).

* carrying out graduate research on Cooperative Education Program of IMS with Freie Universität Berlin

Spectroscopic Studies on Electronic Ferroelectricity in Organic Conductors

Department of Materials Molecular Science
Division of Electronic Properties

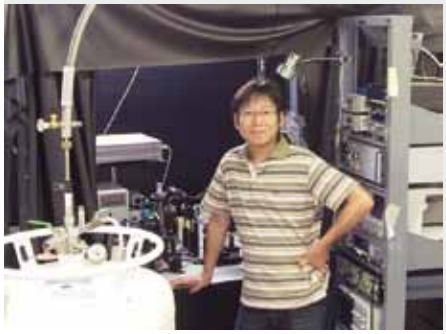

YAMAMOTO, Kaoru Assistant Professor

Organic conductors exhibit unusual physical properties due to the critical nature of valence electrons fluctuating under localizing and delocalizing regime. Recently, we discovered that an organic superconductor, α-(BEDT-TTF)$_2$I$_3$ [BEDT-TTF: bis(ethylenedithio)tetrathiafulvalene], induces optical second-harmonic generation (SHG) along with charge-ordering driven by the repulsive electron-electron interactions.[1)] The SHG activity proves that the organic complex induces macroscopic electric polarization by the electronic transition. To understand the fundamental and functional properties of such "electronic ferroelectrics," we are engaged in the material research and development of experimental technique dedicated for low-temperature SHG microscopy of tiny organic crystals.

1. SHG Microscopy of Ferroelectric Organic Conductor Using Hydrostatic Pressure Apparatus with Argon as a Heat Transfer Medium[2)]

To perform nonlinear microscopy at low-temperatures, one has to dissipate the excessive heat from the photo-irradiated spot of the sample without affecting the physical properties. In the present study, we designed a sapphire-anvil cell, which is usually adopted for high-pressure measurements, as a cooling apparatus used along with liquid-argon as heat-transfer medium. The cryogenic performance of the argon-loaded sapphire cell was examined by the observation of SHG of an organic conductor α'-(BEDT-TTF)$_2$IBr$_2$ at low temperatures.

This α-type compound is unusually susceptible to mechanical stress. In a previous study, we have embedded the single crystals of the compound into a polymer resin and sandwiched them by sapphire plates, and observed the SHG at low temperatures. Because of the difference in thermal shrinkage between the samples and the sapphire plates, the crystals were fragmented with decreasing temperature. The observed image of SHG showed distinct inhomogeneity; the nonlinear optical signal was generated only from limited areas of the crystals, suggesting that the single crystals were divided into ferroelectric and antiferroelectric regions, presumably due to the mechanical stress.

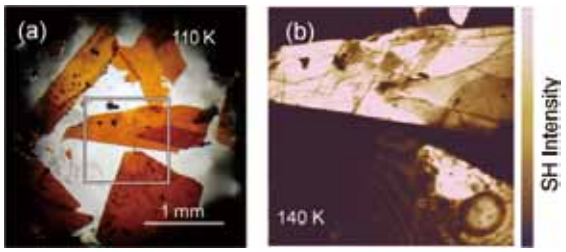

Figure 1. (a) Thin crystals of α'-(BEDT-TTF)$_2$IBr$_2$ in a sapphire-anvil cell loaded with liquid argon. (b) SHG image in the square region of (a) (T = 140 K).

Figure 1(a) shows the transmission image of the filmy thin crystals of the complex mounted in the sapphire cell loaded with liquid argon. The crystals cooled via the heat transfer medium were not completely intact, but the pieces of the cleaved crystals were much larger than the above mentioned fragmented crystals. As shown by the SHG image [Figure 1(b)], the cleaved crystals generated SHG from their whole region. This fact proves that the compound is a bulk ferroelectric matter, and at the same time, indicates that the heat at the irradiated spot was efficiently dissipated via the heat transfer medium without applying severe mechanical stress to the sample.

The successful SHG observation demonstrates that the cooling technique is helpful for low-temperature measurements of nonlinear optical microscopy requiring high-density photo-excitations.

References

1) K. Yamamoto, *et al.*, *J. Phys. Soc. Jpn.* **77**, 074709 (2008).
2) K. Yamamoto, *et al.*, *Phys. Status Solidi C* **9**, 1189 (2012).

Multifunction Integrated Macromolecules for Molecular-Scale Electronics

Research Center for Molecular Scale Nanoscience
Division of Molecular Nanoscience

TANAKA, Shoji Assistant Professor

Recently a single electron tunnel (SET) device has attracted much attention due to the growing demand for ultra-low-power device. A SET device manipulates an electron by means of one-by-one electron transfer, resulting in ultimately low power consumption. However, for room temperature operation, the size of SET device must be as small as a few nm to overcome the thermal fluctuation problems. The process size of a few nm is out of the range of conventional micro-technology. In this project, to establish an innovative fabrication process for SET device systems, we have been developing step-wise synthetic protocols for monomolecular single-electron tunnel devices (**MOSET**) and their integrated circuits.

1. Universal Temperature Crossover Behavior of Electrical Conductance in a Single Oligothiophene Molecular Wire[1)]

We have observed and analyzed a universal temperature crossover behavior of electrical conductance in a single oligothiophene molecular wire. The crossover between the Arrhenius type temperature dependence at high temperature and the temperature-invariant behavior at low temperature is found at a critical molecular wire length of 5.6 nm, where we found a change from the exponential length dependence to the length-invariant behavior. We have derived a scaling function analysis for the origin of the crossover behavior. After assuring that the analysis fits the explanation of the Keldysh Green's function calculation for the temperature dependence, we have applied it to our experimental results and found successfully that our scaling function gives a universal description of the temperature dependence for all over the temperature range.

2. Fabrication of 3- and 4-Terminal Single-Electron Device Structures

To integrate Coulomb islands and tunnel/capacitive junctions in a single molecular skeleton, we have developed a series of molecular building blocks (**1**–**8**). These building blocks make possible to fabricate various type of 3- and 4-terminal monomolecular single-electron tunnel device structures (**11**, **13**, **17**).

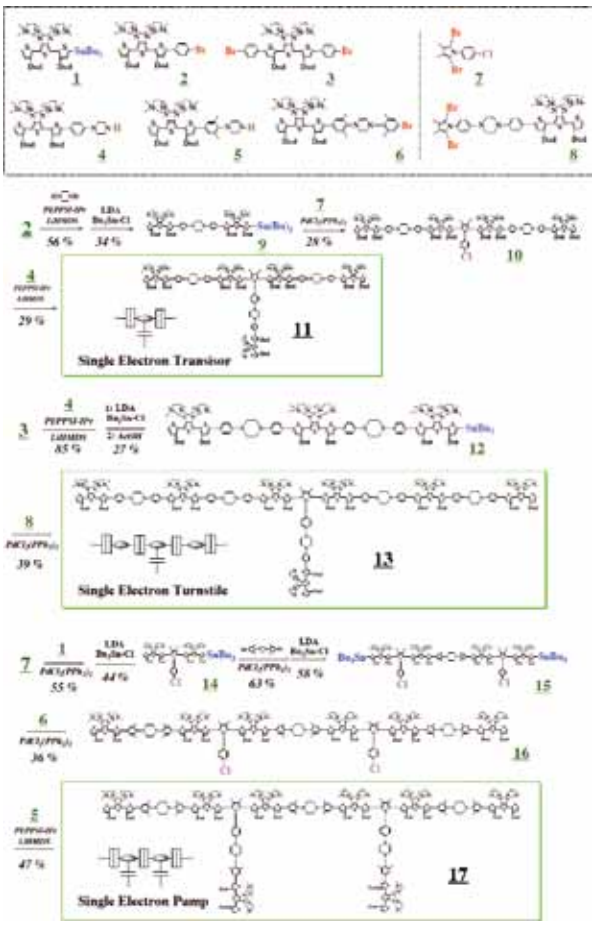

Reference

1) SK. Lee, R. Yamada, S. Tanaka, GS. Chang, Y. Asai and H. Tada, *ACS Nano* **6**, 5078–5082 (2012).

Development of Novel Heterocyclic Compounds and Their Molecular Assemblies for Advanced Materials

Safety Office

TOMURA, Masaaki Assistant Professor

Heterocycles containing sulfur and/or nitrogen atoms are useful as components of functional organic materials since heteroatoms in their rings are helpful to stabilize ions or ion-radical species. In addition, intermolecular interactions caused by heteroatom contacts can be expected to form unique molecular assemblies. In this project, novel functional organic materials based on various heterocycles were synthesized and their physical and structural properties were investigated.

1. Molecular and Crystal Structure of Bis(tetra-*n*-butylammonium) Bis(5,6-dicyanopyrazine-2,3-dithiolato-κ^2*S*,*S*') palladium(II)[1)]

Metal dithiolene complexes have been widely investigated as molecular conductors and superconductors. Several superconductors and single-component molecular metals involving dithiolene complexes have been discovered to date. We have synthesized the title palladium dithiolene complex derived from 2,3-dicyano-5,6-dimercaptopyrazine ligand. The ligand is expected to extend the π-conjugation of the complex resulting in decreased Coulombic repulsion. Intermolecular interactions caused by S···S and S···N heteroatom contacts may increase the dimensionality in the solid state. In the complex the dianion molecule is located on an inversion center. The dianion is a flat molecule with an r.m.s. deviation of 0.034(8) Å of fitted atoms from the least-squares plane. The central Pd atom has a square-planar coordination geometry and the Pd–S distances and the S–Pd–S angle are 2.276(3), 2.294(3) Å and 89.39(10)°, respectively. These values are comparable to those found in bis(tetra-*n*-butylammonium) bis(4,5-dicyanobenzene-1,2-di- thiolato-*S*,*S*')palladium(II) complex. The dianion molecules form a layered structure with an interlayer distance of 6.5 Å. The tetra-*n*-butylammonium cations are inserted between the layers.

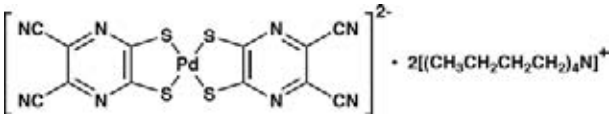

2. Photoinduced Electron-Transfer Reaction of α-Bromomethyl-Substituted Benzocyclic β-Keto Esters with Amines: Selective Reaction Pathways Depending on the Nature of the Amine Radical Cations

Photoinduced electron-transfer reaction of α-bromomethyl-substituted benzocyclic β-keto esters with tertiary amines was investigated. Debrominated β-keto esters and ring-expanded γ-keto esters were obtained as major products. On the basis of mechanistic experiments it was concluded that these products are formed via a reaction sequence of selective carbon–bromine bond cleavage and subsequent competitive hydrogen abstraction and Dowd–Beckwith ring-expansion of the resulting primary alkyl radicals. The characteristic product distribution observed for the type of amine used is rationalized on the basis of selective reaction pathways of generated radical intermediates that depend on the nature of the amine radical cations.

Reference

1) M. Tomura and Y. Yamashita, *Acta Crystallogr., Sect. E: Struct. Rep. Online* **68**, m57–m57 (2012).

Visiting Professors

Visiting Professor
ABE, Manabu *(from Hiroshima University)*

Stretch Effects Induced Molecular Strain in Generating Long-Lived Biradicals

Stretch effects induced by two types of molecular strain were examined by quantum chemical calculations, to design persistent multi-radicals such as localized diradicals and oxyallyls. The cooperative molecular strain (Type-1) induced by the spiro[5.5]undecane and bicyclo[2.1.0]cyclopentane structures was found to significantly destabilize in energy the ring-closed compounds of the diradicals, leading to small energy differences between the diradicals and the σ-bonded compounds. Another stretch effect (Type-2) induced by macrocyclic systems was also found to energetically destabilize the corresponding ring-closed structures of the 1,3-diradicals. The computational studies predict that the two types of stretch effects are quite effective in lowering the energy barriers of the bond-breaking reaction of the ring-closed compounds and in generating long-lived localized diradicals and oxyallyl derivatives.

Visiting Professor
KATO, Tatsuhisa *(from Kyoto University)*

Studies of Molecular Magnetization of Super-Molecules

The encapsulation of C_{60} with γ-cyclodextrin (γ-CD) has been attained by a mechanochemical high-speed vibration (HSV) technique. N@C_{60}, which can be a good magnetic probe giving the information of position as well as of chemical environment, should be soluble in water for the purpose of biological application. Then the HSV technique was applied to the powder of γ-CD and C_{60} containing N@C_{60} at 5%. The obtained molecular complex exhibited the peculiar electron spin resonance (ESR) spectrum of N@C_{60} in water.

We designed the flexible intermolecular communications in a simple molecular architecture by using mechanically interlocked supramolecular motives such as catenanes and rotaxanes, in which two or more molecular components are inseparable but their interactions are flexibly convertible. In a dinuclear Cu^{2+} complex of the four-fold rotaxane, the Cu^{2+}-porphyrin and the Cu^{2+}-phthalocyanine were stacked efficiently on one another to afford spin–spin communication. Spin states of the dinuclear complex were switchable between its protonated form (doublet) and deprotonated form (singlet) reversibly.

Visiting Professor
ASAKURA, Tetsuo *(from Tokyo University of Agriculture and Technology)*

Determination of Molecular Structure with Ultra Fast MAS under High-Field NMR

In single crystal X-ray diffraction analyses of peptides and proteins, it is well-known that the co-ordinates of carbon, nitrogen and oxygen atoms can be obtained in high accuracy, but enough accuracy cannot be obtained for those of hydrogen. Therefore we are trying to determine the accurate ^{1}H positions by the combination of NMR observation by ultra fast magic angle spinning under high field magnetic field and accurate ^{1}H NMR chemical shift calculation. We are applying this novel analytical technique to determine the structures of silk fibroins before and after spinning together with their model peptides. Since such a ^{1}H information is sensitive to both the intra- and inter -molecular structures, it is especially useful in molecular design of biomaterials with silks.

RESEARCH ACTIVITIES

RESEARCH ACTIVITIES

Life and Coordination-Complex Molecular Science

Department of Life and Coordination-Complex Molecular Science is composed of two divisions of biomolecular science, two divisions of coordination-complex molecular science, and one adjunct division. Biomolecular science divisions cover the studies on functions, dynamic structures, and mechanisms for various biomolecules such as sensor proteins, membrane-anchored proteins, biological-clock proteins, metalloproteins, glycoconjugates, and molecular chaperone. Coordination complex divisions aim to develop molecular catalysts and functional metal complexes for transformation of organic molecules, water oxidation and reduction, and molecular materials such as molecular wires. Interdisciplinary alliances in this department aim to create new basic concepts for the molecular and energy conversion through the fundamental science conducted at each division. Professor Koji Tanaka was retired at the end of March, 2012. Professors Shuji Akiyama and Tetsuro Murahashi were appointed as full professors of the Division of Biomolecular Sensing and the Division of Functional Coordination Chemistry, respectively, both in April, 2012.

Bioinorganic Chemistry of Metal-Containing Sensor Proteins

Department of Life and Coordination-Complex Molecular Science
Division of Biomolecular Functions

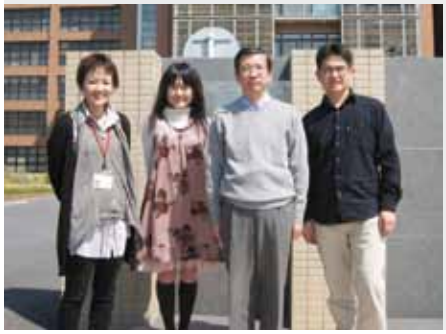

AONO, Shigetoshi	Professor
YOSHIOKA, Shiro	Assistant Professor
SAWAI, Hitomi	IMS Research Assistant Professor
TANIZAWA, Misako	Secretary

The widely studied biological function of heme is to act as a prosthetic group in hemeproteins that show a variety of functions, including oxygen storage and transport, electron transfer, redox catalysis, and sensing of gas molecules. In addition to these functions, a new function of hemeprotein has been found recently, which is a sensor of diatomic gas molecules or redox change.[1)] In these heme-based sensor proteins, the heme acts as the active site for sensing the external signal such as gas molecules and redox change. A new hemeprotein, aldoxime dehydratase (Oxd), also shows a novel biological function of heme, which catalyzes dehydration reaction of organic substrates. Oxd is the first example of hemeproteins that act as a hydro-lyase. Our research interests are focused on the elucidation of the structure-function relationships of these hemeproteins.

1. Bacterial Gas Sensor Proteins Using Transition Metal-Containing Prosthetic Groups as Active Sites[2,3)]

Gas sensor proteins are involved in many biological regulatory systems, including transcription, chemotaxis, and other complex physiological processes. These regulatory systems consist of a sensor and regulatory protein, and, if any, signal transduction proteins that transmit the input signal sensed by the sensor protein to regulator proteins. Sensor proteins are the most upstream component in these regulatory systems, and the sensor and regulator proteins can be distinct molecules, or can sometimes exist in the same molecule as sensor and regulator domains. In both cases, the general scheme is as follows for biological regulatory systems by gas sensor proteins. Once a gas sensor protein/domain senses a gas molecule of its physiological effector, a conformational change of the sensor protein/domain is induced, and then intra- and/or inter-molecular signal transductions proceed to modulate the activity of the regulator protein/domain that is responsible for the regulation of the above biological functions.

HemAT from *Bacillus subtilis* (HemAT-*Bs*) is a heme-containing O_2 sensor protein that acts as a chemotactic signal transducer. Binding of O_2 to the heme in the sensor domain of HemAT-*Bs* induces a conformational change in the protein matrix, and this is transmitted to a signaling domain. To characterize the specific mechanism of O_2-dependent conformational changes in HemAT-*Bs*, we investigated time-resolved resonance Raman spectra of the truncated sensor domain and the full-length HemAT-*Bs* upon O_2 and CO dissociation.

A comparison between the O_2 and CO complexes provides insights on O_2/CO discrimination in HemAT-*Bs*. While no spectral changes upon CO dissociation were observed in our experimental time window between 10 ns and 100 μs, the band position of the stretching mode between the heme iron and the proximal histidine, ν(Fe–His), for the O_2-dissociated HemAT-*Bs* was lower than that for the deoxy form on time-resolved resonance Raman spectra. This spectral change specific to O_2 dissociation would be associated with the O_2/CO discrimination in HemAT-*Bs*. We also compared the results obtained for the truncated sensor domain and the full-length HemAT-*Bs*, which showed that the structural dynamics related to O_2 dissociation for the full-length HemAT-*Bs* are faster than those for the sensor domain HemAT-*Bs*. This indicates that the heme proximal structural dynamics upon O_2 dissociation are coupled with signal transduction in HemAT-*Bs*.

We have also studied the protein dynamics of HemAT-*Bs* following CO photodissociation by time-resolved ultraviolet resonance Raman spectroscopy (UVRR). The UVRR spectra indicated two phases of intensity changes for Trp, Tyr, and Phe bands of both full-length and sensor domain proteins. The

W16 and W3 Raman bands of Trp, the F8a band of Phe, and the Y8a band of Tyr increased in intensity at hundreds of nanoseconds after CO photodissociation, and this was followed by recovery in ~50 μs. These changes were assigned to Trp-132 (G-helix), Tyr-70 (B-helix), and Phe-69 (B-helix) and/or Phe-137 (G-helix), suggesting that the change in the heme structure drives the displacement of B- and G-helices. The UVRR difference spectra of the sensor domain displayed a positive peak for amide I in hundreds of nanoseconds after photolysis, which was followed by recovery in ~50 μs. This difference band was absent in the spectra of the full-length protein, suggesting that the isolated sensor domain undergoes conformational changes of the protein backbone upon CO photolysis and that the changes are restrained by the signaling domain. The time-resolved difference spectrum at 200 μs exhibited a pattern similar to that of the static (reduced–CO) difference spectrum, although the peak intensities were much weaker. Thus, the rearrangements of the protein moiety toward the equilibrium ligand-free structure occur in a time range of hundreds of microseconds.

2. Spectroscopic Analyses of the Heme Environmental Structure of Aldoxime Dehydratase[4)]

Aldoxime dehydratase (Oxd) is a new heme-containing enzyme that works as a hydro-lyase catalyzing dehydration of aldoximes to nitriles. The enzymatic activity of Oxd is dependent on the oxidation state of the heme iron, though the reaction catalyzed by Oxd is not a redox reaction. Ferrous Oxd containing a Fe^{2+}-heme shows the enzymatic activity, but ferric Oxd containing a Fe^{3+}-heme does not. Previous spectroscopic analyses reveal a novel mechanism, where the change in the coordination mode of the substrate plays a crucial role for the regulation of the enzymatic activity. Unlike other heme enzymes, the organic substrate is directly bound to the heme iron in OxdRE. While the oxygen atom of aldoxime is coordinated to the ferric heme, the nitrogen atom of aldoxime is coordinated to the ferrous heme. The dehydration reaction proceeds only via N-coordinated substrate in the ferrous heme.

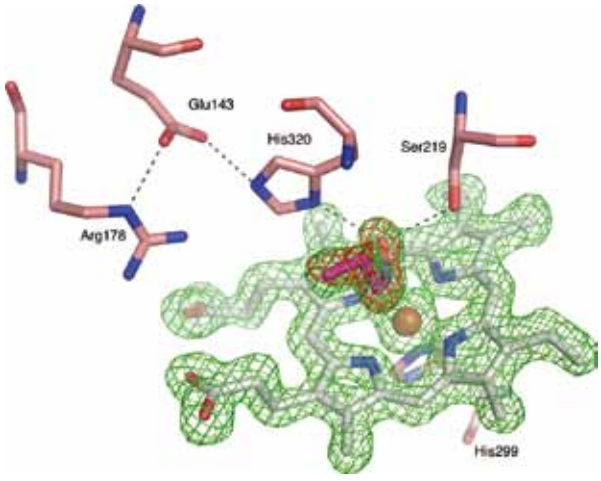

Figure 1. Heme environmental structure of the substrate-bound OxdRE.

In this study, we have elucidated the heme environmental structure of Oxd from *Rhodococcus sp.* N-771 (OxdRE) by analyzing Fourier transform infrared (FTIR) spectra and time-resolved step-scan FTIR spectra of CO-bound Oxd. Two C–O modes of heme at 1945 and 1964 cm^{-1} have been identified and remained unchanged in H_2O/D_2O exchange and in the pH 5.6–8.5 range, suggesting the presence of two conformations at the active site. The "light" minus "dark" difference FTIR spectra indicate that the heme propionates are in both the protonated and deprotonated forms, and the photolyzed CO becomes trapped within a ligand docking site (ν(CO) = 2138 cm^{-1}). The time-resolved step-scan FTIR spectra show that the rate of recombination of CO to the heme is $k_{1945\ cm^{-1}}$ = 126 ± 20 s^{-1} and $k_{1964\ cm^{-1}}$ = 122 ± 20 s^{-1} at pH 5.6, and $k_{1945\ cm^{-1}}$ = 148 ± 30 s^{-1} and $k_{1964\ cm^{-1}}$ = 158 ± 32 s^{-1} at pH 8.5. The rate of decay of the heme propionate vibrations is on a time scale coincident with the rate of rebinding, suggesting that there is a coupling between ligation dynamics in the distal heme environment and the environment sensed by the heme propionates.

The vibrational properties of the CO adduct of OxdRE indicate the formation of a photolabile species in which the proximal histidine and the H-bonding interactions of the negatively charged heme propionates are dominant factors in controlling the strength of the Fe–CO bond. The latter observation indicates that other factors beyond the well-known proximal and distal back-bonding contributions are effective in Oxd. Taken together, these results indicate that the distal residues control the proper orientation of the bound aldoxime and, thus, modulate the heme conformation from inactive to active. Obviously, there is communication linkage between the distal and proximal sites through bond networks suggesting that there is a coupling between ligation dynamics and the environment sensed by the heme propionates. The complexity of the structural implications involved in the transition from oxidized to reduced state in the presence of aldoxime should serve as a basis for uncovering the dynamic processes involved in the reaction mechanism of the enzyme.

References

1) S. Aono, *Dalton Trans.* 3125–3248 (2008).
2) S. El-Mashtoly *et. al., J. Biol. Chem.* **287**, 19973–19984 (2012).
3) Y. Yoshida *et. al., Biochim. Biophys. Acta, Proteins Proteomics* **1824**, 866–872 (2012).
4) E. Pinakoulaki *et. al., J. Phys. Chem. B* **115**, 13012–13018 (2011).

Elucidation of the Molecular Mechanisms of Protein Folding

Department of Life and Coordination-Complex Molecular Science
Division of Biomolecular Functions

KUWAJIMA, Kunihiro	Professor
MAKABE, Koki	Assistant Professor
NAKAMURA, Takashi	IMS Research Assistant Professor
CHEN, Jin	OIIB Research Assistant Professor
TAKENAKA, Toshio	Post-Doctoral Fellow
MIZUKI, Hiroko	Technical Fellow
TANAKA, Kei	Secretary

Kuwajima group is studying mechanisms of *in vitro* protein folding and mechanisms of molecular chaperone function. Our goals are to elucidate the physical principles by which a protein organizes its specific native structure from the amino acid sequence. In this year, we studied the fibrillogenic propensity of the GrEL apical domain and the sequential four-state folding/unfolding of goat α-lactalbumin and its N-terminal variants.

1. Fibrillogenic Propensity of the GroEL Apical Domain: A Janus-Faced Minichaperone

The chaperonin GroEL plays an essential role in promoting protein folding and in protecting against misfolding and aggregation in the cellular environment. In this study, we report that both GroEL and its isolated apical domain form amyloid-like fibrils under physiological conditions, and that the fibrillation of the apical domain is accelerated under acidic conditions. We also found, however, that despite its fibrillation propensity, the apical domain exhibits a pronounced inhibitory effect on the fibril growth of β_2-microglobulin. The analysis of the primary amino-acid sequence by programs, PASTA, TANGO and Zyggregator, which predict aggregation-prone sequences, indicates that the most aggregation-prone sequence is located in residues 260–280, which is coincident with the substrate protein-binding site in the chaperonin GroEL. Therefore, there is a close relationship between the fibrillogenic propensity and the substrate binding of GroEL. Furthermore, the analysis of 1003 sequences of the chaperonin family proteins by the Zyggregator program has shown that the aggregation-prone sequence is present in the substrate-binding site, indicating that the close relationship between the fibrillogenic propensity and the substrate binding is a general property of the chaperonin family.

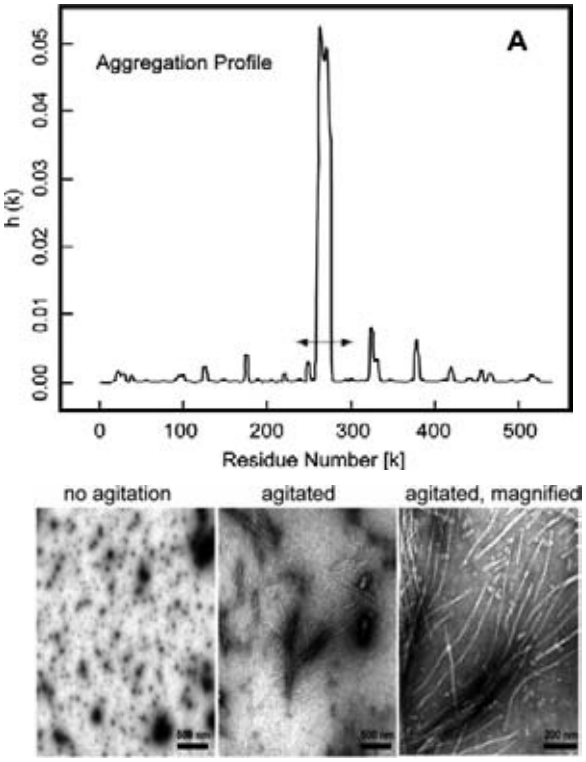

Figure 1. The aggregation profile of GroEL obtained by the analysis with PASTA (A), and the transmission electron microscopic observations of the isolated apical domain at pH 7.0 and 37 °C at 0.1 M NaCl in the presence of 0.5 mM SDS, where the amyloid-like fibrils of the apical domain were formed when the solution was agitated.

2. Sequential Four-State Folding/Unfolding of Goat α-Lactalbumin and Its N-Terminal Variants

Equilibria and kinetics of folding/unfolding of goat α-lactalbumin (GLA) and its two N-terminal variants were studied by circular dichroism spectroscopy. The two variants were wild-type recombinant and Glu1-deletion (E1M) variants expressed in *Escherichia coli*. The presence of an extra methionine at the N terminus in recombinant GLA destabilized the protein by 2 kcal/mol, while the stability was recovered in the E1M variant in which Glu1 was replaced by Met1. Kinetic folding/unfolding reactions of the proteins, induced by stopped-flow concentration jumps of guanidine hydrochloride, indicated the presence of a burst-phase in refolding, and gave chevron plots with significant curvatures in both the folding and unfolding limbs. The folding-limb curvature was interpreted in terms of accumulation of the burst-phase intermediate (I). However, there was no burst phase observed in the unfolding kinetics to interpret the unfolding-limb curvature. We thus assumed a sequential four-state mechanism, in which the folding from the burst-phase intermediate takes place via two transition states separated by a high-energy intermediate (J). We estimated changes in the free energies of the burst-phase intermediate I and two transition states (‡1 and ‡2), caused by the N-terminal variations and also by the presence of stabilizing calcium ions. The Φ values at the N terminus and at the Ca^{2+}-binding site thus obtained increased successively during folding, demonstrating the validity of the sequential mechanism. The stability and the folding behavior of the E1M variant were essentially identical to those of the authentic protein, allowing us to use this variant as a pseudo-wild-type GLA in future studies.

Residue No. / Protein	0	1	2	3	4	5	6	7	8	9	10
Authentic GLA		E	Q	L	T	K	C	E	V	F	Q
Recombinant GLA	M	E	Q	L	T	K	C	E	V	F	Q
E1M variant		M	Q	L	T	K	C	E	V	F	Q

Figure 2. The amino acid sequences of the N-terminal residues of authentic GLA, recombinant GLA, and the E1M variant.

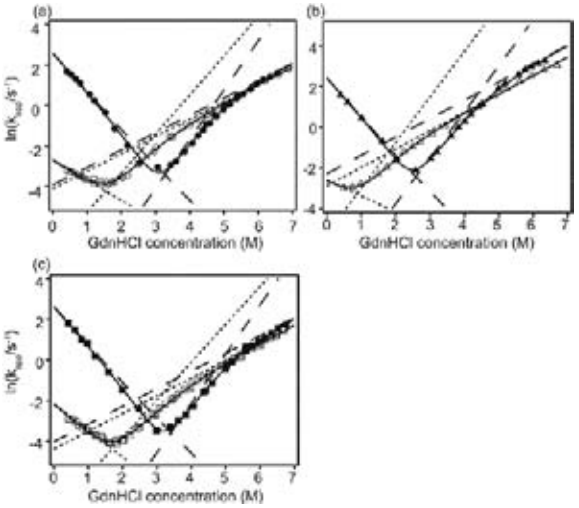

Figure 3. Chevron plots of authentic GLA (a), recombinant GLA (b), and the E1M variant (c) in the holo (filled symbols) and apo (open symbols) forms at pH 7.0 and 25 °C. The solid lines are theoretical curves fitted by the sequential four-state model. The broken lines and dotted lines represent the GdnHCl dependence of logarithms of microscopic rate constants ($\ln(k_1)$, $\ln(k_{-1}k_{-2}/k_2)$ and $\ln(k_{-2})$) of folding and unfolding kinetics; the first two are rate-limited by the transition state 1 (‡1), and the last one by the transitions state 2 (‡2).

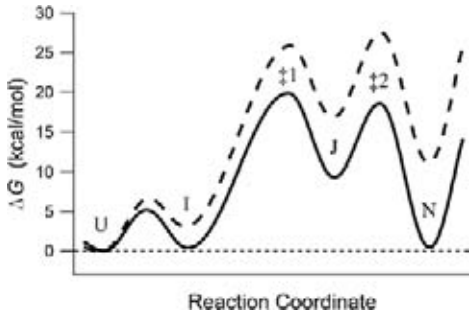

Figure 4. Schematic free-energy profiles of unfolding of GLA under a weakly unfolding condition (solid line) and under a strongly unfolding condition (broken line). Under the weakly unfolding condition, the transition state is located at ‡1, while it is located at ‡2 under the strongly unfolding condition at a high GdnHCl concentration (>5.5*M*). The free-energy profiles shown correspond to those for authentic holo GLA at 3.3*M* GdnHCl (solid line) and at 6.5*M* GdnHCl (broken line). A hypothetical intermediate (J) located between ‡1 and ‡2 is metastable under all conditions, that is, it is higher in free energy than U, I, and N.

References

1) J. Chen, H. Yagi, P. Sormanni, M. Vendruscolo, K. Makabe, T. Nakamura, Y. Goto and K. Kuwajima, *FEBS Lett.* **586**, 1120–1127 (2012).

2) K. Tomoyori, T. Nakamura, K. Makabe, K. Maki, K. Saeki and K. Kuwajima, *Proteins; Struct., Funct., Bioinf.* **80**, 2191–2206 (2012).

Elucidation of Dynamical Structures of Biomolecules toward Understanding the Mechanisms Underlying Their Functions

Department of Life and Coordination-Complex Molecular Science
Division of Biomolecular Functions

KATO, Koichi	Professor
YAMAGUCHI, Takumi	Assistant Professor
KAMIYA, Yukiko	IMS Research Assistant Professor*
YAGI-UTSUMI, Maho	OIIB Research Assistant Professor
YANAGI, Kotaro	IMS Fellow
UEKUSA, Yoshinori	Post-Doctoral Fellow
BOONSRI, Pornthip	Visiting Scientist
BUI DINH, Long	Visiting Scientist
SUGIHARA, Takahiro	Research Fellow
CHANDAK, Mahesh	Graduate Student
ZHANG, Ying	Graduate Student
KUNIHARA, Tomoko	Graduate Student
UNO, Tsuyoshi	Graduate Student†
YAMAMOTO, Sayoko	Graduate Student†
KUMOI, Kentaro	Graduate Student†
OKAWA, Keisuke	Graduate Student†
INAGAKI, Kouya	Graduate Student†
THAMMAPORN, Ratsupa	Graduate Student‡
SUZUKI, Mariko	Technical Fellow
ISONO, Yukiko	Technical Fellow
TANAKA, Kei	Secretary

Our biomolecular studies are based on detailed analyses of structures and dynamics of various biological macromolecules and their complexes at atomic level, using NMR spectroscopy and X-ray crystallography in conjunction with other biophysical, biochemical and molecular biology techniques. Here we report our recent studies of conformations, dynamics, and interactions of oligosaccharides and glycoconjugates along with proteins involved in the ubiquitin (Ub)-proteasome system.

1. Lanthanide-Assisted NMR Analyses of the Conformational Ensemble of Oligosaccharides in Conjunction with Molecular Dynamics Simulations

Conformational flexibility is an important property of biological molecules functioning in living systems, as best exemplified by oligosaccharides. We attempted to combine the lanthanide-assisted NMR method with molecular dynamics (MD) simulations for the evaluation of dynamic conformational ensembles of highly flexible oligosaccharides. In this approach, a metal-chelating tag was covalently attached to the reducing end of the oligosaccharide moieties of gangliosides, which form integral parts of cellular membranes, for observing pseudocontact shifts (PCSs). Upon complexation with paramagnetic lanthanide ions, the tagged GM3 trisaccharide, which is the common core structure shared among the gangliosides, exhibited NMR spectral changes due to PCSs according to the relative positions of the individual atoms with respect to the lanthanide ion coordinated at the tag. The observed PCS values were in excellent agreement with those back-calculated from the vast conformational ensemble of the trisaccharide derived from MD simulations (Figure 1). Thus, the PCS measurements offer a valuable experimental tool for the validation of MD simulation of highly flexible biomolecules.[1)] Furthermore, this approach was successfully applied to the characterization of the conformational dynamics of the branched tetrasaccharide of ganglioside GM2.[2)] The interbranch interactions responsible for the conformational differences between the GM2 tetrasaccahride and the GM3 trisaccharide were identified by the paramagnetic NMR method in conjunction with MD simulations. These results demonstrated the utility of our approach in the evaluation of dynamic conformational ensembles of oligosaccharides, considering their minor conformers in a systematic manner.

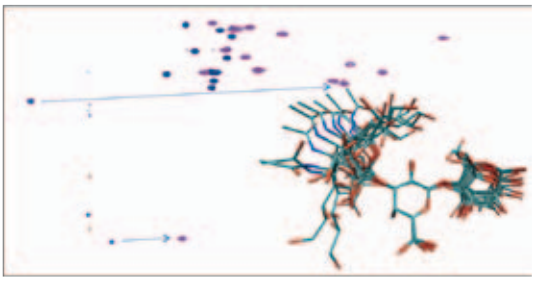

Figure 1. ^{1}H–^{13}C HSQC spectral change of the GM3 trisaccharide tagged with a paramagnetic ion and snapshots of the sugar from an MD-simulated trajectory.

2. Structural Basis for Improved Effector Functions of Antibodies by Engineering of Their Glycans

More than half of proteins in nature are estimated to be modified by sugar chains, which affect the physical and biological properties of proteins. The effector functions of immunoglobulin G (IgG) critically depend on *N*-glycosylation of its Fc region. Removal of the fucose residue from the *N*-glycans of IgG-Fc results in a dramatic enhancement of antibody-dependent cellular cytotoxicity (ADCC) through improved affinity for Fcγ receptor IIIa (FcγRIIIa). We successfully determined the crystal structure of the complex formed between non-fucosylated IgG1-Fc and a soluble form of FcγRIIIa (sFcγRIIIa) with two *N*-glycosylation sites (Figure 2a).[3] The crystal structure demonstrates that one of the two *N*-glycans of sFcγRIIIa mediates the interaction with the *N*-glycan of non-fucosylated Fc, thereby stabilizing the complex. However, fucosylation of the Fc *N*-glycans impairs this interaction because of steric hindrance. On the other hand, our NMR data demonstrated that Tyr296 of the non-fucosylated Fc glycoform exhibits conformational multiplicity in its uncomplexed state, suggesting that conformational selection is governed by the presence or absence of the fucose residue of the Fc *N*-glycan. These findings offer a structural basis for improvement in ADCC of therapeutic antibodies by defucosylation.

3. Conformational Dynamics of Proteins Involved in the Ubiquitin-Proteasome System

While recent progresses have been made in understanding intra-domain conformational fluctuations of proteins, the evaluation of the relative motions of individual domains of multi-domain proteins is still a challenge. We successfully characterized conformational dynamics of Lys-48-linked Ub dimer (diUb) in solution using NMR spectroscopy.[4] Comparison of a chemical shift of wild-type diUb with that of monomeric Ub and cyclic diUb, which mimic the open and closed states (Figure 2b), respectively, with regard to the exposure of hydrophobic surfaces to the solvent indicates that wild-type Lys-48-linked diUb in solution predominantly exhibits the open conformation (75% at pH 7.0), which becomes more populated upon lowering pH. The intrinsic properties of Lys-48-linked Ub chains to adopt the open conformation may be advantageous for interacting with Ub-binding proteins. We also characterized interaction modes of the Ub-like domains of HOIL-1L and HR23 with their specific binding-partners by NMR spectroscopy.[5,6]

Furthermore, we developed a novel technique for real-time monitoring of subunit exchange in homooligomeric proteins, using deuteration-assisted small-angle neutron scattering, and applied it to the tetradecamer of the proteasome α7 subunit.[7]

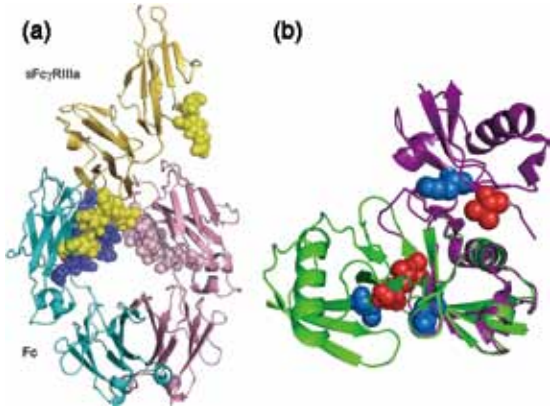

Figure 2. 3D structures of (a) sFcγRIIIa bound to non-fucosylated Fc and (b) wild-type Lys-48-linked diUb. The open form of diUb (purple) was superposed on the closed state (green).

References

1) S. Yamamoto, Y. Zhang, T. Yamaguchi, T. Kameda and K. Kato, *Chem. Commun.* **48**, 4752–4754 (2012).
2) Y. Zhang, S. Yamamoto, T. Yamaguchi and K. Kato, *Molecules* **17**, 6658–6671 (2012).
3) T. Mizushima, H. Yagi, E. Takemoto, M. Shibata-Koyama, Y. Isoda, S. Iida, K. Masuda, M. Satoh and K. Kato, *Genes Cells* **16**, 1071–1080 (2011).
4) T. Hirano, O. Serve, M. Yagi-Utsumi, E. Takemoto, T. Hiromoto, T. Satoh, T. Mizushima and K. Kato, *J. Biol. Chem.* **286**, 37496–37502 (2011).
5) H. Yagi, K. Ishimoto, T. Hiromoto, H. Fujita, T. Mizushima, Y. Uekusa, M. Yagi-Utsumi, E. Kurimoto, M. Noda, S. Uchiyama, F. Tokunaga, K. Iwai and K. Kato, *EMBO Rep.* **13**, 462–468 (2012).
6) Y. Kamiya, Y. Uekusa, A. Sumiyoshi, H. Sasakawa, T. Hirao, T. Suzuki and K. Kato, *FEBS Lett.* **586**, 1141–1146 (2012).
7) M. Sugiyama, E. Kurimoto, H. Yagi, K. Mori, T. Fukunaga, M. Hirai, G. Zaccai and K. Kato, *Biophys. J.* **101**, 2037–2042 (2011).

Awards

YAMAMOTO, Sayoko; Young Scientists Poster Awards, The International Symposium on Nuclear Magnetic Resonance 2011 (2011).
KATO, Koichi; The Erwin von Bälz Prize 2011 (First Prize) (2011).
YAMAGUCHI, Takumi; CSJ Presentation Award 2012, The 92nd Annual Meeting of The Chemical Society of Japan (2012).
ZHANG, Ying; FY2012 Sokendai President's Award (2012).
KUMOI, Kentaro; Young Poster Award, The 12th Annual Meeting of The Protein Science Society of Japan (2012).

* Present Address; Graduate School of Engineering, Nagoya University
† carrying out graduate research on Cooperative Education Program of IMS with Nagoya City University
‡ carrying out graduate research on Cooperative Education Program of IMS with Kasetsart University

Structure-Function Relationship of Metalloproteins

Department of Life and Coordination-Complex Molecular Science
Division of Biomolecular Functions

FUJII, Hiroshi	Associate Professor
KURAHASHI, Takuya	Assistant Professor
CONG, Zhiqi	IMS Fellow
OHTSUKI, Akimichi	Post-Doctoral Fellow
WANG, Chunlan	Graduate Student
TANIZAWA, Misako	Secretary

Metalloproteins are a class of biologically important macromolecules, which have various functions such as oxygen transport, electron transfer, oxidation, and oxygenation. These diverse functions of metalloproteins have been thought to depend on the ligands from amino acid, coordination structures, and protein structures in immediate vicinity of metal ions. In this project, we are studying the relationship between the electronic structures of the metal active sites and reactivity of metalloproteins.

1. Formation of Iron(III) *Meso*-Chloro-Isoporphyrin as a Reactive Chlorinating Agent from Oxoiron(IV) Porphyrin π-Cation Radical[1)]

Oxoiron(IV) porphyrin π-cation radicals are generally known to function as key reactive intermediates in a variety of oxidation reactions catalyzed by heme enzymes such as cytochrome P450. The oxoiron(IV) porphyrin π-cation radical complex has several isoelectronic forms which are two oxidation state equivalents higher than that of the iron(III) porphyrin complex. Isoporphyrins, tautomers of porphyrins with a saturated *meso* carbon, were originally postulated by Woodward, and its metal complex was first reported by Dolphin *et al.*, who prepared a zinc(II) 5'-methoxy-5,10,15,20-tetraphenylisoporphyrin complex by nucleophilic attack of methanol on zinc(II) 5,10,15,20-tetraphenylporhyrin π-dication complex. Since then, iron(III) isoporphyrin complexes, particularly *meso*-tetraaryl derivatives, have been synthesized chemically and electrochemically. However, to our surprise, atom transfer reactions of isoporphyrin complexes to substrates, such as oxygenation and halogenation reactions, have not been studied well. In this study, we show that an oxoiron(IV) porphyrin π-cation radical complex can be converted to iron(III) *meso*-chloro-isoporphyrin complex in the presence of trifluoroacetic acid (TFA) and chloride ion. The formation of the isoporphyrin complex would be due to protonations of the oxo ligand of oxoiron(IV) porphyrin π-cation radical species. More importantly, this study shows that the iron(III) *meso*-chloro-isoporphyrin complex is a reactive reagent for chlorination of aromatic compounds and olefins.

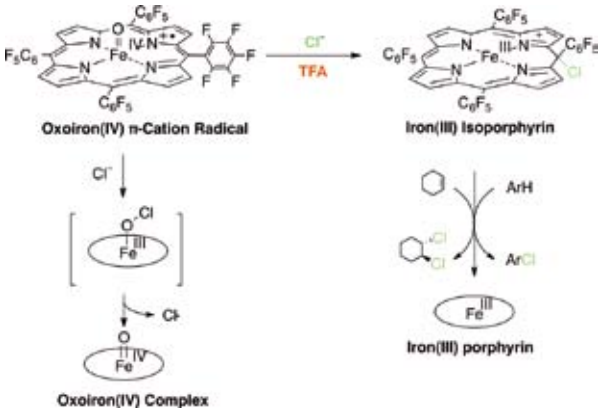

Figure 1. Reaction of oxoiron(IV) porphyrin π-cation radical complex with chloride ion in the presence and absence of proton.

2. The Effect of the Axial Ligand on the Reactivity of the Oxoiron(IV) Porphyrin π-Cation Radical Complex: Higher Stabilization of the Product State Relative to the Reactant State[2)]

The proximal heme axial ligand plays an important role in tuning the reactivity of oxoiron(IV) porphyrin π-cation radical species (compound I) in enzymatic and catalytic oxygenation reactions. To reveal an essence of the axial ligand effect on the reactivity, we investigated from a thermodynamic viewpoint. Compound I model complexes, $(TMP^{+\bullet})Fe^{IV}O(L)$ (where TMP is 5,10,15,20-tetramesitylporphyrin and $TMP^{+\bullet}$ is its π-cation radical), can be provided with altered reactivity by changing the identity of the axial ligand, but the reactivity is not correlated with spectroscopic data (ν(Fe=O), redox potential, and so on) of $(TMP^{+\bullet})Fe^{IV}O(L)$. Surprisingly, a clear correlation was found between the reactivity of $(TMP^{+\bullet})$

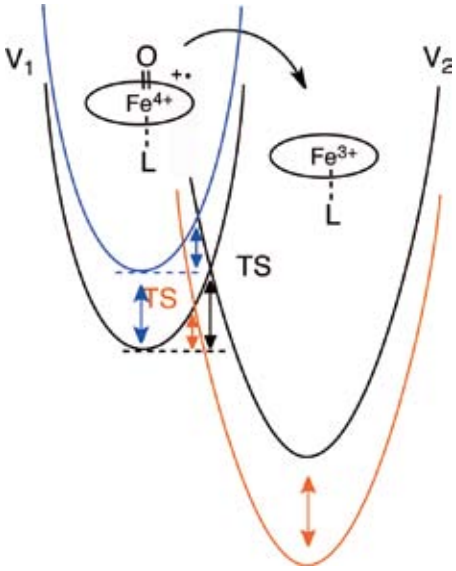

Figure 2. Curve crossing diagram of potential-energy surfaces of the reactant, $(TMP^{+\bullet})Fe^{IV}O(L)$, and product, $(TMP)Fe^{III}(L)$, states. Blue line; Change of stability of $(TMP^{+\bullet})Fe^{IV}O(L)$ and red line; change of stability of $(TMP)Fe^{III}(L)$.

$Fe^{IV}O(L)$ and the Fe^{II}/Fe^{III} redox potential of $(TMP)Fe^{III}L$, the final reaction product. This suggests that the thermodynamic stability of $(TMP)Fe^{III}L$ is involved in the mechanism of the axial ligand effect. Axial ligand-exchange experiments and theoretical calculations demonstrate a linear free-energy relationship, in which the axial ligand modulates the reaction free energy by changing the thermodynamic stability of (TMP) $Fe^{III}(L)$ to a greater extent than $(TMP^{+\bullet})Fe^{IV}O(L)$. The linear free energy relationship could be found for a wide range of anionic axial ligand and for various types of reactions, such as epoxidation, demethylation, and hydrogen abstraction reactions. An essence of the axial ligand effect is neither the electron donor ability of the axial ligand nor the electron affinity of compound I, but the binding ability of the axial ligand (the stabilization by the axial ligand). An axial ligand that binds more strongly makes $(TMP)Fe^{III}(L)$ more stable and $(TMP^{+\bullet})Fe^{IV}O(L)$ more reactive. All results indicate that the axial ligand controls the reactivity of compound I (the stability of the transition state) by the stability of the ground state of the final reaction product and not by compound I itself.

3. Oxidation of Chloride Ion and Subsequent Chlorination of Organic Compounds by Oxoiron(IV) Porphyrin π-Cation Radical Complexes[3)]

Enantioselective transition-metal-catalyzed oxygenation reactions have received much attention because of the demand for organic synthesis strategies and their biological relevance with respect to metalloenzymes. Terminal oxidants such as peroxides, iodosylarenes, and peracids have been utilized as an oxygen source for these oxygenation reactions. Since the terminal oxidants must be stable for easy handling, the primary role of the transition-metal catalyst is to activate a stabilized oxidant and to generate a transient species that remains active enough to transfer an oxygen atom to a substrate. The activation of a terminal oxidant is initiated by binding to the metal complex to form a terminal oxidant adduct of the metal complex. Recently, evidence has been mounting in support of the proposal that the terminal oxidant adduct of a metal complex is not only a precursor to a reactive high valent metal-oxo species, but also itself may serve as a reactive species for an oxygenation reaction. Although terminal oxidant adducts of metal complexes are unstable and reactive compounds in most cases, metal complex adducts with hydrogen peroxide, alkylperoxides, and *m*-CPBA have been isolated and structurally characterized. In contrast to these successful reports, and much to our surprise, there have been no examples of structural characterization of any iodosylarene adducts of metal complexes, although they have emerged as useful oxidants for various organic reactions. The most intensive spectroscopic study was performed by Hill *et al.*, who thoroughly investigated an iodosylbenzene adduct of a manganese porphyrin complex with ^{1}H NMR, IR and ^{127}I Mössbauer spectroscopy. However, the nature of the bonding interaction between iodosylbenzene and the metal ion remains unclear. Here, we report on the preparation and X-ray crystal structure of an iodosylarene adduct of a manganese(IV) salen complex bearing a *trans*-cyclohexane-1,2-diamine linkage as chiral unit.

Figure 3. Synthesis and structural characterization of bis-iodosylmesitylene adduct of manganese(IV) salen complex.

References

1) Z. Cong, T. Kurahashi and H. Fujii, *J. Am. Chem. Soc.* **134**, 4469–4472 (2012).
2) A. Takahashi, D. Yamaki, K. Ikemura, T. Kurahashi, T. Ogura, M. Hada and H. Fujii, *Inorg. Chem.* **51**, 7296–7305 (2012).
3) C. Wang, T. Kurahashi and H. Fujii, *Angew. Chem., Int. Ed.* **51**, 7809–7811 (2012).

Award

WANG, Chunlan; The best pster presentation, The 44th Symposium on Chemical and Biological Oxidation (2011).

Molecular Origin of 24 Hour Period in Cyanobacterial Protein Clock

Department of Life and Coordination-Complex Molecular Science
Division of Biomolecular Sensing

AKIYAMA, Shuji — Professor (April, 2012–)
ABE, Hitomi — Secretary

Circadian (approximately 24 h) clocks are endogenous time-keeping systems encapsulated in living cells, enabling organisms to adapt to daily fluctuation of exogenous environments on the Earth. These time-keeping systems, found ubiquitously from prokaryotes to eukaryotes, share the three characteristics. First, the circadian rhythmicity of the clocks persists even without any external cues (self-sustainability). Second, the period is little dependent on ambient temperature (temperature compensation). Third, the phase of the clock can be reset by external stimuli such as lightning, humidity, or temperature so as to be synchronized to the external phase (synchronization).

KaiC, a core protein of the circadian clock in cyanobacteria, undergoes rhythmic structural changes over approximately 24 h in the presence of KaiA and KaiB (Kai oscillator). This slow dynamics spanning a wide range of both temporal and spatial scales is not well understood, and is central to a fundamental question: what determines the temperature-compensated 24 h period?[1,2] The Kai oscillator reconstitutable *in vitro* is advantageous for studying its dynamic structure through a complementary usage of both X-ray crystallography and solution scattering, its transient response by using physicochemical techniques, and its molecular motion through a collaborative work with computational groups.

Our mission is to explore the frontier in molecular science of the cyanobacterial circadian clock from many perspectives. This Annual Report summarizes our recent activities from April 1, 2012 through August 31, 2012.

1. Tracking the Ticking of Cyanobacterial Clock Protein KaiC in Solution[3)]

The ATPase activity of KaiC *alone* is strongly correlated with the oscillatory period of the Kai oscillator. This correlation suggests that the ATPase activity of KaiC is one of the period-determining factors of the Kai oscillator. Hence, the determination of the structural change of KaiC interlocked with the ATPase activity is of great of importance.

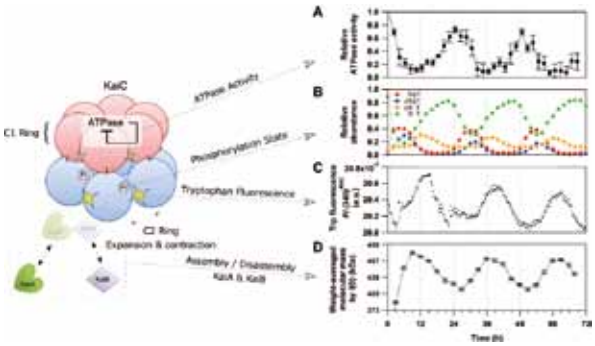

Figure 1. Circadian dynamics of cyanobacterial clock protein KaiC. The C1 and C2 domains in each protomer of KaiC are drawn as red and blue spheres, respectively. Expansion and contraction motions of the C2 ring (B, C) in solution serves as a timing cue for assembly/disassembly of KaiA and KaiB (D), and is interlocked with its C1 ATPase udder a control of negative-feedback regulation (A).

To track the dynamic transition of KaiC in real-time, we recorded the time evolution of intrinsic tryptophan (Trp) fluorescence from KaiC contained in the Kai oscillator. KaiC is a dumbbell-shaped molecule composed of tandemly duplicated N-terminal (C1) and C-terminal (C2) domains. Six protomers are assembled into a hexamer to attain a double-doughnut shape. Two tryptophan (Trp) residues located in the protomer-protomer interface of the C2 domain can serve as a sensitive probe to monitor the potential structural transition of the C2 ring. The intensity of the Trp fluorescence from KaiC revealed a rhythmic fluctuation with the period of approximately 24 h (Figure 1, panel C). So far as we know, this is the first experimental evidence that demonstrated a dynamic

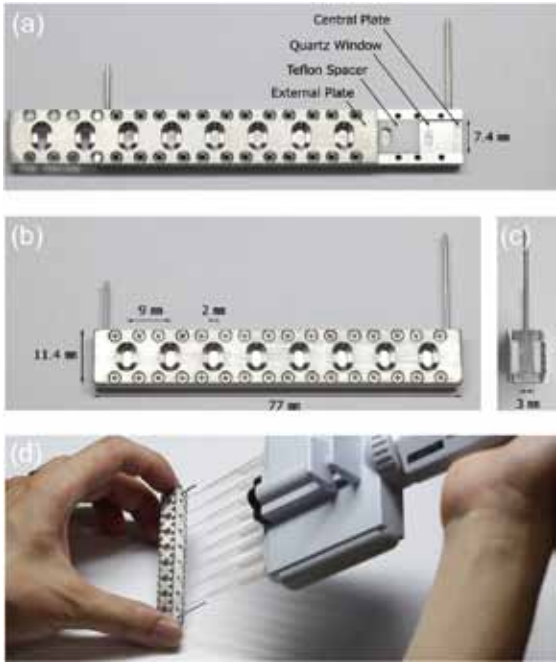

Figure 2. Octuple cuvette. (a) Photograph of the central plate covered by the quartz window, Teflon spacer and external plate, in that order. (b) Front view of the assembly. (c) Side view of the assembly. (d) Filling and removal of solutions using a commercially available eight-channel pipette. The sample volume of each chamber is 25 µl.

structural transition of the C2 ring of KaiC in solution.

Concomitantly with the Trp-fluorescence dynamics, KaiC underwent a periodic change in its phosphorylation state (Figure 1, panel B). KaiC has the two phosphorylation sites, *i.e.*, Ser431 and Thr432, in the C2 domain, and both residues are phosphorylated and then dephosphorylated in a programmed sequence during the phosphorylation cycle as follows: KaiCS/pT → KaiCpS/pT → KaiCpS/T → KaiCS/T (where 'S' represents Ser431, 'pS' represents phosphorylated Ser431, 'T' represents Thr432, and 'pT' represents phosphorylated Thr432). Interestingly, the Trp fluorescence was maximized at the timing when the KaiCpS/T state was populated (Figure 1, panels B and C). The result suggests the Trp fluorescence is an excellent measure of the phosphor-coupled transition of the C2 ring in KaiC.

2. Visualization of Dynamic Structural Changes of KaiC Using Small-Angle X-Ray Solution Scattering Technique[3,4)]

To visualize the C2-ring dynamics confirmed by tracking Trp fluorescence, we measured the small-angle x-ray scattering (SAXS) from KaiC in solution. To obtain the SAXS data of biological samples in solution, one must first record the scattering intensity of the sample (biomacromolecules in solution) and then that of the matching buffer in the separate

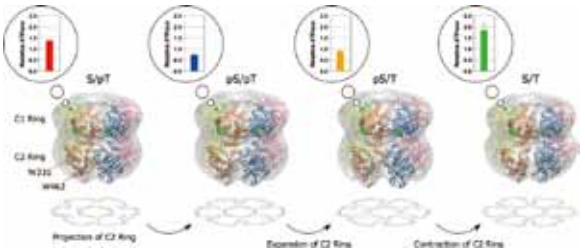

Figure 3. Expansion and contraction motions of C2 ring of KaiC interlocked with ATPase activity.

experiment, and finally find the difference between two intensities. The cuvette used for conventional SAXS experiments has only a single observation chamber in order to ensure the qualitative subtraction of the scattering contributed by the solvent molecules. On the other hand, the use of the single-chamber cuvette makes both the experiment and analysis time-consuming.

To record the SAXS pattern of KaiC both efficiently and qualitatively, we designed and constructed an eight-chamber cuvette (octuplet cuvette), each chamber of which was fabricated so uniformly to ensure the inter-chamber subtraction (Figure 2). The developed cuvette enabled us to acquire SAXS dataset of KaiC roughly 10 times faster without any significant degradation of data quality.

On the basis of the obtained SAXS data, we built low-resolution models of the KaiC hexamer as shown in Figure 3. The overall shape is almost unchanged in the transition from KaiCS/pT to KaiCpS/pT, whereas the radius of the C2 ring is dramatically enlarged in the subsequent transition from KaiCpS/pT to KaiCpS/T. The expanded C2 ring is partly contracted in the transition from KaiCpS/T to KaiCS/T, and is further contracted in the subsequent transition from KaiCS/T to KaiCS/pT. The present model suggests that KaiC ticks through expanding and contracting motions of the C2 ring.

The dynamic motion of the C2 ring uncovered throughout our study is chronobiologically meaningful, we believe, in terms of the elucidation of the key conformational change tightly coupled to the period-determining ATPase of KaiC. Our group is trying to improve spatio-temporal resolution of the experiments so as to draw a more dynamic and detailed picture of KaiC ATPase.

References

1) S. Akiyama, *Cell. Mol. Life Sci.* **69**, 2147–2160 (2012).
2) A. Mukaiyama, T. Kondo and S. Akiyama, *SPring-8 Research Frontiers 2011* 47–48 (2012).
3) Y. Murayama, A. Mukaiyama, K. Imai, Y. Onoue, A. Tsunoda, A. Nohara, T. Ishida, Y. Maéda, T. Kondo and S. Akiyama, *EMBO J.* **30**, 68–78 (2011).
4) S. Akiyama and T. Hikima, *J. Appl. Crystallogr.* **44**, 1294–1296 (2011).

Investigation of Molecular Mechanisms of Channels, Transporters and Receptors in Membrane

Department of Life and Coordination-Complex Molecular Science
Division of Biomolecular Sensing

FURUTANI, Yuji	Associate Professor
KIMURA, Tetsunari	Assistant Professor
TSUKAMOTO, Hisao	IMS Research Assistant Professor
INAGUMA, Asumi	Post-Doctoral Fellow
GUO, Hao	Graduate Student
FUJIWARA, Kuniyo	Graduate Student
SHIMIZU, Atsuko	Secretary

Membrane proteins are important for homeostasis of living cells, which work as ion channels, transporters, various types of chemical and biophysical sensors, and so on. These proteins are considered as important targets for biophysical studies.

Our main goal is to clarify molecular mechanisms of channels, transporters and receptors in cell membrane mainly by using stimulus-induced difference infrared (IR) spectroscopy, which is sensitive to the structural and environmental changes of organic- and bio-molecules. Recently, Dr. Kimura started to construct a microfluidic device to monitor biological and chemical reactions by infrared and fluorescent microscopic techniques. Dr. Tsukamoto has established a protein expression system with mammalian cell line.

1. Anion-Transport Mechanism of a Chloride Ion Pump *p*HR Studied by Time-Resoved FTIR Spectroscopy

pharaonis Halorhodopsin (*p*HR) is a light-driven inward chloride ion pump protein. The ion transportation is performed through the sequential formation of several intermediates (K, L_1, L_2, N and O) during the photocyclic reaction. The structural details of each intermediate state have been studied by various kinds of physicochemical methods, however it is still open question how the structural changes of protein molecule and water molecules are involved in the translocation of a chloride ion inside protein at physiological temperature. To analyze the structural dynamics, we performed the time-resolved Fourier transform infrared (TR-FTIR) spectroscopy in the whole mid-infrared region under various hydration conditions. Measurements under D_2O reveal the structural information of the water inaccessible backbone of protein itself, and those with H_2O or $H_2{}^{18}O$ give an insight on the dynamics of water molecules inside protein. We concluded that the chloride ion release and uptake occurring in the N and O intermediate states are accompanied by the drastic conformational changes in the water-inaccessible transmembrane-helices and the hydrogen- bonding network rearrangement of the internal water molecules in *p*HR (*manuscripts in preparation*).

2. Time-Resolved Difference FTIR Spectroscopy Triggered by Rapid Buffer-Exchange

Attenuated total reflection (ATR) FTIR spectroscopy is a powerful technique to obtain infrared spectra of membrane proteins immersed in aqueous solution.[1)] By exchanging buffer with and without salts, the difference spectra between the two conditions provide the structural information relating to the interaction between protein and ions. In this year, we executed the construction of the kinetic ATR FTIR spectroscopic system, which can follow the chemical and biological reaction triggered by the rapid buffer-exchange, in collaboration with Mr. K. Okamoto in UNISOKU Co. Ltd.

We have developed the photo-triggering system for time-resolved FTIR measurements, but the application of this system has been limited mainly to the photo-inductive chemical reactions. Rapid buffer exchange (<1 ms) allows us to monitor the early stage of reactions, such as substrate or ion binding. For further improvement of the time-resolution, we will construct the flow-flash system.

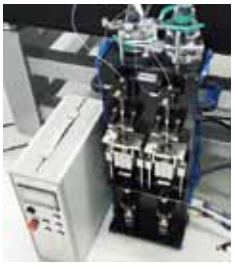

Figure 1. Picture of the rapid buffer-exchange system.

3. Development of a Microfluidic Device to Monitor Biological and Chemical Reactions

Real-time observation is one of the powerful techniques to understand the molecular mechanisms of the self-organization

and molecular association. The solution mixing technique realizes many reaction fields for biological and chemical reactions by changing the buffer condition and can be combined with spectroscopic equipment easily. However, conventional mixing techniques limit their targets because of the large consumption of the sample and the stress of the turbulent mixing. We are developing a novel microfluidic device and trying to reduce both the sample consumption to ~1/1000 and the stress by using sheath flow.

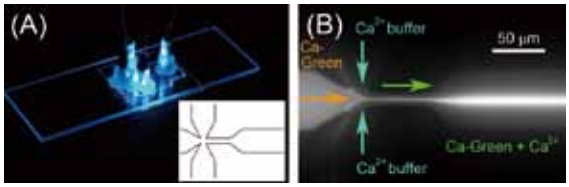

Figure 2. Pictures of the developed microfluidic mixer. (A) Picture of the mixer on the XY-stage of the fluorescence microscope. (inset) Schematic figure of the designed flow channels. (B) Fluorescence image of the Ca-Green mixed with the Ca^{2+} buffer.

Microfluidic devices with the flow channels of micrometer scale are made of a single cast of poly(dimethylsiloxane), PDMS, with the photolithography technique. These devices were combined with the fluorescence microscope and the complete mixing with the time resolution of ~20 μs was confirmed by the fluorescent intensity measurements. We are attempting to combine these devices with FTIR or other fluorescence spectroscopy.

The devices were manufactured with the strong supports of Equipment Development Center of IMS (especially Ms. N. Takada and Mr. M. Aoyama).

4. Investigation of Membrane Proteins Which Are Hardly Expressed in *E. coli*

Heterologous expression system using *E. coli* is established and easy way to obtain large amount of purified proteins, but in general, expression of membrane proteins, in particular mammalian ones, is very difficult. In this year, we have tried to establish a protein expression system using cultured mammalian cells for IR spectroscopic analyses of various membrane proteins, including mammalian ones.

In order to study structure-function relationship using purified proteins, it is very important to select target proteins that can be highly expressed in cell lines. Traditionally the screening of membrane proteins is very painful and time-consuming. However, a powerful method named fluorescence-detected size-exclusion chromatography (FSEC) was recently developed (Kawate and Gouaux, 2006). FSEC method evaluates expression level and properties of target proteins using GFP-tag and size-exclusion chromatograph even without purification (Figure 3). We set up an FSEC system and

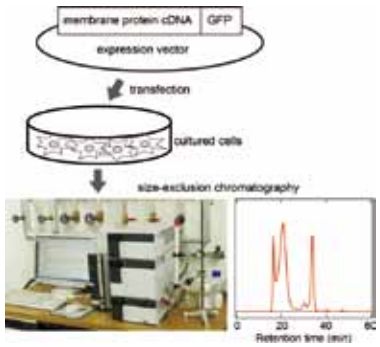

Figure 3. Scheme of the fluorescence-detected size-exclusion chromatography (FSEC).

expressed various membrane proteins with GFP tag to select appropriate proteins. Also, we tried to purify screened proteins and apply them to IR spectroscopic analyses.

Channelrhodopsins (collaboration with Prof. Yawo's group in Tohoku Univ.)

Channelrhodopin is a light-gated cation channels, which is originally identified in *Chlamydomonas*. Currently this protein is used as a tool for "optogenetics" which enables excitation of specific neural cells by irradiation. Prof. Yawo's group has developed several interesting channelrhodopsin mutants that show unique electrophysiological properties. Prof. Yawo kindly provided constructs of the channelrhodopsin mutants to us, and we screened the mutants using FSEC method. Several mutants can be expressed efficiently in mammalian cells, and can be purified. Also, we have already succeeded to measure the difference IR spectra before and after photo-activation of the channelrhodopsins. We are now trying to analyze the spectra and extend to time-resolved measurements with 12.5 μs resolution to reveal real-time analyses of open-close mechanism of the channel protein. (collaboration with Prof. Nureki's group in Univ. of Tokyo)

Mammalian potassium channels (collaboration with Prof. Kubo's group in National Institute for Physiological Sciences (NIPS))

Mammalian potassium channels play important roles in various organs, including brain, heart, kidney and retina. Prof. Kubo's group has revealed structure-function relationship of these channels mainly using electrophysiological method. Prof. Kubo kindly provided constructs of various mammalian potassium channels to us. We tested properties of these channels expressed in cultured cells using FSEC, and found several inwardly rectifying potassium channels can be expressed efficiently and show appropriate properties. In addition, we have just successfully purified the channels. Currently we are trying to measure IR spectra of the purified channels.

Reference

1) Y. Furutani, T. Murata and H. Kandori, *J. Am. Chem. Soc.* **133**, 2860–2863 (2011).

Award

FURUTANI, Yuji; MORINO Foundation research award.

Heterogeneous Catalytic Systems for Organic Chemical Transformations in Water

Department of Life and Coordination-Complex Molecular Science
Division of Complex Catalysis

UOZUMI, Yasuhiro	Professor
OSAKO, Takao	Assistant Professor
HAMASAKA, Go	Assistant Professor
ZHOU, Haifeng	Post-Doctoral Fellow
KOBAYASHI, Noboru	Graduate Student
SAKURAI, Fumie	Graduate Student
TSUJI, Hiroaki	Graduate Student
ITO, Kenichi	Graduate Student
TORII, Kaoru	Technical Fellow
SASAKI, Tokiyo	Secretary
FUKUSHIMA, Tomoko	Secretary

Various transition metal-catalyzed organic molecular transformations in water were achieved under heterogeneous conditions by use of poly(imidazole-palladium), amphiphilic resin-supported palladium complexes, or a microflow device containing a polymeric palladium nanoparticle membrane which were designed and prepared by this research group. The enantioselective carbenoid insertion into phenolic O–H bonds with a new chiral copper(I) imidazoindolephosphine complex has been also developed. In particular, development of a highly active reusable poly(imidazole-palladium) and a microflow device containing a plolymeric Pd nanoparticle membrane for organic transformations in water and the highly enantioselective O–H insertion using a new chiral copper(I) complex are highlights among the achievements of the 2011–2012 period to approach what may be considered ideal chemical processes of next generation. Representative results are summarized hereunder.

1. Self-Assembled Poly(Imidazole-Palladium): A Highly Active, Reusable Catalyst[1,2)]

A polymeric imidazole Pd catalyst (MEPI-Pd) was readily prepared by the coordinative convolution of $(NH_4)_2PdCl_4$ and poly[(*N*-vinylimidazole)-*co*-(*N*-isopropylacrylamide)$_5$] in a methanol/water solution at 80 °C for 30 min. The polymeric Pd catalyst was utilized for the allylic arylation/alkenylation/vinylation of allylic esters and carbonates with aryl/alkenylboronic acids, vinylboronic acid esters, and tetraaryl borates. Even 0.8–40 mol ppm Pd of the catalyst efficiently promoted allylic arylation/alkenylation/vinylation in alcohol and/or water with a catalytic turnover number (TON) of 20,000–1,250,000. Furthermore, the polymeric Pd catalyst efficiently promoted the Suzuki-Miyaura reaction of a variety of inactivated aryl chlorides, as well as aryl bromides, and iodides in water with a TON of up to 3,570,000.

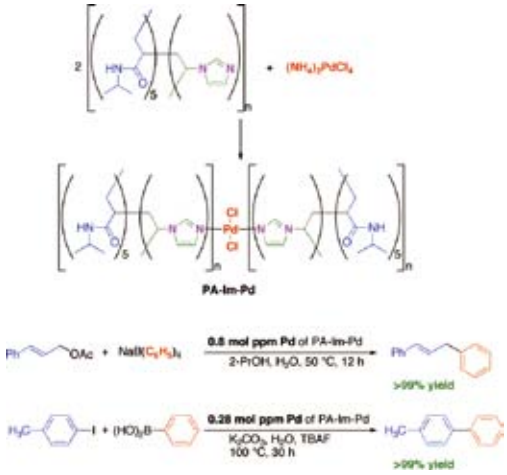

Scheme 1. Preparation of Self-Assembled Poly(Imidazole-Palladium) (top) and Application to Allylic Arylation and Suzuki-Miyaura Reaction.

2. Instantaneous Hydrodehalogenation of Haloarenes by a Microflow Device Containing a Polymeric Pd Nanoparticle Membrane[3)]

An architecture-based system of transition metal catalysis usinWe developed a variety of polymeric Pd nanoparticle membrane-installed microflow devices for the first time. Three types of polymers were convoluted with palladium salts under laminar flow conditions in a microflow reactor to form polymeric Pd membranes at the laminar flow interface. These

membranes were reduced with aqueous sodium formate or with heat to create microflow devices containing polymeric palladium nanoparticle membranes. These microflow devices achieved instantaneous hydrodehalogenation of 10–1,000 ppm of aryl chlorides, bromides, iodides, and triflates, within a residence time of 2–8 s at 50–90 °C using a safe, nonexplosive aqueous sodium formate to quantitatively afford the corresponding hydrodehalogenated products. PCB (10–1,000 ppm) and PBB (1,000 ppm) were completely decomposed under similar conditions, yielding biphenyl as a fungicidal compound.

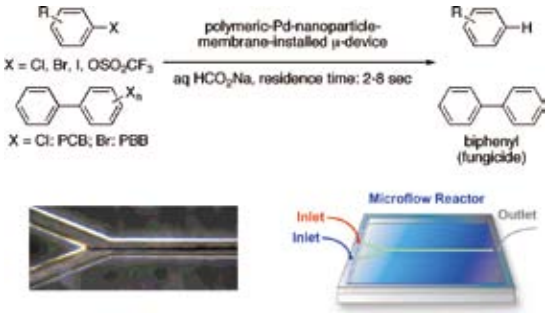

Scheme 2. Instantaneous Hydrodehalogenation of Haloarenes by a Microflow Device Containing a Polymeric Pd Nanoparticles Membrane.

3. C–N and C–S Bond Forming Cross Coupling in Water with Amphiphilic Resin-Supported Palladium Complexes[4)]

Catalytic C–N and C–S bond forming reactions of haloarenes with secondary amines and thiophenols were achieved in water under heterogeneous conditions by the use of immobilized palladium complexes coordinated with the amphiphilic polystyrene-poly(ethylene glycol) resin-supported di(*tert*-butyl)phosphine ligand to afford aryl(dialkyl)amines and diarylsulfides in high yield.

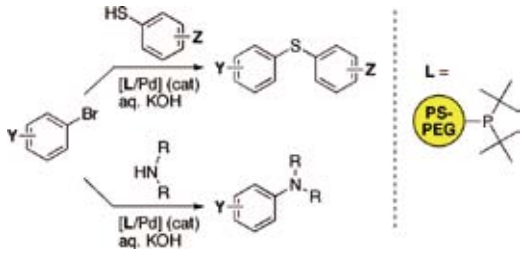

Scheme 3. C–N and C–S Bond Forming Cross Coupling in Water with Amphiphilic Resin-Supported Pd Complexes.

4. Enantioselective Carbenoid Insertion into Phenolic O–H Bonds with a Chiral Copper(I) Imidazoindolephosphine Complex[5)]

The enantioselective O–H carbenoid insertion reaction with a new chiral copper(I) imidazoindolephosphine complex has been developed. The chiral copper(I) complex catalyzed the insertion of carbenoids derived from α-diazopropionates into the O–H bonds of various phenol derivatives to give the corresponding α-aryloxypropionates with up to 91% ee.

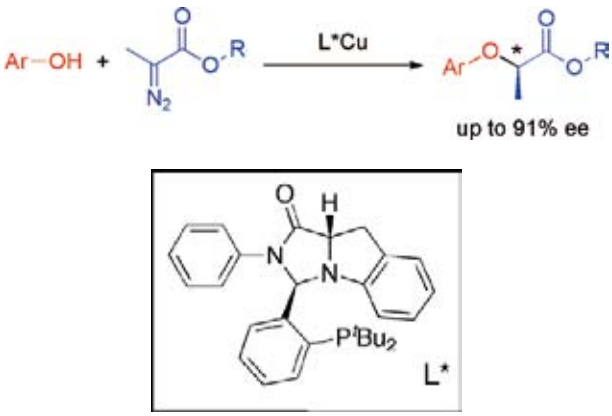

Scheme 4. Enantioselective Carbenoid Insertion into Phenolic O–H Bonds with a Chiral Copper(I) Imidazoindolephosphine Complex.

References

1) S. M. Sarkar, Y. Uozumi and Y. M. A. Yamada, *Angew. Chem., Int. Ed.* **50**, 9437–9441 (2011).
2) Y. M. A. Yamada, S. M. Sarkar and Y. Uozumi, *J. Am. Chem. Soc.* **134**, 3190–3198 (2012).
3) Y. M. A. Yamada, T. Watanabe, A. Ohno and Y. Uozumi, *ChemSusChem* **5**, 293–299 (2012).
4) Y. Hirai and Y. Uozumi, *Chem. Lett.* **40**, 934–935 (2011).
5) T. Osako, D. Panichakul and Y. Uozumi, *Org. Lett.* **14**, 194–197 (2012).

Water Oxidation Catalyzed by Dimeric Ru Complexes

Department of Life and Coordination-Complex Molecular Science
Division of Functional Coordination Chemistry

TANAKA, Koji	Professor (–March, 2012)*
OHTSU, Hideki	Assistant Professor*
KOBAYASHI, Katsuaki	IMS Research Assistant Professor*
PADHI, Sumanta Kumar	Post-Doctoral Fellow
NAKANE, Daisuke	Post-Doctoral Fellow
YAMAGUCHI, Yumiko	Secretary
NOGAWA, Kyoko	Secretary

Artificial photosynthesis aimed at carbon dioxide reduction and water splitting has become a top research theme. Two-electron transfer from or to substrates through redox reactions is requisite for stable molecular transformation. Intermolecular electron transfer, however, always generates free radical species, which often causes undesired side reactions. Success of artificial photosynthesis, therefore, depends on the designing of reaction systems that can provide or take out multi-electrons to or from reaction centers.

Irradiation of $[Ru(bpy)_2(pbn)]^{2+}$ (pbn = 2-(2-pyridyl)-benzo[*b*]-1,5-naphthyridine) with visible light causes proton coupled one-electron reduction, and the subsequent disproportionation affords an NADH model complex, $[Ru(bpy)_2(pbnH_2)]^{2+}$ ($pbnH_2$ = 5,10-dihydro-2-(2-pyridyl)benzo[*b*]-1,5-naphthyridine) (Scheme 1). Smooth conversion from NAD analog to NADH one under visible light irradiation would lead to a new methodology for utilization of water as the hydrogen source in molecular transformation.

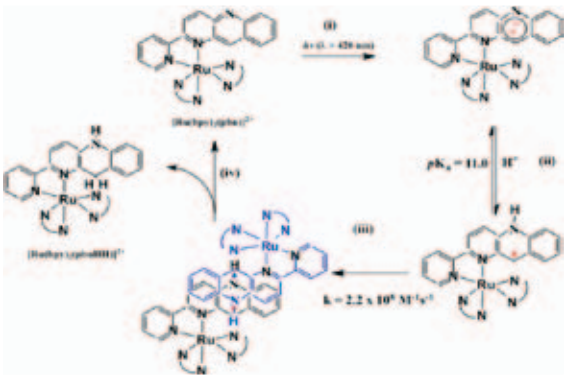

Scheme 1. Photochemical two-electron reduction of $[Ru(bpy)_2(pbn)]^{2+}$.

Three Ru-dioxolene complexes, $[Ru^{II}(Q)(trpy)(OH_2)]^{2+}$, $[Ru^{II}(Q)(trpy)(OH)]^{+}$, and $[Ru^{II}(Sq)(trpy)(O^{-\bullet})]^{0}$ (Q = 3,5-dibutylquinone; Sq = 3,5-dibutylsemiquinone) exist as equilibrium mixtures in water with the pK_a values of 5.5 and 10.5, respectively. A novel oxyl radical complex, $[Ru^{II}(Sq)(trpy)(O^{-\bullet})]^{0}$, undergoes reversible one electron oxidation around 0 V (*vs.* Ag/AgCl), and the subsequent further one electron oxidation creates the unique Ru^{III}–$O^{-\bullet}$ framework in the product (Scheme 2). The oxyl radical and Ru(III) center involved in the product work as simultaneous hydrogen atom and one electron acceptors in two-electron oxidation of alcohols.

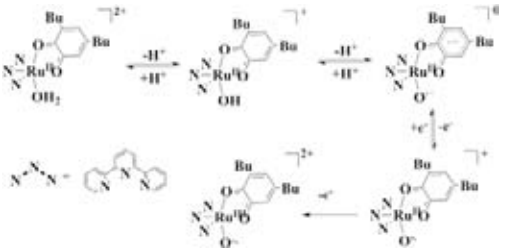

Scheme 2. Two-electron oxidant generation taking advantage of acid-base equilibrium of Ru-aqua(dioxolene) complex.

1. Direct Evidence for O–O Bond Formation in the Four Electron Water Oxidation

The difficulty of water decomposition results from four-electron oxiation of water rather than that of two-electron reduction. Among various water oxidation catalysts reported so far, much attention has been paid to a dinuclear Ru complex, $[Ru_2(OH)_2(Bu_2q)_2(btpyan)]^{2+}$ (Bu_2q = 3,6-di-*tert*-butylquinone, btpyan = 1,8-bis(terpyridyl)-anthracene), known as Tanaka Catalyst because of its high activity toward four-electron oxidation of water. However, any direct evidences for O–O bond formation prior to O_2 evolution have not been obtained so far.

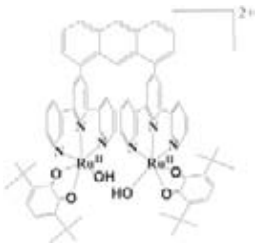

Four redox centers (2 × $Ru^{II/III}$ and 2 × [Q]/[Sq]) of $[Ru_2(OH)_2$

$(Bu_2q)_2(btpyan)]^{2+}$ is attributable to the high catalytic capacity. So, we tried to detect the O–O bond formation process by decreasing the number of redox centers of an Ru dinuclear complex. Two-electron oxidation of $[Ru^{II}_2(Cl)_2(bpy)_2(btpyan)]^{4+}$ at +1.0 V in a range of pH 2.0 to 3.0 forms $[Ru^{IV}_2(=O)_2(bpy)_2(btpyan)]^{4+}$. The controlled potential electrolysis of $[Ru^{II}_2(\mu\text{-}Cl)(bpy)_2(btpyan)]^{3+}$ at +1.60 V in water at pH 2.6 (H_3PO_4/NaH_2PO_4 buffer) catalytically evolved dioxygen. Addition of a CH_3CN (100 μl) solution of $[Ru^{II}_2(\mu\text{-}Cl)(bpy)_2(btpyan)]^{3+}$ (1.0 μmol) into an aqueous solution (10 ml) of $Ce(NH_4)_2(NO_3)_6$ (2.5 mmol) at pH 1.0 (adjusted with HNO_3) also caused O_2 evolution (414 μmol).

The electronic absorption spectra of the reaction mixture showed a transient band at 688 nm that emerged only in O_2 evolution. The transient complex prepared by the electrolysis of $[Ru^{II}_2(\mu\text{-}Cl)(bpy)_2(btpyan)]^{3+}$ in $H_2{}^{16}O$ and $H_2{}^{18}O$ at +1.40 V displayed two absorption bands at 442 and 824 cm^{-1}, and 426 and 780 cm^{-1}, respectively, in the resonance raman spectra with irradiation at 633 nm. The isotope shifts (Δ 16 and 44 cm^{-1}) between $H_2{}^{16}O$ and $H_2{}^{18}O$ are quite consistent with the calculated values of the ν(Ru–O) and ν(O–O) bands of $[Ru_2(\mu\text{-}O_2)(bpy)_2(btpyan)]^{3+}$. If the Ru^{IV}=O bond of $[Ru^{IV}_2(=O)_2(bpy)_2(btpyan)]^{4+}$ generated by the oxidation of $[Ru^{III}_2(OH)(bpy)_2(btpyan)]^{4+}$ has more or less Ru^{III}–O. oxyl radical character, $[Ru^{III}_2(\mu\text{-}O_2)(bpy)_2(btpyan)]^{4+}$ would be produced by the radical coupling of the two oxo groups of $[Ru^{IV}_2(=O)_2(bpy)_2(btpyan)]^{4+}$. The rate of O_2 evolution by chemical oxidation using Ce(IV) is much faster than that of electrochemical reaction at +1.60 V. Nuclear attack of two water to Ru^{III} of $[Ru^{III}_2(\mu\text{-}O_2)(bpy)_2(btpyan)]^{4+}$ will slowly releases O_2 (Scheme 3). On the other hand, Ce(IV) causes further oxidation of $[Ru^{III}_2(\mu\text{-}O_2)(bpy)_2(btpyan)]^{4+}$ to produce $[Ru^{IV}_2(\mu\text{-}O_2)(bpy)_2(btpyan)]^{6+}$, which smoothly evolves O_2 with regeneration of $[Ru^{III}_2(OH)(bpy)_2(btpyan)]^{4+}$ (Scheme 3). In accordance with this, $[Ru^{III}_2(\mu\text{-}O_2)(bpy)_2(btpyan)]^{4+}$ was detected only after Ce(IV) was consumed in O_2 evolution.

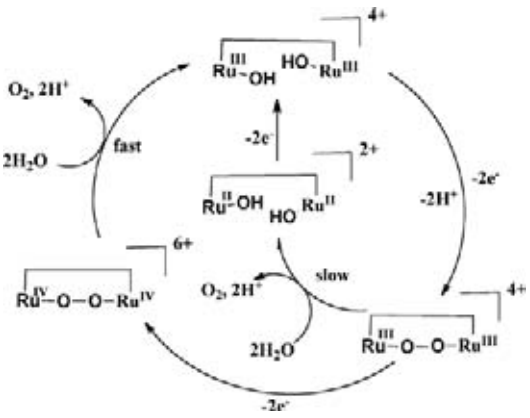

Scheme 3. Four-electron oxidation of water catalyzed by $[Ru^{III}_2(OH)_2(bpy)_2(btpyan)]^{4+}$.

2. Insight for Activity of Tanaka Catalyst toward Water Oxidation

High catalytic ability of $[Ru_2(btpyan)(3,6\text{-}di\text{-}Bu_2Q)_2(OH_2)]^{2+}$ (Tanaka catalyst) toward water oxidation produces disputes about the electronic structures in the catalytic cycle. DFT computational works reported so far are not consistent with each other in the viewpoints of the relative stability between the closed-shell (Ru^{II}-Q) and open-shell (Ru^{III}-SQ) electronic structures, and the pathway to the O–O bond formation. On the other hand, broken-symmetry hybrid density functional computations have provided a rational reaction mechanism for water oxidation (Scheme 4). Deprotonation of waters in ^{1}**1** affords the key tetraradical intermediate ^{1}**3** via one-electron transfer (OET) in ^{1}**2**. The oxygen-radical pair in ^{1}**3** is local triplet diradical (LTD), suppressing facile O–O bond formation by the radical coupling (RC) mechanism. The two-electron removal from ^{1}**3** provides the hexaradical species ^{3}**4**. The oxygen radical pair (^{3}A) is still LTD-type, indicating the necessity of spin inversion (SI) for generation of local singlet diradical (LSD) pair in ^{1}**5**. The RC mechanism in ^{1}**5** is facile, giving the peroxide species ^{1}**6**. The next step for generation of oxygen dianion may become the rate-determining step as shown in ^{1}**7**. The β-spin at the terminal oxygen anion in ^{1}**7** is moved to the Ru_2(III) site with the α-spin to form the singlet pair as shown in ^{1}**8**. The spin exchange (SE) between ↓•Ru_1(III) and SQ_1•↑ to generate ↑•Ru_1(III) and SQ_1•↓ is necessary for one more OET from superoxide anion to ↑•Ru_1(III) to afford triplet molecular oxygen in ^{1}**9**. The SE process is easy because the exchange coupling for the •O–O–Ru(III)• is weak. Thus the SQ_1• radical plays an important role for spin catalysis. The two-electron removal from ^{1}**9** is necessary for reproduction of ^{1}**1**. Thus the BS computational results provide the orbital and spin correlation diagram for water splitting reaction.

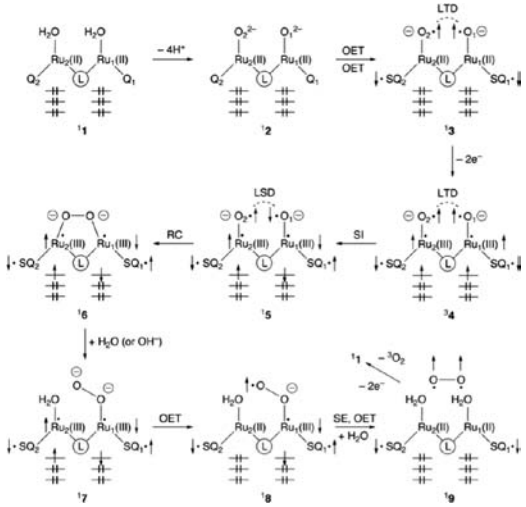

Scheme 4. Proposed mechanism for water oxidation catalyzed by Tanaka catalyst.

* Present Address; Institute for Integrated Cell-Material Sciences, Kyoto University

Synthetic Inorganic and Organometallic Chemistry of Transition Metals

Department of Life and Coordination-Complex Molecular Science
Division of Functional Coordination Chemistry

MURAHASHI, Tetsuro	Professor (April, 2012–)
TACHIBANA, Yuki	Graduate Student*
KIMURA, Seita	Graduate Student*
TANIWAKE, Mayuko	Secretary
NOGAWA, Kyoko	Secretary

Our research focuses on synthesis and structural elucidation of a new class of transition metal complexes. This research leads to development of fundamental concepts of transition metal chemistry as well as applications to catalysis and materials science. Novel synthetic methods are developed to realize transition metal complexes having unique bonding nature. The newly synthesized transition metal complexes are further converted to more reactive forms, and their reaction mechanisms are elucidated. The aspects gained by this research are applied to the understanding and development of molecular catalysis. Furthermore, unique properties of low-dimensional metal-organic hybrid molecules are investigated and developed in our group.

1. Synthesis and Chemical Properties of Metal Chain Sandwich Complexes

The molecular sandwich framework is one of the fundamental structures in transition metal chemistry. It had been believed that the structural concept can be applied only to mono- and dinuclear complexes. Our group revealed that the multinuclear sandwich complexes containing a one-dimensional metal chain or a two-dimensional metal sheet exist stably.[1,2] These findings expand the scope of the structural concept of sandwich compounds (Figure 1).

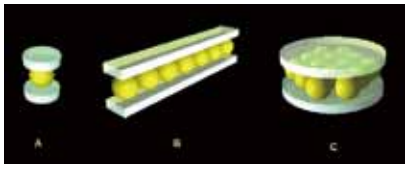

Figure 1. Schematic representation of sandwich compounds: (**A**) mononuclear metallocenes, (**B**) one-dimensional metal chain sandwich complexes, (**C**) two-dimensional metal sheet sandwich complexes. Our group revealed the existence of categories **B** and **C**.

For the one-dimensional metal chain sandwich complexes, we successfully developed a synthetic method that enables the size-selective construction of a metal chain sandwich framework. Furthermore, our laboratory revealed that metal chain sandwich complexes show unique chemical properties such as i) dynamic sliding behavior of polyene ligands on a metal chain and ii) photo-induced flipping of polyene ligands on a metal chain.

Redox-Switchable Metal Assembling and Ligand Coupling in Sandwich Frameworks[3]

In view of the widely developed redox chemistry of metallocenes and other mononuclear sandwich compounds, it is intriguing to elucidate the redox properties of the multinuclear sandwich compounds. Here we disclosed two novel modes of redox-induced reversible structural changes: i) redox-switchable reversible splitting of a Pd_4 chain via translocation, and ii) redox-switchable reversible C–C coupling of π-conjugated ligands in tetrapalladium sandwich complexes (Figure 2). These results provide new aspects for the redox function of (sp^2-carbon)–(multinuclear metal)–(sp^2-carbon) sandwich frameworks.

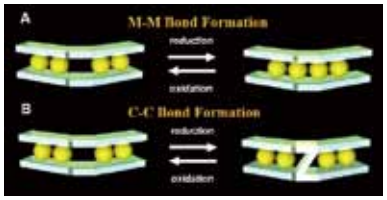

Figure 2. Schematic representations of (**A**) the reversible assembling of dimetal moieties and (**B**) the reversible coupling of ligands.

Oxidation of **1** or **1-OMe** with $AgBF_4$ or $AgPF_6$ (2 equiv.) resulted in the formation of **2** or **2-OMe** (bpbb = 1,2-bis(4-phenyl-1,3-butadienyl)benzene). Reduction of **2** or **2-OMe** with $Fe(C_5H_5)_2$ (2 equiv.) yielded **1** or **1-OMe** (eq. 1). During the two-electron oxidation, the Pd–Pd–Pd–Pd chain is cleaved, and the two Pd_2 units undergo translocation to the outer position during the oxidation process. In the reduction process, the two separate Pd_2 units migrate to the inside position to form the Pd–Pd–Pd–Pd chain. The observed redox behavior is highlighted by the coupling of two events, metal–metal bond formation/cleavage and metal translocation, under the redox control, and provides evidence of redox-switchable movement of multiple metal atoms associated with assembling/disas-

sembling behavior in the space between sp^2-carbon planes.

We also found another mode of the redox-induced structural change featured by the intramolecular reversible C–C bond formation between the two sandwich ligands, by employing **3** (eq. 2).

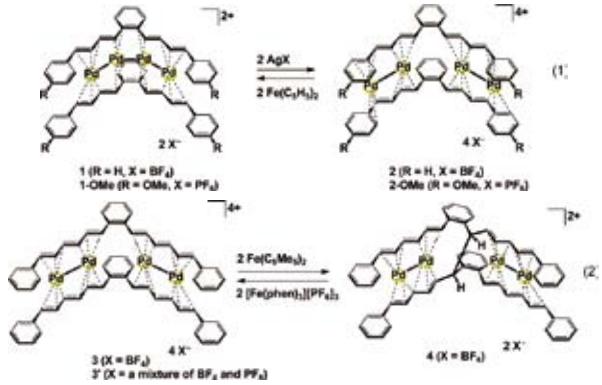

2. Synthesis and Reactivity of Metal Sheet Sandwich Complexes

For the two-dimensional metal sheet sandwich complexes, our group has shown that six-, seven-, eight-, and nine-membered carbocycles, as well as polycyclic arenes behave as the excellent binders for metal sheets. These metal sheet sandwich complexes are stable even in solution. Thus, a reactive form of such metal sheet sandwich complexes may provide a new opportunity to develop sandwich type late transition metal catalysts.

Selective Synthesis of Mixed Metal Pd_2Pt and $PdPt_2$ Complexes of Tropylium[4)]

Our group has reported a series of homonuclear metal sheet sandwich complexes, which have a metal sheet of a single metal element. Here, we reported selective construction of the triangular $PdPt_2$ and Pd_2Pt cores in a common sandwich framework, where a key is to use different carbocyclic ligands for the different composite sandwich; *i.e.*, cycloheptatrienyl for $PdPt_2$, and cycloheptatriene for Pd_2Pt (complexes **5-$PdPt_2$** and **6-Pd_2Pt**).

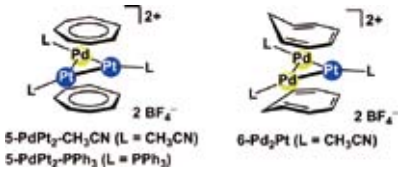

After construction of the Pd_2Pt core, the cycloheptatriene ligands can be converted to cycloheptatrienyl ligands where a (carbocyclic ligand)–(metal triangle)–(carbocyclic ligand) sandwich structure is retained (eq. 3). It was confirmed that the mixed metal core once formed in a cycloheptatrienyl sandwich framework is robust against the intermolecular metal scrambling.

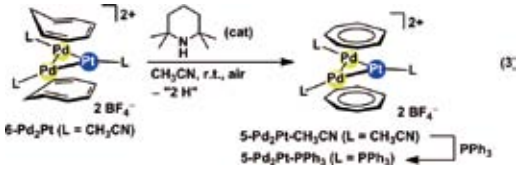

Thus, it has been proven that the mixed-metal triangular trimetal sandwich complexes are synthesizable in a selective manner. The present results expand the scope of the structural variability of multinuclear sandwich complexes from homonuclear to heteronuclear series.

3. Reaction Mechanism of Highly Reactive Pd–Pd Complexes

Our group has shown that a homoleptic dinuclear Pd–Pd complexes of nitriles such as $[Pd_2(CH_3CN)_6][BF_4]_2$ are isolable.[5)] These homoleptic solvento-Pd_2 complexes are highly substitutionally labile, and allow us to investigate reaction mechanism of the Pd–Pd complexes in details. For example, our group has shown that a Pd–Pd moiety adds to various unsaturated hydrocarbons in a syn addition manner.

Dinuclear Addition of a Pd–Pd Moiety to Arenes[6)]

We found that a Pd–Pd moiety undergoes addition reaction to arenes to afford the bi-π-allyl type dipalladium complexes. Previously simple μ–η^2:η^2–(arene)–Pd_2 complexes have been isolated, but now we found that a Pd–Pd moiety undergoes dinuclear addition to several arenes to afford a novel binding mode of arene–Pd_2, namely μ-η^3:η^3–(arene)–Pd^{II}_2 (Figure 3), through isolation and characterization of **8'**, **9**, and **10**. The fact that bi-η^3-allyl type structure is accessible via dinuclear syn-addition of a Pd–Pd moiety suggest possible involvement of a new activation mode of arenes by a Pd–Pd species in some palladium-catalyzed transformations.

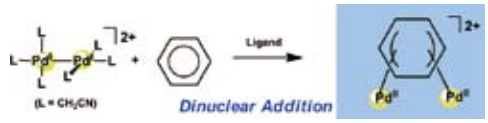

Figure 3. Dinuclear addition of a Pd–Pd moiety to arenes.

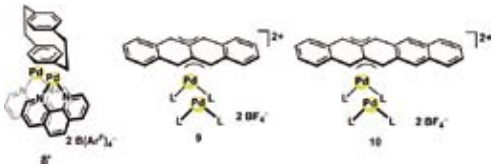

References

1) For the first report on the metal chain sandwich complexes: T. Murahashi, *et al.*, *J. Am. Chem. Soc.* **121**, 10660–10661 (1999).
2) For the first report on the metal sheet sandwich complexes: T. Murahashi, *et al.*, *Science* **313**, 1104–1107 (2006).
3) T. Murahashi, K. Shirato, A. Fukushima, K. Takase, T. Suenobu, S. Fukuzumi, S. Ogoshi and H. Kurosawa, *Nat. Chem.* **4**, 52–58 (2012).
4) T. Murahashi, K. Usui, Y. Tachibana, S. Kimura and S. Ogoshi, *Chem. –Eur. J.* **18**, 8886–8890 (2012).
5) T. Murahashi, *et al.*, *J. Am. Chem. Soc.* **128**, 4377–4388 (2006).
6) T. Murahashi, K. Takase, M. Oka and S. Ogoshi, *J. Am. Chem. Soc.* **133**, 14908–14911 (2011).

* carrying out graduate research on Cooperative Education Program of IMS with Osaka University

Development of Functional Metal Complexes for Artificial Photosynthesis

Department of Life and Coordination-Complex Molecular Science
Division of Functional Coordination Chemistry

MASAOKA, Shigeyuki	Associate Professor
KONDO, Mio	Assistant Professor
YOSHIDA, Masaki	Graduate Student*
NAKAMURA, Go	Graduate Student
OKAMURA, Masaya	Graduate Student
MURASE, Masakazu	Graduate Student†
ITOH, Takahiro	Graduate Student
KUGA, Reiko	Technical Fellow
LIU, Ke	Technical Fellow
KANAIKE, Mari	Technical Fellow
WAKABAYASHI, Kaori	Technical Fellow
TANIWAKE, Mayuko	Secretary

Artificial photosynthesis is a solar energy conversion technology that mimics natural photosynthesis, and poised to be one of the next big breakthroughs in energy. Our group studies chemistry of transition metal complexes for the realization of artificial photosynthesis. Efforts have focused on development of new catalysts for multi-electron transfer reactions and understanding the reaction mechanism. During the last year, we reported (i) a mononuclear ruthenium complex showing multiple proton-coupled electron transfer toward multi-electron transfer reactions,[1] (ii) kinetics and DFT studies on water oxidation catalyzed by a mononuclear ruthenium complex,[2] and (iii) two-step photoexcitation of a platinum complex to produce hydrogen from water.[3] We also demonstrated (iv) the self-assembly of microstructures from dinuclear ruthenium complexes and their structural transformation.[4] The research projects (i), (ii) and (iv) are introduced in this report.

1. A Mononuclear Ruthenium Complex Showing Multiple Proton-Coupled Electron Transfer toward Multi-Electron Transfer Reactions[1]

Proton-coupled electron transfer (PCET) is an important chemical process that involves the concerted transfer of a proton (H^+) and an electron (e^-). It is widely employed to achieve multi-electron transfer reactions such as water oxidation by photosystem II and nitrogen fixation by nitrogenase as well as solar energy conversion in artificial photosynthesis, since high-energy intermediates and/or electrostatic charge buildup during the reactions are generally avoided by going through PCET processes.

In this context, we synthesized and characterized a new ruthenium(II) complex, $[Ru(trpy)(H_2bim)(OH_2)](PF_6)_2$ (**1**) (H_2bim = 2,2'-biimidazole and trpy = 2,2':6',2"-terpyridine), where the H_2bim and M-OH_2 moieties in the molecule are expected to serve as proton-dissociation sites. Electrochemical studies in aqueous solutions under various pH conditions afforded the Pourbaix diagram (potential versus pH diagram) of **1**, where the pK_a values found from the diagram agree well with those determined spectrophotometrically. It was also found that **1** demonstrates four-step PCET reactions to give the four-electron oxidized species, $[Ru^{IV}(trpy)(bim)(O)]^{2+}$, without electrostatic charge buildup during the reactions (Figure 1). The multiple PCET ability of **1** would be applicable to various multi-electron oxidation reactions. Catalysis of electrochemical water oxidation was indeed evaluated in the initial attempt to demonstrate multi-electron oxidation reactions, revealing that the water oxidation potential for **1** is lower than that for 2,2'-bipyridine analogue, $[Ru(trpy)(bpy)(OH_2)]^{2+}$ (**2**) (bpy = 2,2'-bipyridine), which is known as an active catalyst for water oxidation.

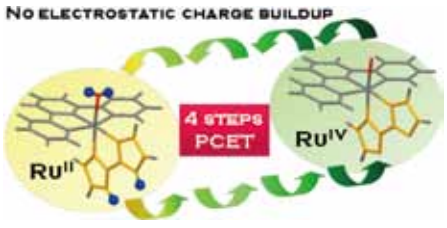

Figure 1. A schematic view of the four-step PCET reaction of **1** to give the four-electron oxidized species, $[Ru^{IV}(trpy)(bim)(O)]^{2+}$.

2. Kinetics and DFT Studies on the Mechanism of Water Oxidation Catalyzed by Mononuclear Ruthenium Complexes[2]

Visible light-induced water splitting is one promising

approach for artificial photosynthesis. This solar-to-fuels conversion consists of the two half-cell reactions; reduction of water to H_2 ($2H^+ + 2e^- \rightarrow H_2$) and oxidation of water to O_2 ($2H_2O \rightarrow O_2 + 4H^+ + 4e^-$). Particularly, development of molecular catalysts for O_2 evolution has been considered more difficult than the hydrogen side, since the O_2 evolution requires removal of four protons and four electrons.

We previously provided two important aspects with regard to this issue as follows. (i) Mononuclear ruthenium catalysts can be classified into two groups based on the rate law observed. One obeys $d[O_2]/dt = k[\text{catalyst}][Ce^{4+}]$ and the other obeys $d[O_2]/dt = k[\text{catalyst}]^2$, where the rate is first- and second-order to the catalyst concentration, respectively. (ii) A radical coupling of the oxo atom from Ru catalyst and the radical-like O(hydroxo) atom from hydroxocerium(IV) species plays an important role in the O–O bond formation in the former monoruthenium-catalyzed O_2 evolution reactions. However, our previous studies has not provided the spectroscopic evidence of the highest-valence intermediate for the Ru species prior to the O–O bond formation.

In this work, the reaction mechanism of the Ce^{4+}–driven water oxidation catalyzed by $[Ru(trpy)(bpy)(OH_2)]^{2+}$ (**2**, Ru^{II}-OH_2). As a result, the Ru^{V}=O species, together with other intermediates in the multi-step electron transfer processes, were spectrophotometrically followed by use of the global kinetic analysis using the singular value decomposition (SVD) method. We also demonstrate that each spectral component can be rationally reproduced by TD-DFT (time-dependent density functional theory) calculation. Moreover, it is also found that the Ru^{V}=O species can be written as the resonance structure of the Ru^{IV}-$O^{\bullet}$ species (Ru^{V}=O ↔ Ru^{IV}-$O^{\bullet}$), indicating that the Ru^{V}=O species bears a substantial radical character at the O(oxo) atom. This study suggests that a radical-radical coupling of Ru^{V}=O and hydroxocerium(IV) species predominates the major path leading to the dioxygen formation.

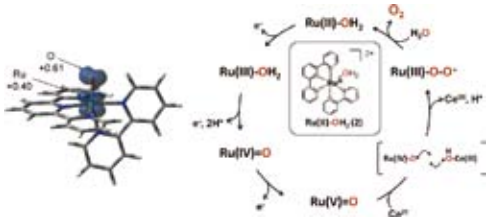

Figure 2. (Left) The optimized structure of the Ru^{V}=O species in the doublet state. The distribution of the Mulliken atomic spin density is also overlaid. The spin density is located on the 3d orbital of the ruthenium ion (+0.40) and the 2p orbital of the O(oxo) atom (+0.61). (Right) A proposed catalytic cycle of the Ce^{4+}–driven water oxidation catalyzed by **2**.

3. Self-Assembly of Tubular Structures from Dinuclear Ruthenium Complexes and Their Structural Transformation[4)]

Controlled self-assembly of metal complexes is of high scientific and technological importance for the development of multi-functional materials and devices. Among various types of metal complexes, mixed-valence complexes have attracted much attention because of their wide range of interesting physical and chemical properties from charge-transfer interactions between metal ions linked via bridging ligands. In particular, low-dimensional assembly of such mixed-valence complexes gives rise to specific electronic, magnetic, and optical properties. Ideally, the characteristics of such systems would be tunable by controlling the spatial arrangement of the mixed-valence complexes, resulting in electric interaction among metal complexes without linkage of covalent or coordination.

In this work, we have demonstrated that the lipid-packaged mixed-valence complex displays morphological changes with aging of the solution in dichloromethane. Formation of a bilayer structure causes morphological evolution from microtapes to microtubes, giving rise to changes in absorption spectral intensities. Moreover, these morphological and spectral changes can be reversed by standing or shaking. The technique of combination of lipid molecules and *discrete* coordination compounds makes it possible to design flexible, reversible and signal responsive supramolecular coordination systems. The concept of lipid packaging could also be expanded of other useful coordination compounds, and should allow us to further develop the nanochemistry of coordination materials.

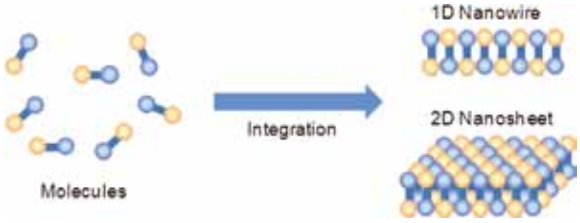

Figure 3. Schematic illustration of the assembly of discrete metal complexes for constructing nanostructures.

References

1) M. Okamura, M. Yoshida, R. Kuga, K. Sakai, M. Kondo and S. Masaoka, *Dalton Trans.*, in press.
2) A. Kimoto, K. Yamauchi, M. Yoshida, S. Masaoka and K. Sakai, *Chem. Commun.* **48**, 239–241 (2012).
3) M. Kobayasi, S. Masaoka and K. Sakai, *Angew. Chem., Int. Ed.* **51**, 7431–7434 (2012).
4) K. Kuroiwa, M. Yoshida, S. Masaoka, K. Kaneko, K. Sakai and N. Kimizuka, *Angew. Chem., Int. Ed.* **51**, 656–659 (2012).

Award

KONDO, Mio; The 5th Shiseido Female Researcher Science Grant (2012).

* carrying out graduate research on Cooperative Education Program of IMS with Kyushu University

† carrying out graduate research on Cooperative Education Program of IMS with Nagoya Institute of Technology

Visiting Professors

Visiting Professor
SASAI, Hiroaki *(from Osaka University)*

Design and Synthesis of Novel Enantioselective Catalysts and Their Application

Synthesis of optically active complex molecules using catalytic amount of chiral compounds plays an important role in pharmaceutical industrial processes. Our group engages in the development of novel enantioselective catalyses which involve asymmetric domino reaction promoted by an acid-base type organocatalyst, oxidative coupling of 2-naphthol derivatives using dinuclear vanadium(V) catalysts, spiro bis(isoxazoline) ligand (SPRIX) accelerated Pd catalyses, *etc*. Recently we have realized a highly enantioselective intramolecular Rauhut-Currier reactions catalyzed by an amino acid derived organocatalyst. In addition, an umpolung acetoxylation of Pd enolate derived from alkynyl cyclohexadienones was found to be promoted by Pd-SPRIX catalyst.

Visiting Associate Professor
UEMURA, Takashi *(from Kyoto University)*

Polymer Chemistry in Coordination Nanospaces

One of the most outstanding challenges in polymer materials science is the fabrication of systems that allow the controlled arrangement of monomers to be polymerized to materials useful for a desired purpose. We are developing strategies to control polymerizations in nanochannels of Metal–Organic Frameworks (MOFs) composed of metal ions and organic ligands. Use of their regulated and tunable channels for a field of polymerization can allow multi-level controls of the resulting polymer structures, such as molecular weight, stereoregularity, reaction positions, and monomer sequences. In addition, construction of nanocomposites between MOFs and polymers provides new material platforms to accomplish many optical and electronic functions.

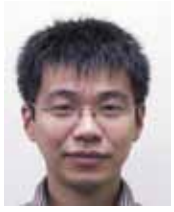

Visiting Associate Professor
SUDO, Yuki *(from Nagoya University)*

Understanding and Controlling the Photoactive Proteins

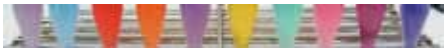

Light is one of the most important energy sources and signals providing critical information to biological systems. Rhodopsin molecules are photochemically reactive membrane-embedded proteins, with seven transmembrane α-helices which bind the chromophore retinal (vitamin A aldehyde). A striking characteristic of these photoactive proteins is their wide range of seemingly dissimilar functions. We are investigating them by using various techniques such as biophysical, molecular biological, biochemical, genetical and spectroscopic methods. In addition, rhodopsin molecules have great potential for controlling cellular activity by light. We are also focusing on the development of novel photocontrollable tools for the life scientists.

RESEARCH FACILITIES

The Institute includes five research facilities. This section describes their latest equipment and activities. For further information please refer to previous IMS Annual Review issues (1978–2011).

UVSOR Facility

KATOH, Masahiro	Director, Professor
SHIGEMASA, Eiji	Associate Professor
KIMURA, Shin-ichi	Associate Professor
ADACHI, Masahiro	Assistant Professor
IWAYAMA, Hiroshi	Assistant Professor
MATSUNAMI, Masaharu	Assistant Professor
OHIGASHI, Takuji	Assistant Professor
KONOMI, Taro	Assistant Professor
HORIGOME, Toshio	Technical Associate
NAKAMURA, Eiken	Technical Associate
YAMAZAKI, Jun-ichiro	Technical Associate
HASUMOTO, Masami	Technical Associate
SAKAI, Masahiro	Technical Associate
HAYASHI, Kenji	Technical Associate
KONDO, Naonori	Technical Associate
TOKUSHI, Tetsunari	Technical Fellow
HAGIWARA, Hisayo	Secretary

Outline of UVSOR

Since the first light in 1983, UVSOR has been successfully operated as one of the major synchrotron light sources in Japan. After the major upgrade of the accelerators in 2003, UVSOR was renamed to UVSOR-II and became one of the world brightest low energy synchrotron light source. In 2012, it was upgraded again and has been renamed to UVSOR-III. The brightness of the electron beam was increased further. Totally, six undulators were installed. It is operated fully in the top-up mode, in which the electron beam intensity is kept constant.

The UVSOR accelerator complex consists of a 15 MeV injector linac, a 750 MeV booster synchrotron, and a 750 MeV storage ring. The magnet lattice of the storage ring consists of four extended double-bend cells with distributed dispersion function. The storage ring is normally operated under multi-bunch mode with partial filling. The single bunch operation is also conducted about two weeks per year, which provides pulsed synchrotron radiation (SR) for time-resolved experiments.

Eight bending magnets and four undulators are available for providing SR. The bending magnet with its radius of 2.2 m provides SR with the critical energy of 425 eV. There are twelve beam-lines operational at UVSOR, two beam-lines under commissioning, one under construction. The operational beam-lines can be classified into two categories. Nine of them are the so-called “Open beamlines,” which are open to scientists of universities and research institutes belonging to the government, public organizations, private enterprises and those of foreign countries. The other three beam-lines are the so-called “In-house beamlines,” which are dedicated to the use of the research groups within IMS. We have 1 soft X-rays (SX) station equipped with a double-crystal monochromator, 7 EUV and SX stations with a grazing incidence monochromator, 3 VUV stations with a normal incidence monochromator, 1 (far) infrared station equipped with FT interferometers.

Figure 1. UVSOR electron storage ring and synchrotron radiation beam-lines.

Collaborations at UVSOR

Variety of investigations related to molecular/material science is carried out at UVSOR by IMS researchers. In addition, many researchers outside IMS visit UVSOR to conduct their own research work. The number of visiting researchers per year tops about 800, whose affiliations extend to 60 different institutes. International collaboration is also pursued actively and the number of visiting foreign researchers reaches over 80, across 10 countries. UVSOR invites new/continuing proposals for research conducted at the open beamlines twice a year. The proposals from academic and public research organizations (charge-free) and from enter-

prises (charged) are acceptable. The fruit of the research activities using SR at UVSOR is published as a UVSOR ACTIVITY REPORT annually. The refereed publications per year count more than 60 since 1996.

Recent Developments of the Facility

In 2011, a new undulator system dedicated for coherent light production was constructed as shown in Figure 2. This new undulator will be used for coherent light generation both in the UV-VUV range and in the THz range. This will be also used for the resonator free electron laser.

In spring, 2012, we had three month shut-down for a reconstruction work towards UVSOR-III. We have replaced all the bending magnets in the storage ring with combined function ones which are capable of producing defocussing fields as well as the dipole fields. A new in-vacuum undulator was installed. This will be used for a scanning transmission X-ray microscope (STXM) beam-line, which is also under construction.

Figure 2. New Undulators installed in 2011. The upper is the variable polarization optical klystron undulator which will be used for coherent light generation. The lower is the in-vacuum undulator for the STXM beam-line.

Reserch Highlight 2011

A New Two-Dimensional Topological Insulator —Successful Formation of a Bilayer Bismuth

Topological insulators are a new state of matter which is gaining increased attention in condensed matter physics. While the bulk is an insulator, they have metallic edge (surface states) and these edge states have similar properties with magnets even though the bulk is not a magnet. There are hopes to develop novel devices utilizing this intriguing property.

In this work,[1)] a way to fabricate a new two-dimensional topological insulator has been found. The remarkable thing about this material is that it is only two-atomic layers (bilayer) thick made of bismuth. While it is not impossible to make such a thin material in the atomic scale (for example, the Noble physics prize in 2010 was awarded to physicists who studied graphene, a single atomic-layer sheet of carbon), it still remains to be a big challenge. The present finding should accelerate researches to further understand the exotic properties of topological insulators as well as for application in atomic-scale devices and quantum computation.

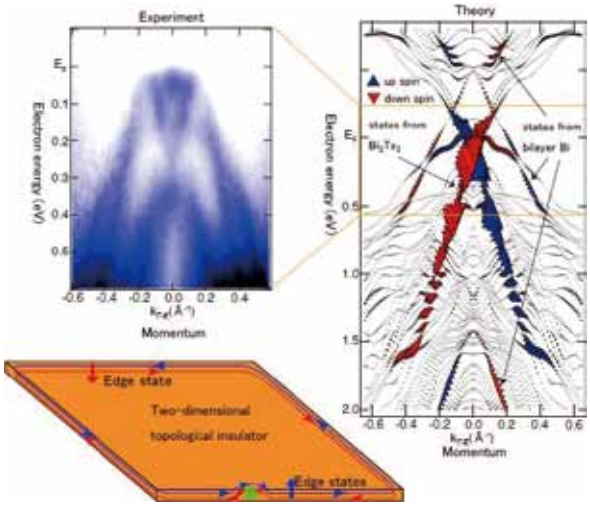

Figure 3. The experimental band dispersion of Bi(111) bilayer on Bi_2Te_3 measured experimentally (left) and its corresponding first-principles calculations (right). The left bottom figure shows the schematic drawing of a two-dimensional topological insulator.

Reference

1) T. Hirahara, G. Bihlmayer, Y. Sakamoto, M. Yamada, **H. Miyazaki**, **S. Kimura**, S. Blugel and S. Hasegawa, *Phys. Rev. Lett.* **107**, 166801 (5 pages) (2011).

Research Center for Molecular Scale Nanoscience

YOKOYAMA, Toshihiko	Director, Professor
HIRAMOTO, Masahiro	Professor
SUZUKI, Toshiyasu	Associate Professor
NAGATA, Toshi	Associate Professor
SAKURAI, Hidehiro	Associate Professor
NISHIMURA, Katsuyuki	Associate Professor
TADA, Mizuki	Associate Professor
TANAKA, Shoji	Assistant Professor
SAKAMOTO, Yoichi	Assistant Professor
HIGASHIBAYASHI, Shuhei	Assistant Professor
KAJI, Toshihiko	Assistant Professor
NAKAO, Satoru	Post-Doctoral Fellow (Nanotechnology Platform)
KANEKO, Yasushi	Technical Fellow (Nanotechnology Platform manager)
SUZUKI, Hiroko	Secretary
WATANABE, Yoko	Secretary
FUNAKI, Yumiko	Secretary
TOYAMA, Yu	Secretary (Nanotechnology Platform)

Research Center for Molecular Scale Nanoscience was established in 2002 with the mission of undertaking comprehensive studies of "Molecular Scale Nanoscience." The Center consists of one division staffed by full-time researchers (Division of Molecular Nanoscience), two divisions staffed by adjunctive researchers (Divisions of Instrumental Nanoscience and Structural Nanoscience), one division staffed by visiting researchers (Division of Advanced Molecular Science). Their mandates are

1) Fabrication of new nanostructures based on molecules
2) Systematic studies of unique chemical reactions
3) Systematic studies of physical properties of these nanostructures.

As a public research management, the Center has been conducting Nanotechnology Network Project (April 2007–March 2012) and Nanotechnology Platform Program (July 2012–March 2022) of the Ministry of Education, Culture, Sports, Science and Technology (MEXT) as a representative organization, and provided various kinds of nanotechnology public support programs to Japanese and foreign researchers. Details of these projects will be described in the other section in this book.

Through the MEXT projects, the Center offers public usage of the advanced ultrahigh magnetic field NMR (Nuclear Magnetic Resonance, 920 MHz) spectrometer not only for solution specimens but for solid samples. Since 2004 a number of collaborating researches with the 920MHz NMR measurements have been examined. Figure shows the apparatus, together with a typical example of the NMR spectra, where one can easily find much better resolving power than that of a standard 500 MHz NMR spectrometer. (1) dynamic structures of biological macromolecules, (2) structure of bioactive natural products, (3) characterization of metal ion complexes and so forth. We will continuously call for the collaborating research applications using the 920MHz NMR spectrometer with a view to use the NMR of a wide scientific tolerance (*e.g.* structural biology, organic chemistry, catalyst chemistry, *etc.*).

Figure 1. 920 MHz NMR spectrometer and an example measured using 920 and 500 MHz spectrometers. Much higher resolution in 920 MHz can be clearly seen.

Laser Research Center for Molecular Science

OKAMOTO, Hiromi	Director, Professor
KATOH, Masahiro	Professor
OHMORI, Kenji	Professor
OHSHIMA, Yasuhiro	Professor
TAIRA, Takunori	Associate Professor
FUJI, Takao	Associate Professor
ISHIZUKI, Hideki	Assistant Professor
NOMURA, Yutaka	Assistant Professor
OKANO, Yasuaki	Technical Associate
MASUDA, Michiko	Secretary
KAWAI, Shigeko	Secretary

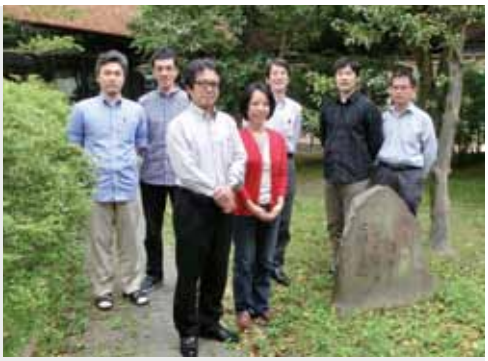

The Center aims to develop new experimental apparatus and methods to open groundbreaking research fields in molecular science, in collaboration with the Department of Photo-Molecular Science. Those new apparatus and methods will be served as key resources in advanced collaborations with the researchers from the community of molecular science. The main targets are (1) advanced photon sources covering wide energy ranges from terahertz to soft X-day regions; (2) novel quantum-control schemes based on intense and ultrafast lasers; and (3) high-resolution optical imaging and nanometric microscopy. The center also serves as the core of the joint research project “Extreme Photonics” between IMS and RIKEN.

Two of full-time associate professors and their research groups belong to the Center. The groups promote research projects targeting mainly on developments of novel laser light sources for molecular science. The Center also possesses several general-purpose instruments for laser-related measurements, and lends them to researchers in IMS who conduct laser-based studies, so as to support and contribute to their advanced researches.

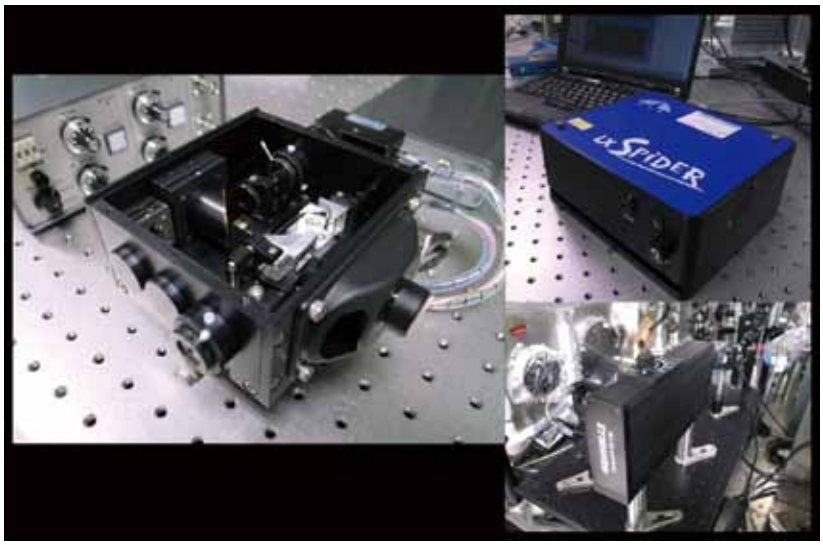

Figure 1. (left) A Fringe-Resolved Autocorrelation (FRAC) apparatus for sub-10 fs pulse characterization designed in the Center. (upper right) Spectral Phase Interferometry for Direct Electric-Field Reconstruction (SPIDER) and (lower right) Frequency-Resolved Optical Gating (FROG) apparatuses for general-purpose ultrashort pulse characterization.

Instrument Center

OHSHIMA, Yasuhiro	Director
YAMANAKA, Takaya	Technical Associate
TAKAYAMA, Takashi	Technical Associate
FUJIWARA, Motoyasu	Technical Associate
OKANO, Yoshinori	Technical Associate
MIZUKAWA, Tetsunori	Technical Associate
MAKITA, Seiji	Technical Associate
NAKANO, Michiko	Technical Associate
SAITO, Midori	Technical Associate
UEDA, Tadashi	Technical Associate
OTA, Akiyo	Secretary
NAKAGAWA, Nobuyo	Secretary

Instrument Center was organized in April of 2007 by integrating the general-purpose facilities of Research Center for Molecular Scale Nanoscience and Laser Research Center for Molecular Science. The mission of Instrument Center is to support the in-house and external researchers in the field of molecular science, who intend to conduct their research by utilizing general-purpose instruments. The staffs of Instrument Center maintain the best condition of the machines, and provide consultation for how to use them. The main instruments the Center now maintains in Yamate campus are: Nuclear magnetic resonance (NMR) spectrometers (JEOL JNM-ECA 600, and JNM-LA500), matrix assisted laser desorption ionization (MALDI) mass spectrometer (Voyager DE-STR), powder X-ray diffractometer (Rigaku RINT-Ultima III), circular dichroism (CD) spectrometer (JASCO JW-720WI), differential scanning calorimeter (MicroCal VP-DSC), and isothermal titration calorimeter (MicroCal iTC200). In the Myodaiji campus, the following instrument are installed: Electron spin resonance (ESR) spectrometers (Bruker E680, E500, EMX Plus), superconducting quantum interference devices (SQUID; Quantum Design MPMS-7 and MPMS-XL7), powder X-ray diffractometer (MAC Science MXP3), and single-crystal X-ray diffractometers (Rigaku Mercury CCD-1, CCD-2, RAXIS IV, and 4176F07), thermal analysis instruments (TA TGA2950, DSC2920, and SDT2960), fluorescence spectro-photometer (SPEX Fluorolog2), X-ray fluorescence spectrometer (JEOL JSX-3400RII), UV-VIS-NIR spectro-photometer (Hitachi U-3500), Raman microscope (Renishaw INVIA REFLEX532), excimer/dye laser system (Lambda Physics LPX105i/LPD3002), Nd^{+}:YAG-laser pumped OPO laser (Spectra Physics GCR-250/ Lambda Physics Scanmate OPPO), excimer laser (Lambda Physics Complex 110F), and picosecond tunable laser system (Spectra Physics Tsunami/Quantronix Titan/Light Conversion TOPAS). In addition to these, the following instruments have newly been added as the open facilities maintained by the Center: Electron spectrometers for chemical analysis (ESCA) (Omicron EA-125), high-resolution transmission electron microscope (TEM; JEOL JEM-3100FEF), scanning electron microscope (SEM; JEOL JEM-6700F(1), JED-2201F), focused ion beam (FIB) machine (JEOL JEM-9310FIB(P)), elemental analyzer (J-Science Lab Micro Corder JM10), NMR spectrometers (JEOL JNM-ECA920 and JNM-ECS400), and FTIR spectrometer (Bruker IFS 66v/S). In the fiscal year of 2011, Instrument Center accepted more than 80 applications from institutions outside IMS. Instrument Center also maintains helium liquefiers in the both campus and provides liquid helium to users. Liquid nitrogen is also provided as general coolants used in many laboratories in the Institute. The staffs of Instrument Center provide consultation for how to treat liquid helium, and provide various parts necessary for low-temperature experiments. Instrument Center supports also the Inter-University Network for Common Utilization of Research Equipments.

Figure 1. 600 MHz NMR spectrometer (JEOL JNM-ESA600).

Figure 2. Pulse ESR for Q-band (Bruker E680).

Figure 3. Raman microscope (Renishaw INVIA REFLEX532).

Equipment Development Center

KATOH, Masahiro	Director
MIZUTANI, Nobuo	Technical Associate
AOYAMA, Masaki	Technical Associate
YANO, Takayuki	Technical Associate
KONDOU, Takuhiko	Technical Associate
YOSHIDA, Hisashi	Technical Associate
UTCHIYAMA, Kouichi	Technical Associate
TOYODA, Tomonori	Technical Associate
NAGATA, Masaaki	Technical Associate
TAKADA, Noriko	Technical Associate
MIYASHITA, Harumi	Technical Fellow
SUGITO,Shouji	Technical Fellow
URANO, Hiroko	Secretary

Researches and developments of novel instruments demanded in the forefront of molecular science, including their design and fabrication, are the missions of this center. Technical staffs in the three work sections, mechanics, electronics and glass works are engaged in developing state-of-the-art experimental instruments, in collaboration with scientists. We expanded our service to other universities and research institutes since 2005, to contribute to the molecular science community and to improve the technology level of the center staffs. A few selected examples of our recent developments are described below.

Development of Seven-Axes Adjustable Stage for Manufacturing of Multi-Channel Biosensor

We are developing fine processing technologies using photo-fabrication as a new supporting technology.

We process penetrated micro-holes of about 1 to 2 μm in diameter with X-ray lithography at the specific positions on PMMA (poly-methyl-methacrylate) boards which are used for researches of biosensors, such as transferring signal of nerve cells, and so on.

We have developed a seven-axes adjustable stage for the alignment of the X-ray mask and the PMMA board accurately and conveniently. The positioning accuracy of less than 10 μm was succcessfully demonstrated.

Figure 1. Seven axes adjustable stage.

Development of Microfluidic Mixer for Research of Structural Changes in Proteins

We are developing a microfluidic mixer, which is used to investigate structural changes in proteins by mixing of two or more solutions combining with a fluorescence microscope. This is another example of the application of the photo-fabrication.

For this device, we have to produce micro-flow-channels of 10 μm width and 50 μm depth. Since it is hard to produce by ordinary machining, we have been developing techniques based on photolithography and PDMS (poly-dimethyl-siloxane) molding. We have successfully produced a microfluidic mixser as shown in Figure 2.

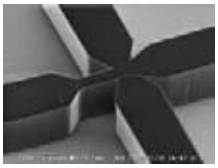

Figure 2. Microfluidic mixer.

BPM System Using Coaxial Switches and ARM Microcontroller through LAN

For the commissioning work after the remodeling of the UVSOR electron storage ring, which started from April 2012, we have developed a beam position monitor (BPM) system, which is capable of measuring the electron beam orbit, turn by turn. The sensor head of BPM consists of four electrodes mounted on the beam pipe. The beam position can be deduced from the difference between the induced fast electric pulse voltages on the electrodes by the beam. The electric signals are recorded by a digital oscilloscope which has four channels. The key technique of the system is switching of the BPM signals remotely from control room.

In UVSOR, there are 24 BPM heads. By using the newly developed signal switching system (Figure 3), we can select one BPM head (four signals) from 8 BPM heads. Coaxial switches of 16 SPDT types and 4 SP4T types are used. (Figure 4)

Figure 3. BPM system.

We control totally 20 coaxial switches by 'mbed,' the ARM microcontroller development kit. The control application is configured in a HTML file and JavaScript library, which can handle multiple I/O ports. The 'mbed' responds as a HTTP server when we access from LAN, and the control application is displayed on the Web browser, which enables us to select remotely the BPM signals.

Figure 4. Block diagram of BPM system.

Research Center for Computational Science

SAITO, Shinji	Director, Professor
EHARA, Masahiro	Professor
OKUMURA, Hisashi	Associate Professor
OONO, Hitoshi	Assistant Professor
ISHIDA, Tateki	Assistant Professor
KIM, Kang	Assistant Professor
FUKUDA, Ryoichi	Assistant Professor
ITOH, G. Satoru	Assistant Professor
MIZUTANI, Fumiyasu	Technical Associate
TESHIMA, Fumitsuna	Technical Associate
NAITO, Shigeki	Technical Associate
SAWA, Masataka	Technical Associate
IWAHASHI, Kensuke	Technical Associate
MATSUO, Jun-ichi	Technical Associate
NAGAYA, Takakazu	Technical Associate
TOYA, Akiko	Secretary
ISHIHARA, Mayumi	Secretary

Research Center for Computational Science provides state-of-the-art computational resources to academic researchers in molecular science and related fields, *e.g.* quantum chemistry, molecular simulations, and solid state physics. The computer systems consist of Fujitsu PRIMERGY RX300 and PRIME HPC FX10, SGI UV1000, and Hitachi SR16000. Over 650 users, 190 project groups, in molecular science have used in 2011. The large scale calculations, for example the formation of fullerenes, conformation searches using non-Boltzmann ensemble methods, and nonlinear spectroscopy of liquids, have been performed with the systems. The Center also provides a number of application programs, for example including Gaussian 09, GAMESS, Molpro, AMBER, and NAMD. The Center offers the Quantum Chemistry Literature Database, which has been developed by the Quantum Chemistry Database Group in collaboration with staff members of the Center. The latest release, QCLDB II Release 2008, contains 118,989 data of quantum chemical studies. Detailed information on the hardware and software at the Center is available on the web site (http://ccportal.ims.ac.jp/).

In addition to the provision of computational resources, the Center contributes to the so-called next-generation supercomputer project which is conducted by the government. In 2010, Computational Material Science Initiative (CMSI) was established, after the research field which consists of molecular science, solid state physics, and material science was selected as one of the research fields which scientific breakthroughs are expected by using the supercomputer. The Center contributes to CMSI by providing approximately 20% of its computational resource.

Figure 1. Fujitsu PRIMERGY RX300.

Figure 2. SGI UV1000.

Okazaki Institute for Integrative Bioscience

AONO, Shigetoshi	Professor
KUWAJIMA, Kunihiro	Professor
KATO, Koichi	Professor
FUJII, Hiroshi	Associate Professor
KURAHASHI, Takuya	Assistant Professor
YOSHIOKA, Shiro	Assistant Professor
YAMAGUCHI, Takumi	Assistant Professor
NAKAMURA, Takashi	IMS Research Assistant Professor
SAWAI, Hitomi	IMS Research Assistant Professor
CHEN, Jin	OIIB Research Assistant Professor
YAGI-UTSUMI, Maho	OIIB Research Assistant Professor
TANIZAWA, Misako	Secretary
TANAKA, Kei	Secretary

The main purpose of Okazaki Institute for Integrative Bioscience (OIIB) is to conduct interdisciplinary, molecular research on various biological phenomena such as signal transduction, differentiation and environmental response. OIIB, founded in April 2000, introduces cutting edge methodology from the physical and chemical disciplines to foster new trends in bioscience research. OIIB is a center shared by and benefited from all three institutes in Okazaki, thus encouraging innovative researches adequately in advance of academic and social demands. The research groups of three full professors and one associate professor who have the position in IMS join OIIB. The research activities of these groups are as follows.

Aono group is studying the bioinorganic chemistry of hemeproteins that show a novel function. They elucidated the structure and function relationships of the heme-based sensor proteins in which a heme is the active site for sensing gas molecules such as CO and O_2. They are also studying the structure and function relationships of HrtR that is an heme-sensing transcriptional regulator responsible for heme homeostasis in *Lactococcus lactis*. Kato group is studying structure, dynamics, and interactions of biological macromolecules primarily using ultra-high field nuclear magnetic resonance (NMR) spectroscopy. In particular, they conducted studies aimed at elucidating the dynamic structures of glycoconjugates and proteins for integrative understanding of the mechanisms underlying their biological functions. In this year, they successfully provided atomic views of conformational dynamics and intermolecular interactions of proteins involved in the ubiquitin-proteasome system and molecular recognition events on mammalian cell membranes. Kuwajima group is studying mechanisms of *in vitro* protein folding and mechanisms of molecular chaperone function. Their goals are to elucidate the physical principles by which a protein organizes its specific native structure from the amino acid sequence. In this year, they studied the structural fluctuations of the *Escherichia coli* chaperonin GroEL/ES complex by hydrogen/deuterium-exchange 2D NMR techniques. Fujii group is studying molecular mechanisms of metalloenzymes, which are a class of biologically important macromolecules having various functions such as oxygen transport, electron transfer, oxygenation, and signal transduction, with synthetic model complexes for the active site of the metalloenzymes. In this year, they studied molecular mechanisms of metalloenzymes relating to monooxygenation reactions and denitification processes.

OIIB is conducting the research program, “Integrated Bioscience to Reveal the Entire Life System with Studies of Biofunctional Molecules” and “Research on the Molecular Mechanisms of Biological Responses toward Environmental- and Biological-molecules.” In these research programs, the studies on the following subjects have been carried out: (i) functional analyses of higher-ordered biological phenomena, (ii) comprehensive screening of biofunctional molecules, (iii) computer simulations of higher-ordered biological systems and biofunctional molecules, (iv) molecular mechanisms of response to environmental molecules, of differentiation of germ cells, and of cellular stress-response and defense against stress, (v) studies on perturbation of biological functions induced by environmental molecules, (vi) studies on normal physiological functions regulated by biological molecules, and (vii) construction of integrated data base on the biological influences of environmental molecules.

Safety Office

UOZUMI, Yasuhiro	Director
TOMURA, Masaaki	Assistant Professor
TANAKA, Shoji	Assistant Professor
SUZUI, Mitsukazu	Technical Associate
NAGATA, Masaaki	Technical Associate
UEDA, Tadashi	Technical Associate
TAKAYAMA, Takashi	Technical Associate
SAKAI, Masahiro	Technical Associate
MAKITA, Seiji	Technical Associate
KONDO, Naonori	Technical Associate
ONITAKE, Naoko	Secretary
TSURUTA, Yumiko	Secretary

The Safety Office was established in April 2004. The mission of the Office is to play a principal role in the institute to secure the safety and health of the staffs by achieving a comfortable workplace environment, and improvement of the working conditions. In concrete terms, it carries out planning, work instructions, fact-findings, and other services for safety and health in the institute. The Office is comprised of the following staffs: The Director of the Office, Safety-and-Health Administrators, Safety Office Personnel, Operational Chiefs and other staff members appointed by the Director General. The Safety-and-Health Administrators patrol the laboratories in the institute once every week, and check whether the laboratory condition is kept sufficiently safe and comfortable to conduct researches. The Office also edits the safety manuals and gives safety training courses, for Japanese and foreign researchers.

Public Affairs Office

OHSHIMA, Yasuhiro	Head	NAKAMURA, Rie	Technical Fellow
HARADA, Miyuki	Technical Associate		

It is increasingly important for an institution conducting basic reach like IMS to communicate its objective, function, and activities not only to members of the scientific community, but also to ordinary people in society. For this mission, Public Affair Office conducts various operations. They include: 1) publishing several periodicals printed in Japanese or English, such as activity report, annual review, IMS letters, and brochures, 2) maintaining and renovating the homepage of the Institute, 3) managing the press releases to presenting recent achievements, 4) maintaining the exhibition room and managing laboratory tours by visitors to facilities in IMS. It is also in charge of organizing Molecular Science Forum, a lectureship held trimonthly for providing variety of lectures on interesting scientific topics to people living in Okazaki city. In addition, to cultivate scientific literacy and adoration to science, in particular, among younger generation, Public Affair Office participates to several activities co-jointly held by educational organizations in the city.

Archives

OHSHIMA, Yasuhiro	Head	SUZUKI, Satomi	Secretary
MINAMINO, Satoshi	Technical Associate		

IMS was founded in 1975, following the incubation period of 14 years since the term “molecular science” was officially used for the first time in Japanese community of chemistry and physics. Archives of IMS, established in early 2006, have been collecting mainly the important materials in such an early period around the foundation of IMS. At present, 7 hundreds of archives have been preserved. Among them, documents and publications have been photo-copied and converted to digital files or microfilms.

Technical Division

SUZUI, Mitsukazu	Head
OMARU, Tadakazu	Technical Fellow
MIZUNO, Hitoshi	Technical Fellow

Secretary for Director-General

MIZUNO, Hisayo	Secretary

Information Office

OHHARA, Kyoko	Secretary
SUGIYAMA, Kayoko	Secretary
TSURUTA, Yumiko	Secretary
KAMO, Kyoko	Secretary

The Technical Division is an organization of the technical staff which supports research facilities of IMS. The technical staffs are assigned to support the research by using their professional skills of mechanical engineering, electrical engineering, instrumental analysis, optical technology, computer engineering, cryogenic technology, and the SOR technology, *etc*.

In addition, the Technical Division supports IMS facilities by managing Safety Office, Research groups, Public Affairs Office, Archives and Information Office.

The annual meeting for technical staff of research Institute and Universities was organized in 1975 and since then the meeting has been regularly held every year. We aim toward a higher technology and exchange discussion concerning the various technical problems related to our technology.

Special Research Projects

IMS has special research projects supported by national funds. Seven projects in progress are:

(a) Next Generation Integrated Nanoscience Simulation Software
Development & Application of Advanced High-Performance Supercomputer Project
(b) The Ministry of Education, Culture, Sports, Science and Technology
"Construction of Innovative High Performance Computing Infrastructure (HPCI)"
HPCI Strategy Program Field 2 "—New Materials and Energy Creation—"
(c) Extreme Photonics
(d) MEXT Nanotechnology Network Program and Nanotechnology Platform Program
Platform of Molecule and Material Synthesis
(e) Inter-University Network for Efficient Utilization of Research Equipments
(f) Consortium for Photon Science and Technology (C-PhoST)
(g) Quantum Beam Technology Program

These seven projects are being carried out with close collaboration between research divisions and facilities. Collaborations from outside also make important contributions. Research fellows join these projects.

(a) Next Generation Integrated Nanoscience Simulation Software Development & Application of Advanced High-Performance Supercomputer Project

A national project entitled, "Next Generation Integrated Nanoscience Simulation Software" was initiated on April 1, 2006 at Institute for Molecular Science (IMS). The project was a part of the "Development & Application of Advanced High-Performance Supercomputer Project" of MEXT, which aimed to develop a next generation supercomputer and application software to meet the need in the computational science nation-wide.

The primary mission of our project was to resolve following three fundamental problems in the field of nanoscience, all of which were crucial to support society's future scientific and technological demands: (1) "Next Generation Energy" (*e.g.*, effective utilization of the solar energy), (2) "Next Generation Nano Biomolecules" (*e.g.*, scientific contributions toward overcoming obstinate diseases), and (3), "Next Generation Nano Information Function and Materials" (*e.g.*, molecular devices). In these fields, new computational methodologies and programs were to be developed to clarify the properties of nanoscale substances such as catalysts (enzymes), bio-materials, molecular devises, and so forth, by making the best use of the next generation supercomputer.

Among many application programs developed in the project, we selected six programs, three from the molecular science and three from the solid state physics, as "core applications" in the nano-science, and concentrating our effort to tune those programs to the next generation machine, K-computer. The programs in molecular science are concerned with molecular dynamics simulation, quantum chemistry, and statistical mechanics of liquids.

This project was completed successfully as of the end of March, 2012. 46 programs have been released to the public via Portal site for Application Software Library (PAL). Over 1800 science papers have been submitted during the project.

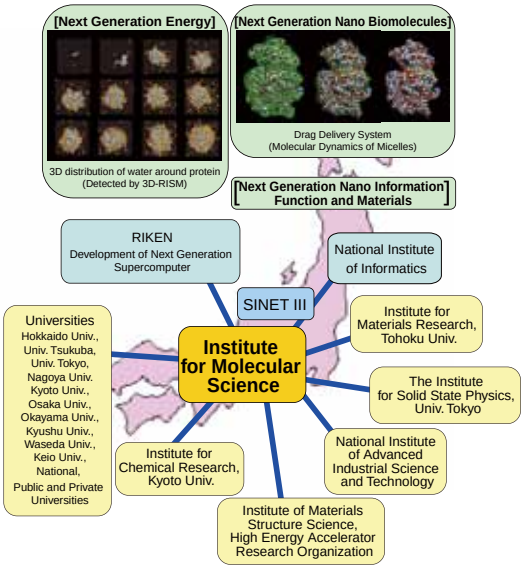

(b) The Ministry of Education, Culture, Sports, Science and Technology "Construction of Innovative High Performance Computing Infrastructure (HPCI)" HPCI Strategy Program Field 2 "New Materials and Energy Creation"

HPCI strategy programs aim to promote scientific research using "K-computer," the next-generation supercomputer at RIKEN Advanced Institute for Computational Science. In the strategic filed 2, the Institute for Solid State Physics (ISSP) of the University of Tokyo, Institute for Molecular Science (IMS), and Institute for Material Research (IMR) of Tohoku University were selected as strategic organizations. The project started in September 2010 for "Computational Material Science: Turning the Headwaters of Basic Science into a Torrent of Innovations in Functional Materials and Energy Conversion" as a strategic target. To promote the activities of the strategic organizations, a new community "Computational Materials Science Initiative (CMSI)" consisting of research fields of condensed matter physics, molecular science and materials science was launched.

Theoretical and Computational Chemistry Initiative (TCCI) at IMS completed the activities of fiscal year 2011: (1)TCCI established its organization for research and promotion in the field of computational molecular science, (2)TCCI recruited 14 researchers and 2 professors, (3)TCCI organized the second TCCI workshop, one symposium for interactions with experimental chemistry, and the other one for industry-academic partnership, and (4)TCCI also sponsored the fifteenth summer school of Molecular Simulations, two TCCI winter colleges (molecular simulations, and quantum chemistry), and one workshop for massively parallel programming.

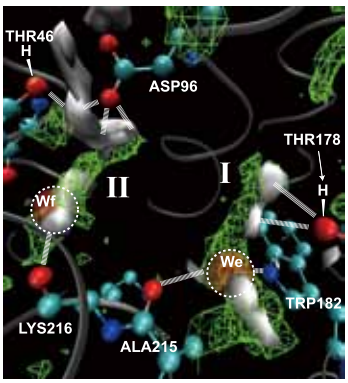

3D distribution function of water in a protein computed with the MC-MOZ method.

In the following years, TCCI is going to pursue the activities above and promote the research using K-computer and the computational molecular science field.

(c) Extreme Photonics

Institute for Molecular Science has a long-standing tradition of promoting spectroscopy and dynamics of molecules and molecular assemblies. Accordingly, photo-molecular science is one of the major disciplines in molecular science. This field is not confined in the traditional spectroscopy, but makes solid basis for other disciplines including nanoscience and bioscience, *etc*. Therefore, continuing developments in spectroscopy and microscopy are vital to enhance our abilities to elucidate more complex systems in time and spatial domains. In order to achieve full developments of photo-molecular science, we need to pursue three branches in developing: (1) new light source, (2) new spatio-temporally resolved spectroscopy, and (3) new methods to control atomic and molecular dynamics. Since 2005, we have started the program of "Extreme Photonics" in collaboration with the RIKEN institute. Currently 6 groups in IMS are involved in this program, and the specific research titles are as follows:

(1) Development of new light sources

TAIRA, Takunori	Micro Solid-State Photonics
FUJI, Takao	Coherent Synthesis of Femtosecond Pulses over the UV-IR Range
KATOH, Masahiro	Coherent Synchrotron Radiation

(2) Development of new spatio-temporally resolved spectroscopy

OKAMOTO, Hiromi	Development of Extreme Time-Resolved Near-Field Spectroscopy

(3) Development of new methods to control atomic and molecular dynamics

OHMORI, Kenji	Development of Attosecond Coherent Control and Its Applications
OHSHIMA, Yasuhiro	Quantum-State Manipulation of Molecular Motions by Intense Coherent Laser Pulses

(d) MEXT Nanotechnology Network Program and Nanotechnology Platform Program Platform of Molecule and Material Synthesis

The Nanotechnology Network Project of the Ministry of Education, Culture, Sports, Science and Technology (MEXT) was completed in March 2012. IMS participated in this project as a core organization (project leader: YOKOYAMA, Toshihiko, Prof. & Director of Research Center for Molecular Scale Nanoscience) with Nagoya University (representative: BABA, Yoshinobu, Prof.), Nagoya Institute of Technology (representative: HIHARA, Takehiko, Prof.) and Toyota Technological Institute (representative: SAKAKI, Hiroyuki, Prof. & Vice President of TTI), and established a nanotechnology support

center in central Japan area in 2007–2012. In 2011 Apr.–2012 Mar., the number of accepted projects applied to IMS amounted 138 including 63 in-house applications and the total number of days is 989 including 387 days for in-house use.

In July 2012, a new program started, which is named Nanotechnology Platform Program supported by MEXT and will continue for ten years. This program has three platforms of nanostructure analysis, nanoprocessing, and molecule and material synthesis, together with the center of the platforms. Each platform consist of about ten organizations all over Japan. IMS conducts a representative organization of the platform of Molecule and Material Synthesis, and Research Center for Molecular Scale Nanoscience is a steering center of this project. All the organizations in this platform are shown in Figure.

In order to support Japanese nanotechnology researches not only for universities and government institutes but also for private companies, we will open various kinds of our equipments with total supports including data analysis. The list of the supporting elements is given in Table. We will promote applications not only to each element, but to combined usage of several supporting elements such as nanobiotechnology and green nanotechnology.

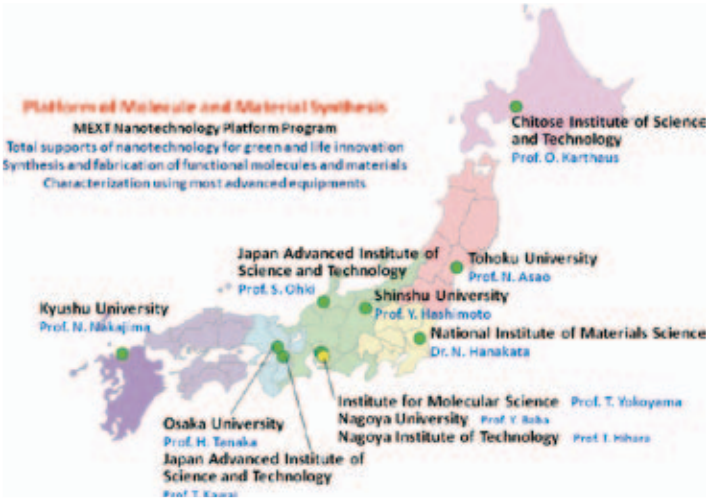

List of Supports in IMS (Nanotechnology Platform Program)

Supporting Element		Responsible Persons		Charging Persons	Remarks
Platform Management		T. Yokoyama Y. Kaneko		Y. Funaki Y. Toyama	
Organization Management in IMS		T. Yokoyama			
Electron Microscopy	300kV Transmission Electron Microscopy	Y. Ohshima		M. Saito	
	Field Emission Scanning Electron Microscopy Focus Ion Beam Processing			S. Nakao	
UVSOR Synchrotron Radiation	Scanning Transmission X-Ray Microscopy	M. Katoh	N. Kosugi	T. Ohigashi	From Apr. 2013
	X-Ray Magnetic Circular Dichroism		T. Yokoyama	T. Nakagawa Y. Takagi	From Apr. 2013
Molecular Properties	Electron Spectroscopy for Chemical Analysis	Y. Ohshima	N. Kosugi	M. Sakai	
	Electron Spin Resonance		T. Nakamura	K. Furukawa M. Fujiwara	
	Superconducting Quantum Interference Device		Y. Ohshima	M. Fujiwara	From Apr. 2013
	Microscopic Raman Spectroscopy		H. Yamamoto	K. Yamamoto M. Uruichi	
	Fourier Transform Far Infrared Spectroscopy				
920 MHz NMR	Solutions	Y. Ohshima	K. Kato	T. Yamaguchi M. Nakano	800 and 600MHz NMR will be supplied in 2013
	Solids		K. Nishimura	M. Nakano	
Functional Molecular Synthesis and Molecular Device Fabrication	Organic Thin Film Solar Cells	T. Yokoyama	M. Hiramoto	T. Kaji	
	Organic Field Effect Transistors		H. Yamamoto	K. Yamamoto M. Uruichi	
	Molecular Catalysts		M. Tada		
	Functional Organic Synthesis		H. Sakurai		
	Functional Metal Complex Synthesis		T. Nagata		
	Large Scale Quantum Mechanical Calculations		M. Ehara		

(e) Inter-University Network for Efficient Utilization of Research Equipments

It is highly important to improve the supporting environment for research and education in the field of science and engineering. Nowadays, advanced research instruments are indispensable for conducting research and education in high standard. To install such sophisticated instruments, significant amount of budgets is necessary. In 2007, for constructing a national-wide network to provide the easy access to high-level equipments to researchers and students in universities all over Japan, the 5 year project "Functioning of Inter-University Network for Efficient Utilization of Chemical Research Equipments," was launched. The network maintains an internet machine-time reservation and charging system by the help of equipment managers and accounting sections in each university. More than 50 universities all over Japan have been participating to the network. They are grouped into 12 regions and in each region the regional committee discusses and determines the operation of regional network system with the hub university chairing. There is no barrier for every user to access to any universities beyond his/her regional group. From 2009, the registered equipments are open to the researchers and students of every public and private universities. Since 2010, the project name has been changed as "Inter-University Network for Efficient Utilization of Research Equipments," still keeping the original strategy and stable functioning. In July 2012, the number of user registrants amounts to more than 7500 in 92 universities/institutions covering more than 1800 laboratories in Japan. Usage of the network reaches to a few thousands per month since April 2010, and keeps growing in numbers.

(f) Consortium for Photon Science and Technology (C-PhoST)

In order to establish strong bases in the research and education in optical science, a new 10-year program "Photon Frontier Network" has been started in 2008 by the Ministry of Education, Culture, Sports, Science and Technology (MEXT). Consortium for Photon Science and Technology (C-PhoST) is the one of two research consortia of Photon Frontier Network. It is composed of 4 Core Organizations headed by Principal Investigators (written in parentheses): JAEA (R. Kodama, supported by A. Sugiyama), Osaka University (R. Kodama), Kyoto University (S. Noda) and Institute for Molecular Science (K. Ohmori). The major strength of this Consortium is the collaboration between the specialists in three fields: High power lasers, semiconductor lasers, and coherent control. Emphasis will be placed in the education to foster young researchers capable of taking leaderships in scientific projects through participation to the forefront researches taking place at C-PhoST and also participation to international collaboration activities.

(g) Quantum Beam Technology Program

Quantum Beam Technology Program of MEXT/JST is aimed to develop technologies and applications of quantum beams such as photon beam, electron/positron beam, neutron beam, ion beam and so on produced by particle accelerators. This program is also aimed to train and educate young researchers and students in this research field. We proposed a development study using the UVSOR accelerators, "Light source development study using electron storage ring and laser" in collaboration with Nagoya University and Kyoto University. Graduate students of SOKENDAI and Nagoya University and a few postdoctoral fellows would be involved in this study. This proposal was approved in 2008 as a five year program.

Under the support of this program, we have been developing technologies to produce coherent light beam in the terahertz and the vacuum ultra-violet ranges using the UVSOR-II electron storage ring and lasers. By injecting a laser beam into the UVSOR-II electron storage ring, a density modulation at the radiation wavelength on the electron beam circulating in the storage ring can be produced. Such an electron beam emits coherent synchrotron radiation at the wavelength and its harmonics.

We have modified the configuration of the storage ring to produce a space for this development. We have constructed a new optical klystron type undulator system and two new beam-lines to extract the terahertz light and the VUV light. We have reinforced the laser system which is synchronized with the electron acceleration. These developments and constructions were completed until the end of 2011. First demonstration on producing the coherent terahertz radiation was successful. Some users experiments using these coherent light beam will be tried during the fiscal year 2012.

Okazaki Conference

The 71st Okazaki Conference
New Perspectives on Molecular Science of Glycoconjugates

(October 12–14, 2011)

Organizers: S. Wakatsuki (*KEK*), K. Kato (*IMS*), R. Kato (*KEK*), Y. Yamaguchi (*RIKEN*), T. Satoh (*Nagoya City Univ.*), Y. Kamiya (*IMS*)

Invited Overseas Speakers: M. von Itzstein (*Griffith Univ.*), K.-H. Khoo (*Academia Sinica*), J. C. Paulson (*Scripps Res. Inst.*), T. Peters (*Univ. Lübeck*), R. J. Woods (*Univ. Georgia*)

The 71st Okazaki Conference "New perspectives on molecular science of glycoconjugates" was held on October 12–14, 2011. We had 73 participants including 24 invited speakers and 18 poster presenters. The purpose of this conference was to provide a forum where researchers from various fields related to glycoscience come together and exchange their idea.

Carbohydrate chain is called "third life chain" along with nucleic acid and protein and its biological importance has been widely recognized in recent years. However, molecular science of glycoconjugates has remarkably lagged behind those of other biomolecules. This is because carbohydrate chain structures are not directly encoded in the genome and exhibit microheterogeneities along with significant degrees of freedom in internal motion. Moreover, biological functions of the carbohydrate chains are promoted through their cluster formation mediated by weak intermolecular interactions. Thus, decoding processes of *glycocodes* involves a lot of important issues that remain to be addressed in fields of molecular science.

The conference opened with an introductory lecture by Prof. Paulson (Scripps Res. Inst.), which was followed by a variety of topics delivered by researchers from different disciplines including leading glycoscientists. Every talk elicited active discussion with naïve and pertinent questions and comments, which made the conference exciting, enjoyable, and memorable, opening up the possibilities of new collaborations among the participants. Finally, we discussed perspectives on novel molecular science approaches towards understanding of the mechanisms underlying glycoconjugate functions. The conference was so successful that invited overseas speakers remarked that it was one of the best conferences they had ever participated in. We anticipated that the exciting three-day event would be a prelude to new wave of molecular science for providing atomic views of dynamic glycoconjugate functions.

The 71st Okazaki Conference "New Perspectives on Molecular Science of Glycoconjugates," October 12–14, 2011.

Joint Studies Programs

As one of the important functions of an inter-university research institute, IMS facilitates joint studies programs for which funds are available to cover the costs of research expenses as well as the travel and accommodation expenses of individuals. Proposals from domestic scientists are reviewed and selected by an interuniversity committee.

(1) Special Projects

A. Development of Polarized Quantum Beam Sources and their Applications to Molecular Science

KATOH, Masahiro *(IMS)*
KOBAYASHI, Kensei (*Yokohama Natl. Univ.*)
YAMAMOTO, Naoto (*Nagoya Univ.*)
SODA, Kazuo (*Nagoya Univ.*)
YABUTA, Hikaru (*Osaka Univ.*)
KIMURA, Shin-ichi *(IMS)*

By using particle accelerator technologies, polarized quantum beams of various kinds can be produced. At the UVSOR facility, circular polarized coherent synchrotron radiation ranging from visible to deep UV can be produced by using resonator free electron laser.[1)] We have demonstrated that such polarized radiation is a powerful tool for molecular science.[2,3)] In this joint study program, we are going to develop techniques to produce polarized quantum beams of various kinds and explore their applications.

It was successfully demonstrated at UVSOR to produce circular VUV light beam by using a technique called Coherent Harmonic Generation (CHG).[4)] Towards higher intensity, a new undulator system called optical klystron was developed and installed in the ring (Figure 1). Its basic performance has been confirmed by observing the spontaneous synchrotron radiation spectra. A first CHG experiment will be done in autumn, 2012.

It was also successfully demonstrated at UVSOR to produce a polarized gamma-ray source by using a technique called Laser Compton Scattering (LCS). Laser photons are injected to the electron beam and are scattered off, and they are converted to gamma-rays via inverse Compton scattering process.[5)] The polarity of the gamma-rays can be changed by changing that of the laser photons. The possible applications are now being explored.

In Nagoya University, a polarized electron source has been developed based on an electron gun technology using GaAs photocathode. The spin polarization higher than 90% has been demonstrated.[6)] In collaboration with Nagoya University, a spin polarized electron source is now under commissioning at UVSOR. The first experiment on bio-molecular science will be carried out in autumn 2012. The application in the field of inverse photoelectron spectroscopy is now under preparation.

Figure 1. Variable Polarization Optical Klystron at UVSOR-III.

References

1) M. Hosaka, S. Koda, M. Katoh, J. Yamazaki, K. Hayashi, Y. Takashima, T. Gejo and H. Hama, *Nucl. Instrum. Methods Phys. Res., Sect. A* **483**, 146–151 (2002).
2) J. Takahashi, H. Shinojima, M. Seyama, Y. Ueno, T. Kaneko, K. Kobayashi, H. Mita, M. Adachi, M. Hosaka and M. Katoh, *Int. J. Mol. Sci.* **10**, 3044–3064 (2009).
3) T. Nakagawa, T. Yokoyama, M. Hosaka and M. Katoh, *Rev. Sci. Instrum.* **78**, 023907 (2007).
4) M. Labat, M. Hosaka, M. Shimada, M. Katoh and M. E. Couprie, *Phys. Rev. Lett.* **101**, 164803 (2008).
5) Y. Taira, M. Adachi, H. Zen, T. Tanikawa, M. Hosaka, Y. Takashima, N. Yamamoto, K. Soda and M. Katoh, *Nucl. Instrum. Methods Phys. Res., Sect. A* **637**, 5116–5119 (2011).
6) N. Yamamoto, X. G. Jin, A. Mano, T. Ujihara, Y. Takeda, S. Okumi, T. Nakanishi, T. Yasue, T. Koshikawa, T. Ohshima, T. Saka and H. Horinaka, *J. Phys.: Conf. Series* **298**, 012017 (2011).

(2) Research Symposia

(From Oct. 2011 to Sep. 2012)

Dates	Theme	Chair
Nov. 1– 2, 2011	Molecular Science for Supra-Functional Molecular Systems by Using Experimental and Theoretical Methods	**SEKIYA, Hiroshi** **FURUTANI, Yuji**
Mar. 13, 2012	Synposium for Young Inorganic Chemsts Aiming at the Innovation	**MIZUTA, Tsutomu** **MASAOKA, Shigeyuki**
Mar. 15–16, 2012	Symposium on Integral Researches toward the Next Generation of Molecular Science	**MATSUMOTO, Yoshiteru** **FURUTANI, Yuji**
Jun. 1– 2, 2012	Recent Development of Experimental and Theoretical Methodology on Liquids and Soft Matters: Basic Properties and Applications to Novel Devices	**NISHIYAMA, Katsura** **OKUMURA, Hisashi**
Jul. 30–31, 2012	New Avenue for Investigating Molecular Structure via Laser Spectroscopy and Magnetic Measurements	**BABA, Masaaki** **OHSHIMA, Yasuhiro**
Jun. 16–17, 2012	Preparatory Meeting for the 52nd Molecular Science Summer School & the 1st Symposium for Young Molecular Scientists	**YAMAZAKI, Kaoru** **FURUTANI, Yuji**

(3) Numbers of Joint Studies Programs

Categories		Oct. 2011–Mar. 2012	Apr. 2012–Sep. 2012	Total
Special Projects		0	1	1
Research Symposia		3	2	5
Research Symposia for Young Researchers		0	1	1
Cooperative Research		55	51	106
Use of Facility	Instrument Center	41	51	92
	Equipment Development Center	7	7	14
Use of UVSOR Facility		78	56	134
Use of Facility Program of the Computer Center				179*

* from April 2011 to March 2012

Collaboration Programs

(a) IMS International Program

IMS has accepted many foreign scientists and hosted numerous international conferences since its establishment and is now universally recognized as an institute that is open to foreign countries. In 2004, IMS initiated a program to further promote international collaborations. As a part of this program, IMS faculty members can (1) nominate senior foreign scientists for short-term visits, (2) invite young scientists for long-term stays, and (3) undertake visits overseas to conduct international collaborations.

Leader	Title	Partner
UOZUMI, Yasuhiro	Development of Novel Polymer-Supported Transition Metal Catalysts and Their Application to Selective Organic Transformations	Korea: HAN, Jinwook and group members
YOKOYAMA, Toshihiko	A Development of Uniaxial Magnetic Anisotropy in $Fe_{1-x}Co_x$ Films Grown on Vicinal Surfaces	Germany: PRZYBYLSKI, Marek and group members Turkey: YILDIZ, Fikret
OKAMOTO, Hiromi	Plasmon Characteristics of Hybrid Metal Nanorods	Korea: LIM, Jong Kuk and group members
TAIRA, Takunori	Study of the Coupling between Angular-Quasi-Phase-Matching, Pockels Effect and Bragg Diffraction: Application to the Modulation of Parametric Processes	France: BOULANGER, Benoît and group members
SHIGEMASA, Eiji	Deexcitation Dynamics of Core Excited States Studied by High-Resolution Electron Spectroscopy	France: SIMON, Marc and group members
KATO, Koichi	Ultra High-Field NMR Study of Post-Translational Modifications of Proteins	Korea: LEE, Weontae and group members
SAKURAI, Hidehiro	Synthesis and Properties of Functionalized Buckybowls	Germany: LENTZ, Dieter and group members Korea: KAWANO, Masaki and group members India: SASTR, G. Narahari Thailand: SOMSOOK, Ekasith and group members
KATOH, Masahiro	Beam Dynamics in Free Electron Laser Oscillator	France: BIELAWSKI, Serge and group members
JIANG, Donglin	Synthesis and Fucntions of Two-Dimensional Polymers	China: DONG, Yuping and group members
KIMURA, Shin-ichi	Optical and Photoelectrical Studies on Electronic Structure of Strongly Correlated 3d and 4f Electron Systems	Korea: KWON, Yong-Seung and group members

KOSUGI, Nobuhiro	Research and Development of Scanning Transmission X-Ray Microscopy (STXM)	Canada: HITCHCOCK, Adam P. Germany: RUEHL, Eckart U. S. A.: TYLISZCZAK, Tolek

(b) IMS-Asian Core Program "Molecular Science in East Asian Region toward Post-Nano-Science"

In 2006, Institute for Molecular Science (IMS) started Asian Core Program on "Frontiers of material, photo- and theoretical molecular sciences" (2006–2011). This program, which was sponsored by Japan Society for the Promotion of Science (JSPS), aimed to develop a new frontier in the molecular sciences and to foster the next generation of leading researchers through the collaboration and exchange among IMS and core Asian institutions: Institute of Chemistry, Chinese Academy of Science (ICCAS, China); The College of Natural Science, Korea Advanced Institute of Science and Technology (KAIST, Korea); and Institute of Atomic and Molecular Sciences, Academia Sinica (AIMS, Taiwan). After this JSPS Asian Core Program was successfully completed in March 2011, we have launched IMS Asian Core Program on "Molecular Science in East Asian Region toward Post-Nano-Science" to further promote collaborations with these four key institutes. Within the framework of this IMS Asian Core Program, an educational program, Asian Winter School, with three key institutes are planned within JFY 2012. In addition, several international seminars and collaborations which were spun off from the previous JSPS Asian Core Program are also in progress within the frame work of IMS International Collaboration and so on.

(c) Exchange Program for East Asian Young Researchers "Improvement of Fundamental Research Base for Environmental and Energy Problems"

At the Second East Asia Summit (EAS), held in January 2007, Mr. Shinzo Abe, Prime Minister of Japan, announced a plan to invite about 6,000 young people to Japan mainly from the EAS member states every year for the next five years. Based on this plan, the Government of Japan has launched the Japan-East Asia Network of Exchange for Students and Youths (JENESYS) Programme, under which it is conducting a variety of exchange activities. As a part of the JENESYS Programme, the Japan Society for the Promotion of Science (JSPS) and Japan Student Services Organization (JASSO) have launched the "Exchange Program for East Asian Young Researchers." Aimed at promoting researcher exchanges with East Asian countries, this program supports initiatives by Japanese universities and research institutions to invite young researchers (JSPS) and graduate students (JASSO) from those countries. By supporting exchange programs implemented by Japanese universities and research institutions, the "Exchange Program for East Asian Young Researchers" works to establish and expand networks with researchers mainly from Asian countries. It also helps to develop high-caliber human resources and to create a regional science and technology community. IMS is a center of the basic research of physical/chemistry fields in Japan and has a role for the center of both domestic and international collaboration. From 2008, IMS has organized the JENESYS program for chemistry/physics fields. IMS provides the opportunity for young researchers from Asian countries to stay in the laboratories related to the basic research for environmental and energy problem. Through the experience, we encourage them to continue the basic research in their own countries as well as to build up the future collaboration. IMS welcomed totally 15 young researchers in 2011 season from Thailand, Indonesia, Malaysia, Vietnam, Philippines, and India.

OKAMOTO, Hiromi
Photo-Molecular Science

The Chemical Society of Japan Award for Creative Work
"Nano-Optical Studies on Physical and Chemical Characteristics of Noble Metal Nanostructures"

The Chemical Society of Japan Award for Creative Work is awarded to researchers who have made a leading contribution to the fundamentals and applications of chemistry. Since appointed as a professor in IMS, Prof. Okamoto developed and established a new measurement methodology for the studies of excited states of nanomaterials based mainly on scanning near-field optical microscopy. He used the developed method to reveal fundamental optical characteristics of plasmonic noble metal nanostructures. The achievements were highly evaluated and the Society concluded that Prof. Okamoto deserves the award.

OHMORI, Kenji
Photo-Molecular Science

Humboldt Research Award
"Pioneering Development of Spatiotemporal Quantum Engineering with Precisions on the Picometer and Attosecond Scales"

Kenji Ohmori, Professor and Chairman of the Department of Photo-Molecular Science, has been awarded Humboldt Research Award. The award has been founded by Alexander von Humboldt foundation funded by the government of Federal Republic of Germany. It is awarded in recognition of a researcher's entire achievements to date in a variety of disciplines such as humanities, social sciences, natural sciences, and engineering, and is presented to academics whose fundamental discoveries, new theories, or insights have had a significant impact on their own discipline and who are expected to continue producing cutting-edge achievements in the future. It is considered to be the most prestigious academic award in Germany, and 42 Humboldt Research Awardees have subsequently been awarded Nobel Prize. The award has been granted to Professor Ohmori for his pioneering development of spatiotemporal quantum engineering with precisions on the picometer and attosecond scales.

KATO, Koichi
Life and Coordination-Complex Molecular Science

The Erwin von Bälz Prize 2011 (First Prize)
"Molecular Mechanism Underling Initiation of Amyloidogenesis and Its Application to Development of Disease-Modifying Drugs for Alzheimer Disease"

Professor Koichi Kato was awarded the first prize in the Erwin von Bälz Prize 2011 together with Dr. Katsuhiko Yanagisawa (Director of the National Center for Geriactrics and Gerontology's Center for Development of Advanced Medicine for Dementia) and Dr. Katsumi Matsuzaki (Professor of the Graduate School of Pharmaceutical Sciences, Kyoto University) for their paper on "Molecular Mechanism Underling Initiation of Amyloidogenesis and Its Application to Development of Disease-Modifying Drugs for Alzheimer Disease." This prize was awarded by Boehringer Ingelheim GmbH interlinking the bestowal to the awardees with its gratitude and its wish for continuing close and successful collaboration between Japanese and German Medicine.

TAIRA, Takunori
Laser Research Center for Molecular Science

SPIE Fellow
"Significant Achievement in the Field of Solid-State Lasers and Nonlinear Optics"

SPIE, the international society for optics and photonics, was founded in 1955 to advance light-based technologies. Serving more than 225,600 constituents from approximately 150 countries, the Society advances emerging technologies through interdisciplinary information exchange, continuing education, publications, patent precedent, and career and professional growth. Fellows are Members of distinction who have made significant scientific and technical contributions in the multidisciplinary fields of optics, photonics, and imaging. They are honored for their technical achievement, for their service to the general optics community, and to SPIE in particular. More than 900 SPIE members have become Fellows since the Society's inception in 1955.

FURUTANI, Yuji
Life and Coordination-Complex Molecular Science

Morino Foundation for Molecular Science (2012)
"Investigation of Molecular Mechanisms of Signal Transduction and Energy Conversion of Membrane Proteins and Specific Reactions in Nanospaces Mimicking Protein Function by Using Infrared Spectroscopy"

KURASHIGE, Yuki
Theoretical and Computational Molecular Science

Young Researcher Award from National Institute of Natural Science
"Development of Quantum-Chemical Density-Matrix Renormalization Group Theory and Applications to Electronic-Structure of Metalloenzymes"

AWARDS

YOSHIDA, Norio Theoretical and Computational Molecular Science	Young Scientist Award of the Japan Association of Solution Chemisty 2011 "Theoretical Study on Chemical Processes in Solution by Integral Equation Theory"
KAJI, Toshihiko Research Center for Molecular Scale Nanoscience	31st Young Scientist Oral Presentation Award from The Japan Society of Applied Physics "Co-Evaporant Induced Crystallization of Donor:Acceptor Blends in Organic Solar Cells"
SAWAI, Hitomi Life and Coordination-Complex Molecular Science	The 5th Shiseido Female Researcher Science Grant "Elucidation of the Molecular Mechanisms for Intracellular Heme Homeostasis" The Chemical Society of Japan Presentation Award 2012 "Molecular Mechanism of Functional Regulation by Heme for the Novel Transcriptional Regulator, HesR"
YAMAGUCHI, Takumi Life and Coordination-Complex Molecular Science	The Chemical Society of Japan Presentation Award 2012 "Paramagnetic-Tagging for Development of NMR Conformational Analyses of Oligosaccharides"
KONDO, Mio Life and Coordination-Complex Molecular Science	The 5th Shiseido Female Researcher Science Grant "Construction of Water Splitting System via the Control of Electron Transfer at Interface"
AOYAMA, Masaki Equipment Development Center	The Chemical Society of Japan Award for Technical Achievements "Fabrication of Experimental Devices for Molecular Science by Advanced Machining Technology"

Visitors from abroad are always welcome at IMS and they have always played an important role in the research activities of the Institute. The foreign scientists who visited IMS during the past year (September 2011–August 2012) are listed below.

(1) MONKASHO (Ministry of Education, Culture, Sports, Science and Technoogy, Japan) or JSPS (Japan Society for the Promotion of Science) Invited Fellow

Prof. Panda Gautam	CSIR	India	Oct. '11–Jul. '12
Dr. Khemthong Pongtanawat	Natl. Natnotechnology Center	Thailand	Oct. '11–Nov. '11

(2) IMS Visiting Scientist

Dr. Le Quang Hong	Inst. of Material Res. and Engineering	Vietnam	Sep. '11–Jan. '12
Prof. Jeong Dae Hong	Seoul Natl. Univ.	Korea	Sep. '11–Jan. '12
Prof. Lablanquie Pascal	LCPMR, Univ. Pierre et Marie Curie	France	Sep. '11–Jan. '12
Ms. Chidthong Rungtiwa	Nakhon Pathom Rajabhat Univ.	Thailand	Sep. '11–Mar. '12
Prof. Zhao Xiang	Xi'an Jiaotong Univ.	China	Sep. '11–Feb. '12
Dr. Dang JingShuang	Xi'an Jiaotong Univ.	China	Sep. '11–Feb. '12
Ms. Promkatkaew Malinee	Kasetsart Univ.	Thailand	Oct. '11–Feb. '12
Dr. Vailikhit Veeramol	Kasetsart Univ.	Thailand	Oct. '11–Jan. '12
Prof. Bongsoo Kim	Changwon Univ.	Korea	Oct. '11–Dec. '11
Ms. Lim Min Hwee	Natl. Univ. of Singapore	Singapore	Oct. '11–Mar. '12
Dr. Kaewmati Patcharin	Mahidol Univ.	Thailand	Oct. '11–Jan. '12
Mr. Jeon Seong Hwan	Pohang Univ. of Sci. and Tech.	Korea	Oct. '11–Jan. '12
Prof. Borve Knut	Univ. of Bergen	Norway	Oct. '11–Nov. '11
Dr. Guritamu Violeta	Univ. of Geneva	Germany	Oct. '11–Jan. '12
Mr. Jung Sung Won	Pohang Univ. of Sci. and Tech.	Korea	Oct. '11–Jan. '12
Dr. Arulmozhiraja Sundaram	The Australian Natl. Univ.	India	Oct. '11–Mar. '12
Prof. Sastry G. Narahari	Indian Inst. of Chem. Tech.	India	Oct. '11–Apr. '12
Mr. Choavarit Kamonsakikul	Mahidol Univ.	Thailand	Oct. '11–Apr. '12
Dr. Chalupsky Jakub	Inst. of Organic Chem. and Biochem. Gilead Sci. Res. Cent.	Czech	Nov. '11–Dec. '11
Mr. Koedtruad Anucha	Chulalongkorn Univ.	Thailand	Nov. '11–Jan. '12
Dr. Chiang Hsin-lin	Natl.Tsing Hua Univ. Inst. of Phys. Academia Sinica	Taiwan	Nov. '11–Feb. '12
Dr. Chen Fei	Fudan Univ.	China	Dec. '11–Jan. '12
Dr. Ge Qingqin	Fudan Univ.	China	Dec. '11–Jan. '12
Dr. Zhou Xin	IMS	China	Dec. '11–Mar. '12
Mr. Lee Chul	Univ. of Seoul	Korea	Dec. '11–Jan. '12
Mr. Kim Jooyun	Univ. of Seoul	Korea	Dec. '11–Jul. '12
Prof. Wiesner Karoline	Univ. of Bristol	U.K.	Jan. '12–Jul. '12
Dr. Dahlsten Oscar	Natl. Univ. of Singapore	Sweden	Jan. '12–Jun. '12
Dr. Hartl Ingmar	IMRA AMERICA	U.S.A	Jan. '12–Aug. '12
Dr. Kurzynski Pawel	Natl. Univ. of Singapore	Singapore	Jan. '12–Jun. '12
Mr. Min Byeon-Hun	Sungkyunkwan Univ.	Korea	Jan. '12–Jul. '12
Prof. Song Yun Young	Sungkyunkwan Univ.	Korea	Jan. '12–Jul. '12
Prof. Kwon Yong-Seung	Sungkyunkwan Univ.	Korea	Jan. '12–Jul. '12
Ms. Rungnim Chompoonut	Chiang Mai Univ.	Thailand	Feb. '12–May '12
Prof. Aka Gerard	Ecole Natl. Suprieure de Chimie de Paris	France	Feb. '12–Apr. '12
Dr. Wang Heng	IMS	Japan	Feb. '12
Prof. Liu Hsiang-Lin	Natl. Taiwan Normal Univ.	Taiwan	Feb. '12–Jul. '12
Prof. Sommerfeld Thomas	Southeastern Louisiana Univ.	U.S.A	Feb. '12–Jun. '12
Mr. Hudson Reuben	McGill Univ.	Canada	Feb. '12–Jun. '12
Ms. Koo Jin Young	Pohang Univ. of Sci. and Tech.	Korea	Feb. '12–Aug. '12
Prof. Ebbesen W. Thomas	ISIS, Univ. of Strasbourg and CNRS	France	Feb. '12–Jun. '12
Dr. Yang Tao	Xi'an Jiaotong Univ.	China	Feb. '12–Apr. '12
Mr. Tarsang Ruangchai	Ubon Ratchathani Univ.	Thailand	Feb. '12–Jul. '12
Ms. Maitarad Phornphimon	Shanghai Univ.	Thailand	Feb. '12–Aug. '12
Prof. Piecuch Piotr	Michigan State Univ.	U.S.A	Feb. '12–Aug. '12
Prof. Cheng Yuang-Chung	Natl. Univ. of Taiwan	Taiwan	Feb. '12–.Jul. '12
Ms. Thammaporn Ratsupa	IMS	Japan	Feb. '12–Jan. '13

Ms. Meeprasert Jittima	Natl. Nanotechnology Cent.	Thailand	Feb. ’12–Oct. ’12
Prof. Lim Jong Kuk	Chosun Univ.	Korea	Feb. ’12–Aug. ’12
Ms. Jo Jihee	Chosun Univ.	Korea	Feb. ’12–Aug. ’12
Dr. Volety Srinivas	CCMB	India	Feb. ’12–Jun. ’12
Prof. Ruehl Eckart	Free Univ. of Berlin	Germany	Feb. ’12–Jul. ’12
Prof. Simon Marc	Univ. Pierre et Marie Curie	France	Feb. ’12–Jun. ’12
Dr. Guillemin Renaud	Univ. Pierre et Marie Curie	France	Feb. ’12–Jun. ’12
Prof. Segonds Patricia	Joseph Fourier Univ.	France	Feb. ’12–Apr. ’12
Prof. Piancastelli Maria-Novel	Univ. Pierre et Marie Curie	France	Feb. ’12–Jun. ’12
Dr. Tan Si-Hui	Agency for Sci.,Tech. and Res.	Singapore	Feb. ’12–Jun. ’12
Dr. Skrzypczyk Paul	Univ. of Cambridge	U.K.	Feb. ’12–Jun. ’12
Prof. Lablanquie Pascal	LCPMR, Univ. Pierre et Marie Curie	France	Mar. ’12–Mar. ’12
Dr. Probst Petra	The Karksruhe Inst. of Tech.	Germany	Mar. ’12–Apr. ’12
Ms. Seo Jeong Jin	Yonsei Univ.	Korea	Mar. ’12–Jun. ’12
Ms. Kyung Won Shik	Yonsei Univ.	Korea	Mar. ’12–Jun. ’12
Prof. Przybylski Marek	Max-Planck-Inst. für Mikrostrukturphysik	Poland	Mar. ’12–Apr. ’12
Prof. Loiseau Pascal	Ecole Natl. Suprieure de Chimie de Paris(Paris6)	France	Mar. ’12–Apr. ’12
Mr. Ilas Simon	Ecole Natl. Suprieure de Chimie de Paris(Paris6)	France	Mar. ’12–Aug. ’12
Prof. Yildiz Fikret	Gebze Inst. of Tech.	Turkey	Mar. ’12–Apr. ’12
Mr. Dabrowski Maciej	Max-Planck-Inst. für Mikrostrukturphysik	Poland	Mar. ’12–Apr. ’12
Prof. Boulanger Benoit	Joseph Fourier Univ.	France	Mar. ’12–Aug. ’12
Prof. Ni Huagang	Zhejiang Sci.-Tech. Univ.	China	Mar. ’12–Sep. ’12
Ms. Sophiphun Onsulang	Sranaree Univ. of Tech.	Thailand	Mar. ’12–Apr. ’12
Dr. Chou Ming-Hsien	HC Photonics Co.	Taiwan	Mar. ’12–Aug. ’12
Mr. Wu Yang	Donghua Univ.	China	Mar. ’12
Prof. Ufuktepe Yulsel	Univ. of Cukurova	Turkey	Mar. ’12–Jul. ’12
Dr. Szwaj Chirisophe	Univ. des Sci. et Tech. de Lille	France	Apr. ’12–Jun. ’12
Ms. Roussel Elenore	Univ. des Sci. et Tech. de Lille	France	Apr. ’12–Jun. ’12
Prof. Bielawski Serge	Univ. des Sci. et Tech. de Lille	France	Apr. ’12–Jun. ’12
Prof. Joye Alain	Fourier Inst.	France	Apr. ’12–Aug. ’12
Prof. Kwon Yong-Seung	Daegu Gyeongbuk Inst. of Sci. and Tech.	Korea	May ’12–Aug. ’12
Dr. Min Byeon Hun	Daegu Gyeongbuk Inst. of Sci. and Tech.	Korea	May ’12–Aug. ’12
Prof. Song Yun Young	Jeju College of Tech.	Korea	May ’12–Aug. ’12
Ms. Boonsri Pornthip	Univ. of Kasetsart	Thailand	Jun. ’12–Aug. ’12
Prof. Bagchi Biman	Indian Inst. of Sci.	India	Jul. ’12–Aug. ’12
Ms. Lin Jianbin	Sun Star Co. Ld.	China	Aug. ’12–Mar. ’14
Mr. Leloup Valentin	Chimie Paris Tech.	France	Aug. ’12
Ms. Jinasan Atchaleeya	Mahidol Univ.	Thailand	Aug. ’12–Nov. ’12

(3) Visitor to IMS

Prof. Matsika Sopiridoula	Temple Univ.	Canada	Sep. ’11–Dec. ’11
Dr. Roca-Sanjuan Daniel	Univ. of Uppsala	Sweden	Oct. ’11
Prof. D. M. Harris Kenneth	Cardiff Univ.	U.K.	Oct. ’11–Dec. ’11
Prof. Fleming Graham	Univ. of California, Berkeley	U.S.A.	Oct. ’11–Jan. ’12
Prof. Sprik Michiel	Univ. of Cambridge	U.K.	Nov. ’11–Jan. ’12
Ms. Zhu Tong	Shenyang Pharmaceutical Univ.	China	Jan. ’12–Aug. ’12
Mr. Ou Shin Sei	Okayama Univ.	Japan	Jan. ’12–Aug. ’12
Prof. Gruebelle Martin	Univ. of Illinois	U.S.A.	Jan. ’12–Jul. ’12
Mr. Ngamsomprasert Niti	Chulalongkorn Univ.	Thailand	Feb. ’12–Apr. ’12
Ms. Nitnara Supamas	Bank of Thailand	Thailand	Feb. ’12–Apr. ’12
Prof. Berry Richard Stephen	Univ. of Chicago	U.S.A.	Feb. ’12–Jun. ’12
Prof. Biswas Ranjit	S. N. Bose Natl. Cent. for Basic Sci.	India	Feb. ’12–Jun. ’12
Prof. Petek Hrvoje	Univ. of Pittsuburgh	U.S.A.	Mar. ’12–Jun. ’12
Prof. Liu Zhongfan	Peking Univ.	China	Mar. ’12–Apr. ’12
Prof. Xi Zhengfeng	Peking Univ.	China	Mar. ’12–Apr. ’12
Prof. Xi Rimo	Nankai Univ.	China	Mar. ’12–Apr. ’12
Prof. Li Yongfang	Inst. of Chem., Chinese Acad. of Sci.	China	Mar. ’12–Apr. ’12

Prof. Scholes Gregory	Univ. of Toronto	Canada	Mar. ’12–Jun. ’12
Prof. Zhang Guobin	NSRL, Univ. of Sci. and Tech. of China	China	Mar. ’12–Jun. ’12
Dr. Wang Ping	Allied Adv. Materials Co.	China	Apr. ’12–Apr. ’12
Mr. Gao Jia	Lanzhou Univ.	China	May. ’12–Sep. ’12

Scientists who would like to visit IMS under programs (1) is invited to make contact with IMS staff in their relevant field.

Theoretical and Computational Molecular Science

T. TSUCHIYA, M. WIELOPOLSKI, N. SAKUMA, N. MIZOROGI, T. AKASAKA, T. KATO, D. M. GULDI and S. NAGASE, "Stable Radical Anions inside Fullerene Cages: Formation of Reversible Electron Transfer Systems," *J. Am. Chem. Soc.* **133**, 13280–13283 (2011).

X. DING, L. CHEN, Y. HONSHO, X. FENG, O. SAENGSAWANG, J. -D. GUO, A. SAEKI, S. SEKI, S. IRLE, S. NAGASE, V. PARASUK and D. JIANG, "An n-Channel Two-Dimensional Covalent Organic Framework," *J. Am. Chem. Soc.* **133**, 14510–14513 (2011).

K. SAWAI, Y. TAKANO, M. IZQUIERDO, S. FILIPPONE, N. MARTIN, Z. SLANINA, N. MIZOROGI, M. WAELCHLI, T. TSUCHIYA, T. AKASAKA and S. NAGASE, "Enantioselective Synthesis of Endohedral Metallofullerenes," *J. Am. Chem. Soc.* **133**, 17746–17752 (2011).

M. SAITO, T. KUWABARA, K. ISHIMURA and S. NAGASE, "Synthesis of a Novel Lithocene that has Aromatic-Like Nature without Nonaromatic Rings," *Chem. –Asian J.* **6**, 2907–2910 (2011).

H. LEI, J. -D. GUO, J. C. FETTINGER, S. NAGASE and P. P. POWER, "Synthesis, Characterization, and CO Elimination of Ferrio-Substituted Two-Coordinate Germylenes and Stannylenes," *Organometallics* **30**, 6316–6322 (2010).

S. A. MIAN, X. GAO, S. NAGASE and J. JANG, "Adsorption of Catechol on a Wet Silica Surface: Density Functional Theory Study," *Theor. Chem. Acc.* **130**, 333–339 (2011).

L. WANG, J. ZHENG, J. ZHOU, R. QIN, H. LI, W. -N. MEI, S. NAGASE and J. LU, "Tuning Graphene Nanoribbon Field Effect Transistors via Controlling Doping Level," *Theor. Chem. Acc.* **130**, 483–489 (2011).

Y. OHTSUKA and S. NAGASE, "Projector Monte Carlo Method Based on Slater Determinants: A New Sampling Method for Singlet State Calculations," *Theor. Chem. Acc.* **130**, 501–505 (2011).

G. LUO, L. WANG, H. LI, R. QUI, J. ZHOU, L. LI, Z. GAO, W. -N. MEI, J. LU and S. NAGASE, "Polarized Nonresonant Raman Spectra of Graphene Nanoribons," *J. Phys. Chem. C* **115**, 24463–24468 (2011).

J. ZHOU, L. WANG, R. QIN, J. ZHENG, W. N. MEI, P. A. DOWBEN, S. NAGASE, Z. GAO and J. LU, "Structure, Electronic, and Transport Properties of Transition Metal Intercalated Graphene and Graphene-Hexagonal-Boron- Nitride Bilayer," *J. Phys. Chem. C* **115**, 25273–25280 (2011).

X. LU, K. NAKAJIMA, Y. IIDUKA, H. NIKAWA, N. MIZOROGI, Z. SLANINA, T. TSUCHIYA, T. AKASAKA and S. NAGASE, "Structural Elucidation and Regioselective Functionalization of An Unexplored Carbide Cluster Metallofullerene $Sc_2C_2@C_s(6)$-C_{82}," *J. Am. Chem. Soc.* **133**, 19553–19558 (2011).

Z. SLANINA, F. UHLIK, S. -L. LEE, L. ADAMOWICZ, T. AKASAKA and S. NAGASE, "Calculations of Metallofullerene Yields," *J. Comput. Theor. Nanosci.* **8**, 2233–2239 (2011).

X. GAO, D. JIANG, Y. ZHAP, S. NAGASE, S. ZHANG and Z. CHEN, "Theoretical Insights into the Structures of Graphene Oxide and Its Chemical Conversion between Graphene," *J. Comput. Theor. Nanosci.* **8**, 2406–2422 (2011).

H. KURIHARA, X. LU, Y. IIDUKA, H. NIKAWA, N. MIZOROGI, Z. SLANINA, T. TSUCHIYA, S. NAGASE and T. AKASAKA, "X-Ray Structures of $Sc_2C_2@C_{2n}$ (n = 40, 41, 42): In-Depth Understanding of the Core-Shell Interplay in Carbide Cluster Metallofullerenes," *Inorg. Chem.* **51**, 746–750 (2012).

H. KURIHARA, X. LU, Y. IIDUKA, N. MIZOROGI, Z. SLANINA, T. TSUCHIYA, S. NAGASE and T. AKASAKA, "$Sc_2@C_{3v}(8)$-C_{82} *vs.* $Sc_2C_2@C_{3v}(8)$-C_{82}: Drastic Effect of C_2 Capture on the Redox Properties of Scandium Metallofullerenes," *Chem. Commun.* **48**, 1290–1292 (2012).

S. SATO, H. NIKAWA, S. SEKI, L. WANG, G. LUO, J. LU, M. HARANAKA, T. TSUCHIYA, S. NAGASE and T. AKASAKA, "Co-Crystal of Paramagnetic Endohedral Metallofullerene La@C_{82} and Nickel Porphyrin with High Electronic Mobility," *Angew. Chem., Int. Ed.* **51**, 1589–1591 (2012).

H. KURIHARA, X. LU, Y. IIDUKA, H. NIKAWA, N. MIZOROGI, Z. SLANINA, T. TSUCHIYA, S. NAGASE and T. AKASAKA, "Chemical Understanding of Carbide Cluster Metallofullerenes: A Case Study on $Sc_2C_2@C_{2v}(5)$-C_{80} with Complete X-Ray Crystallographic Characterizations," *J. Am. Chem. Soc.* **134**, 3139–3144 (2012).

X. ZHAO, W. -Y. GAO, T. YANG, J. -J. ZHENG, L. -S. LI, L. HE, R. -J. GAO and S. NAGASE, "Violating the Isolated Pentagon Rule (IPR): Endohedral Non-IPR C_{98} Cages of $Gd_2@C_{98}$," *Inorg. Chem.* **51**, 2039–2045 (2012).

H. -X. YEONG, S. -H. ZHANG, H. -W. XI, J. -D. GUO, K. H. LIM, S. NAGASE and C. -W. SO, "An Amidinate-Stabilized Germatrisila-cyclobutadiene Ylide," *Chem. –Eur. J.* **18**, 2685–2691 (2012).

S. KARTHIKEYAN and S. NAGASE, "Origins of the Stability of Imidazole-Imidazole, Benzene-Imidazole, and Benzene-Indole Dimers: CCSDS(T)/CBS and SAPT Calculations," *J. Phys. Chem. A* **116**, 1694–1700 (2012).

M. SAITO, Y. HASHIMOTO, T. TAJIMA, K. ISHIMURA, S. NAGASE and M. MINOURA, "Molecular Structure of Dibenzo[*a*,*e*] pentalenen Anion Radical and its Electronic State," *Chem. –Asian. J.* **7**, 480–483 (2012).

Y. MAEDA, M. YAMADA, T. HASEGAWA, T. AKASAKA, J. LUO and S. NAGASE, "Interaction of Single-Walled Carbon Nanotubes with Amine," *NANO* **7**, 1130001 (10 pages) (2012).

H. KURIHARA, Y. IIDUKA, Y. RUBIN, M. WAELCHLI, N. MIZOROGI, Z. SLANINA, T. TSUCHIYA, S. NAGHASE and T. AKASAKA, "Unexpected Formation of a $Sc_3C_2@C_{80}$ Bisfulleroid Derivative," *J. Am. Chem. Soc.* **134**, 4092–4095 (2012).

T. AGOU, Y. SUGIYAMA, T. SASAMORI, H. SAKAI, Y. FURUKAWA, N. TAKAGI, J. -D. GUO, S. NAGASE, D. HASHIZUME and N. TOKITOH, "Synthesis of Kinetically Stabilized 1,2-Dihydorodisilenes," *J. Am. Chem. Soc.* **134**, 4120–4123 (2012).

X. LU, T. AKASAKA and S. NAGASE, "Soluble and Tubular Higher Fullerenes that Encapsulate Metals," *Angew. Chem., Int. Ed.* **51**, 2812–2814 (2012).

R. QUHE, J. ZHENG, G. LUO, Q. LIU, R. QIN, J. ZHOU, D. YU, S. NAGASE, W. -N. MEI, Z. GAO and J. LU, "Tunable and Sizable Band Gap of Single Layer Graphene Sandwiched between Hexagonal Boron Nitride," *NPG Asia Materials* **4**, e6 (10 pages) (2012).

N. KANO, A. FURUTA, T. KANBE, J. YOSHINO, Y. SHIBATA, T. KAWASHIMA, N. MIZOROGI and S. NAGASE, "2,2'-Diborylazo-benzenes with Double N–B Coordination: Control of Fluorescent Properties by Substituents and Redox Reactions," *Eur. J. Inorg. Chem.* 1584–1587 (2012).

C. A. CAPUTO, J. -D. GUO, S. NAGASE, J. C. FETTINGER and P. P. POWER, "Reversible and Irreversible Higher-Order Cycloaddition Reactions of Polyolefins with a Multiple-Bonded Heavier Group 13 Alkene Analogue: Contrasting the Behavior of Systems with π–π, π–π* and π–n_+ Frontier Molecular Orbital Symmetry," *J. Am. Chem. Soc.* **134**, 7155–7164 (2012).
M. SUZUKI, X. LU, S. SATO, H. NIKAWA, N. MIZOROGI, Z. SLANINA, T. TSUCHIYA, S. NAGASE and T. AKASAKA, "Where Does the Metal Cation Stay in Gd@C_{2v}(9)-C_{82}? A Single-Crystal X-Ray Diffraction Study," *Inorg. Chem.* **51**, 5270–5273 (2012).
C. XU, G. LUO, Q. LIU, J. ZHENG, Z. ZHANG, S. NAGASE, Z. GAO and J. LU, "Giant Magnetoresistance in Silicene Nanoribbons," *Nanoscale* **4**, 3111–3117 (2012).
Z. D. BROWN, J. -D. GUO, S. NAGASE and P. P. POWER, "Experimental and Computational Study of Auxiliary Molecular Effects on the Mechanism of the Addition of Hydrazines to a Low-Valent Germanium Complex," *Organometallics* **31**, 3768–3772 (2012).
X. LU, K. NAKAJIMA, Y. IIDUKA, H. NIKAWA, T. TSUCHIYA, N. MIZOROGI, Z. SLANINA, S. NAGASE and T. AKASAKA, "The Long-Believed Sc_2@C_{2v}(17)-C_{84} Is Actually Sc_2C_2@C_{2v}(9)-C_{82}: Unambiguous Structure Assignment and Chemical Functionalization," *Angew. Chem., Int. Ed.* **51**, 5889–5892 (2012).
Q. ZHENG, G. LUO, Q. LIU, R. QUHE, J. ZHENG, K. TANG, Z. GAO, S. NAGASE and J. LU, "Structural and Electronic Properties of Bilayer and Trilayer Graphdiyne," *Nanoscale* **4**, 3990–3996 (2012).

Y. NEGISHI, K. MUNAKATA, W. OHGAKE and K. NOBUSADA, "Effect of Copper Doping on Electronic Structure, Geometric Structure, and Stability of Thiolate-Protected Au_{25} Nanoclusters," *J. Phys. Chem. Lett.* **3**, 2209–2214 (2012).
Y. NEGISHI, K. IGARASHI, K. MUNAKATA, W. OHGAKE and K. NOBUSADA, "Palladium Doping of Magic Gold Cluster $Au_{38}(SC_2H_4Ph)_{24}$: Formation of $Pd_2Au_{36}(SC_2H_4Ph)_{24}$ with Higher Stability than $Au_{38}(SC_2H_4Ph)_{24}$," *Chem. Commun.* **48**, 660–662 (2012).

Y. KURASHIGE and T. YANAI, "Second-Order Perturbation Theory with a DMRG Self-Consistent Field Reference Function: Theory and Application to the Study of Chromium Dimer," *J. Chem. Phys.* **135**, 094104 (9 pages) (2011).
T. YANAI and T. SHIOZAKI, "Canonical Transcorrelated Theory with Projected Slater-Type Geminals," *J. Chem. Phys.* **136**, 084107 (9 pages) (2012).
T. YANAI, Y. KURASHIGE, E. NEUSCAMMAN and G. K.-L. CHAN, "Extended Implementation of Canonical Transformation Theory: Parallelization and a New Level-Shifted Condition," *Phys. Chem. Chem. Phys.* **14**, 7809–7820 (2012).

N. YOSHIDA, Y. KIYOTA and F. HIRATA, "The Electronic-Structure Theory of a Large-Molecular System in Solution: Application to the Intercalation of Proflavine with Solvated DNA," *J. Mol. Liq.* **159**, 83–92 (2011).
Y. KIYOTA, N. YOSHIDA and F. HIRATA, "Affinity of Small Ligands to Myoglobin Studied by the 3D-RISM Theory," *J. Mol. Liq.* **159**, 93–98 (2011).
T. IMAI, N. MIYASHITA, Y. SUGITA, A. KOVALENKO, F. HIRATA and A. KIDERA, "Functionality Mapping on Internal Surfaces of Multidrug Transporter AcrB Based on Molecular Theory of Solvation: Implications for Drug Efflux Pathway," *J. Phys. Chem. B* **115**, 8288–8295 (2011).
D. J. SINDHIKARA, N. YOSHIDA, M. KATAOKA and F. HIRATA, "Solvent Penetration in Photoactive Yellow Protein R52Q Mutant: A Theoretical Study," *J. Mol. Liq.* **164**, 120–122 (2011).
Y. KIYOTA, N. YOSHIDA and F. HIRATA, "A New Approach for Investigating the Molecular Recognition of Protein: Toward Structure-Based Drug Design Based on the 3D-RISM Theory," *J. Chem. Theory Comput.* **7**, 3803–3815 (2011).
D. SINDHIKARA, N. YOSHIDA and F. HIRATA, "Placevent: An Algorithm for Predicting of Explicit Solvent Atom Distribution—Application to HIV-1 Protease and F-ATP Synthase," *J. Comput. Chem.* **33**, 1536–1543 (2012).
J. HONG, N. YOSHIDA, S.-H. CHONG, C. LEE, S. HAM and F. HIRATA, "Elucidating the Molecular Origin of Hydrolysis Energy of Pyrophosphate in Water," *J. Chem. Theory Comput.* **8**, 2239–2246 (2012).
Y. MARUYAMA and F. HIRATA, "Modified Anderson Method for Acceleating 3D-RISM Calculations Using Graphics Processor Unit," *J. Chem. Theory Comput.* **8**, 2239–2246 (2012).

Y. TANAKA and K. YONEMITSU, "Nonlinear Conduction by Melting of Stripe-Type Charge Order in Organic Conductors with Triangular Lattices,'' *J. Phys. Soc. Jpn.* **80**, 103702 (4 pages) (2011).
K. YONEMITSU, "Theory of Photoinduced Phase Transitions in Molecular Conductors: Interplay between Correlated Electrons, Lattice Phonons and Molecular Vibrations,'' *Crystals* **2**, 56–77 (2012).
K. YONEMITSU, N. MAESHIMA and Y. TANAKA, "Interplay between Correlated Electrons and Quantum Phonons in Charge-Ordered and Mott-Insulating Organic Compounds,'' *Acta Phys. Pol., A* **121**, 372–374 (2012).
H. UEMURA, N. MAESHIMA, K. YONEMITSU and H. OKAMOTO, "Dimerization-Induced Spin-Charge Coupling in One-Dimensional Mott Insulators Revealed by Femtosecond Reflection Spectroscopy of Rb-Tetracyanoquinodimethane Salts,'' *Phys. Rev. B* **85**, 125112 (7 pages) (2012).
K. YONEMITSU, "Roles of Molecular Vibrations in Photoinduced Insulator-to-Metal and Neutral-to-Ionic Transitions,'' *Phys. Status Solidi B* **249**, 975–978 (2012).
Y. TANAKA and K. YONEMITSU, "Theory of Nonlinear Conduction for Charge-Ordered States in Quasi-Two-Dimensional Organic Conductors,'' *Phys. Status Solidi C* **9**, 1186–1188 (2012).
K. NISHIOKA and K. YONEMITSU, "Theory of Photoinduced Melting of Charge Order in $Et_2Me_2Sb[Pd(dmit)_2]_2$,'' *Phys. Status Solidi C* **9**, 1213–1215 (2012).
M. MIYAZAKI, K. YAMAJI, T. YANAGISAWA and K. YONEMITSU, "Renormalization of Hopping Integrals in Coexistence Phase of Stripe and *d*-Wave Superconductivity in Two-Dimensional Hubbard Model,'' *Physics Procedia* **27**, 64–67 (2012).
K. NISHIOKA, K. NASU and K. YONEMITSU, "Two-Pulse Excitation for Efficient Formation of an sp^3 Nanodomain with Frozen Shear in a Graphite Crystal,'' *J. Phys.: Condens. Matter* **24**, 205402 (6 pages) (2012).

M. HIGASHI and S. SAITO, "Direct Simulation of Excited-State Intramolecular Proton Transfer and Vibrational Coherence of 10-Hydroxybenzo[h]quinoline in Solution," *J. Phys. Chem. Lett.* **2**, 2366–2371 (2011).

J. LIU, W. H. MILLER, G. S. FANOURGAKIS, S. S. XANTHEAS, S. IMOTO and S. SAITO, "Insights in Quantum Dynamical Effects in the Infrared Spectroscopy of Liquid Water from a Semiclassical Study with an Ab Initio-Based Flexible and Polarizable Force Field," *J. Chem. Phys.* **135**, 244503 (14 pages) (2011).

T. YAGASAKI and S. SAITO, "Energy Relaxation of Intermolecular Motions in Supercooled Water and Ice: A Molecular Dynamics Study," *J. Chem. Phys.* **135**, 244511 (9 pages) (2011).

N. YAMAMOTO, O. KAMBARA, K. YAMAMOTO, A. TAMURA, S. SAITO and K. TOMINAGA, "Temperature and Hydration Dependence of Low-Frequency Spectra of Poly-L-Glutamic Acid with Different Secondary Structures Studied by Terahertz Time-Domain Spectroscopy," *Soft Matter* **8**, 1997–2006 (2012).

S. K. PADHI, R. FUKUDA, M. EHARA and K. TANAKA, "Comparative Study of C^N and N^C Type Cyclometalated Ruthenium Complexes with a NAD^+/NADH Function," *Inorg. Chem.* **51**, 8091–8102 (2012).

S. SURAMITR, S. PHALINYOT, P. WOLSCHANN, R. FUKUDA, M. EHARA and S. HANNONGBUA, "Photophysical Properties and Photochemistry of *EE*-, *ZE*-, and *ZZ*-1,4-diethoxy-2,5-bis[2-(thien-2-yl)ethyenyl]benzene in Solution: Theory and Experiment," *J. Phys. Chem. A* **116**, 924–937 (2012).

K. BOBUATONG, S. KARANJIT, R. FUKUDA, M. EHARA and H. SAKURAI, "Aerobic Oxidation of Methanol to Formic Acid on Au_{20}^- Cluster: Theoretical Study on Reaction Mechanism," *Phys. Chem. Chem. Phys.* **14**, 3103–3111 (2012).

M. TASHIRO, K. UEDA and M. EHARA, "Double Core-Hole Shake-up Satellite Spectra of N_2 and CO Molecules," *Chem. Phys. Lett.* **521**, 45–51 (2012).

Y. MAKITA, K. IKEDA, K. SUGIMOTO, T. FUJITA, T. DANNO, K. BOBUATONG, M. EHARA, S. FUJIWARA and A. OGAWA, "Enhancement of Catalytic Reactivity of Zinc(II) Complex by a Cyclotriveratrylene-Capped Structure," *J. Organomet. Chem.* **706-707**, 26–29 (2012).

S. YAMANAKA, K. KANDA, T. SAITO, Y. KITAGAWA, T. KAWAKAMI, M. EHARA, M. OKUMURA, H. NAKAMURA and K. YAMAGUCHI, "Does B3LYP Correctly Describe Megnetism of Manganese Complexes with Various Oxidation Numbers and Various Structural Motifs?" *Chem. Phys. Lett.* **519-520**, 134–140 (2012).

R. FUKUDA and M. EHARA, "Excited States and Electronic Spectra of Annulated Dinuclear Free-Base Phthalocyanines," *J. Chem. Phys.* **136**, 114304 (15 pages) (2012).

D. SHIMADA, R. KUSAKA, Y. INOKUCHI, M. EHARA and T. EBATA, "Nonradiative Decay Dynamics of Methyl 4-Hydroxycinnamate and Its Hydrated Complex Revealed by Picosecond Pump-Probe Spectroscopy," *Phys. Chem. Chem. Phys.* **14**, 8999–9005 (2012).

S. K. PADHI, R. FUKUDA, M. EHARA and K. TANAKA, "Photo-Isomerization and Proton-Coupled Electron Transfer (PCET) Promoted Water Oxidation by Mononuclear Cyclometalated Ruthenium Catalysts," *Inorg. Chem.* **51**, 5386–5392 (2012).

M. EHARA and T. SOMMERFELD, "CAP/SAC-CI Method for Calculating Resonance States of Metastable Anions," *Chem. Phys. Lett.* **537**, 107–112 (2012).

N. BERRAH, L. FANG, T. OSIPOV, B. MURPHY, K. UEDA, E. KUKK, R. FEIFEL, P. VAN DER MEULEN, P. SALE, H. SCHMIDT, R. THOMAS, M. LARSSON, R. RICHTER, K. C. PRINCE, J. D. BOZEK, C. BOSTEDT, S. WADA, M. N. PIANCASTELLI, M. TASHIRO and M. EHARA, "Double Core-Hole Spectroscopy for Chemical Analysis with an Intense X-Ray Femtosecond Laser," *Proc. Natl. Acad. Sci. U. S. A.* **108**, 16912–16915 (2011).

M. TASHIRO, K. UEDA and M. EHARA, "Auger Decay of Molecular Double Core Hole States," *J. Chem. Phys.* **135**, 022139 (14 pages) (2011).

O. TAKAHASHI, M. TASHIRO, M. EHARA, K. YAMASAKI and K. UEDA, "Molecular Double Core Hole Electron Spectroscopy of Nucleobases," *J. Phys. Chem. A* **115**, 12070–12082 (2011).

P. POOLMEE, M. EHARA and H. NAKATSUJI, "Photophysical Properties and Vibrational Structure of Ladder-Type Penta p-Phenylene and Carbazole Derivatives Based on SAC-CI Calculations," *Theor. Chem. Acc.* **130**, 161–173 (2011).

H. OKUMURA, "Temperature and Pressure Denaturation of Chignolin: Folding and Unfolding Simulation by Multibaric-Multithermal Molecular Dynamics Method," *Proteins: Struct., Funct., Bioinf.* **80**, 2397–2416 (2012).

S. G. ITOH, A. DAMAJANOVIC and B. R. BROOKS, "pH Replica-Exchange Method Based on Discrete Protonation States," *Proteins: Struct., Funct., Bioinf.* **79**, 3420–3436 (2011).

T. MORISHITA, S. G. ITOH, H. OKUMURA and M. MIKAMI, "Free-Energy Calculation via Mean-Force Dynamics Using a Logarithmic Energy Landscape," *Phys. Rev. E* **85**, 066702 (2012).

Y. SUSA, Y. SHIKANO and A. HOSOYA, "Optimal Probe Wavefunction of Weak-Value Amplification," *Phys. Rev. A* **85**, 052110 (7 pages) (2012).

H. SHIROTA and T. ISHIDA, "Microscopic Aspects in Dicationic Ionic Liquids through the Low-Frequency Spectra by Femtosecond Raman-Induced Kerr Effect Spectroscopy," *J. Phys. Chem. B* **115**, 10860–10870 (2011).

T. KAWATSU, K. MATSUDA and J. HASEGAWA, "Bridge-Mediated Excitation Energy Transfer Pathways through Protein Media: A Slater Determinant-Based Electronic Coupling Calculation Combined with Localized Molecular Orbitals," *J. Phys. Chem. A* **115**, 10814–10822 (2011).

J. HASEGAWA and K. MATSUDA, "Theoretical Study of the Excited States and the Redox Potentials of Unusually Distorted β-Trifluoromethylporphycene," *Theor. Chem. Acc.* **130**, 175–185 (2011).

T. KAWATSU, K. MATSUDA and J. HASEGAWA, "Singlet Excitation Energy Transfer Mediated by Local Exciton Bridge," *J. Phys. Chem. C* **116**, 13865–13876 (2012).

T. MORISHITA, S. G. ITOH, H. OKUMURA and M. MIKAMI, "Free-Energy Calculation via Mean-Force Dynamics Using a Logarithmic Energy Landscape," *Phys. Rev. E* **85**, 066702 (5 pages) (2012).
T. MORISHITA, "Compressed Exponential Relaxation in Liquid Silicon: Universal Feature of the Crossover from Ballistic to Diffusive Behavior in Single-particle Dynamics," *J. Chem. Phys.* **137**, 024510 (6 pages) (2012).

Photo-Molecular Science

Y. HARADA, K. IMURA, H. OKAMOTO, Y. NISHIJIMA, K. UENO and H. MISAWA, "Plasmon-Induced Local Photocurrent Changes in GaAs Photovoltaic Cells Modified with Gold Nanospheres: A Near-Field Imaging Study," *J. Appl. Phys.* **110**, 104306 (7 pages) (2011).
H. J. WU, Y. NISHIYAMA, T. NARUSHIMA, K. IMURA and H. OKAMOTO, "Sub-20-fs Time-Resolved Measurements in an Apertured Near-Field Optical Microscope Combined with a Pulse-Shaping Technique," *Appl. Phys. Express* **5**, 062002 (3 pages) (2012).

A. MIZOGUCHI, Y. OHSHIMA and Y. ENDO, "The Study for the Incipient Solvation Process of NaCl in Water: The Observation of the NaCl–$(H_2O)_n$ (n = 1, 2, and 3) Complexes by Using Fourier-Transform Microwave Spectroscopy," *J. Chem. Phys.* **135**, 064307 (11 pages) (2011).
M. TSUBOUCHI, M. NAGAI and Y. OHSHIMA, "Terahertz Tomography of Photo-Induced Carrier Based on Pump-Probe Spectroscopy Using Counter-Propagation Geometry," *Opt. Lett.* **37**, 3528–3530 (2012).

H. S. KATO, H. YAMANE, N. KOSUGI and M. KAWAI, "Characterization of an Organic Field-Effect Thin-Film Transistor in Operation Using Fluorescence-Yield X-Ray Absorption Spectroscopy," *Phys. Rev. Lett.* **107**, 147401 (5 pages) (2011).
C. MIRON, C. NICOLAS, O. TRAVNIKOVA, P. MORIN, Y.-P. SUN, F. GEL'MUKHANOV, N. KOSUGI and V. KIMBERG, "Imaging Molecular Potentials Using Ultrahigh-Resolution Resonant Photoemission," *Nat. Phys.* **8**, 135–138 (2012).
R. FLESCH, E. SERDAROGLU, F. BLOBNER, P. FEULNER, X. O. BRYKALOVA, A. A. PAVLYCHEV, N. KOSUGI and E. RÜHL, "Gas-to-Solid Shift of C 1s-Excited Benzene," *Phys. Chem. Chem. Phys.* **14**, 9397–9402 (2012).
V. KIMBERG, T. GEJO, M. OURA, T. TOKUSHIMA, Y. HORIKAWA, H. ARAI, S. SHIN and N. KOSUGI, "Rydberg-Valence Mixing and Interchannel Coupling in Resonant Oxygen 1s Inelastic X-Ray Scattering of O_2," *Phys. Rev. A* **85**, 032503 (5 pages) (2012).
M. NAGASAKA, N. KOSUGI and E. RÜHL, "Structures of Small Mixed Krypton-Xenon Clusters," *J. Chem. Phys.* **136**, 234312 (7 pages) (2012).
T. MARUYAMA, S. SAKAKIBARA, S. NARITSUKA, W. NORIMATSU, M. KUSUNOKI, H. YAMANE and N. KOSUGI, "Band Alignment of a Carbon Nanotube/N-Type 6H-SiC Heterojunction Formed by Surface Decomposition of SiC Using Photoelectron Spectroscopy," *Appl. Phys. Lett.* **101**, 092106 (4 pages) (2012).
J. W. CHIOU, S. C. RAY, S. I. PENG, C. H. CHUANG, B. Y. WANG, H. M. TSAI, C. W. PAO, H.-J. LN, Y. C. SHAO, Y. F. WANG, S. C. CHEN, W. F. PONG, Y. C. YEH, C. W. CHEN, L.-C. CHEN, K.-H. CHEN, M.-H. TSAI, A. KUMAR, A. GANGULY, P. PAPAKONSTANTINOU, H. YAMANE, N. KOSUGI, T. REIGIER, L. LIU and T. K. SHAM, "Nitrogen-Functionalized Graphene Nanoflakes (GNFs:N): Tunable Photoluminescence and Electronic Structures," *J. Phys. Chem. C* **116**, 16251–16258 (2012).

H. KATAYANAGI and K. MITSUKE, "Mass-Analyzed Velocity Map Imaging of Doubly Charged Photofragments from C_{70}," *J. Chem. Phys.* **135**, 144307 (8 pages) (2011).
K. MITSUKE, H. KATAYANAGI, B. P. KAFLE and MD. S. I. PRODHAN, "Design of Velocity Map Imaging Spectrometer Equipped with a Mass Gate Discriminating Particular Photofragments," *ISRN Phys. Chem.* **2012**, 959074 (9 pages) (2012).

Y. TAIRA, M. ADACHI, H. ZEN, T. TANIKAWA, M. HOSAKA, Y. TAKASHIMA, N. YAMAMOTO, K. SODA and M. KATOH, "Feasibility Study of Ultra-Short Gamma-Ray Pulse Generation by Laser-Compton Scattering in an Electron Storage Ring," *Nucl. Instrum. Methods Phys. Res., Sect. A* **637**, 5116–5119 (2011).
N. YAMAMOTO, M. SHIMADA, M. ADACHI, H. ZEN, T. TANIKAWA, Y. TAIRA, S. KIMURA, M. HOSAKA, Y. TAKASHIMA, T. TAKAHASHI and M. KATOH, "Ultra-Short Coherent Terahertz Radiation from Ultra-Short Dips in Electron Bunches Circulating in a Storage Ring," *Nucl. Instrum. Methods Phys. Res., Sect. A* **637**, 5112–5115 (2011).
Y. TAIRA, M. ADACHI, H. ZEN, T. TANIKAWA, N. YAMAMOTO, M. HOSAKA, Y. TAKASHIMA, K. SODA and M. KATOH, "Generation of Energy-Tunable and Ultrashort-Pulse Gamma Ray via Inverse Compton Scattering in an Electron Storage Ring," *Nucl. Instrum. Methods Phys. Res., Sect. A* **652**, 696–700 (2011).
I. KATAYAMA, H. SHIMOSATO, M. BITO, K. FURUSAWA, M. ADACHI, M. SHIMADA, H. ZEN, S. KIMURA, N. YAMAMOTO, M. HOSAKA, M. KATOH and M. ASHIDA, "Electric Field Detection of Coherent Synchrotron Radiation in a Storage Ring Generated Using Laser Bunch Slicing," *Appl. Phys. Lett.* **100**, 111112 (4 pages) (2012).

H. MIYAZAKI, T. HAJIRI, T. ITO, S. KUNII and S. KIMURA, "Momentum-Dependent Hybridization Gap and Dispersive In-Gap State of the Kondo Semiconductor SmB_6," *Phys. Rev. B* **86**, 075105 (4 pages) (2012).
Y. S. KWON, J. B. HONG, Y. R. JANG, H. J. OH, Y. Y. SONG, B. H. MIN, T. IIZUKA, S. KIMURA, A. V. BALATSKY and Y. BANG, "Evidence of a Pseudogap for Superconducting Iron-Pnictide $Ba_{0.6+\delta}K_{0.4-\delta}Fe_2As_2$ Single Crystals from Optical Conductivity Measurements," *New J. Phys.* **14**, 063009 (11 pages) (2012).
S. KIMURA, E. NAKAMURA, K. IMURA, M. HOSAKA, T. TAKAHASHI and M. KATOH, "Design of a Dedicated Beamline for THz Coherent Synchrotron Radiation at UVSOR-III," *J. Phys: Conf. Series* **359**, 012009 (5 pages) (2012).
T. TAKAHASHI, T. IIZUKA, T. MORI and S. KIMURA, "Development of a Scanning Near-Field Sub-THz-Wave Microscopy with Coherent Transition Radiation," *J. Phys: Conf. Series* **359**, 012016 (6 pages) (2012).

J. ONOE, T. ITO, H. SHIMA, H. YOSHIOKA and S. KIMURA, "Observation of Riemannian Geometric Effects on Electronic States," *Europhys. Lett.* **98**, 27001 (5 pages) (2012).

T. IIZUKA, T. MIZUNO, B. H. MIN, Y. S. KWON and S. KIMURA, "Existence of Heavy Fermions in the Antiferromagnetic Phase of $CeIn_3$," *J. Phys. Soc. Jpn.* **81**, 043703 (4 pages) (2012).

T. HAJIRI, T. ITO, R. NIWA, M. MATSUNAMI, B. H. MIN, Y. S. KWON and S. KIMURA, "Three-Dimensional Electronic Structure and Interband Nesting in the Stoichiometric Superconductor LiFeAs," *Phys. Rev. B* **85**, 094509 (6 pages) (2012).

T. INUSHIMA, D. K. MAUDE, H. LU, W. J. SCHAFF, T. IIZUKA, S. KIMURA, A. YAMAMOTO and K. FUKUI, "Superconducting Properties of InN with Low Carrier Density near the Mott Transition," *J. Phys. Soc. Jpn.* **81**, 044704 (9 pages) (2012).

I. KATAYAMA, H. SHIMOSATO, M. BITO, K. FURUSAWA, M. ADACHI, M. SHIMADA, H. ZEN, S. KIMURA, N. YAMAMOTO, M. HOSAKA, M. KATOH and M. ASHIDA, "Electric Field Detection of Coherent Synchrotron Radiation in a Storage Ring Generated Using Laser Bunch Slicing," *Appl. Phys. Lett.* **100**, 111112 (4 pages) (2012).

J. ONOE, T. ITO, S. KIMURA, H. SHIMA, Y. TODA and H. YOSHIOKA, "One-Dimensional Uneven Peanut-Shaped C_{60} Polymer: A Quantum Electronic System in Riemannian Space," *Fullerene, Nanotubes, Carbon Nanostruct.* **20**, 1–16 (2012).

W. JUNG, Y. KIM, B. KIM, Y. KOH, C. KIM, M. MATSUNAMI, S. KIMURA, M. ARITA, K. SHIMADA, J. H. HAN, J. KIM, B. CHO and C. KIM, "Warping Effects in the Band and Angular-Momentum Structures of the Topological Insulator Bi_2Te_3," *Phys. Rev. B* **84**, 245435 (6 pages) (2011).

F. NAKAMURA, Y. KOUSA, A. A. TASKIN, Y. TAKEICHI, A. NISHIDE, A. KAKIZAKI, M. D'ANGELO, P. LEFEVRE, F. BERTRAN, A. TALEB-IBRAHIMI, F. KOMORI, S. KIMURA, H. KONDO, Y. ANDO and I. MATSUDA, "Topological Transition in $Bi_{1-x}Sb_x$ Studied as a Function of Sb-Doping," *Phys. Rev. B* **84**, 235308 (8 pages) (2011).

S. KIMURA, T. IIZUKA, H. MIYAZAKI, T. HAJIRI, M. MATSUNAMI, T. MORI, A. IRIZAWA, Y. MURO, J. KAJINO and T. TAKABATAKE, "Optical Study of Charge Instability in $CeRu_2Al_{10}$ in Comparison with $CeOs_2Al_{10}$ and $CeFe_2Al_{10}$," *Phys. Rev. B* **84**, 165125 (7 pages) (2011).

T. HIRAHARA, G. BIHLMAYER, Y. SAKAMOTO, M. YAMADA, H. MIYAZAKI, S. KIMURA, S. BLUGEL and S. HASEGAWA, "Interfacing 2D and 3D Topological Insulators: Bi(111) Bilayer on Bi_2Te_3," *Phys. Rev. Lett.* **107**, 166801 (5 pages) (2011).

S. TANAKA, M. MATSUNAMI and S. KIMURA, "Observation of Anomalous Peaks in the Photoelectron Spectra of Highly Oriented Pyrolytic Graphite: Folding of the Band due to the Surface Charge Density Wave Transition," *Phys. Rev. B* **84**, 121411(R) (5 pages) (2011).

Y. HIKOSAKA, P. LABLANQUIE, F. PENENT, J. PALAUDOUX, L. ANDRIC, K. SOEJIMA, E. SHIGEMASA, I. H. SUZUKI, M. NAKANO and K. ITO, "Energy Correlation among Three Photoelectrons Emitted in Core-Valence-Valence Triple Photoionization of Ne," *Phys. Rev. Lett.* **107**, 113005 (5 pages) (2011).

P. LABLANQUIE, S-M. HUTTULA, M. HUTTULA, L. ANDRIC, J. PALAUDOUX, J. H. D. ELAND, Y. HIKOSAKA, E. SHIGEMASA, K. ITO and F. PENENT, "Multi-Electron Spectroscopy: Auger Decays of the Argon 2s Hole," *Phys. Chem. Chem. Phys.* **13**, 18355–18364 (2011).

P. LABLANQUIE, T. P. GROZDANOV, M. ŽITNIK, S. CARNIATO, P. SELLES, L. ANDRIC, J. PALAUDOUX, F. PENENT, H. IWAYAMA, E. SHIGEMASA, Y. HIKOSAKA, K. SOEJIMA, M. NAKANO, I. H. SUZUKI and K. ITO, "Evidence of Single-Photon Two-Site Core Double Ionization of C_2H_2 Molecules," *Phys. Rev. Lett.* **107**, 193004 (5 pages) (2011).

M. NAGASONO, J. R. HARRIES, H. IWAYAMA, T. TOGASHI, K. TONO, M. YABASHI, Y. SENBA, H. OHASHI, T. ISHIKAWA and E. SHIGEMASA, "Observation of Free-Electron-Laser-Induced Collective Spontaneous Emission (Super-Fluorescence)," *Phys. Rev. Lett.* **107**, 193603 (4 pages) (2011).

A. HISHIKAWA, M. FUSHITANI, Y. HIKOSAKA, A. MATSUDA, C.-N. LIU, T. MORISHITA, E. SHIGEMASA, M. NAGASONO, K. TONO, T. TOGASHI, H. OHASHI, H. KIMURA, Y. SENBA, M. YABASHI and T. ISHIKAWA, "Enhanced Nonlinear Double Excitation of He in Intense Extreme Ultraviolet Laser Fields," *Phys. Rev. Lett.* **107**, 243003 (5 pages) (2011).

R. MOSHAMMER, TH. PFEIFER, A. RUDENKO, Y.-M. JIANG, L. FOUCAR, M. KURKA, K. U. KÜHNEL, C. D. SCHRÖTER, J. ULLRICH, O. HERRWERTH, M. F. KLING, X.-J. LIU, K. MOTOMURA, H. FUKUZAWA, A. YAMADA, K. UEDA, K. L. ISHIKAWA, K. NAGAYA, H. IWAYAMA, A. SUGISHIMA, Y. MIZOGUCHI, S. YASE, M. YAO, N. SAITO, A. BELKACEM, M. NAGASONO, A. HIGASHIYA, M. YABASHI, T. ISHIKAWA, H. OHASHI, H. KIMURA and T. TOGASHI, "Second-Order Autocorrelation of XUV FEL Pulses via Time Resolved Two-Photon Single Ionization of He," *Opt. Express* **19**, 21698 (9 pages) (2011).

E. SHIGEMASA and N. KOSUGI, "Molecular Inner-Shell Spectroscopy: ARPIS Technique and its Applications," A*dv. Chem. Phys*. **147**, 75–126 (2012).

T. GEJO, T. TAMURA, K. HONMA, E. SHIGEMASA, Y. HIKOSAKA and Y. TAMENORI, "Angle-Resolved Metastable Fragment Yields Spectra of N_2 and CO in K-Edge Excitation Energy Region," *J. Chem. Phys.* **136**, 054201 (7 pages) (2012).

R. BHANDARI and T. TAIRA, "> 6 MW Peak Power at 532 nm from Passively Q-Switched Nd:YAG/Cr^{4+}:YAG Microchip Laser," *Opt. Express* **19**, 19135–19141 (2011).

R. BHANDARI and T. TAIRA, "Megawatt Level UV Output from [110] Cr^{4+}:YAG Passively Q-Switched Microchip Laser," *Opt. Express* **19**, 22510–22514 (2011).

W. KONG and T. TAIRA, "Lens-Less Edge-Pumped High Power Microchip Laser," *Appl. Phys. Lett.* **100**, 141105 (4 pages) (2012).

R. BHANDARI, T. TAIRA, A. MIYAMOTO, Y. FURUKAWA and T. TAGO, "> 3 MW Peak Power at 266 nm Using Nd:YAG/ Cr^{4+}:YAG Microchip Laser and Fluxless-BBO," *Opt. Mater. Express* **2**, 907–913 (2012).

W. KONG, A. SUGITA and T. TAIRA, "Generation of Hermite-Gaussian Modes and Vortex Arrays Based on 2D Gain-Distribution Controlled Microchip Laser," *Opt. Lett.* **37**, 2661–2663 (2012).

T. FUJI, Y.-I. SUZUKI, T. HORIO and T. SUZUKI, "Excited-State Dynamics of CS_2 Studied by Photoelectron Imaging with a Time Resolution of 22 fs," *Chem. –Asian J.* **6**, 3028–3034 (2011).
N. KUSE, A. OZAWA, Y. NOMURA, I. ITO and Y. KOBAYASHI, "Injection Locking of Yb-Fiber Based Optical Frequency Comb," *Opt. Express* **20**, 10509–10518 (2012).
N. ISHII, S. ADACHI, Y. NOMURA, A. KOSUGE, Y. KOBAYASHI, T. KANAI, J. ITATANI and S. WATANABE, "Generation of Soft X-Ray and Water Window Harmonics Using a Few-Cycle, Phase-Locked, Optical Parametric Chirped-Pulse Amplifier," *Opt. Lett.* **37**, 97–99 (2012).

A. ITO, T. INOUE, K. TAKEHARA, N. SHIMIZU, Y. KITAJIMA and K. SHINOHARA, "Application of XANES Profiles to X-Ray Spectromicroscopy for Biomedical Specimens: Part I. Discrimination of Macromolecules with Sulfur Atoms," *J. X-Ray Sci. Technol.* **19**, 249–260 (2011).
T. INOUE, K. TAKEHARA, N. SHIMIZU, Y. KITAJIMA, K. SHINOHARA and A. ITO, "Application of XANES Profiles to X-Ray Spectromicroscopy for Biomedical Specimens: Part II. Mapping Oxidation State of Cysteine in Human Hair," *J. X-Ray Sci. Technol.* **19**, 313–320 (2011).

Materials Molecular Science

N. ISHIGURO, T. SAIDA, T. URUGA, O. SEKIZAWA, S. NAGAMATSU, K. NITTA, T. YAMAMOTO, S. OHKOSHI, Y. IWASAWA, T. YOKOYAMA and M. TADA, "Operando Time-Resolved X-Ray Absorption Fine Structure Study for Surface Events on a Pt_3Co/C Cathode Catalyst in a Polymer Electrolyte Fuel Cell during Voltage-Operating Processes," *ACS Catal.* **2**, 1319–1330 (2012).
K. EGUCHI, Y. TAKAGI, T. NAKAGAWA and T. YOKOYAMA, "Growth Process and Magnetic Properties of Iron Nanoparticles Deposited on Si_3N_4/Si(111)-(8×8)," *Phys. Rev. B* **85**, 174415 (8 pages) (2012).
H. WANG, S. HAMANAKA, Y. NISHIMOTO, S. IRLE, T. YOKOYAMA, H. YOSHIKAWA and K. AWAGA, "In Operando XAFS Studies of Polyoxometalate Molecular Cluter Batteries: Polyoxometalates as Electron Sponges," *J. Am. Chem. Soc.* **134**, 4918–4924 (2012).
K. HILD, G. SCHÖNHENSE, H. J. ELMERS, T. NAKAGAWA, T. YOKOYAMA, K. TARAFDER and P. M. OPPENEER, "Dominance of the First Excitation Step for Magnetic Circular Dichroism in Near-Threshold Two-Photon Photoemission," *Phys. Rev. B* **85**, 014426 (10 pages) (2012).
H. WANG, S. HAMANAKA, T. YOKOYAMA, H. YOSHIKAWA and K. AWAGA, "In-Situ XAFS Studies of Mn12 Molecular-Cluster Batteries: Super-Reduced Mn12 Clusters in Solid-State Electrochemistry," *Chem. –Asian J.* **6**, 1074–1079 (2011).

Y. UEMURA, Y. INADA, K. K. BANDO, T. SASAKI, N. KAMIUCHI, K. EGUCHI, A. YAGISHITA, M. NOMURA, M. TADA and Y. IWASAWA, "*In Situ* Time-Resolved XAFS Study on the Structural Transformation and Phase Separation of Pt_3Sn and PtSn Alloy Nanoparticles on Carbon in the Oxidation Process," *Phys. Chem. Chem. Phys.* **13**, 15833–15844 (2011).
S. MURATSUGU, K. SODEYAMA, F. KITAMURA, S. TSUKADA, M. TADA, S. TSUNEYUKI and H. NISHIHARA, "Normal and Inverted Redox Potentials and Structural Changes Tuned by Medium Effects in $M_2Mo(\eta^5\text{-}C_5Me_5)_2(S_2C_6H_4)_2(CO)_2]$ (M: Co, Rh)," *Chem. Sci.* **2**, 1960–1968 (2011).
Y. YANG, Z. WENG, S. MURATSUGU, N. ISHIGURO, S. OHKOSHI and M. TADA, "Preparation and Catalytic Performances of a Molecularly Imprinted Ru-Complex Catalyst with an NH_2 Binding Site on a SiO_2 Surface," *Chem. –Eur. J.* **18**, 1142–1153 (2012).
N. MAITY, C. WATTANAKIT, S. MURATSUGU, N. ISHIGURO, Y. YANG, S. OHKOSHI and M. TADA, "Sulfoxidation on a SiO_2-Supported Ru Complex Using O_2/Aldehyde System," *Dalton Trans.* **41**, 4558–4565 (2012).
N. ISHIGURO, T. SAIDA, T. URUGA, O. SEKIZAWA, S. NAGAMATSU, K. NITTA, T. YAMAMOTO, S. OHKOSHI, Y. IWASAWA, T. YOKOYAMA and M. TADA, "Operando Time-Resolved X-Ray Absorption Fine Structure Study for Surface Events on a Pt_3Co/C Cathode Catalyst in a Polymer Electrolyte Fuel Cell during Voltage-Operating Processes," *ACS Catal.* **2**, 1319–1330 (2012).

F. IWASE, K. SUGIURA, K. FURUKAWA and T. NAKAMURA, "^{13}C NMR Study of the Magnetic Properties of the Quasi-One-Dimensional Conductor $(TMTTF)_2SbF_6$," *Phys. Rev. B* **84**, 115140 (7 pages) (2011).
A. FUNABIKI, H. SUGIYAMA, T. MOCHIDA, K. ICHIMURA, T. OKUBO, K. FURUKAWA and T. NAKAMURA, "Physical Properties of a Molecular Conductor $(BEDT\text{-}TTF)_2I_3$ Nanohybridized with Silica Nanoparticles by Dry Grinding," *RSC Adv.* **2**, 1055–1060 (2012).
M. KANO, H. MORI, K. MATSUBAYASHI, M. ITOI, M. HEDO, T. P. MURPHY, S. W. TOZER, Y. UWATOKO and T. NAKAMURA, "Anisotropy of Upper Critical Field in a One-Dimensional Organic System, $(TMTTF)_2PF_6$ under High Pressure," *J. Phys. Soc. Jpn.* **81**, 024716 (7 pages) (2012).

X. DING, X. FENG, A. SAEKI, S. SEKI, A. NAGAI and D. JIANG, "Conducting Metallophthalocyanine 2D Covalent Organic Frameworks: The Role of Central Metals in Controlling π-Electronic Functions," *Chem. Commun.* **48**, 8952–8954 (2012).
X. FENG, X. DING and D. JIANG, "Covalent Organic Frameworks," *Chem. Soc. Rev.* 2012, DOI:10.1032/C2CS35157A (Tutorial Review).
X. LIU, Y. XU and D. JIANG, "Conjugated Microporous Polymers as Molecular Sensing Devices: Microporous Architecture Enables Rapid Response and Enhances Sensitivity in Fluorescence-On and Fluorescence-Off Sensing," *J. Am. Chem. Soc.* **134**, 8738–8742 (2012).
X. FENG, L. CHEN, Y. HONSHO, O. SAENGSAWANG, L. LIU, L. WANG, A. SAEKI, S. IRLE, S. SEKI, Y. DONG and D. JIANG, "An Ambipolar Covalent Organic Framework with Self-Sorted and Periodic Electron Donor-Acceptor Ordering," *Adv. Mater.* **24**, 3026–3031 (2012).
X. FENG, L. LIU, Y. HONSHO, A. SAEKI, S. SEKI, S. IRLE, Y. DONG, A. NAGAI and D. JIANG, "High-Rate Charge Carrier Transport in Porphyrin Covalent Organic Frameworks: Switching from Hole to Electron, and to Ambipolar," *Angew. Chem., Int. Ed.* **51**, 2618–2622 (2012).
A. NAGAI, Z. GUO, X. FENG, S. JIN, X. CHEN, X. DING and D. JIANG, "Pore Surface Engineering in Covalent Organic Frameworks," *Nat. Commun.* 2:536 doi: 10.1038/ncomms1542 (2011).

Y. XU, L. CHEN, Z. GUO, A. NAGAI and D. JIANG, "Light-Emitting Conjugated Polymers with Microporous Network Architecture: Interweaving Scaffold Promotes Electronic Conjugation, Facilitates Exciton Migration, and Improves Luminescence," *J. Am. Chem. Soc*. **133**, 17622–17625 (2011).
X. DING, L. CHEN, Y. HONSHO, X. FENG, O. SAENGSAWANG, J. GUO, A. SAEKI, S. SEKI, S. IRLE, S. NAGASE, P. VUDHICHAI and D. JIANG, "An n-Channel Two-Dimensional Covalent Organic Framework," *J. Am. Chem. Soc*. **133**, 14510–14513 (2011).

T. IIJIMA and K. NISHIMURA, "^{2}H Quadrupolar Carr-Purcell-Meiboom-Gill NMR for Paramagnetic Solids," *Chem. Phys. Lett.* **514**, 181–186 (2011).

M. KUBO, T. KAJI and M. HIRAMOTO, "*pn*-Homojunction Formation in Single Fullerene Films," *AIP Adv.* **1**, 032177 (5 pages) (2011).
N. ISHIYAMA, M. KUBO, T. KAJI and M. HIRAMOTO, "Doping-Based Control of the Energetic Structure of Photovoltaic Co-Deposited Films," *Appl. Phys. Lett.* **99**, 133301 (3 pages) (2011).
Y. SHINMURA, M. KUBO, N. ISHIYAMA, T. KAJI and M. HIRAMOTO, "*pn*-Control and *pn*-Homojunction Formation of Metal-Free Phthalocyanine by Doping," *AIP Adv.* **2**, 032145 (6 pages) (2012).

E. KAYAHARA, Y. SAKAMOTO, T. SUZUKI and S. YAMAGO, "Selective Synthesis and Crystal Structure of [10]Cycloparaphenylene," *Org. Lett.* **14**, 3284–3287 (2012).

H. KON and T. NAGATA, "Syntheses, Properties and Photoreactions of the Hybrid Molecules Consisting of a Co^{II} Mononuclear Complexes and Porphyrins," *Chem. –Eur. J.* **18**, 1781–1788 (2012).
Y. MIYAKE, T. NAGATA, H. TANAKA, M. YAMAZAKI, M. OHTA, R. KOKAWA and T. OGAWA, "Entropy-Controlled 2D Supramolecular Structures of *N*,*N*'-Bis(*N*-alkyl)-naphthalenediimides on a HOPG Surface," *ACS Nano* **6**, 3876–3887 (2012).
M. NAKAMURA, H. TAHARA, K. TAKAHASHI, T. NAGATA, H. UOYAMA, D. KUZUHARA, S. MORI, T. OKUJIMA, H. YAMADA and H. UNO, "π-Fused Bis-BODIPY as a Candidate for NIR Dyes," *Org. Biomol. Chem.* **10**, 6840–6849 (2012).

K. MAEYAMA, T. TSUKAMOTO, M. SUZUKI, S. HIGASHIBAYASHI and H. SAKURAI, "Synthesis of Aromatic Polyketones Bearing 1,1'-Binaphthyl-2,2'-dioxy Units through Suzuki-Miyaura Coupling Polymerization," *Chem. Lett.* **40**, 1445–1446 (2011).
R. N. DHITAL, A. MURUGADOSS and H. SAKURAI, "Dual Roles of Polyhydroxy Matrices for Homocoupling of Arylboronic Acid Catalysed by Gold Nanoclusters Under Acidic Conditions," *Chem. –Asian J.* **7**, 55–59 (2012).
S. HIGASHIBAYASHI, R. B. NASIR BAIG, Y. MORITA and H. SAKURAI, "Selective Synthesis of C_3 Symmetric Functionalized Sumanenes," *Chem. Lett.* **41**, 84–86 (2012).
R. SHOMURA, S. HIGASHIBAYASHI, H. SAKURAI, Y. MATSUSHITA, A. SATO and M. HIGUCHI, "Chiral Phenylazomethine Cage," *Tetrahedron Lett.* **53**, 783–785 (2012).
A. MURUGADOSS, N. KAI and H. SAKURAI, "Synthesis of Bimetallic Gold-Silver Alloy Nanoclusters by Simple Mortar Grinding," *Nanoscale* **4**, 1280–1282 (2012).
D. VIJAY, H. SAKURAI, V. SUBRAMANIAN and G. N. SASTRY, "Where to Bind in Buckybowls? The Dilemma of a Metal Ion," *Phys. Chem. Chem. Phys.* **14**, 3057–3065 (2012).
K. BOBUATONG, S. KARANJIT, R. FUKUDA, M. EHARA and H. SAKURAI, "Aerobic Oxidation of Methanol to Formic Acid on Au_{20}^{-}: A Theoretical Study on the Reaction Mechanism," *Phys. Chem. Chem. Phys.* **14**, 3103–3111 (2012).
S. MEBS, M. WEBER, P. LUGER, B. M. SCHMIDT, H. SAKURAI, S. HIGASHIBAYASHI, S. ONOGI and D. LENTZ, "Experimental Electron Density of Sumanene, a Bowl Shaped Fullerene Fragment; Comparison with the Related Corannulene Hydrocarbon," *Org. Biomol. Chem.* **10**, 2218–2222 (2012).
H. KITAHARA and H. SAKURAI, "*Anti*-Addition Mechanism in the Intramolecular Hydroalkoxylation of Alkene Catalyzed by PVP-Stabilized Nanogold," *Molecules* **17**, 2579–2586 (2012).
S. HIGASHIBAYASHI, R. TSURUOKA, Y. SOUJANYA, U. PURUSHOTHAM, G. N. SASTRY, S. SEKI, T. ISHIKAWA, S. TOYOTA and H. SAKURAI, "Trimethylsumanene: Enantioselective Synthesis, Substituent Effect on Bowl Structure, Inversion Energy, and Electron Conductivity," *Bull. Chem. Soc. Jpn.* **85**, 450–467 (2012).
J.-J. CHEN, S. ONOGI, Y.-C. HSIEH, C.-C. HSIAO, S. HIGASHIBAYASHI, H. SAKURAI and Y.-T. WU, "Palladium-Catalyzed Arylation of Methylene-Bridged Polyarenes: Synthesis and Structures of 9-Arylfluorene Derivatives," *Adv. Synth. Catal.* **354**, 1551–1558 (2012).
R. N. DHITAL and H. SAKURAI, "Anomalous Efficacy of Bimetallic Au/Pd Nanoclusters in C–Cl Bond Activation and Formal Metathesis-Type C–B Bond Activation at Room Temperature," *Chem. Lett.* **41**, 630–632 (2012).
Q.-T. TAN, S. HIGASHIBAYASHI, S. KARANJIT and H. SAKURAI, "Enantioselective Synthesis of a Chiral Nitrogen-Doped Buckybowl," *Nat. Commun.* 3:891 doi: 10.1038/ncomms1896 (2012).
S. ONOGI, S. HIGASHIBAYASHI and H. SAKURAI, "Microwave-Assisted Synthesis of Methyl (1*S*,2*R*,4*S*,5*R*)-7-Aza-5- hydroxybicyclo[2.2.1]heptan-2-carboxylate through Unexpected Stereoselective Substitution Reaction," *Tetrahedron Lett.* **53**, 3710–3712 (2012).
Y. MORITA, S. NAKAO, S. HAESUWANNAKIJ, S. HIGASHIBAYASHI and H. SAKURAI, "Emission Amplification by Sumanene Nanocrystals in an *Onigiri*-Type Organic–Organic Assembly," *Chem. Commun.* **48**, 9050–9052 (2012).

K. YAMAMOTO, A. A. KOWALSKA and K. YAKUSHI, "Second-Harmonic Generation Microscopy of Ferroelectric Organic Conductor Using Hydrostatic Pressure Apparatus with Ar as a Heat Sink," *Phys. Status Solidi C* **9**, 1189–1192 (2012).
K. YAMAMOTO, A. A. KOWALSKA, Y. YUE and K. YAKUSHI, "*E-mv* Coupling of Vibrational Overtone in Organic Conductors: Relationship to Optical Nonlinearities and Ferroelectricity," *Phys. B* **407**, 1775–1778 (2012).

S. C. LEE, A. UEDA, H. KAMO, K. TAKAHASHI, M. URUICHI, K. YAMAMOTO, K. YAKUSHI, A. NAKAO, R. KUMAI, R. KOBAYASHI, H. NAKAO, Y. MURAKAMI and H. MORI, "Charge-Order Driven Proton Arrangement in a Hydrogen-Bonded Charge-Transfer Complex Based on a Pyridyl-Substituted TTF Derivative," *Chem. Commun.* **48**, 8673–8675 (2012).
K. KODAMA, M. KIMATA, T. YAMAKUCHI, N. KURITA, A. HARADA, H. SATSUKAWA, T. TERASHIMA, S. UJI and K. YAMAMOTO, K. YAKUSHI, "Charge Transport in Charge-Ordered States of Two-Dimensional Organic Conductors, α-(BEDT-TTF)$_2$I$_3$ and α'-(BEDT-TTF)$_2$IBr$_2$," *J. Phys. Soc. Jpn.* **81**, 044703 (7 pages) (2012).
R. B. MORGUNOV, A. I. DMITRIEV, A. S. CHERNEN'KAYA, K. YAKUSHI, K. YAMAMOTO and Y. TANIMOTO, "Spin Dynamics of Charge Carriers in the Process of Their Localization in α'-(BEDT-TTF)$_2$IBr$_2$ Single Crystals," *J. Exp. Theor. Phys.* **111**, 857–864 (2011).

SK. LEE, R. YAMADA, S. TANAKA, GS. CHANG, Y. ASAI and H. TADA, "Universal Temperature Crossover Behavior of Electrical Conductance in a Single Oligothiophene Molecular Wire," A*CS Nano* **6**, 5078–5082 (2012).

M. TOMURA and Y. YAMASHITA, "Bis(tetra-*n*-butylammonium) Bis(5,6-dicyanopyrazine-2,3-dithiolato-κ^2*S*,*S*')palladium(II)," *Acta Crystallogr., Sect. E: Struct. Rep. Online* **68**, m57–m57 (2012).

Y. YAMADA, M. OKAMOTO, K. FURUKAWA, T. KATO and K. TANAKA, "Switchable Inetrmolecular Communication in a Four-Fold Rotaxane," *Angew. Chem., Int. Ed.* **51**, 709–713 (2012).
D. SAKAMAKI, A. ITO, K. TANAKA, K. FURUKAWA, T. KATO and M. SHIRO, "1,3,5-Benzenetriamine Double- and Triple-Decker Molecules," *Angew. Chem., Int. Ed.* **51**, 8281–8285 (2012).
T. WAKAHARA, T. KATO, K. MIYAZAWA and W. HARNEIT, "N@C$_{60}$ as a Structural Probe for Fullerene Nanomaterials," *Carbon* **50**, 1699–1712 (2012).

Y. NISHIYAMA, Y. ENDO, T. NEMOTO, H. UTSUMI, K. YAMAUCHI, K. HIOKA and T. ASAKURA, "Very Fast Magic Angle Spinning ^{1}H-^{14}N 2D Solid-State NMR: Sub-Micro-Liter Sample Data Collection in a Few Minutes," *J. Magn. Reson.* **208**, 44–48 (2011).
T. ASAKURA, H. NISHI, A. NAGANO, A. YOSHIDA, Y. NAKAZAWA, M. KAMIYA and M. DEMURA, "NMR Analysis of the Fibronection Cell-Adhesive Sequence, Arg-Gly-Asp, in a Redombinant Silk-Like Protein and a Model Peptide," *Biomacromolecules* **12**, 3910–3916 (2011).
K. SUGANUMA, K. HORIUCHI, H. MATSUDA, H. N. CHENG, A. AOKI and T. ASAKURA, "Stereoregularity of Poly(lactic acid) and Their Model Compounds as Studied by NMR and Quantum Chemical Calculations," *Macromolecules* **44**, 9247–9253 (2011).
A. NAGANO, H. SATO, Y. TANIOKA, Y. NAKAZAWA, D. KNIGHT and T. ASAKURA, "Characterization of a Ca Binding-Amphipathic Silk-Like Protein and Peptide with the Sequence (Glu)$_8$(Ala-Gly-Ser-Gly-Ala-Gly)$_4$ with Potential for Bone Repair," *Soft Matter* **8**, 741–748 (2012).
K. YAZAWA, E. YAMAGUCHI, D. KNIGHT and T. ASAKURA, "^{13}C Solid State NMR Study of the ^{13}C-Labeled Peptide, (E)$_8$GGLGGQGAG(A)$_6$GGAGQGGYGG as a Model for the Local Structure of *Nephila Clavipes* Dragline Silk (MaSpl) before and after Spinning," *Biopolymers* **97**, 347–354 (2012).
T. ASAKURA, M. OKONOGI, K. HORIGUCHI, A. AOKI, H. SAITO, D. P. KNIGHT and M. P. WILLIAMSON, "Two Different Packing Arrangements of Antiparallel Polyalanine," *Angew. Chem., Int. Ed.* **51**, 1212–1215 (2012).
S. KUROKI, M. KANEKIYO, K. YAZAWA, K. ISOBE and T. ASAKURA, "^{1}H MRI Study of Small-Diameter Silk Vascular Grafts in Water," *Polym. J.* **44**, 868–875 (2012).
K. YAZAWA, E. YAMAGUCHI, A. AOKI, Y. NAKAZAWA, Y. SUZUKI and T. ASAKURA, "A Two Dimensional Spin Diffusion NMR Study on the Local Structure of a Water Soluble Model Peptide for *Nephila Clavipes* Dragline Silk (MaSp1) before and after Spinning," *Polym. J.* **44**, 913–917 (2012).
Y. NAKAZAWA, A. ASANO, C. NAKAZAWA, T. TSUKATANI and T. ASAKURA, "Structural Characterization of the Silk-Polyurethane Composite Material for the Biomaterials Using Solid-State NMR," *Polym. J.* **44**, 802–807 (2012).

Life and Coordination-Complex Molecular Science

Y. YOSHIDA, H. ISHIKAWA, S. AONO and Y. MIZUTANI, "Structural Dynamics of Proximal Heme Pocket in HemAT-Bs Associated with O_2 Dissociation," *Biochim. Biophys. Acta, Proteins Proteomics* **1824**, 866–872 (2012).
S. EL-MASHTOLY, M. KUBO, Y. GU, H. SAWAI, S. NAKASHIMA, T. OGURA, S. AONO and T. KITAGAWA, "Site-Specific Protein Dynamics in Communication Pathway from Sensor to Signaling Domain of Oxygen Sensor Protein, HemAT-Bs: Time-Resolved Ultraviolet Resonance Raman Study," *J. Biol. Chem.* **287**, 19973–19984 (2012).
H. SAWAI, H. SUGIMOTO, Y. SHIRO, H. ISHIKAWA, Y. MIZUTANI and S. AONO, "Structural Basis for Oxygen Sensing and Signal Transduction of the Heme-Based Sensor Protein Aer2 from *Pseudomonas aeruginosa*," *Chem. Commun.* **48**, 6523–6525 (2012).
E. PINAKOULAKI, C. KOUTOUPAKIS, H. SAWAI, A. PAVLOU, Y. KATO, Y. ASANO and S. AONO, "Aldoxime Dehydratase: Probing the Heme Environment Involved in the Synthesis of the Carbon-Nitrogen Triple Bond," *J. Phys. Chem. B* **115**, 13012–13018 (2011).

T. RATHNAYAKA, M. TAWA, T. NAKAMURA, S. SOHYA, K. KUWAJIMA, M. YOHDA and Y. KURODA, "Solubilization and Folding of a Fully Active Recombinant *Gaussia* Luciferase with Native Disulfide Bonds by Using a SEP-Tag," *Biochim. Biophys. Acta, Proteins Proteomics* **1814**, 1775–1778 (2011).

J. CHEN, H. YAGI, P. SORMANNI, M. VENDRUSCOLO, K. MAKABE, T. NAKAMURA, Y. GOTO and K. KUWAJIMA, "Fibrillogenic Propensity of the GroEL Apical Domain: A Janus-Faced Minichaperone," *FEBS Lett.* **586**, 1120–1127 (2012).

K. TOMOYORI, T. NAKAMURA, K. MAKABE, K. MAKI, K. SAEKI and K. KUWAJIMA, "Sequential Four-State Folding/Unfolding of Goat α-Lactalbumin and Its N-Terminal Variants," *Proteins* **80**, 2191–2206 (2012).

S. HANASHIMA, K. KATO and Y. YAMAGUCHI, "^{13}C-NMR Quantification of Proton Exchange at LewisX Hydroxyl Groups in Water," *Chem. Commun.* **47**, 10800–10802 (2011).

M. SUGIYAMA, E. KURIMOTO, H. YAGI, K. MORI, T. FUKUNAGA, M. HIRAI, G. ZACCAI and K. KATO, "Kinetic Asymmetry of Subunit Exchange of Homooligomeric Protein as Revealed by Deuteration-Assisted Small-Angle Neutron Scattering," *Biophys. J.* **101**, 2037–2042 (2011).

T. HIRANO, O. SERVE, M. YAGI-UTSUMI, E. TAKEMOTO, T. HIROMOTO, T. SATOH, T. MIZUSHIMA and K. KATO, "Conformational Dynamics of Wild-Type Lys-48-Linked Diubiquitin in Solution," *J. Biol. Chem.* **286**, 37496–37502 (2011).

T. MIZUSHIMA, H. YAGI, E. TAKEMOTO, M. SHIBATA-KOYAMA, Y. ISODA, S. IIDA, K. MASUDA, M. SATOH and K. KATO, "Structural Basis for Improved Efficacy of Therapeutic Antibodies on Defucosylation of Their Fc Glycans," *Genes Cells* **16**, 1071–1080 (2011).

H. YAGI, E. OHNO, S. KONDO, A. YOSHIDA and K. KATO, "Development and Application of Multidimensional HPLC Mapping Method for *O*-Linked Oligosaccharides," *Biomolecules* **1**, 48–62 (2011).

L. MAURI, R. CASELLATO, M. G. CIAMPA, Y. UEKUSA, K. KATO, K. KAIDA, M. MOTOYAMA, S. KUSUNOKI and S. SONNINO, "Anti-GM1/GD1a Complex Antibodies in GBS Sera Specifically Recognize the Hybrid Dimer GM1-GD1a," *Glycobiology* **22**, 352–360 (2012).

D. FUJITA, K. SUZUKI, S. SATO, M. YAGI-UTSUMI, E. KURIMOTO, Y. YAMAGUCHI, K. KATO and M. FUJITA, "Synthesis of a Bridging Ligand with a Non-Denaturated Protein Pendant: Toward Protein Encapsulation in a Coordination Cage," *Chem. Lett.* **41**, 313–315 (2012).

K. TAKAGI, S. KIM, H. YUKII, M. UENO, R. MORISHITA, Y. ENDO, K. KATO, K. TANAKA, Y. SAEKI and T. MIZUSHIMA, "Structural Basis for Specific Recognition of Rpt1p, an ATPase Subunit of the 26 S Proteasome, by the Proteasome-Dedicated Chaperone Hsm3p," *J. Biol. Chem.* **287**, 12172–12182 (2012).

S. YAMAMOTO, Y. ZHANG, T. YAMAGUCHI, T. KAMEDA and K. KATO, "Lanthanide-Assisted NMR Evaluation of a Dynamic Ensemble of Oligosaccharide Conformations," *Chem. Commun.* **48**, 4752–4754 (2012).

Y. KAMIYA, Y. UEKUSA, A. SUMIYOSHI, H. SASAKAWA, T. HIRAO, T. SUZUKI and K. KATO, "NMR Characterization of the Interaction between the PUB Domain of Peptide:*N*-Glycanase and Ubiquitin-Like Domain of HR23," *FEBS Lett.* **586**, 1141–1146 (2012).

S. KIM, A. NISHIDE, Y. SAEKI, K. TAKAGI, K. TANAKA, K. KATO and T. MIZUSHIMA, "New Crystal Structure of the Proteasome-Dedicated Chaperone Rpn14 at 1.6 Å Resolution," *Acta Crystallogr., Sect. F: Struct. Biol. Cryst. Commun.* **68**, 517–521 (2012).

H. YAGI, K. ISHIMOTO, T. HIROMOTO, H. FUJITA, T. MIZUSHIMA, Y. UEKUSA, M. YAGI-UTSUMI, E. KURIMOTO, M. NODA, S. UCHIYAMA, F. TOKUNAGA, K. IWAI and K. KATO, "A Non-Canonical UBA-UBL Interaction Forms the Linear-Ubiquitin-Chain Assembly Complex," *EMBO Rep.* **13**, 462–468 (2012).

H. YAGI, S. WATANABE, T. SUZUKI, T. TAKAHASHI, Y. SUZUKI and K. KATO, "Comparative Analyses of *N*-Glycosylation Profiles of Influenza A Viruses Grown in Different Host Cells," *Open Glycoscience* **5**, 2–12 (2012).

N. SRIWILAIJAROEN, S. KONDO, H. YAGI, H. HIRAMATSU, S. NAKAKITA, K. YAMADA, H. ITO, J. HIRABAYASHI, H. NARIMATSU, K. KATO and Y. SUZUKI, "Bovine Milk Whey for Preparation of Natural *N*-Glycans: Structural and Quantitative Analysis," *Open Glycoscience* **5**, 41–50 (2012).

Y. ZHANG, S. YAMAMOTO, T. YAMAGUCHI and K. KATO, "Application of Paramagnetic NMR-Validated Molecular Dynamics Simulation to the Analysis of a Conformational Ensemble of a Branched Oligosaccharide," *Molecules* **17**, 6658–6671 (2012).

H. YAGI, T. SAITO, M. YANAGISAWA, R. K. YU and K. KATO, "Lewis X-Carrying *N*-Glycans Regulate the Proliferation of Mouse Embryonic Neural Stem Cells via the Notch Signaling Pathway," *J. Biol. Chem.* **287**, 24356–24364 (2012).

Z. CONG, T. KURAHASHI and H. FUJII, "Oxidation of Chloride Ion and Subsequent Chlorination of Organic Compounds by Oxoiron(IV) Porphyrin π-Cation Radical Complexes," *Angew. Chem., Int. Ed.* **50**, 9935–9939 (2011).

Z. CONG, T. KURAHASHI and H. FUJII, "Formation of Iron(III) *Meso*-Chloro-Isoporphyrin as a Reactive Chlorinating Agent from Oxoiron(IV) Porphyrin π-Cation Radical," *J. Am. Chem. Soc.* **134**, 4469–4472 (2012).

C. WANG, T. KURAHASHI and H. FUJII, "Structure and Reactivity of Iodosylarene Adduct of Manganese(IV) Salen Complex," *Angew. Chem., Int. Ed.* **51**, 7809–7811 (2012).

A. TAKAHASHI, D. YAMAKI, K. IKEMURA, T. KURAHASHI, T. OGURA, M. HADA and H. FUJII, "The Effect of the Axial Ligand on the Reactivity of the Oxoiron(IV) Porphyrin π-Cation Radical Complex: Higher Stabilization of the Product State Relative to the Reactant State," *Inorg. Chem.* **51**, 7296–7305 (2012).

T. SATO, S. NOZAWA, A. TOMITA, M. HOSHINO, S. KOSHIHARA, H. FUJII and S. ADACHI, "Coordination and Electronic Structure of Ruthenium(II)-*tris*-2,2'-Bipyridine in the Triplet Metal-to-Ligand Charge Transfer Excited State Observed by Picosecond Time-Resolved Ru *K*-Edge XAFS," *J. Phys. Chem. C* **116**, 14232–14236 (2012).

J. ZHU, T. KURAHASHI, H. FUJII and G. WU, "Solid-State ^{17}O NMR and Computational Studies of terminal Transition Metal Oxo Compounds," *Chem. Sci.* **3**, 391–397 (2012).

Y. MURAYAMA, A. MUKAIYAMA, K. IMAI, Y. ONOUE, A. TSUNODA, A. NOHARA, T. ISHIDA, Y. MAEDA, T. KONDO and S. AKIYAMA, "Tracking and Visualizing the Circadian Ticking of the Cyanobacterial Clock Protein KaiC in Solution," *EMBO J.* **30**, 68–78 (2011).
S. AKIYAMA and T. HIKIMA, "Octuple Cuvette for Small-Angle X-Ray Solution Scattering," *J. Appl. Crystallogr.* **44**, 1294–1296 (2011).

K. KATAYAMA, Y. FURUTANI, H. IMAI and H. KANDORI, "Protein-Bound Water Molecules in Primate Red- and Green-Sensitive Visual Pigments," *Biochemistry* **51**, 1126–1133 (2012).

Y. HIRAI and Y. UOZUMI, "C–N and C–S Bond Forming Cross Coupling in Water with Amphiphilic Resin-supported Palladium Complexes," *Chem. Lett.* **40**, 934–935 (2011).
H. OHTA, Y. UOZUMI and Y. M. A. YAMADA, "Highly Active Copper-Network Catalyst for the Direct Aldol Reaction," *Chem. –Asian J.* **6**, 2545–2549 (2011).
G. HAMASAKA, T. MUTO and Y. UOZUMI, "A Novel Amphiphilic Pincer Palladium Complex: Design, Preparation and Self-Assembling Behavior," *Dalton Trans.* **40**, 8859–8868 (2011).
H. OHTA, Y. YUYAMA, Y. UOZUMI and Y. M. A. YAMADA, "In-Water Dehydrative Alkylation of Ammonia and Amines with Alcohols by a Polymeric Bimetallic Catalyst," *Org. Lett.* **13**, 3892–3895 (2011).
S. M. SARKAR, Y. UOZUMI and Y. M. A. YAMADA, "A Highly Active and Reusable Self-Assembled Poly(Imidazole/Palladium) Catalyst: Allylic Arylation/ Alkenylation," *Angew. Cham., Int. Ed.* **50**, 9437–9441 (2011).
T. OSAKO, D. PANICHAKUL and Y. UOZUMI, "Enantioselective Cabenoid Insertion into Phenolic O–H Bonds with a Chiral Copper(I) Imidazoindolephosphine Complex," *Org. Lett.* **14**, 194–197 (2011).
Y. M. A. YAMADA, S. M. SARKAR and Y. UOZUMI, "Self-Assembled Poly(imidazole-palladium): Highly Active, Reusable Catalyst at Parts per Milion to Parts per Billion Levels," *J. Am. Chem. Soc.* **134**, 3190–3198 (2012).
Y. M. A. YAMADA, T. WATANABE, A. OHNO and Y. UOZUMI, "Development of Polymeric Palladium-Nanoparticle Membrane-Installed Microflow Devices and Their Application in Hydrodehalogenation," *ChemSusChem* **5**, 293–299 (2012).
K. INAMOTO, C. HASEGAWA, K. HIROYA, Y. KONDO, T. OSAKO, Y. UOZUMI and T. DOI, "Use of Dimethil Carbonate as a Solvent Greatly Enhances the Biaryl Coupling of Aryl Iodides and Organoboron Reagents without Adding Any Transisiton Metal Catalyst," *Chem. Commun.* **48**, 2912–2914 (2012).

T. TERATANI, T. KOIZUMI, T. YAMAMOTO, K. TANAKA and T. KANBARA, "Deprotonation/Protonation of Coordinated Secondary Thioamide Units of Pincer Ruthenium Complexes: Modulation of Voltammetric and Spectroscopic Characterization of the Pincer Complexes," *Dalton Trans.* **40**, 1–8 (2011).
T. WADA, J. T. MUCKERMAN, E. FUJITA and K. TANAKA, "Substituents Dependent Capability of Bis(ruthenium-dioxolene-terpyridine) Complexes toward Water Oxidation," *Dalton Trans.* **40**, 2225–2233 (2011).
S. K. PADHI and K. TANAKA, "Proton-Induced Dynamic Equilibrium between Cyclometalated Ruthenium rNHC (Remote N-Heterocyclic Carbene) Tautomers with an NAD^+/NADH Function," *Inorg. Chem.* **50**, 5321–5323 (2011).
B. COHEN, D. POLYANSKY, P. ACHORD, D. CABELLI, J. MUCKERMAN, K. TANAKA, R. THUMMEL, R. ZONG and E. FUJITA, "Steric Effects for Proton, Hydrogen-Atom, and Hydride Transfer Reactions with Geometric Isomers of NADH-Model Ruthenium Complexes," *Faraday Discuss.* **155**, 129–144 (2012).
T. WADA, H. OHTSU and K. TANAKA, "Catalytic Four-Electron Oxidation of Water via Intramolecular Coupling of the Oxo Ligands of Bis(ruthenium-bipyridine) Complex," *Chem. –Eur. J.* **18**, 2374–2381 (2012).
H. OHTSU and K. TANAKA, "Drastic Difference in the Photo-Driven Hydrogenation Reactions of Ruthenium Complexes Containing NAD Model Ligands," *Chem. Commun.* **48**, 1796–1798 (2012).
S. PADHI, R. FUKUDA, M. EHARA and K. TANAKA, "Comparative Study of C^N and N^C Type Cyclometalated Ruthenium Complexes with an NAD^+/NADH Function," *Inorg. Chem.* **51**, 8091–8102 (2012).
S. PADHI, R. FUKUDA, M. EHARA and K. TANAKA, "Photoisomerization and Proton-Coupled Electron Transfer (PCET) Promoted Water Oxidation by Mononuclear Cyclometalated Ruthnium Catalysts," *Inorg. Chem.* **51**, 5386–5392 (2012).
K. TANAKA, H. ISOBE, S. YAMANAKA and K. YAMAGUCHI, "Similarities of Artificial Photosystems by Ruthenium Oxo Complexes and Native Water Splitting Systems," *Proc. Natl. Acad. Sci. U. S. A.* **109**, 15600–15605 (2012).
H. OHTSU and K. TANAKA, "An Organic Hydride Transfer Reaction of a Ruthenium NAD Model Complex Leading to Carbon Dioxide Reduction," *Angew. Chem., Int. Ed.* **51**, 9792–9795 (2012).

T. MURAHASHI, K. USUI, Y. TACHIBANA, S. KIMURA and S. OGOSHI, "Selective Construction of Pd_2Pt and $PdPt_2$ Triangles in a Sandwich Framework: Carbocyclic Ligands as Scaffolds for a Mixed-Metal System," *Chem. –Eur. J.* **18**, 8886–8890 (2012).

M. KOBAYASHI, S. MASAOKA and K. SAKAI, "Photoinduced Hydrogen Evolution from Water Based on a Z-Scheme Photosynthesis by a Simple Platinum(II) Terpyridine Derivative," *Angew. Chem., Int. Ed.* **51**, 7431–7434 (2012).
M. KOBAYASHI, S. MASAOKA and K. SAKAI, "Synthesis, Crystal Structure, Spectroscopic and Electrochemical Properties, and H_2-Evolving Activity of a New $[PtCl(terpyridine)]^+$ Derivative with Viologen-Like Redox Properties," *Dalton Trans.* **41**, 4903–4911 (2012).
H. A. EL-GHAMRY, K. SAKAI, S. MASAOKA, K. Y. EL-BARADIE and R. M. ISSA, "Preparation, Characterization, Biological Activity and 3D Molecular Modeling of Mn(II), Co(II), Ni(II), Cu(II), Pd(II) and Ru(III) Complexes of Some Sulfadrug Schiff Bases," *Chin. J. Chem.* **30**, 881–890 (2012).
H. A. EL-GHAMRY, K. SAKAI, S. MASAOKA, K. Y. EL-BARADIE and R. M. ISSA, "Synthesis and Characterization of Self-Assembled Coordination Polymers of N-diaminomethylene-4-(3-formyl-4-hydroxy-phenylazo)-benzenesulfonamide," *J. Coord. Chem.* **65**, 780–794 (2012).

LIST OF PUBLICATIONS

A. KIMOTO, K. YAMAUCHI, M. YOSHIDA, S. MASAOKA and K. SAKAI, "Kinetics and DFT Studies on Water Oxidation by Ce^{4+} Catalyzed by $[Ru(terpy)(bpy)(OH_2)]^{2+}$," *Chem. Commun.* **48**, 239–241 (2012).

K. KUROIWA, M. YOSHIDA, S. MASAOKA, K. KANEKO, K. SAKAI and N. KIMIZUKA, "Self-Assembly of Tubular Microstructures from Mixed-Valence Metal Complexes and Their Reversible Transformation via External Stimuli," *Angew. Chem., Int. Ed.* **51**, 656–659 (2012).

K. YAMAUCHI, S. MASAOKA and K. SAKAI, "Stability of Pt(II)-Based H_2-Evolving Catalysts against H_2 in Aqueous Solution," *Dalton Trans.* **40**, 12447–12449 (2011).

S. TAKIZAWA, T. M.-N. NGUYEN, A. GROSSMANN, D. ENDERS and H. SASAI, "Enantioselective Synthesis of α-Alkylidene-γ-Butyrolactones: Intramolecular Rauhut-Currier Reaction Promoted by Acid/Base Organocatalysts," *Angew. Chem., Int. Ed.* **51**, 5423–5426 (2012).

Y. YOSHIDA, S. TAKIZAWA and H. SASAI, "Synthesis of Spiro Bis(1,2,3-triazolium) Salts as Chiral Ionic Liquids," *Tetrahedron Lett.* **52**, 6877–6879 (2011).

S. TAKIZAWA, K. KIRIYAMA, K. IEKI and H. SASAI, "Bifunctional Spiro-Type Organocatalyst with High Enantiocontrol: Application to the Aza-Morita–Baylis–Hillman Reactions," *Chem. Commun.* **47**, 9227–9229 (2011).

K. TAKENAKA, M. AKITA, Y. TANIGAKI, S. TAKIZAWA and H. SASAI, "Enantioselective Cyclization of 4-Alkenoic Acids via an Oxidative Allylic C–H Esterification," *Org. Lett.* **13**, 3506–3509 (2011).

K. TAKENAKA, S. HASHIMOTO, S. TAKIZAWA and H. SASAI, "Chlorinative Cyclization of 1,6-Enynes by Enantioselective Pd^{II}/Pd^{IV} Catalysis," *Adv. Synth. Catal.* **353**, 1067–1070 (2011).

C. RAMALINGAN, K. TAKENAKA and H. SASAI, "Pd(II)-SPRIX Catalyzed Enantioselective Construction of Pyrrolizines/Pyrroloindoles Employing Molecular Oxygen as the Sole Oxidant," *Tetrahedron* **67**, 2889–2894 (2011).

S. TAKIZAWA, N. INOUE and H. SASAI, "An Enantioselective Organocatalyzed Aza-MBH Domino Process: Application to the Facile Synthesis of Tetrahydropyridines," *Tetrahedron Lett.* **52**, 377–380 (2011).

T. UEMURA, N. UCHIDA, A. ASANO, A. SAEKI, S. SEKI, M. TSUJIMOTO, S. ISODA and S. KITAGAWA, "Highly Photoconducting π-Stacked Polymer Accommodated in Coordination Nanochannels," *J. Am. Chem. Soc.* **134**, 8360–8363 (2012).

N. YANAI, T. UEMURA, M. INOUE, R. MATSUDA, T. FUKUSHIMA, M. TSUJIMOTO, S. ISODA and S. KITAGAWA, "Guest-to-Host Transmission of Structural Changes for Stimuli-Responsive Adsorption Property," *J. Am. Chem. Soc.* **134**, 4501–4504 (2012).

N. YANAI, T. UEMURA, W. KOSAKA, R. MATSUDA, T. KODANI, M. KOH, T. KANEMURA and S. KITAGAWA, "Inclusion and Dielectric Properties of a Vinylidene Fluoride Oligomer in Coordination Nanochannels," *Dalton Trans.* **41**, 4195–4198 (2012).

N. YANAI, K. KITAYAMA, Y. HIJIKATA, H. SATO, R. MATSUDA, Y. KUBOTA, M. TAKATA, M. MIZUNO, T. UEMURA and S. KITAGAWA, "Gas Detection by Structural Variations of Fluorescent Guest Molecules in a Flexible Porous Coordination Polymer," *Nat. Mater.* **10**, 787–793 (2011).

Theoretical and Computational Molecular Science

Z. SLANINA, F. UHLIK, S. -D. LEE, T. AKASAKA and S. NAGASE, "Stability Computation for Fullerenes and Metallofullenes," in *Handbook of Carbon Nano Materials*, F. D'Souza and K. M. Kadish, Eds., World Scientific, **Vol. 4**, pp. 381–429 (2012).
S. NAGASE, "Quantum Chemistry Calculations of Large Molecules: Multiply Bonded Compounds and Endohedral Metallofullerenes," in *CSJ Current Review 08 Computational Chemistry of Macromolecular System*, Chem. Soc. Jpn., Ed., Kagaku Doujin, pp. 100–105 (2012). (in Japanese)

M. EHARA and R. FUKUDA, "Computational Materials Chemistry for Photofunctional Molecules Based on the Highly Accurate Electronic Structure Theory," in *Expected Materials for the Future*, NTS; Tokyo, **12**, pp. 15–22 (2012).

H. OKUMURA, S. G. ITOH and Y. OKAMOTO, "Generalized-Ensemble Algorithms for Simulations of Complex Molecular Systems" in *Practical Aspects of Computational Chemistry II An Overview of the Last Two Decades and Current Trends*, J. Leszczynski and M.K. Shukla, Eds., Springer; Dordrecht, pp. 69–101 (2012).

Y. SHIKANO, *Time in Weak Value and Discrete Time Quantum Walk: From Quantum Measurement to Quantum Dynamics*, LAP Lambert Academic Publishing; Saarbrucken (2012).

T. ISHIDA, "The Unique Physical and Chemical Properties of Ionic Liquids through Interionic Interactions: Theoretical Investigation with Molecular Dynamics Simulations," in *Handbook of Ionic Liquids: Properties, Applications and Hazards*, J. Mun and H. Sim, Eds., Nova Science Publishers Inc.; Hauppauge, NY, pp. 395–417 (2012).

Photo-Molecular Science

H. OKAMOTO, "Near-Field Optical Microscopy," in *Daigakuin Kogi Butsuri Kagaku 2nd Ed., III. Solid State Physics and Chemistry*, K. Awaga, M. Kotani and T. Yokoyama, Eds., Tokyo Kagaku Dojin; Tokyo, pp. 272–278 (2012). (in Japanese)
K. IMURA and H. OKAMOTO, "Near-Field Optical Microscopy of Localized Surface Plasmons Excited in Noble Metal Nanostructures," *Laser Kenkyu (Rev. Laser Eng.)* **40**, 571–578 (2012). (in Japanese)

E. SHIGEMASA and N. KOSUGI, "Molecular Inner-Shell Spectroscopy: ARPIS Technique and Its Applications," *Adv. Chem. Phys.* **147**, 75–126 (2011).

M. KATOH and S. BIELAWSKI, "Coherent Terahertz Synthesizer," *Nat. Photonics* **Vol. 6**, 76–77 (2012).

T. TAIRA, "Micro Solid-State Photonics," *Parity* **26**, 11–13 (2011). (in Japanese)
T. TAIRA and G. AKA, "Introduction: Advances in Optical Materials (AIOM) Feature," *Opt. Mater. Express* **1**, 523–524 (2011).
T. TAIRA, "Domain-Controlled Laser Ceramics toward Giant Micro-Photonics," *Opt. Mater. Express* **1**, 1040–1050 (2011). (Invited)
H. ISHIZUKI and T. TAIRA, "Large-Aperture, Axis-Slant Quasi-Phase Matching Device Using Mg-Doped Congruent $LiNbO_3$," *Opt. Mater. Express* **1**, 1376–1382 (2011). (Invited)
B. BOULANGER, S. T. CUNDIFF, D. J. GAUTHIER, M. KARLSSON, Y. LU, R. A. NORWOOD, D. SKRYABIN and T. TAIRA, "Focus Issue Introduction: Nonlinear Optics," *Opt. Mater. Express* **1**, 1393–1398 (2011).
N. PAVEL, M. TSUNEKANE and T. TAIRA, "All-Poly-Crystalline Ceramics Nd:YAG/Cr^{4+}:YAG Monolithic Micro-Lasers with Multiple-Beam Output," in *Laser Systems for Applications*, Krzysztof Jakubczak, ISBN 978-953-307-429-0, InTech; Croatia, Chapter 4, pp. 59–82 (2011).
T. TAIRA, Editor of "Solid-State Laser Metals," "Solid-State Lasers," in *Advanced Solid-State Lasers*, Laser Society of Japan, Ed., OHM Press; Tokyo, Chapter 3, pp. 33–96, Chapter 4, pp. 97–147 (2011). (in Japanese)
T. TAIRA, "Pulse Gap High Intensity Laser—Giant Micro-Photonics—," *J. Jpn. Soc. Laser Technology* **37**, 1–5 (2012). (in Japanese)
S. HAYASHI, K. NAWATA, H. SAKAI, T. TAIRA, H. MINAMIDE and K. KAWASE, "High-Power, Single-Longitudinal-Mode Terahertz-Wave Generation Pumped by a Microchip Nd:YAG Laser," *Opt. Express* **20**, 2881–2886 (2012).
M. TSUNEKANE, K. KANEHARA and T. TAIRA, "Next Generation of Ignition by Micro-Laser," *Mater. Sci. Tech. Jpn.*, Materials Science Society of Japan, **49**, 72–77 (2012). (in Japanese)
J. AKIYAMA and T. TAIRA, "Micro-Domain Control for Laser Ceramics," *Ceramics Japan* **47**, 249–252 (2012).
Y. SATO, J. AKIYAMA and T. TAIRA, "Micro-Domain Controlled Anisotropic Laser Ceramics Assisted by Rare-Earth Trivalent," in *Proc. SPIE on CD-ROM*, Pacific Rim Laser Damage 2011, SPIE; Washington, **8206**, pp. 82061T (8 pages) (2012).

Y. NOMURA, C.-T. CHEN, S. WATANABE and Y. KOBAYASHI, "Development of Narrowband, Coherent Quasi-CW Vacuum Ultraviolet Light Source," *Kagaku Kogyo* **64**, Kagaku Kogyosha; Kawasaki, pp. 36–41 (2012). (in Japanese)

Materials Molecular Science

K. AWAGA, M. KOTANI and T. YOKOYAMA, "Chemistry and Properties of Solids," in *Graduate Lectures in Physical Chemistry*, 2nd Ed, Vol. 3, Tokyo Kagaku Dojin (2012). (in Japanese)
T. YOKOYAMA, "Photoelectron Spectroscopy," in *Instrumental Analysis of Metal Complexes II*, H. Oshio, Ed., Textbook of Complex Chemistry VII, Sankyo, Section 17, p.356–391 (2012). (in Japanese)
T. YOKOYAMA, "Synchrotron Radiation: Application to Magnetic Researches," *Magne*, Magnetics Jpn., **6**, p.240–247 (2011). (in Japanese)

M. TADA, "Cluster Cataysts," *Hyomen Gijyutsu*, **62-10**, 491–495 (2011). (in Japanese)
M. TADA, "Structure of a Single Catalyst Particle Observed by Ultra-Thin X-Ray Beam," *Kagaku*, **66**, 33–36 (2011). (in Japanese)
M. TADA, "Micro-XAFS Characterization of Catalyst Particles Using X-Ray Microbeam," *SPring-8 User Information*, **Vol. 16 No.4**, 81–84 (2011). (in Japanese)

M. HIRAMOTO, "Characteristics of Solar Cells Using Carbon Materials in Codeposited Layers," in *Carbon—From Fundamentals to Application*, K. Tanaka, S. Higashihara and H. Shinohara, Eds., Kagaku Dojin, Chap. 14, Section 5.2, pp. 460–470 (2011). (in Japanese)
M. HIRAMOTO, "Long-Term Durability of Small Molecular Type Organic Solar Cells," in *Technology on Long-term Durability for Organic Devices and Materials*, Joho Kiko, pp. 142–146 (2011). (in Japanese)
M. HIRAMOTO, M. KUBO, N. ISHIYAMA and T. KAJI, "pn-Control by Doping and Organic Thin-Film Solar Cells," in *Cutting-Edge Research in Organic Thin-Film Solar Cells*, Y. Matsuo, Ed., CMC Publishing, Chap. 3, Section 2, pp. 122–136 (2012). (in Japanese)
T. KAJI and M. HIRAMOTO, "Crystallization of Small Molecular Codeposited Films by Liquid Coevaporant Molecules," in *Cutting-Edge Research in Organic Thin-Film Solar Cells*, Y. Matsuo, Ed., CMC Publishing, Chap. 4, Section 2, pp. 173–180 (2012). (in Japanese)
M. HIRAMOTO, "Operation Principles of Organic Solar Cells," *Kogyo Zairyo*, **59(9)**, 23–26 (2011). (in Japanese)
M. HIRAMOTO, "Organic Thin-Film Solar Cells," *Molecular Science*, **6**, A0052 (2012). (in Japanese)
M. HIRAMOTO and M. KUBO, "Small-Molecular-Type Organic Thin-Film Solar Cells—Doping Technology," *Mirai Zairyo*, **12(6)**, 38–43 (2012). (in Japanese)
T. KAJI, "New Vacuum Evaporation Technology for Small-Molecular-Type Organic Thin-Film Solar Cells," *Molecular Electronics and Bioelectronics*, **23(1)**, 39–44 (2012). (in Japanese)
T. KAJI, "Crystallization of Small Molecular Organic Semiconductor Thin-Films by Molecular Diffusion and Solar Cell Application," *Molecular Electronics and Bioelectronics*, **23(2)**, 103–104 (2012). (in Japanese)
T. KAJI, "Photocurrent Enhancement of Organic Thin-Film Solar Cells by Advanced Vacuum Evaporation Technique," *Gekkan Displays*, **18(7)**, 28–34 (2012). (in Japanese)

H. TSUNOYAMA, Y. LIU, T. AKITA, N. ICHIKUNI, H. SAKURAI, S. XIE and T. TSUKUDA, "Size-Controlled Synthesis of Gold Clusters as Efficient Catalysts for Aerobic Oxidation," *Catal. Surv. Asia* **15**, 230–239 (2011).
H. SAKURAI, "Uniformal Synthesis and Chirality Control of Carbon Nanotubes Based on Organic Synthesis," *Kagaku Kogyo*, **63**, 140–145 (2012). (in Japanese)

T. ASAKURA, *The NMR World is Expanding—The Enthusiastic Messages from 40 Researchers—*, T. ASAKURA, Ed., CORONA Publishing Co., Ltd.; Tokyo Japan, pp. 26–29, 82–85, 122–125 (2011). (in Japanese)
T. ASAKURA, "The New Silk Road," *Highlighting JAPAN*, **5(2)**, pp. 26–27 (2011).
A. NAGANO, Y. SUZUKI, Y. NAKAZAWA, J. T. GERIG and T. ASAKURA, "NMR Characterization and Product Design of Novel Silk-Based Biomaterials," in *NMR Spectroscopy of Polymers: Innovative Strategies for Complex Macromolecules*, H. N. CHENG, T. ASAKURA and A. ENGLISH, Eds., pp. 281–297 (2011).
Y. NAKAZAWA, Y. SUZUKI, H. SAITO and T. ASAKURA, "The Interaction of Aβ(1-40) Peptide with Lipid Bilayers and Ganglioside as Studied by Multinuclear Solid-State NMR," in *NMR Spectroscopy of Polymers: Innovative Strategies for Complex Macromolecules*, H. N. CHENG, T. ASAKURA and A. ENGLISH, Eds., pp. 299–316 (2011).
T. ASAKURA, "Attack! Laboratory in Japan (7th): By Elucidation of the Preparation Mechanism of Stronger Silk Fiber than Iron Fiber by Silkworm, Development of Excellent Artificial Graft by the Silk Fiber Will Be Attained," http://www.blwisdom.com/pr/laboratory/07/. (in Japanese)
T. ASAKURA, "Road to Development of New Materials from Silk by Elucidation of Mysteries in Spinning Mechanism and Unique Structure of Silk," *HEALTHIST*, Special Issue in 2012 pp. 28–32 (2012). (in Japanese) and (in English)

Life and Coordination-Complex Molecular Science

S. AONO, "Novel Bacterial Gas Sensor Proteins with Transition-Metal-Containing Prosthetic Groups as Active Sites," *Antioxd. Redox Signal.* **16**, 678–686 (2012).

K. YANAGISAWA, K. MATSUZAKI and K. KATO, "Molecular Mechanism Underlying Initiation of Amyloidogenesis and Its Application to Development of Disease-Modifying Drugs for Alzheimer Disease," *Saishin-igaku*, **67**, 138–158 (2012). (in Japanese)
K. KATO, "Structural Biology of Post-Translational Modifications of Proteins," *Yakugaku Zasshi*, **132**, 563–573 (2012). (in Japanese)
Y. KAMIYA, T. SATOH and K. KATO, "Molecular and Structural Basis for *N*-Glycan-Dependent Determination of Glycoprotein Fates in Cells," *Biochim. Biophys. Acta, Gen. Subj.* **1820**, 1327–1337 (2012).

S. AKIYAMA, "Structural and Dynamic Aspects of Protein Clocks: How Can They Be So Slow and Stable?" *Cell. Mol. Life Sci.* **Vol. 69**, 2147–2160 (2012).
A. MUKAIYAMA, T. KONDO and S. AKIYAMA, *SPring-8 Research Frontiers 2011*, 47–48 (2012).

Y. UOZUMI, "Allylic and Aromatic Substitution Reactions," in *Science of Synthesis Water in Organic Synthesis*, pp. 511–534 (2012).

K. TANAKA, "Metal Catalyzed Redox Reactions of Small Inorganic and Organic Molecules Aimed at Energy Conversion," *J. Synth. Org. Chem. Jpn.* **Vol. 69 (No. 4)**, 360–369 (2011). (in Japanese)
K. TANAKA, "Metal Complexes Aimed at Reversible Conversion between Chemical Energy and Electrical One," *Func. Mater.* **Vol. 32 (No. 1)**, 28–37 (2012).

T. UEMURA and S. KITAGAWA, "Polymerization in Confined Geometries," in *Synthesis of Polymers: New Structures and Methods*, D. A. Schlüter, C. Hawker and J. Sakamoto, Eds., Wiley-VCH; Weinheim, pp. 1011–1026 (2012).
T. UEMURA, "Polymer Synthesis in Coordination Nanospaces," *Bull. Chem. Soc. Jpn.* (Award Accounts) **84**, 1169–1177 (2011).
T. UEMURA, "Polymer Friendly Metal-Organic Frameworks," in *Supramolecular Soft Matter: Applications in Materials and Organic Electronics*, T. Nakanishi, Ed., John Wiley & Sons; Hoboken, pp. 175–189 (2011).

INDEX

to “Research Activities”

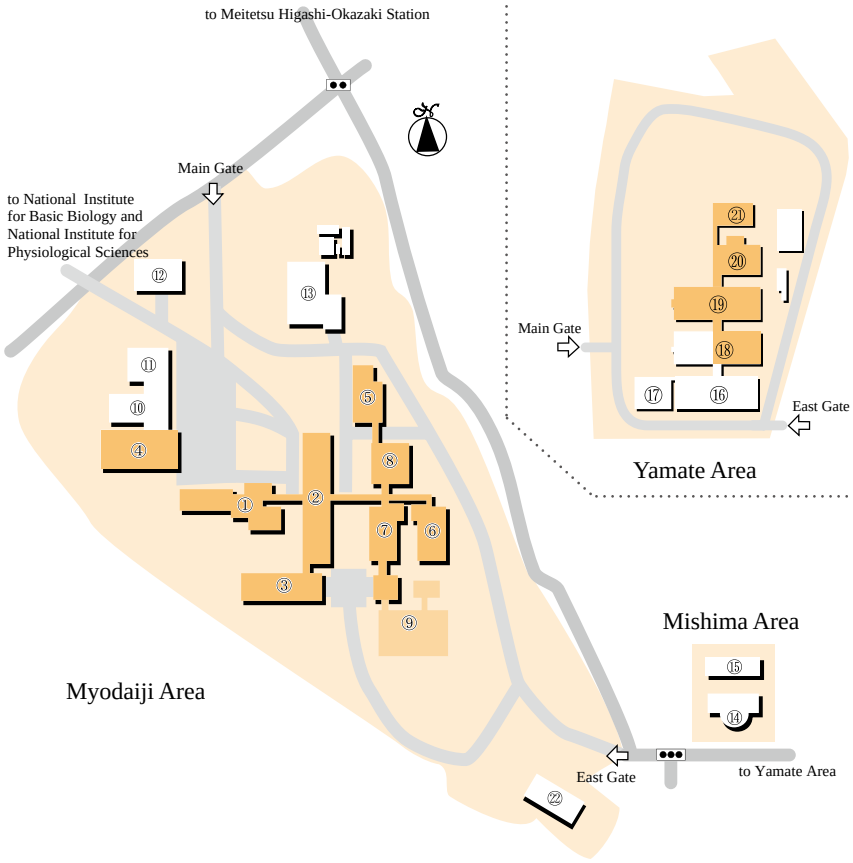

1. Research Office Building
2. Main Laboratory Building
3. South Laboratory Building
4. Research Center for Computational Science
5. Low-Temperature Facilities Building
6. Instrument Center
7. Laser Research Center for Molecular Science
8. Equipment Development Center
9. UVSOR Facility
10. Central Administration
11. Library
12. Faculty Club
13. Power Station
14. Okazaki Conference Center
15. Mishima Lodge
16. Yamate Bldg. 1A
17. Yamate Bldg. 1B
18. Yamate Bldg. 2
19. Yamate Bldg. 3
20. Yamate Bldg. 4
21. Yamate Bldg. 5
22. Myodaiji Lodge

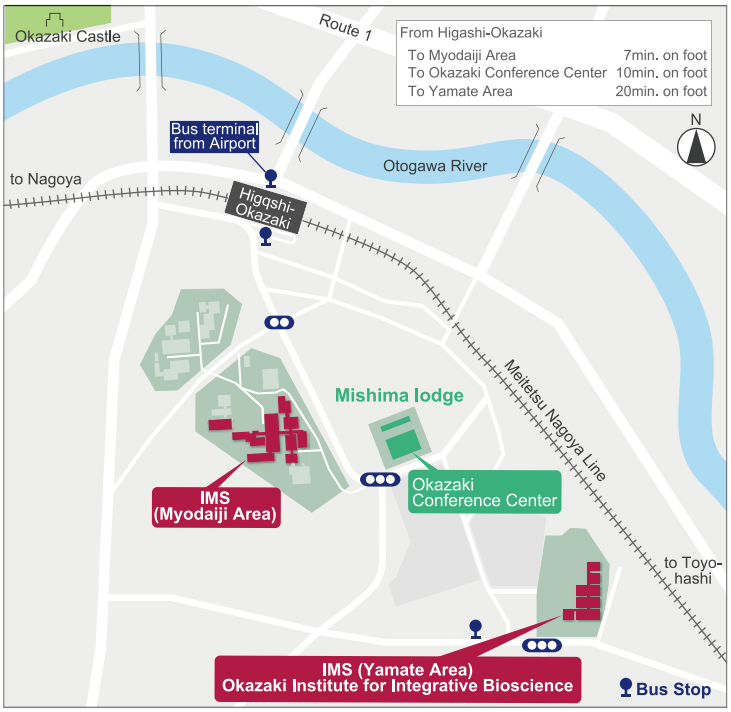

NATIONAL INSTITUTES OF NATURAL SCIENCES

Institute for Molecular Science

Since 1975